



**Federal Aviation
Administration**

DOT/FAA/AFS400/2016/R/01
Flight Technologies and Procedures Division, AFS-400
Washington, DC 20591

**Safety Study on Simultaneous
Independent Approaches Using
Established on Required Navigation
Performance Approach Procedures
with Track-to-Fix Design**

June 2016

Technical Report

Version: V_6

NOTICE

This document is disseminated under the sponsorship of the U.S. Department of Transportation in the interest of information exchange. The United States Government assumes no liability for the contents or use thereof.

The United States Government does not endorse products or manufacturers. Trade or manufacturers' names appear herein solely because they are considered essential to the objective of this report.

1. Report No. DOT/FAA/AFS400/2016/R/01			2. Government Accession No.			3. Recipient's Catalog No.		
4. Title and Subtitle Safety Study on Simultaneous Independent Approaches Using Established on Required Navigation Performance Approach Procedures with Track-to-Fix Design						5. Report Date June 2016		
6. Author(s) Jason Walls, AFS-450; Cody Nichols, AFS-450; Dr. Gerry McCartor, AFS-450; Dr. Richard Greenhaw, AFS-450; Lane Ramirez, AFS-450; Mark Reisweber, AFS-440; Douglas Rodzon, AFS-440; Warren Smith, AJI-121; Blair Dulli, Digital iBiz; Gary Foster, SAIC						7. Performing Organization Code AFS-450		
8. Performing Organization Name and Address Flight Systems Laboratory, AFS-450 6500 S MacArthur Blvd., STB Annex, RM 217 Oklahoma City, OK 73169						9. Type of Report and Period Covered Safety Study/Technical Report		
10. Sponsoring Agency Name and Address Federal Aviation Administration Flight Technologies and Procedures Division, AFS-400 470 L'Enfant Plaza, SW Washington, DC 20024								
11. Supplementary Notes								
12. Abstract The Federal Aviation Administration conducted a safety study on simultaneous independent approaches using Established on Area Navigation Global Positioning System approach procedures to dual or triple parallel runways. The established on required navigation performance concept utilizes required navigation performance technology to safely direct aircraft from initial approach fixes on the downwind leg to simultaneous independent approach paths for dual or triple parallel runways without required vertical separation of aircraft on adjacent final approach courses since the aircraft are considered "established". Data was collected from three separate human-in-the-loop (HITL) tests: Pilot HITL test phases 1 and 2, and a controller HITL test. The phase 1 pilot test included a flight crew HITL test simulation conducted in our A330 and B737 flight simulators located at the Mike Monroney Aeronautical Center (MMAC) in Oklahoma City, OK. The controller HITL test was conducted in the ATC lab simulator, also located at the MMAC. The phase 2 pilot test included a flight crew HITL test simulation conducted in an ERJ 145 simulator located at the CAE Simuflite Training Facility at the Dallas/Fort Worth International Airport. The analysis indicates that aircraft-to-aircraft collision risk is below 1×10^{-9} per operation for simultaneous independent track-to-fix fly-by turn procedures to dual parallel runways separated by 3,600 feet or greater and to triple parallel runways separated by 3,900 feet or greater using a 10° intercept to the final approach course. These results are constrained by the Traffic Alert and Collision Avoidance System and final monitor aid results contained in this study.								
13. Key Words Area Navigation (RNAV) Airport Surveillance Radar (ASR)-9 Blunder Closely Spaced Parallel Operations (CSPO) Established on Required Navigation Performance (RNP) (EoR) Final Monitor Aid (FMA) Human Factors Human-in-the-Loop (HITL) Instrument Landing System (ILS) No Transgression Zone (NTZ) Required Navigation Performance (RNP) Required Navigation Performance Approach (RNP APCH) Traffic Alert and Collision Avoidance System (TCAS) TCAS Resolution Advisory (RA) TCAS Traffic Advisory Track to Fix (TF) Vertical Navigation (VNAV)						14. Distribution Statement Uncontrolled		
15. Security Classification of This Report Unclassified						16. Security Classification of This Page Unclassified		

DOT F1700.7

Table of Contents

Executive Summary	10
1 Introduction	12
1.1 Background	13
2 Purpose and Scope	14
3 Overall Methodology	15
4 Pilot HITL Tests	18
4.1 Test Design.....	18
4.1.1 Test Environment	18
4.1.2 Test Scenarios	20
4.1.2.1 Nominal Scenarios	21
4.1.2.2 Controller Directed Go-Around Scenarios.....	21
4.1.2.3 Flight Guidance Failures Scenarios.....	22
4.1.2.4 Wind and Turbulence Event Scenarios	23
4.1.2.5 Controller Directed Breakout	23
4.1.3 Human Factors Data Collection	23
4.1.3.1 Post-Run Questionnaire.....	24
4.1.3.2 Direct Observations.....	24
4.1.3.3 Debriefing.....	24
4.2 Nominal Analysis	24
4.2.1 Nominal Lateral Performance	25
4.2.1.1 Flight Technical Error	26
4.2.1.2 Total System Error	28
4.2.2 Nominal Vertical Performance.....	30
4.2.3 Nominal Along-Track Performance.....	31
4.2.4 Nominal Human Factor Analysis	33
4.3 Off-Nominal Analysis	34
4.3.1 Controller Directed Go-Around Performance.....	35
4.3.1.1 Take-Off/Go-Around Response in VNAV1 Aircraft.....	35
4.3.1.2 Take-Off/Go-Around Response in VNAV2 Aircraft.....	35
4.3.2 Flight Guidance Failure Performance	37
4.3.2.1 Failure Recovery Initiation from Track Data	38
4.3.2.2 Failure Recovery Initiation Including In-Flight Events	38
4.3.2.3 Vertical Responses during Failure Recovery	41
4.3.2.4 Flight Guidance Failure Human Factors Analysis	43
4.3.3 Wind and Turbulence Event Performance	44

4.3.3.1	Wind and Turbulence Event Lateral Performance	45
4.3.3.2	Wind and Turbulence Event Human Factors Performance	46
4.3.4	Controller Directed Breakout Performance	47
4.3.4.1	Breakout Initiation Performance	47
4.3.4.2	Breakout Human Factors Analysis	48
4.3.5	Nominal to Off-Nominal Overview	49
5	Controller HITL Test	51
5.1	Test Design	51
5.1.1	Test Environment	51
5.1.2	Test Scenarios	52
5.1.3	Human Factors Data Collection	55
5.1.3.1	Post-Shift Questionnaires	55
5.1.3.2	Direct Observations	55
5.1.3.3	Debriefing	55
5.2	Human Factors Analysis	55
5.2.1	Aspect Ratio	56
5.2.2	Phraseology	57
5.2.3	Controller Scan Pattern	57
5.2.4	Controller Comfort	57
5.3	Controller Response Time Analysis	59
6	Modeling and Simulation	61
6.1	Normal Collision Risk	61
6.2	Non-Normal Collision Risk	64
6.2.1	Dual Non-Normal Collision Risk Model Methodology	65
6.2.2	Triple Non-Normal Collision Risk Model Methodology	77
6.2.3	Sensitivity Analysis	79
6.2.4	Controller Directed Breakout	83
6.2.5	Vertical Navigation Considerations	86
6.3	Implementation Risks	88
6.3.1	Nuisance Final Monitor Aid Caution Alerts	88
6.3.2	Traffic Alert and Collision Avoidance System	90
6.3.3	Instrument Approach Procedure Design	94
7	Key Findings and Conclusions	97
8	References	99
	Appendix A: Flight Crew Demographics	102
	Appendix B: Scenario Matrix List for Phase 1 Pilot Test	104
	Appendix C: Scenario Matrix for Phase 2 Pilot Test	109

Appendix D: Post-Run Questionnaire for Pilot Tests	111
Appendix E: Re-engagement of Managed NAV Algorithm for Pilot Test	112
Appendix F: Failure Recovery Initiation Reaction Time for Pilot Test	115
Appendix G: Controller Test Matrix	133
Appendix H: Post-Shift Questionnaire for Controller Test	136
Appendix I: Post-Simulation Debriefing Questionnaire for Controller Test	138
Appendix J: Deviation Recognition Algorithm for Controller Test	140
Appendix K: Final Monitor Aid Model Description	144
Appendix L: Hsu-Anderson Reich Greenhaw Model	155
Appendix M: Sensitivity Analysis Details	158

List of Figures

Figure 1-1: EoR Concept	12
Figure 3-1: Test EoR Track-to-Fix Configuration	16
Figure 4-1: Instrument Approach Procedure Charts Used for Testing	19
Figure 4-2: Event Positions	21
Figure 4-3: Nominal Ground Tracks by Aircraft Type	26
Figure 4-4: Flight Management System Cross-Track Error	27
Figure 4-5: Flight Management System Cross-Track Error by Flight Guidance	28
Figure 4-6: Lateral Total System Error	29
Figure 4-7: Vertical Performance by Aircraft Type	31
Figure 4-8: Indicated Airspeed by Aircraft Type	32
Figure 4-9: ATC Speed Command versus No-ATC Speed Command	32
Figure 4-10: Time in Approach to Length of Approach Scatterplot	33
Figure 4-11: Post-Run Questionnaire Responses Nominal Runs By Aircraft Type .	34
Figure 4-12: VNAV1 TO/GA	35
Figure 4-13: VNAV2 TO/GA	36
Figure 4-14: Times for Pilots to Engage Managed NAV after TO/GA	37
Figure 4-15: Lateral Response Time	39
Figure 4-16: No Visual Contact Lateral Response Time	40
Figure 4-17: No Visual Contact, Go-Around Lateral Response Time	41
Figure 4-18: Distance from Extended Runway Centerline	42
Figure 4-19: Height Above or Below the Glidepath by Distance from the Extended Runway Centerline	43
Figure 4-20: Questionnaire Responses to Flight Guidance Failures by Aircraft Type	44
Figure 4-21: Wind and Turbulence Event Ground Tracks by Aircraft Type	45

Figure 4-22: Total System Error Nominal versus Wind and Turbulence Event	46
Figure 4-23: Questionnaire Responses for Wind Event	47
Figure 4-24: Pilot Reaction Time to Air Traffic Control Directed Breakout	48
Figure 4-25: Nominal versus Off-Nominal Questionnaire Responses	50
Figure 5-1: Scenario 1 – Navigation System Error	53
Figure 5-2: Scenario 2 – Course Deviation	54
Figure 5-3: Scenario 3 – Wrong Runway Selection	54
Figure 5-4: Post-Run Questionnaire Data	58
Figure 5-5: Histogram of Controller Response Times from Deviation Start	60
Figure 6-1: Lateral Separation Distribution and Region of Overlap	62
Figure 6-2: Distribution of Vertical Separation with Region of Overlap	63
Figure 6-3: Geometry of Non-Normal Collision Risk Model	66
Figure 6-4: Collision Risk	69
Figure 6-5: Distance Required to Maintain SMS Target Level of Safety Given a Lateral Path Deviation at Any Angle Relative to the Final Approach Course and Vertical Separation of 0 ft at Intersection	70
Figure 6-6: Distance Required to Maintain SMS Target Level of Safety Given a Lateral Path Deviation at Any Angle Relative to the Final Approach Course and Vertical Separation of 200 ft at Intersection	71
Figure 6-7: 10° Heading Change Joining a Final Approach Course	72
Figure 6-8: Minimum Vertical Separation	74
Figure 6-9: Vertical Profile	75
Figure 6-10: Horizontal and Vertical Overlap Given S	76
Figure 6-11: Triple Approach Concept	77
Figure 6-12: Sample Triple Geometries	78
Figure 6-13: Sensitivity to Runway Spacing	80
Figure 6-14: Sensitivity to Extra Length Added to Leg	80
Figure 6-15: Sensitivity to EoR Vertical Angle	81
Figure 6-16: Sensitivity to Altitude Separation at Glideslope Intercept	82
Figure 6-17: Sensitivity to Third Turn Angle	82
Figure 6-18: Sensitivity to Groundspeed	83
Figure 6-19: Sensitivity to Correction Bank Angle	83
Figure 6-20: Time from Fault to Intersection	85
Figure 6-21: FMA 10 Second Predictor Overshoot Towards NTZ Geometry	89
Figure 6-22: Nuisance Alert Rates (# of Nuisance Alerts / # of EoR Approaches) ...	90
Figure 6-23: TCAS Rate Calculation Method	92
Figure 6-24: Downwind Leg Distance Acceptance Estimation	95

List of Tables

Table 4-1: Go-Arounds on Nominal Approaches	25
Table 4-2: Contingency Table for Non-Normal Error Rates.....	37
Table 4-3: Go-Arounds on Wind and Turbulence Approaches	44
Table 6-1: Simplified Model Collision Risks $\sigma_{Xv} = \sigma_{Yv} = 54.84$, as observed in VNAV equipped aircraft	64
Table 6-2: Simplified Model Collision Risks $\sigma_{Xv} = \sigma_{Yv} = 192.2$, as observed in aircraft not equipped with VNAV	64
Table 6-3: Hsu-Anderson-Reich-Greenhaw Model of Normal Collision Risk Results	64
Table 6-4: Collision Risk during the 10° Turn without Vertical Separation at Intersection	71
Table 6-5: Required Air Traffic Control and Pilot Response Time.....	86
Table 6-6: Near Sea-Level Runway Pair/3,600 ft Separation/No Stagger.....	87
Table 6-7: 10° Interception Added Leg Length TCAS RA Rate; Sensitivity Level 3	92
Table 6-8: 10° Interception Added Leg Length TCAS RA Rate; Sensitivity Level 4	93
Table 6-9: Procedure Stagger TCAS RA Rate; Sensitivity Level 3	93
Table 6-10: Procedure Stagger TCAS RA Rate; Sensitivity Level 4	93

Executive Summary

In response to a request from the House of Representatives Committee on Transportation and Infrastructure, Subcommittee on Aviation, the Federal Aviation Administration (FAA) collaborated with the aviation industry to address one of the Established on Required Navigation Performance (RNP) (EoR) focus areas within the Performance Based Navigation (PBN) priority.

Current aircraft separation standards require a minimum of 1,000 ft vertically or 3 nautical miles (NM) horizontally between aircraft, until they are established on an approach procedure aligned to the runway. The EoR concept considers an aircraft established on the downwind portion of the procedure, thereby eliminating the Air Traffic Control (ATC) requirement of 1,000 ft or 3 NM separation once established. The benefits from this concept support the PBN priority area. They include increased fuel savings from shorter downwind tracks, reduced pilot and controller workload from predictable/repeatable paths, more stabilized approaches, and reduced controller and pilot communications.

In an effort to assess the safety of the EoR concept, the primary purpose of this study was to evaluate the aircraft-to-aircraft collision risk of EoR operations. A secondary purpose was to assess pilot and controller comfort and workload while conducting EoR operations. Based on a recommendation from the NextGen Advisory Committee, this study evaluated the use of area navigation (RNAV) Global Positioning System (GPS) approaches using track-to-fix to track-to-fix (TF-TF) fly-by transitions by aircraft that may not have vertical guidance. As with existing parallel approach operations, an autopilot or flight director is required. We did not presume any special training would be associated with this type of operation for the three tests conducted for this study.

We conducted three human-in-the-loop (HITL) tests to collect data on the pilot and controller response to non-normal scenarios. The tests were conducted using a procedure layout designed for Denver International Airport in Denver, Colorado which represents a conservative case for other airports.

Using the results of the tests, we developed models and simulations to estimate normal and non-normal collision risk, the rate of the nuisance Traffic Alert and Collision Avoidance System (TCAS) resolution advisories (RA)s, and the rate of the nuisance final monitor aid (FMA) caution alerts.

The results indicate that dual EoR operations meet the target level of safety for collision risk (less than 1×10^{-9}) for any configuration with runways spaced 3,600 ft or greater using a 10° intercept of the final approach course. With runways separated by 3,900 ft or more, triples have less than 1×10^{-9} collision risk per operation if the final approach course is intercepted using a 10° leg. A 10° intercept of the final approach course and an at-or-below 210 knot speed restriction on the downwind leg are required to prevent consistent overshooting of the extended runway centerline. Additionally, extending the length of the 10° intercept leg, decreasing the angle of the turn prior to the 10° intercept leg, or increasing the runway spacing are effective methods to further reduce collision risk.

FMA and TCAS may generate nuisance alerts at runways spaced less than 4,800 ft, especially if the length of the 10° intercept leg is not sufficient to keep high convergence areas separated. These results apply to GPS based RNAV and RNP aircraft with or without vertical guidance using TF fly-by turn procedure design, and may be combined with Instrument Landing System (ILS) or Ground-Based Augmentation System (GBAS) Landing System (GLS) straight-in approaches.

The collision risk in this study does not incorporate the risk of wrong runway selection. The risk of a pilot flying the wrong approach can be eliminated through procedure design alone by ensuring an aircraft is on a path that is unique to the intended landing runway prior to being considered established on the approach. Procedure designs that do not incorporate this concept will invalidate the collision risks presented in this report unless mitigations are evaluated and validated via a safety assessment involving all stakeholders.

1 Introduction

In response to a request from the House of Representatives Committee on Transportation and Infrastructure, Subcommittee on Aviation, the FAA collaborated with the aviation industry through the NextGen Advisory Committee to develop an implementation plan for a number of high-priority NextGen capabilities. The plan's foundation was earlier committee work, which recommended the FAA focus on NextGen capabilities in four areas: Multiple Runway Operations, PBN, Surface Operations, and Data Communications. The resulting plan, the NextGen Priorities Joint Implementation Plan, was submitted to Congress in October 2014. This safety study addresses one of the EoR focus areas within the PBN priority.

Current aircraft separation standards require a minimum of 1,000 ft vertically or 3 NM horizontally between aircraft, until they are established on an approach procedure aligned to the runway. Downwind lengths for vectored approaches can be extended during increased traffic rates as controllers attempt to adhere to current separation standards. The EoR concept of operations adapts the approach procedure to an RNAV (GPS) or RNAV (RNP) approach that begins with a segment aligned with the downwind leg. [1] By taking advantage of the reliability and performance of the aircraft's navigation system, this study evaluates the potential risks of considering aircraft established on the RNAV approach and applying parallel approach separation criteria during the turn to final, using no transgression zones (NTZ) between parallel approach paths. The differences between existing radar-vectored interceptions of the final approach course and conceptual EoR operations can be seen in figure 1-1. The key difference is the shorter and repeatable flight paths required by EoR operations as compared to vectored aircraft to intercept the final approach course. This results in efficiency gains to the National Airspace System.

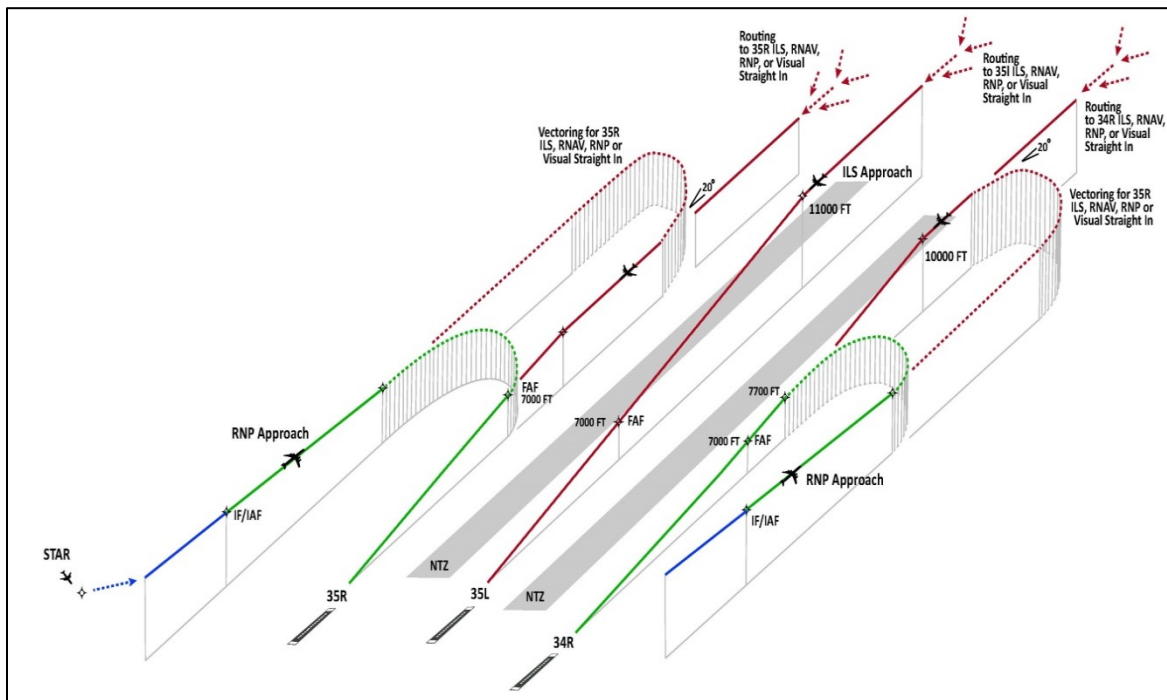


Figure 1-1: EoR Concept

1.1 Background

In February 2011, the Performance-Based Operations Aviation Rulemaking Committee issued a recommendation to the FAA Associate Administrator for Aviation Safety to consider implementation of the EoR concept. [2] After reviewing the recommendation, the FAA contracted Boeing to perform a safety analysis for dependent operations. [3] AFS-400 also performed a data collection on dependent simultaneous operations at Seattle, Washington. [4] Subsequent to the publication of the final Boeing report in March 2014, dependent operations applying the EoR concept have been implemented at the Seattle Terminal Radar Approach Control (TRACON) facility. [5] Additionally, the FAA completed an analysis for RNP authorization required curved path approaches to runways separated by more than 9,000 ft. [6] That analysis supported approval of a change to the separation standards to allow simultaneous independent parallel operations between an RNP authorization required curved approach and a straight-in ILS, RNAV with vertical guidance, GLS, or another RNAV (RNP) approach with a radius-to-fix (RF) leg(s) or an RNAV straight-in to runways spaced more than 9,000 ft. Simultaneous approaches utilizing this separation standard have already been implemented at Denver International Airport, and other locations are currently being evaluated. [7] The MITRE Center for Advanced Aviation System Development is analyzing the feasibility of the concept and operations as implemented at Seattle and Denver. [8, 9, 10, 11]

The International Civil Aviation Organization (ICAO) categorizes RNAV (GPS) approaches as RNP approach (APCH) and RNAV (RNP) approaches as either RNP 0.3, advanced RNP (A RNP), or RNP AR APCH.

2 Purpose and Scope

In an effort to assess the safety of the EoR concept, the primary purpose of this study was to evaluate the aircraft-to-aircraft collision risk of EoR operations. A secondary purpose was to assess pilot and controller comfort and workload while conducting EoR operations. Based on a recommendation from the NextGen Advisory Committee, this study evaluated the use of RNAV (GPS) or RNP APCH procedures using TF-TF fly-by turn transitions by aircraft that may not have vertical guidance. As with existing parallel approach operations, an autopilot or flight director is required. To be consistent with current parallel operations to runways spaced more than 4,300 ft apart, we did not presume any special training would be associated with this type of operation for the three tests conducted for this study. This study assumed that a high-resolution color monitor with alert algorithms, such as the FMA with an NTZ between parallel runways spaced 9,000 ft or less, will be used for EoR operations. This study also assumed that each final approach course has an established monitor controller with override transmit and receive capabilities on the appropriate control tower frequency during EoR operations.

While characterizing the models of aircraft performance on these proposed operations, we also identified some potential implementation issues. These issues included nuisance alerts, procedure design, and participant acceptance.

3 Overall Methodology

In prior safety studies, the analysis of simultaneous independent operations assumed that collision risk was dominantly controlled by a non-normal event where an aircraft suddenly departs from the approach. [12, 13] The deviating aircraft would continue at a constant heading toward the other approach for an extended period of time without the flight crew responding to any radio communications. This type of scenario was called a non-responding blunder. This scenario was considered to be a conservative case to evaluate the safety of parallel operations. Most experts did not attempt to assign a cause for this type of deviation, but those that did listed a variety of failures including airborne equipment failures, ground equipment failures, and human errors. [14]

It was assumed that the proposed EoR operations would be safe to runway spacings down to 3,600 ft if the aircraft exhibited lateral performance typical for RNAV (GPS) approach procedures. Based on this assumption, we concluded that the non-normal collision risk posed the greatest collision risk for this operation. We decided to reconsider methods previously used to determine the risk presented by situations where aircraft deviate from the instrument approach procedure track. We only considered non-normal scenarios where an aircraft that was established on the approach suddenly deviated from the approach path. This is because prior Flight Technologies and Procedures Division (AFS-400) studies of Closely Spaced Parallel Operations (CSPO) have already demonstrated that straight-in procedures are safe and any failure to become established on the approach path would be clear by the time that aircraft reached the final approach course. [13]

Although it is impossible to catalog and test every equipment failure or event that could cause the aircraft to deviate from the approach procedure, it is possible to come to an understanding of how aircraft and flight crews respond to non-normal conditions by causing some representative failures under experimental observation. Previous studies focused on normally performing aircraft and flight crews executing evasive (breakout) maneuvers away from a deviating aircraft on a parallel approach. They did not require data to support how the pilots in the deviating aircraft flew off course or would respond to the deviation. In addition, previous AFS-400 collision risk studies focused on pilot reaction times to a blundering aircraft. This study attempts to capture both how flight crews react to equipment failures that can potentially cause path deviations from the approach course, and how quickly the flight crew reaction to return to course was performed. To this end, flight crews were not provided guidance regarding how they should resolve non-normal conditions.

To model this system, we needed three different categories of data:

- Normal aircraft-pilot system performance data based on the tests, in-service data, and navigation equipment specifications;
- Response data from flight crews who deviate from the approach path, and subsequent controller corrections; and
- Response data from flight crews and controllers during conditions of impending collision caused by unexpected deviations from aircraft on an adjacent approach.

A prototype procedure design was developed for these tests. The FAA conducted several outreach meetings with industry and considered several operational factors in developing

the prototype procedure design. The selected design used four TF fly-by turns to transition from the downwind initial approach segment to the aligned final approach segment: a 60° turn (1st turn), a second 60° turn (2nd turn), a 50° turn (3rd turn), and a final 10° turn (4th turn). The 10° turn was selected to improve the effectiveness of the collision risk mitigations and improve compatibility with existing traffic alerting systems. The prototype procedure design included an at-or-below 210 knot speed restriction at the initial approach fix and an at-or-below 180 knot speed restriction at the 10° turn waypoint. The approach speeds were developed in coordination with industry during the kick-off of this safety analysis and during development of instrument approach procedures for simultaneous dependent EoR operations at Seattle-Tacoma International Airport. They have been identified as an operationally acceptable method of maintaining stable, consistent flight paths during EoR operations. The test EoR configuration used symmetric, head-to-head, co-altitude approach procedures as it was assumed to represent the worst-case scenario for test purposes, see figure 3-1.

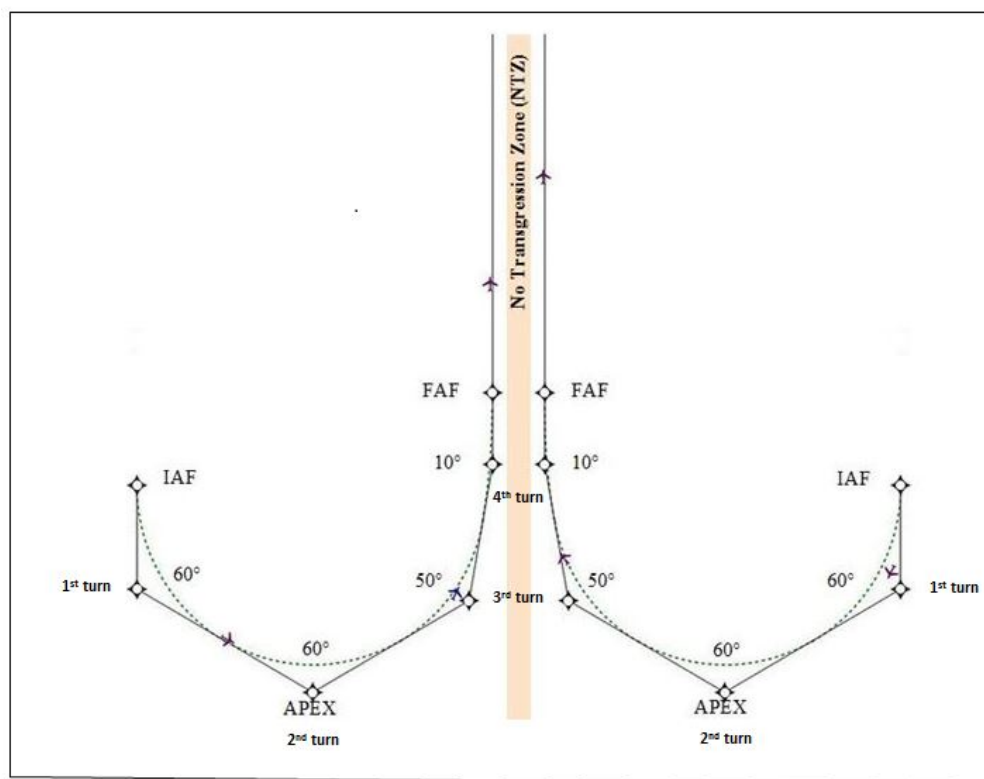


Figure 3-1: Test EoR Track-to-Fix Configuration

The RNAV approach procedure was designed in accordance with the effective United States Standard for Terminal Instrument Procedures (TERPS) at the time of the publication of this report. Each leg has a minimum length to assure that it can be flown under various wind conditions, resulting in a minimum distance between the downwind initial approach fix and the extended runway centerline. The achievable distance was compared to the current tracks at all qualifying airports to confirm the perpendicular distance between the downwind leg and the extended runway centerline was compatible with the existing ground tracks, see section 6.3.3.

This study presents strategic information about how the collision risk and nuisance alert models behave as key variables are changed. This information is provided throughout this report to better inform regulatory bodies in the FAA. Furthermore, the collision risk calculations will include more of the intermediate steps as we layer on the mitigations used in simultaneous operations today.

Finally, this report was developed while collaborating with industry, National Air Traffic Controllers Association (NATCA), the FAA Air Traffic Organization, and regulatory stakeholders through a series of meetings and continuous outreach.

4 Pilot HITL Tests

From January 12 to February 6, 2015 and May 9 through 19, 2015, we conducted high-fidelity HITL testing to collect data from 630 EoR approaches. This represents 112 hours of experimentally controlled and professionally observed flights.

4.1 Test Design

The pilot HITL tests were designed to achieve the following objectives:

- Objective 1: Collect pilot reaction times and responses to non-normal events that may cause a track deviation;
- Objective 2: Collect pilot reaction times and responses to a controller breakout command from the final monitor in response to a blundering aircraft when the subject flight crew is flying the adjacent approach track normally; and
- Objective 3: Evaluate pilot perception of comfort and workload, while simulating an airspace that includes the EoR operations.

The following describes how we designed the test to achieve these objectives.

4.1.1 Test Environment

To evaluate the responses of industry pilots flying EoR approaches with approved VNAV, we used the FAA narrow-body Boeing 737-800NG (B737), designated VNAV1, and the wide-body Airbus A330, designated as VNAV2, full-motion level D flight simulators at the Mike Monroney Aeronautical Center in Oklahoma City, Oklahoma. During the second HITL test, we evaluated the response of industry pilots flying EoR approaches without approved VNAV in the Embraer ERJ 145 full-motion flight simulator at the CAE Simuflite Training Center in Dallas, Texas. [16] The non-VNAV simulator was used to collect data on aircraft with minimal avionics and especially aircraft without approved vertical navigation guidance. Each flight deck was equipped consistent with the majority of such aircraft in the fleet. Furthermore, we tested pilots that were qualified and current in each aircraft under test, and were active 14 CFR Part 121 air carrier line pilots. Each flight crew was composed of pilots from the same airline. Care was taken in the selection of the sample flight crews to not bias the sample toward any particular demographic, see appendix A for flight crew demographics.

For two out of nine flight crews in the A330 simulator, A330 pilots were not available, so we substituted A320 flight crews due to the similarity of the A330/A320 cockpit. Additionally, three subject pilots were unexpectedly absent during their assigned test day. In these cases, we substituted type-rated FAA personnel. Data collected during these days were marked and treated separately in the analysis. Due to engineering limitations in the ERJ 145 simulator, flight crews had to manually enter the flight plan before each approach. This simulator was equipped with a Honeywell FMZ2000 Flight Management System (FMS), and many of the flight crews were unfamiliar with this system. To mitigate this issue, flight crews were provided a checklist to standardize flight plan entry throughout the ERJ 145 test. Additionally, this FMS was running an older software version, NZ 5.2, which prevented the course deviation indicator from transitioning from terminal to approach scaling. This was not a significant issue because we only tested the initial and intermediate approach segments from the initial approach fix (IAF) to the final approach fix (FAF). The course deviation indicator is not required to scale from RNP 1

to RNP 0.3 until the FAF while flying RNAV (GPS) approaches. Terminal scaling is equivalent to RNP 1, which is equivalent to the scaling during the approach segments tested. However, it might have impacted the test data by reducing the urgency of the correction in the few cases where the aircraft continued in non-normal flight past the FAF. Finally, to avoid pilot responses to RAs during non-normal conditions, TCAS was set to traffic alert-only. This setting was explained to crews in test pre-briefings. See section 6.3.2 for further discussion on TCAS.

As described in section 3 and further discussed in section 6.3.3, we selected one instrument approach procedure design to collect the data needed in these HITL tests. The approach was designed for runways 35L and 35R at Denver International Airport to collect data from an airport with a high field elevation, see figure 4-1. These approach plates are shown full size in appendix B. The specific procedure design tested was built using operational expert feedback and consideration for pilot and controller acceptance, false FMA caution alerts, false TCAS RAs, and the distance that the downwind leg would be abeam the airport. For further discussion on the nuisance alerts, see section 6.3. To normalize the aircraft state and flight crew, we initiated all approaches 2 NM prior to the IAF at a typical arrival altitude.

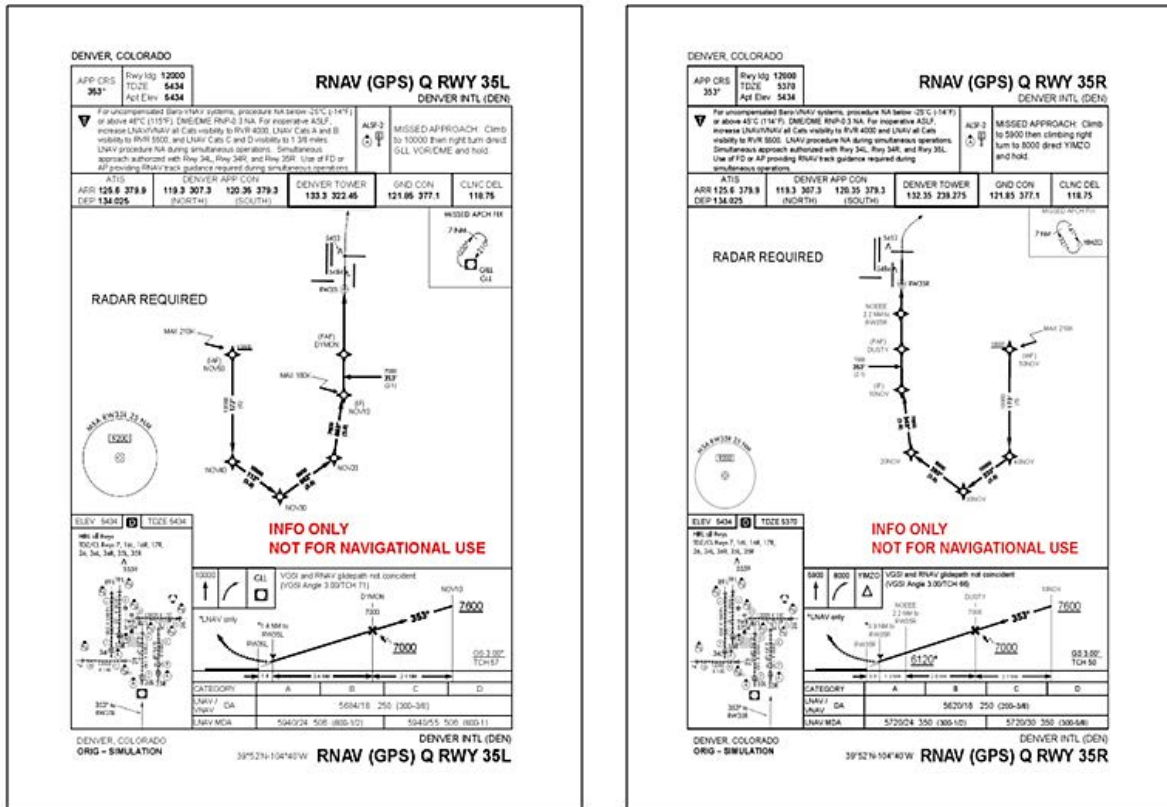


Figure 4-1: Instrument Approach Procedure Charts Used for Testing

We included simulated traffic in the surrounding airspace and appropriate air traffic control services. For the VNAV simulators, simulated traffic and air traffic control services were provided from an attached ATC lab simulator. This lab provided the capability to simulate multiple aircraft concurrently. The ATC lab simulator was not available at the CAE facility where the non-VNAV test was held, so nearby traffic was

simulated using recorded traffic features. During the tests, one controller communicated to the other nearby traffic and the other communicated with the subject flight crew simulating the appropriate radio traffic on the tower frequency. The controllers used in the pilot tests were not certified professional controllers. Since they were not test subjects, we refer to them as non-subject controllers throughout this section.

Weather was selected to be worse than normal. We used the 99th percentile historical winds in the direction that operational experts believed was most likely to induce an overshoot for the subject aircraft on the interception of the final approach course, that is, a quartering tailwind relative to the final approach course at 47 knots at 10,000 ft mean sea level and 15 knots at the ground. All approaches were also flown in dusk lighting conditions. We varied between two weather categories during the test. The first weather condition was representative of marginal visual meteorological conditions (MVMC). The runway visual range was greater than 6,000 ft with broken clouds at 2,000 ft above ground level. The second weather condition was representative of instrument meteorological conditions (IMC). The runway visual range and ceiling were set to the procedure lateral navigation (LNAV) minimums, that is, 5,500 ft and 600 ft respectively.

4.1.2 Test Scenarios

We wanted data on lateral path deviations from a wide range of causes. To achieve this, we induced events designed to cause possible path deviations during selected approaches. Additionally, we wanted information about an event where the controller breaks the pilot of a normally performing aircraft out of the approach path. These events were included in the different scenario types used during the test. For example, we had eight scenarios per day that we will refer to as nominal scenarios. In each scenario, we changed the weather, the flight guidance system in use, that is, autopilot or hand-flying with flight director, the location and timing of the events, and which pilot was flying. By combining these variables with the scenario types and eliminating those combinations that we did not anticipate would produce useful data, we generated a list of scenarios. The order of this list was randomized for each flight crew. See appendix B for the scenario matrix list used during the pilot phase 1 test, and appendix C for the pilot phase 2 test.

Operational experience indicates that various weather conditions on arrival or controller spacing requirements could induce different speed profiles during the approach. To introduce realistic variation in the speed profiles, we scripted a rare-normal event that occurred during some of our other scenarios. During the start of the 1st turn in figure 4-2, the non-subject controller would provide the following direction: “INCREASE AIRSPEED TO 210 UNTIL FURTHER ADVISED”. This type of speed variation could be expected and, therefore, it is categorized as a normal flight condition.

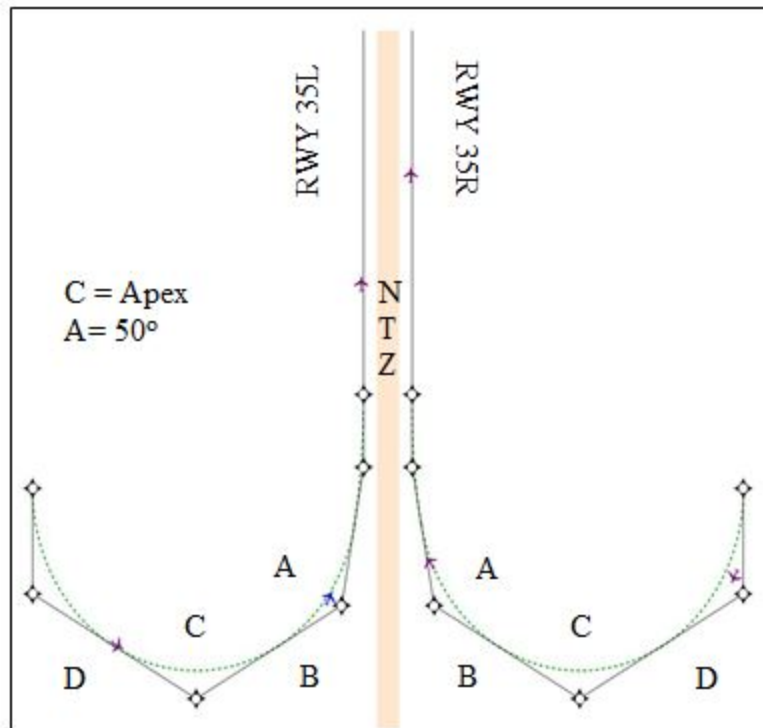


Figure 4-2: Event Positions

The scenarios selected for this test could influence the final result of the safety study because we were attempting to expand the data collected from this limited set of lateral deviation conditions to all possible lateral deviation conditions. To mitigate the risk associated with scenario selection, we involved stakeholders as early as possible. Before testing, we invited experienced industry pilots who had attended the initial FAA EoR stakeholder meeting to fly proposed scenarios and provide input on the test design. The scenarios selected were a result of feedback from these stakeholders. We continued this activity when expanding the testing to the non-VNAV case by collaborating with regional carriers and inviting experienced non-VNAV pilots to review the test setup. Additional inputs were gathered from experts throughout the FAA including the chief scientist for avionics.

4.1.2.1 Nominal Scenarios

Nominal scenarios are approaches where no abnormal events occur when the pilot is flying the approach. These scenarios represent the typical EoR operation. The 8 nominal scenarios out of the 24 approaches flown per flight crew are the experimental control. Besides providing control data, these runs help improve test realism and flight crew immersion.

4.1.2.2 Controller Directed Go-Around Scenarios

Although aircraft failing to complete an approach for which they have been cleared is somewhat rare, this event should represent normal operations. When it occurs, it is typically associated with failing to visually acquire the airport before the decision altitude. This type of go-around occurs when the aircraft is at a low altitude and on the final approach course. However, a cancelled approach clearance due to a runway

obstruction or some other cause could occur earlier in the approach when the aircraft is higher above the ground. When an approach clearance has been cancelled, pilots have the option to either use take off/go around (TO/GA) to provide flight guidance and climb power, or they can follow controller directions manually without selecting TO/GA.

In the VNAV1 simulator, selecting TO/GA while flying the test approach procedure disengaged the autopilot which, if engaged, could have caused a course deviation. The FAA VNAV2 simulator did not have TO/GA lateral navigation at the time of the test, so when TO/GA was selected, the lateral navigation mode switched from lateral navigation mode to track mode. Both of these conditions simulate a pilot error while using the automation which could have resulted in lateral path deviations. In the non-VNAV simulator, TO/GA could not be selected when higher than 2,500 ft above ground level. Since the point where this scenario would have occurred was higher than 2,500 ft above ground level, we did not include this scenario when testing non-VNAV flight crews.

To induce the TO/GA deviations, the non-subject controllers issued the following direction: “(call sign), CANCEL APPROACH CLEARANCE, FLY THE RNAV TRACK, CLIMB AND MAINTAIN ONE ZERO THOUSAND.” This phraseology was determined with the assistance of the Air Traffic Organization (ATO) safety representative to AFS-400, a Denver support specialist, and the EoR NATCA representative. To increase the probability that the flight crew would elect to actuate the TO/GA switch, we only triggered this event during the 3rd turn at the lowest altitude, at position **A** in figure 4-2. We did not simulate go-around instructions for aircraft that were established on the approach but closer to touchdown than our subject aircraft. Even though this would have added more realism to our test, we decided not to include go-around instructions for simulated traffic in order to increase the probability of inducing non-normal flight conditions.

4.1.2.3 Flight Guidance Failures Scenarios

These scenarios were intended to represent lateral path deviations caused by an equipment failure. We designed an event that would cause a deviation from the approach until the flight crew took an action to correct their trajectory. These failures maintained the aircraft state at the time of the failure; therefore, we triggered them just before a turn. To avoid the risk of test subjects being influenced by the learning effect as a result of a limited number of equipment failure scenarios being used during the testing procedure, multiple equipment failures were chosen and were considered equivalent from a testing standpoint. To further reduce flight crew learning effect throughout the test, we initiated the failure at two points: before 20NOV/NOV20 and before 30NOV/NOV30. These positions are represented by **B** and **D** on figure 4-2.

To achieve a comparable effect for each flight crew, we had to fail systems specific to each aircraft type. In the VNAV1 case, we failed the flight director. This appeared in the cockpit as the flight director bar disappearing from the primary flight display. The flight crew was unable to re-engage the flight director; however, the flight director on the pilot monitoring side was still available. In the VNAV2 simulator, we failed a component in the flight management computer (FMC). In the non-VNAV simulator, we failed the Attitude Heading Reference System (AHRS). The flight guidance provided on the primary flight display of the pilot flying behaved as if the heading had not changed (stuck heading) from the time that the failure occurred. Correct heading guidance was provided

on the pilot monitoring side, and it could be switched to the pilot flying side using a reversion switch.

4.1.2.4 Wind and Turbulence Event Scenarios

Collaboration with industry pilots during the pre-test resulted in the inclusion of a high wind condition with every equipment failure the flight crew experienced. During the initial planning stages of the pilot test, we did not intend to introduce a wind condition as a possible failure. However, discussions with AFS-400 personnel in conjunction with feedback from industry pilots following the pilot pre-test led us to the conclusion that the high winds we used represented a non-normal event even without any other failure. To incorporate that feedback, we reduced the winds during the equipment failure scenarios for the pilot test, and we introduced a new scenario with extreme winds. This scenario simulated a wind gust that suddenly increased the speed of the aircraft, making the ground track difficult to maintain.

We configured the gust to smoothly increase to 105 knots with increased turbulence before smoothly decreasing to the typical environmental conditions, see section 4.1.1. The event lasted for approximately 10 seconds. This event was initiated before the 30NOV/NOV30 or before 20NOV/NOV20. See position **D** and position **B** in figure 4-2.

4.1.2.5 Controller Directed Breakout

This type of scenario has been used in pilot HITL tests for other simultaneous independent operations. It assumes that an aircraft has blundered off the other approach and will hit the subject aircraft and assesses the time it takes for a pilot to execute breakout procedures after a controller issues a breakout command. We collected data on this event because the turning aircraft and flight crew are in a different configuration than when established on the final approach course. The breakout occurred near the 10° heading change as the aircraft turned to the final approach course. We also did not provide any special briefing regarding breakout procedures using an attention all users page.

The non-subject controllers initiated the breakout using one of two phraseologies. For some runs they used the phraseology specified in the Order 7110.65, *Air Traffic Control*, [17] for dual and triple precision runway monitor (PRM) approaches:

“TRAFFIC ALERT, (call sign), TURN (left/right) IMMEDIATELY HEADING (degrees), CLIMB AND MAINTAIN (altitude).”

In other cases, they excluded the words “TRAFFIC ALERT” and used the following phraseology: “(Call sign), TURN (left/right) IMMEDIATELY HEADING (degrees), CLIMB AND MAINTAIN (altitude).”

Non-subject controllers varied the breakout terminology during the VNAV1 and VNAV2 pilot tests. However, the non-subject controllers only used Order 7110.65 phraseology during the non-VNAV pilot test. We have frequently observed this omission during air traffic control HITL tests; therefore, we included it for realism.

4.1.3 Human Factors Data Collection

The following three methods were used to collect human factors data:

4.1.3.1 Post-Run Questionnaire

After each approach, pilots were given a post-run questionnaire, see appendix D. These questions evaluated pilot perceptions of difficulty, comfort, and workload compared to normal duties and functions. Questions were limited to expedite completion and also reduce the latency of memory retrieval.

Question 1 assessed each subject pilot's perception of the difficulty of the approach; question 2, their comfort; question 3, each subject pilot's perception of their individual workload; and, question 4, their perception of the collective flight crew workload. Questions 5 and 6 were answered on only those approaches when flight crews experienced off-nominal conditions. These assessed each subject pilot's comfort with recognizing a deviation from the approach and their comfort with taking the necessary action to resolve that deviation.

4.1.3.2 Direct Observations

Observation data was collected by two observers in the cockpit: one human factors observer and one pilot observer. All flight scenarios were carefully scripted to modify flight crew activity. During periods in the flight sequence when a flight crew had to perform non-normal functions, the observers monitored both primary and secondary task completion. During periods of heightened activity, workload, reaction times, latency of task completion, or task shedding may have changed. When observed, the following events were recorded and analyzed:

- Missed radio calls;
- Query of non-subject controllers for a clearance repeat;
- Inappropriate response to a radio call;
- Misunderstood clearance or incorrect reaction;
- Errors using FMC or navigation system;
- Missed or incomplete checklist;
- Latency in radio response; and
- Deviation from the intended path.

4.1.3.3 Debriefing

The human factors observers administered a questionnaire and debriefing at the end of each day with the intent of soliciting each pilot's and crew's overall perception of performance of all of that day's runs. The debriefing covered data collection execution, review of post-run questionnaire responses and any issues that arose during the simulation. Open feedback and discussion from the flight crew and between all members of the test team was encouraged.

Although there was some variation, major themes of questioning were consistent across all flight crews. Besides some generic information regarding employment, experience, and training, we asked about the realism of the test, the flight crew's comfort with the operation, changes in workload, comfort during non-normal conditions, and the flight crew's comfort with the breakout. Breakouts in reference to human factors are further discussed in section 4.3.4.2.

4.2 Nominal Analysis

As discussed in section 4.1.2.1, the nominal scenarios are representative of the typical operation of EoR. Although it has a smaller fleet mix than the anticipated participants for

these operations, this data provided 201 approaches with high quality track information that informed models of these approaches during normal operations. The three most significant parameters needed to model normal approach performance are the lateral path, vertical path, and speed profile variations.

Table 4-1 shows that nearly 5% (10 out of 201) of all aircraft went around during nominal approaches. The go-arounds were mostly correlated with scenarios that required flight crews to hand-fly with flight director guidance and with IMC conditions. This indicates that these variables may be more stressing than other variables tested. Note that we do not believe that this go-around rate will be representative of implemented EoR operations. Rather, the rate appears to be the result of above average test wind speeds and lack of familiarity with the instrument approach procedure. Therefore, the go-arounds were filtered out for the following analysis because they were not representative of the target set of EoR operations that resulted in a landing.

Table 4-1: Go-Arounds on Nominal Approaches

	Go-Around	Overall	Percent		Go-Around	Overall	Percent	
IMC	9	132	6.82%		Autopilot	0	101	0.0%
MVMC	1	69	1.45%		Flight Director	10	100	10.0%
Total	10	201	4.98%		Total	10	201	4.98%

4.2.1 Nominal Lateral Performance

The ground tracks reflect relatively little variation compared to some data observed in-service, see figure 4-3. This may be due to the single wind condition used throughout the test. Furthermore, the tracks have less variation before the 1st turn than later in the approach. We initiated all flights at the same position, so it is expected that some time must pass before typical variance is observed across the sample. By the time they reached the part of the approach where we were interested in aircraft behavior, the variance had normalized. Pilots performed well when the approach was flown under normal conditions.

In this section, we are interested in lateral total system error, or cross-track error, which is the total distance between an aircraft’s position and its desired path. Because the path in the test approaches were defined with TF fly-by turns, each FMS calculated the RNAV track for the transitions differently. This raised some difficult questions about how to measure cross-track error for these approaches. To address this difficulty, we looked at the cross-track error in two ways, as described in the following sections.

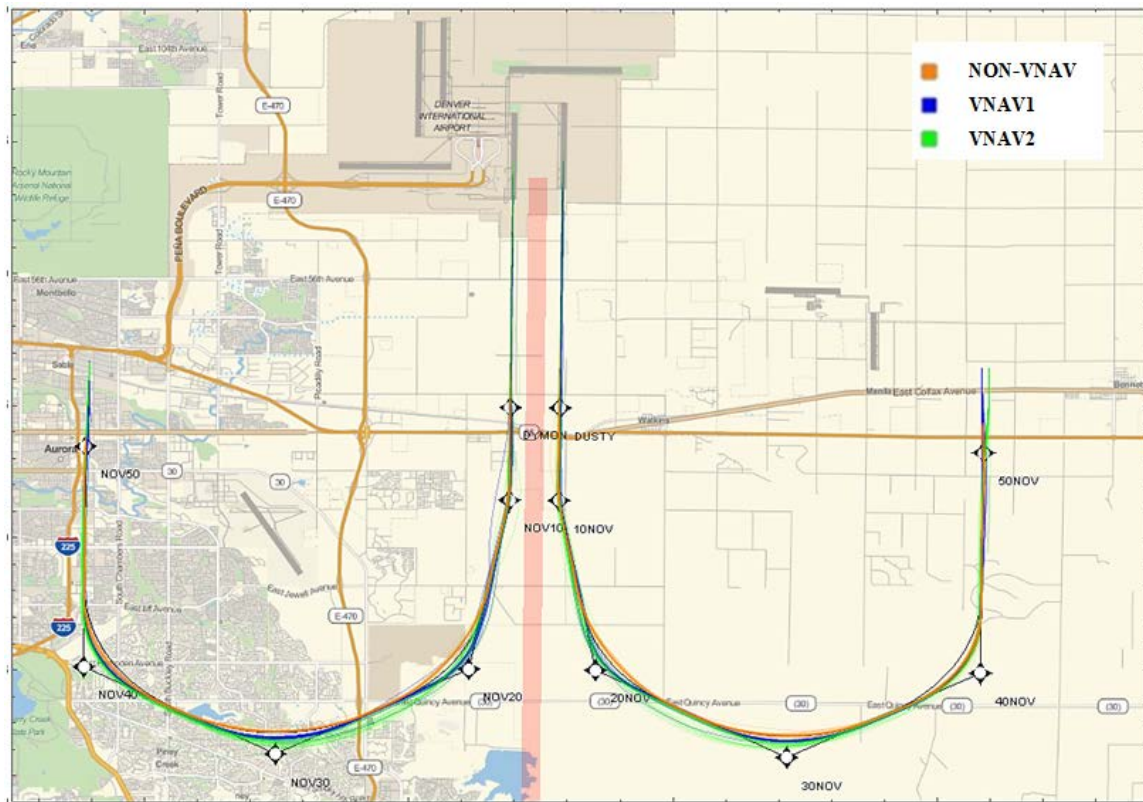


Figure 4-3: Nominal Ground Tracks by Aircraft Type

4.2.1.1 Flight Technical Error

In the VNAV aircraft, the FMC calculates a continuous lateral RNAV path and provides guidance to maintain that path. In the non-VNAV aircraft, when the aircraft reaches the lead point for the next turn, the FMC internal cross-track error measures the distance from the next straight line TF leg. To further illustrate the lower fidelity of the non-VNAV simulator’s FMC, we observed that the navigation display would occasionally display lateral deviation opposite to the steering guidance on the primary flight display. Therefore, we have a good estimate of flight technical error from the FMS in the VNAV simulators, while in the non-VNAV simulator we do not.

In figures 4-4 through 4-8, the x-axis is labeled distance travelled. This is the distance traveled along the TF legs that compose this approach procedure. By using this as our x-axis, we are able to normalize all approaches for variations in path length and time in the approach. The following figures show data collected for both left and right approaches. Only the left approach waypoints are labeled (NOV50 through NOV10), but represent the right approach data collected as well (50NOV through 10NOV).

Figure 4-4 shows the FMC cross-track error where a positive error is an error to the outside of the turn. The most noticeable feature of this image is the consistent overshoot in the VNAV2 aircraft between waypoints NOV30 and NOV20. This is also visible in figure 4-5. The observers noted that VNAV2 crews consistently overshoot this turn, especially during the scenarios with a higher speed profile. Although the crews were aware of the overshoot, they appeared to accept it. Due to the orientation of the approach procedures, this overshoot is not a significant contributor to collision risk. The VNAV1

aircraft performed notably better than the VNAV2 aircraft. Our observers attributed this to quick cross-track deviation detection and correction facilitated by monitoring cross-track with navigation display scaling and navigation performance scales.

Based on our operational expertise, we modelled flight technical error using a Gaussian distribution (also known as a normal distribution or bell-curve) with a standard deviation of 0.050 NM. [15] Besides the VNAV2 overshoot, the variance of the flight technical error displayed here is less than the variance of the proposed distribution.

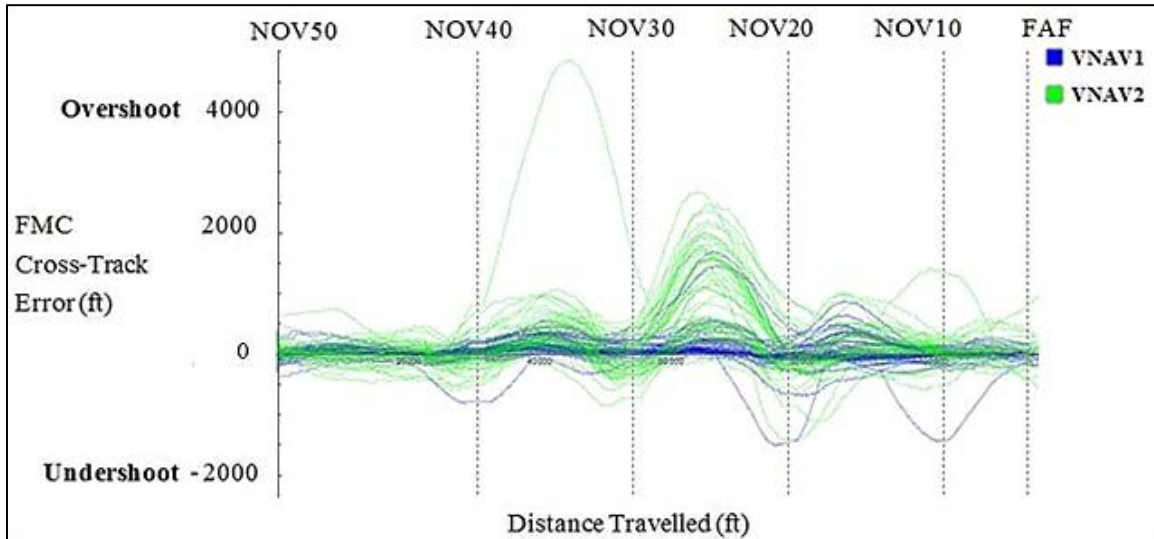


Figure 4-4: Flight Management System Cross-Track Error

Figure 4-5 illustrates how overshoots in the VNAV2 aircraft are similar regardless of whether autopilot is engaged or pilots are hand-flying with flight director. The flight technical error improves when autopilot is engaged in the VNAV1 aircraft, which is expected due to the decrease in human error. This indicates that the VNAV2 overshoot is not a result of pilot behavior, but rather overall size and maneuverability of the aircraft. For the collision risk analysis, we assumed that aircraft would not consistently overshoot the 4th turn to the final approach course. This assumption is reasonable because the characteristics associated with a turn that requires a 5° to 10° bank angle are substantially different from a 50° or 60° heading change, which requires a 25° bank angle. Operational expertise and our test observations indicate that the 10° heading change is unlikely to generate consistent overshoot.

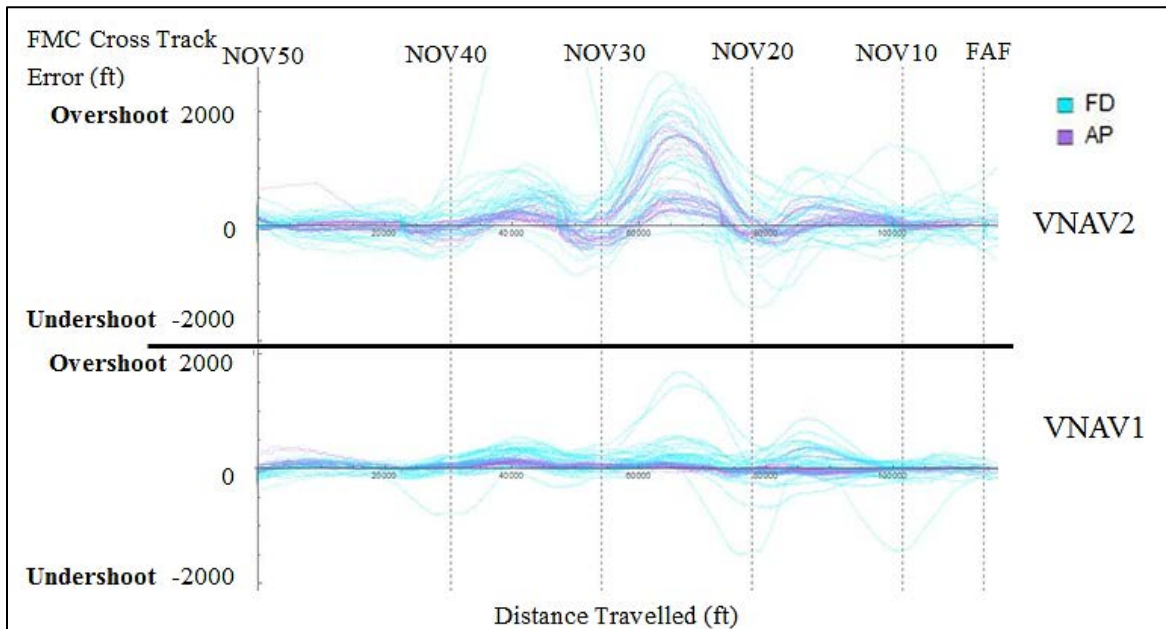
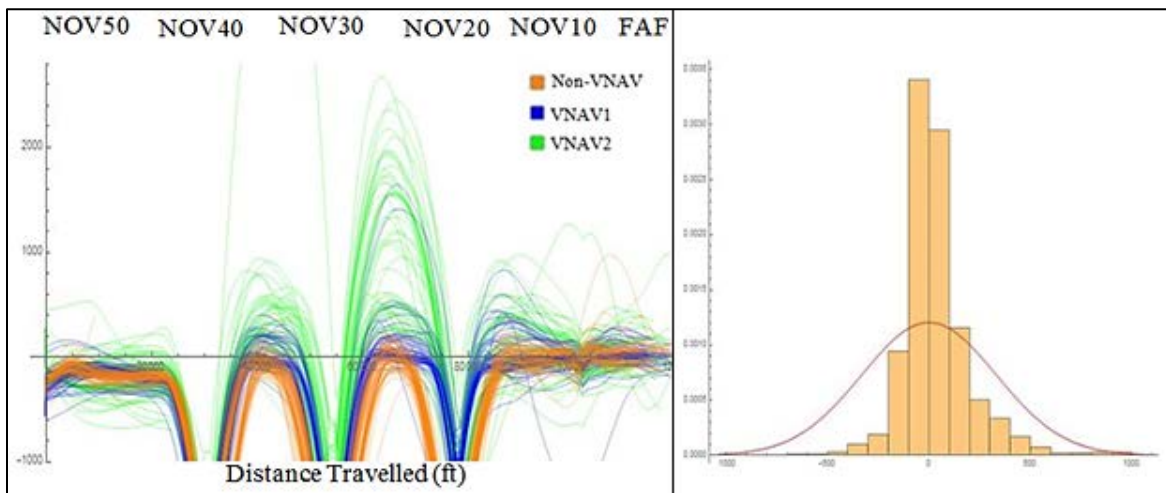


Figure 4-5: Flight Management System Cross-Track Error by Flight Guidance

4.2.1.2 Total System Error

Actual aircraft position is based on total system error, which is the vector sum of flight technical error, navigation system error, and path definition error. Because the TF-TF fly-by turn theoretical transition area allows for many different desired paths, the total system error is difficult to calculate from aircraft position data. However, we are mostly interested in aircraft errors toward the other approach path. Although it may not capture small errors during the turn, we can consider the straight-line approach procedure without the transitions to be the ideal path for calculating total system error. Figure 4-6 shows the total system error calculated from the straight-line approach procedure. The dips below the x-axis are due to the TF fly-by turns, and they are expected. Note that the position correlated error information on the y-axis of figure 4-6 (a) is the same as the error measured for the histogram seen in figure 4-6 (b).



(a) Lateral Total System Error

(b) Lateral Total System Error Histogram

Figure 4-6: Lateral Total System Error

The non-VNAV tracks are very similar to those of the VNAV1 aircraft, and we can conservatively model their error using a Gaussian distribution with standard deviation equal to 0.05447 NM. This is the result of convolving the assumed flight technical error distribution with a distribution for the path definition error and navigation system error assumed to be a Gaussian distribution with a standard deviation of 40 meters, per operational expert opinion.

Except for approaches that are very close together (e.g., 0.01 NM), the Laplace distribution (based on a given RNAV or RNP value) gives larger collision likelihoods than the corresponding Gaussian distribution due to its fatter tails. However, for modeling the typical lateral behavior of RNP and RNAV (GPS) operations, these likelihoods may be too conservative; that is, too large. Therefore, the Gaussian values may be more reasonable.

Since the turning segments of EoR contribute negligible amounts to the approach collision likelihood, use of Laplace distributions will provide negligible increases over the use of Gaussian distributions for those segments would. The use of Gaussian distributions on the straight segments follows the use of such distributions for RNP terminal operations, especially in view of AC 90-105, appendix 1, paragraph 2.a. [16] In addition, we have seen more than one data analysis that supports the conclusion that, for typical lateral terminal area behavior, RNP operations using GPS sensors and RNAV operations using GPS sensors can be modeled with the same distributions for collision risk purposes. Therefore, we accept the proposed Gaussian distribution for total system error with a standard deviation of 0.05447 NM.

The overshoot in the VNAV2 aircraft also appears in the total system error. However, after the aircraft become established on the 10° leg, overshoot decreases. The error near the extended runway centerline, which is most significant for the normal collision risk, can be modeled by the proposed distribution for all airframes.

The errors measured in the non-VNAV simulator were surprising given that the test observers noted that this simulator had significantly reduced performance monitoring

capabilities. The non-VNAV simulator multi-function display (MFD) navigation map consistently presented an artifact where the ownship icon would oscillate from one side to the other over a two to five second period. This observed motion occurred in a start-stop skipping fashion. When questioned during debriefing, crews consistently stated that this behavior was expected and consistent with aircraft on the line. The recorded track data indicated a smooth, on-course track for all nominal runs in the non-VNAV simulator. However, from the flight deck MFD, it was not possible to detect the precision which the aircraft was tracking. The MFD was only used by crews to provide a general position relative to fixes on the flight path and the course deviation indicator was used to determine lateral track compliance. From the cockpit, they did not observe the nominal performance experienced by our non-VNAV sample.

4.2.2 Nominal Vertical Performance

Prior studies of simultaneous procedures have assumed a requirement for vertical navigation, so we have less historical understanding of how modern aircraft without VNAV perform.

Figure 4-7 shows the vertical paths of each aircraft type. The first three approach fixes were coded at or above 10,000 ft mean sea level. The initial aircraft position was set to simulate coming off of an optimized profile descent. The VNAV2 arrived at this starting position at a lower altitude than the VNAV1 and non-VNAV aircraft, hence the lower starting altitude. The histograms demonstrate the relationship between the vertical errors over the area of interest in each aircraft type, showing that the VNAV1 had the most consistent vertical path, followed by the VNAV2, then the non-VNAV.

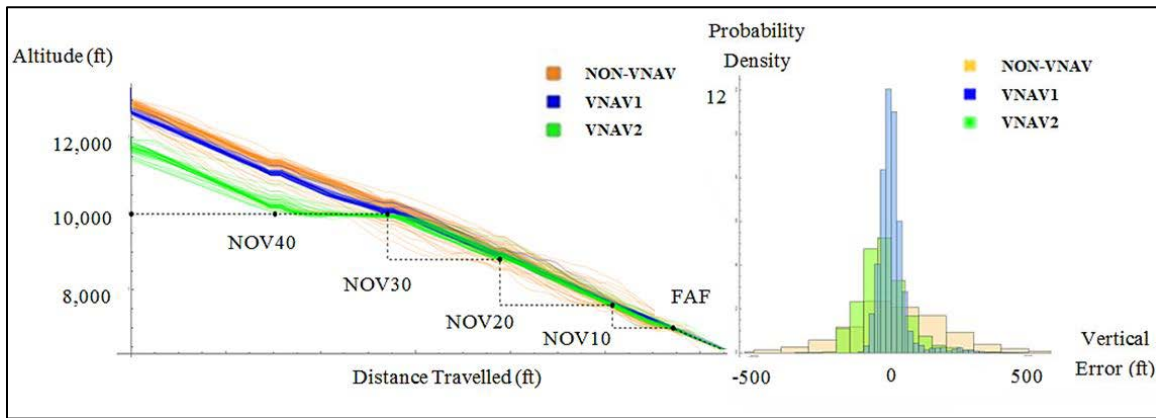


Figure 4-7: Vertical Performance by Aircraft Type

Both the VNAV aircraft have approved vertical navigation using either VNAV in the VNAV1 case or managed descent mode in the VNAV2 case. The non-VNAV aircraft is not approved for vertical guidance and, therefore, pilots are taught to manage approaches vertically using various techniques such as the constant angle non-precision approach technique. As a result, vertical path compliance appeared to be more workload intensive for the non-VNAV pilots. Overall, the non-VNAV vertical paths do not look like a series of step down altitudes, but look similar to the VNAV1 and VNAV2 vertical paths with a wider variance. The standard deviation observed in the VNAV1 dataset was 54.84 ft; the standard deviation in the VNAV2 dataset was 87.54 ft; and the standard deviation in the non-VNAV case was 192.2 ft.

4.2.3 Nominal Along-Track Performance

Figure 4-8 shows that aircraft had a wide range of speeds while flying the approach nominally. Observers noticed many different techniques for slowing the aircraft. The variability in deceleration techniques do not lend themselves to statistical modeling. Therefore, we use this data to inform assumptions in the collision risk calculations, but we did not statistically model it.

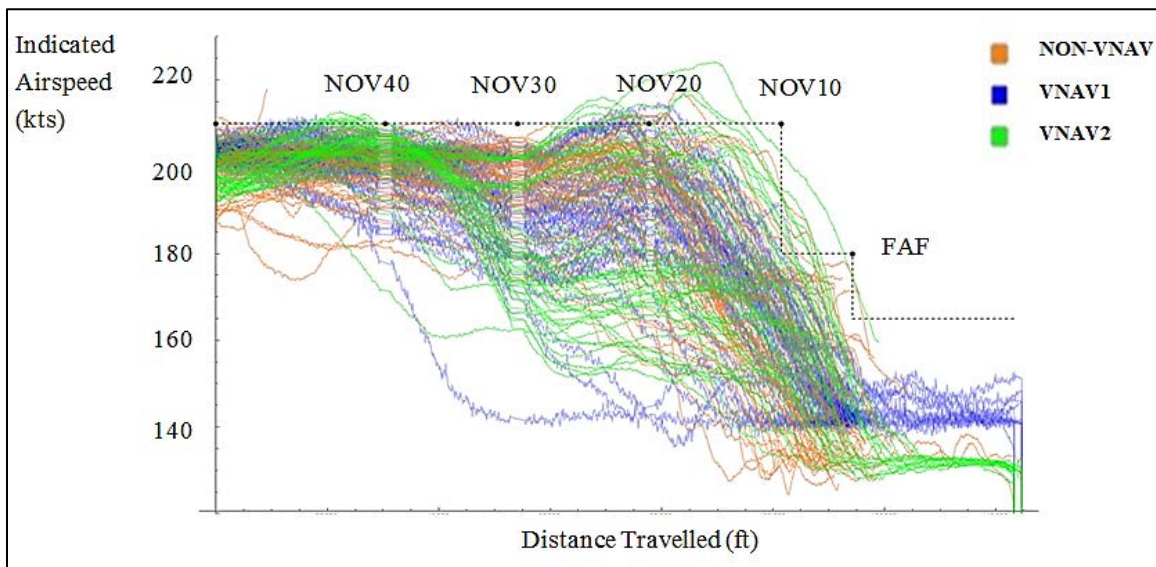


Figure 4-8: Indicated Airspeed by Aircraft Type

As described in section 4.1.2, controllers introduced variation in approach speeds by providing 210 knot speed commands during some of the test runs. The effect of maintaining higher approach speeds can be seen in figure 4-9.

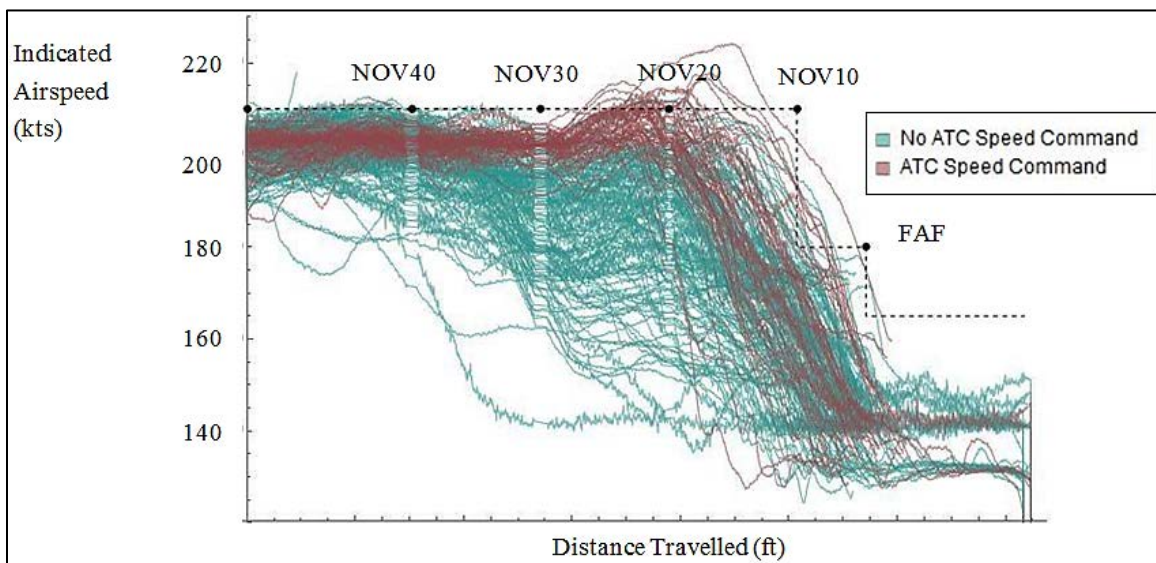


Figure 4-9: ATC Speed Command versus No-ATC Speed Command

Some experts and stakeholders have expressed concern about controllers managing the diverse path lengths associated with a TF fly-by turn procedure design. Figure 4-10 demonstrates that the variability reduces the correlation between path lengths and time spent on the approach. Although an RF procedure design would reduce variability in path length, if the speed variation is similar, it would not eliminate variability in time spent on the approach. Unless speed variations are also restricted during RF approaches, it may not provide the anticipated relief for air traffic control sequencing and spacing. It appears that both RF and TF approach procedures may present challenges when merging

EoR traffic with traffic flying the extended final approach. This emphasizes the important relationship between EoR operations and decision support tools.

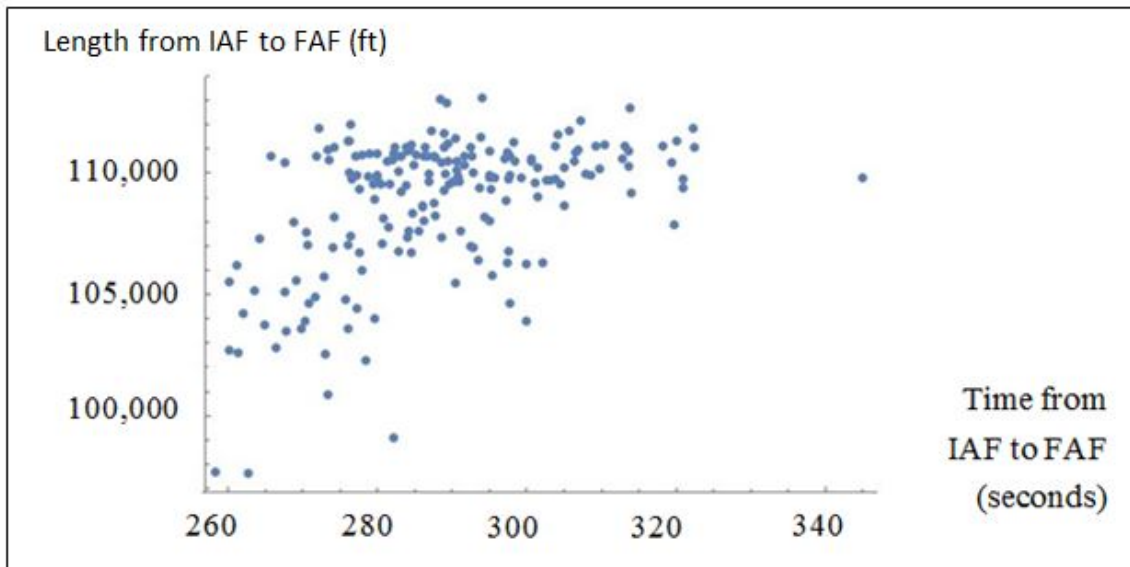


Figure 4-10: Time in Approach to Length of Approach Scatterplot

4.2.4 Nominal Human Factor Analysis

In the box charts throughout this report, the shaded boxes represent 50% of responses. The whiskers indicate the range of responses, and the thick horizontal black line represents the mean. In some charts, a white line may appear within the shaded box. This line represents the median of the data. If a box is not present, 50% or more respondents answered with the median value. In each group of three, the first box is the non-VNAV pilot responses, the second box is the VNAV2, and the third box is the VNAV1.

The responses to the post-run questionnaire, as seen in figure 4-11, indicate that crews did not report difficulty, discomfort, or high workload with the nominal EoR approaches. Using this figure as an example, the first group of boxes represents the responses to the question: “Compared to your typical approach, rate the level of difficulty performing this operation.” The second box in the group indicates that 50% of VNAV2 pilots responded with either “same as typical approach” by marking a 5 or “somewhat more difficult” by marking a 6 on the questionnaire. The long whisker above the box indicates that at least one VNAV2 pilot responded to this question with “much more difficult” by marking a 9. The long whisker below this box indicates that at least one VNAV2 pilot responded to this question with “much easier” by marking a 1. The black line indicates that the mean response is approximately 5.25. The white line is not visible, meaning that the median of the data falls on the boundary of the box. In this case, 5 is the median response.

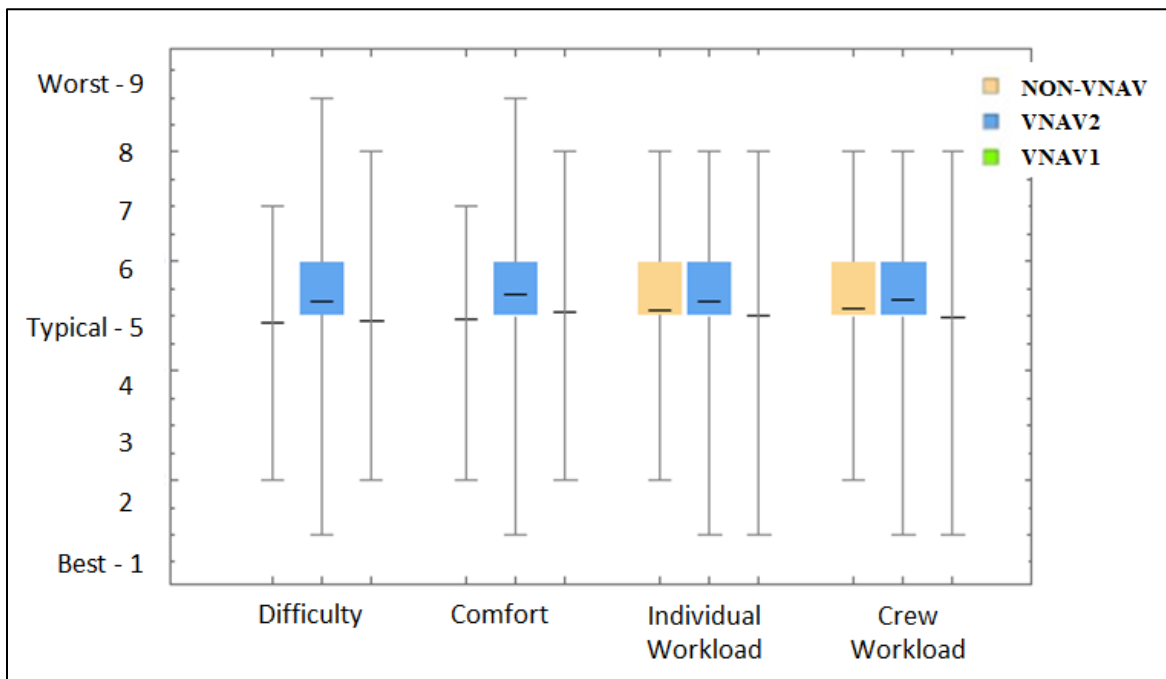


Figure 4-11: Post-Run Questionnaire Responses Nominal Runs By Aircraft Type

Several of the VNAV pilots preferred flying RF legs as opposed to TF legs, but no pilots indicated that TF legs were unacceptable. Several pilots voiced concerns about the head-to-head geometry flown in the test.

4.3 Off-Nominal Analysis

We tested three off-nominal scenarios. First, we failed an element of the flight guidance system that could cause a deviation from the approach. Second, the non-subject controllers cancelled the approach clearance during the 3rd turn to possibly cause automation conflicts during the go-around procedures. Finally, we subjected the flight crew to extreme wind conditions. For more information on these failure types, see section 4.1.2.

When pilots were faced with off-nominal scenarios, they recognized the situation then engaged in some or all of following activities:

- Transferred control of the aircraft to the other pilot;
- Turned the aircraft away from the parallel traffic;
- Contacted air traffic control; and/or
- Executed a go-around.

From the flight guidance failures and the go-around automation issues, we identified the tracks that experienced non-normal conditions and extracted the time that it took for the flight crew to correct. The wind scenarios increased cross-track error by inducing elevated energy states.

Additionally, we collected pilot performance data when issued a breakout as a specific test condition.

4.3.1 Controller Directed Go-Around Performance

The controller directed go-around was an event that simulated a deviation initiated by the pilot instead of a deviation from an equipment failure. The details of how we attempted to induce the pilot errors are very specific; however, they inform a response to a wide range of pilot errors using cockpit automation. This is different than the failures in the flight guidance failure events, which occurred without any pilot trigger. However, these different types of events had very similar results.

The phraseology used to direct go-arounds was understood by flight crews. On a few occasions, flight crews requested a heading from the controller. The non-subject controllers complied and issued a heading.

4.3.1.1 Take-Off/Go-Around Response in VNAV1 Aircraft

In the VNAV1 simulator, pressing the TO/GA switch automatically disengages the autopilot if it is engaged when it is flying an RNAV (GPS) approach. However, the autopilot disconnection did not cause any significant deviations during the test because LNAV guidance was still available due to the TO/GA to LNAV capability. The maximum cross-track errors reported by the FMC in each approach are recorded in figure 4-12. Any measurable overshoots from the autopilot disconnection would likely be less than the maximum FMC cross-track error, so further study of this data is not necessary.

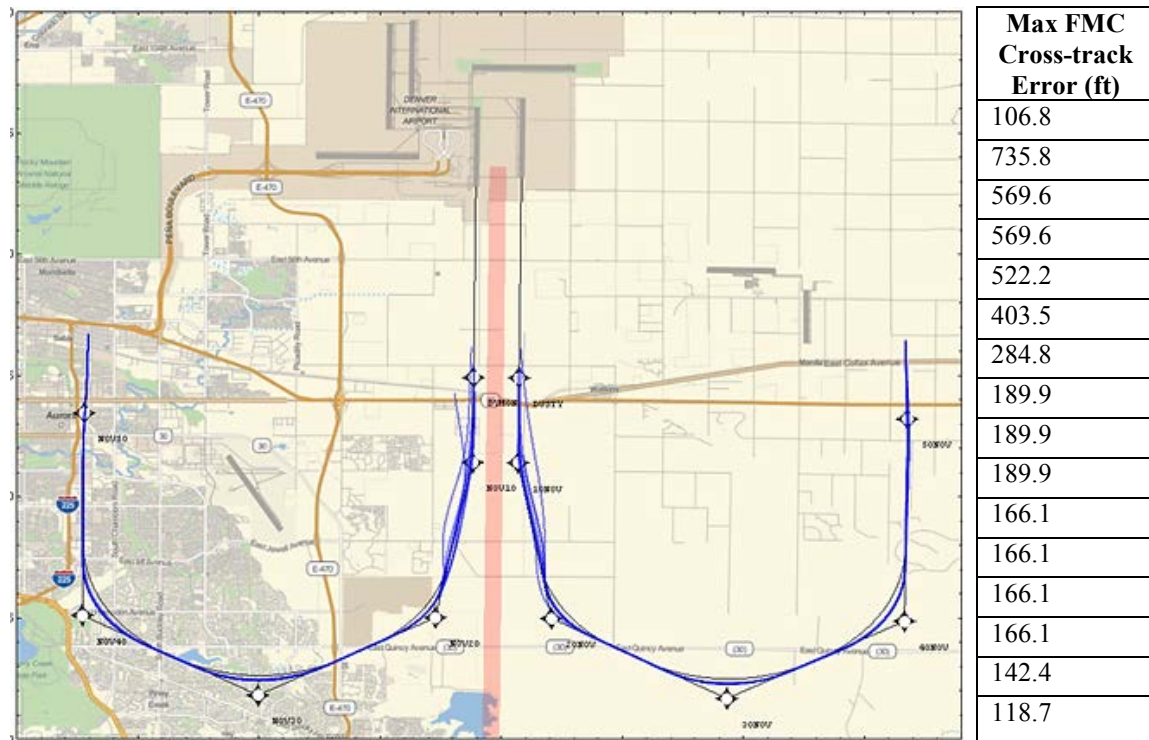


Figure 4-12: VNAV1 TO/GA

4.3.1.2 Take-Off/Go-Around Response in VNAV2 Aircraft

As discussed in section 4.1.2.2, some versions of the VNAV2 aircraft enter track lateral navigation mode when TO/GA is selected, potentially resulting in course deviation if selected while the aircraft is turning. Figure 4-13 is a composite image of VNAV2 tracks where TO/GA was selected. Not every scenario involving the controller directed

go-around resulted in the crew selecting TO/GA. Many crews manually controlled the aircraft to climb or set a new altitude using the altitude selector on the flight control unit. Furthermore, some of the crews that engaged go-around mode did not experience any deviation from the approach course, because they selected managed navigation immediately after selecting TO/GA as trained.

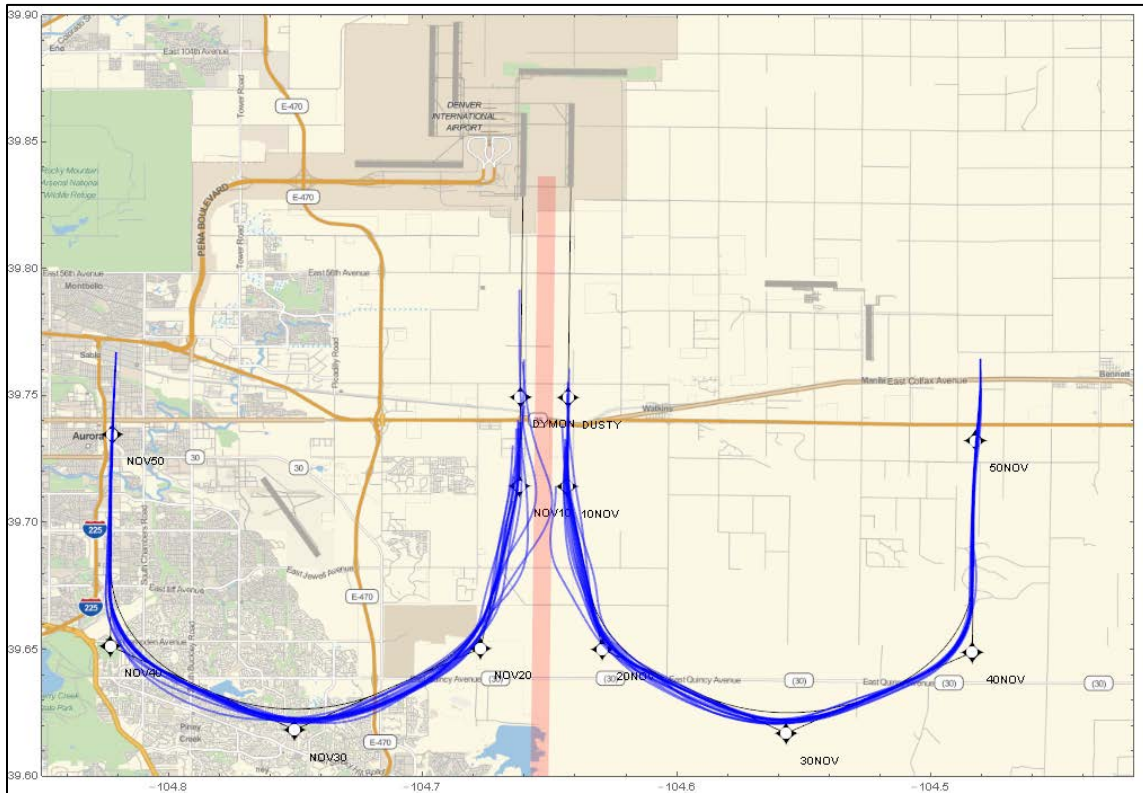


Figure 4-13: VNAV2 TO/GA

There is not a significant correlation between any variable and the rate that flight crews used the TO/GA switch except certain flight crews consistently used TO/GA while others did not. When the non-subject controllers directed crews to maintain a higher speed, they were more likely to experience a deviation by using TO/GA to execute the go-around. This is statistically true with 95% confidence.

When aircraft experienced a deviation, we extracted a reaction time. TO/GA selection is marked in the data, which indicates the start of the deviation. The full flight simulators did not capture when pilots re-engaged managed navigation. Therefore, we developed an algorithm to estimate when the flight crew re-engaged LNAV. This algorithm is described in detail in appendix E. Figure 4-14 is the histogram of the reaction times that result from subtracting the time that the TO/GA switch was actuated from the time the flight crew re-engaged managed navigation (managed NAV).

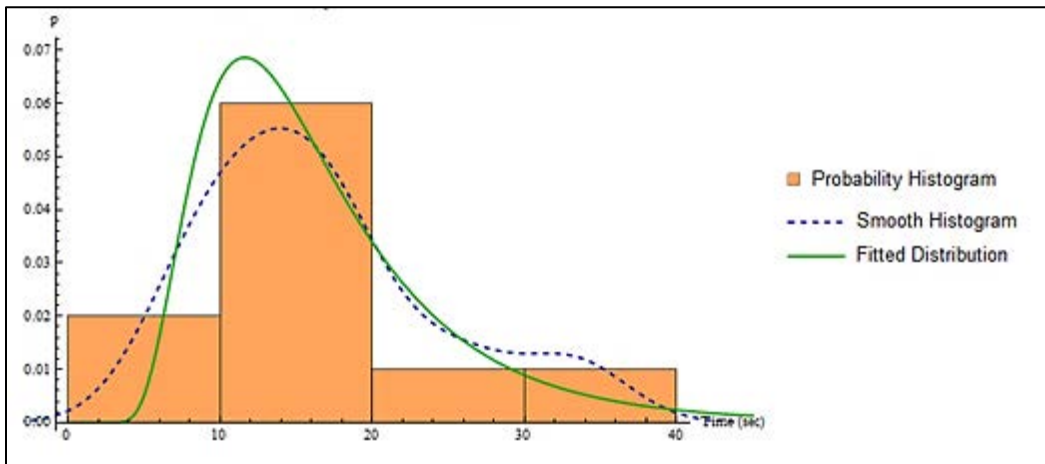


Figure 4-14: Times for Pilots to Engage Managed NAV after TO/GA

We modeled the response times for this failure condition using an unbounded Johnson distribution with shape parameters $\gamma = -11.07$ and $\delta = 1.864$, location parameter $\mu = 2.233$, and scale parameter $\sigma = 0.06599$.

4.3.2 Flight Guidance Failure Performance

Between all three airframes, we subjected flight crews to the flight guidance malfunctions 100 times. By simulating these failures with the flight crews, we hoped to cause situations where the aircraft developed large path errors. The flight crews responded to some failures in such a way that the aircraft continued to track the approach normally. To isolate approaches with non-normal behavior, we filtered out tracks that overshot the path toward the other runway by less than two standard deviations from the assumed normal behavior distribution. Out of the 100 approaches with failures, 67 exhibited non-normal cross-track error. On 24 of these approaches, pilots reported seeing the other traffic. These were considered not representative of a conservative non-normal condition because the pilots could have been reacting to stimuli not available during instrument conditions. Therefore, they were also excluded from the data analysis.

The rate at which crews displayed non-normal error characteristics given a failure appears to be correlated with the aircraft type as seen in table 4-2. This may indicate that the selected failures in each aircraft had different severity. However, the failures are similar enough that the reaction times can be measured using the same algorithms.

Table 4-2: Contingency Table for Non-Normal Error Rates

	Number of Approaches that Exhibited Non-Normal Error Characteristics	Total Number of Approaches	Percent of Non-normal Aircraft
VNAV1 / FD	11	32	34.38
VNAV2 / FMC	21	32	65.63
Non-VNAV / AHRS	35	36	97.22
Total	67	100	67.00

4.3.2.1 Failure Recovery Initiation from Track Data

To ensure that results were comparable between aircraft types, we built a test for reaction times based on aircraft state information.

First, we did not consider times before we triggered the malfunction in each approach. Then we removed times after we could obviously identify that the correction had taken full effect. The way that we identified the full correction was to examine the time-series of the cross-track error and not consider any of the times after the first apparent local maximum.

Next, we refined the reaction start using a bank angle time series smoothed with a Gaussian filter. This is a moving average with Gaussian weights which we set to use a radius of eight seconds and a standard deviation of four seconds. These values were selected based on analyst expertise. The maximum smoothed bank indicated a significant peak in the data. Finally, we calculated the last time that the measured bank was less than 60% of the maximum bank angle prior to the identified peak.

4.3.2.2 Failure Recovery Initiation Including In-Flight Events

The simulators exported more variables than aircraft state information, and we used this additional data to augment the response time calculation. The main questions that we can answer with this extra data are:

- Was someone hand-flying, and if so, who;
- Did the flight crew initiate a go-around; and
- What flight guidance was engaged?

Two data analysis algorithms were needed to answer these questions. With the first algorithm, we detected a go-around that did not use TO/GA from the altitude and rate of climb data. Using the second algorithm, we determined who was hand-flying based on the roll inputs.

To detect the go-around we first smoothed the vertical speed using a Gaussian filter with a radius of 12 seconds and a standard deviation of 6 seconds. These values were selected based on analyst expertise. Then, the aircraft was considered to be climbing any time that the smoothed vertical speed was greater than 100 ft/min. The initiation and termination of these periods of climb were recorded.

To calculate which pilot was hand-flying, we used the roll force exerted on each pilot's control wheel. Based on the nominal data, we developed thresholds for determining if either pilot was flying. We applied a Gaussian filter with a radius of eight seconds and a standard deviation of four seconds to the unsigned roll force. Each time that the pilot supplying the most smoothed wheel force changed or both wheels had no smoothed roll force above the threshold, we recorded the time. When the smoothed roll force compared to the threshold, times were corrected for the last time that the inputs fell within the threshold before the change. This helped ensure that the times were not biased by smoothing.

By combining the results from these algorithms with other simulator outputs, the data gave a clear picture of the sequence of events on each approach. For the 10 longest reaction times, we used observer notes along with analytical, pilot, and human factors experts to corroborate the data and clearly describe what happened in each case. These

results can be seen in appendix F.

For the collision risk model, we needed both the time of the lateral correction and, if the aircraft executed a go-around, when this occurred relative to the lateral correction. While processing the data, we identified that distribution was substantially different when the pilots made visual contact with the other aircraft, see figures 4-15 and 4-16.

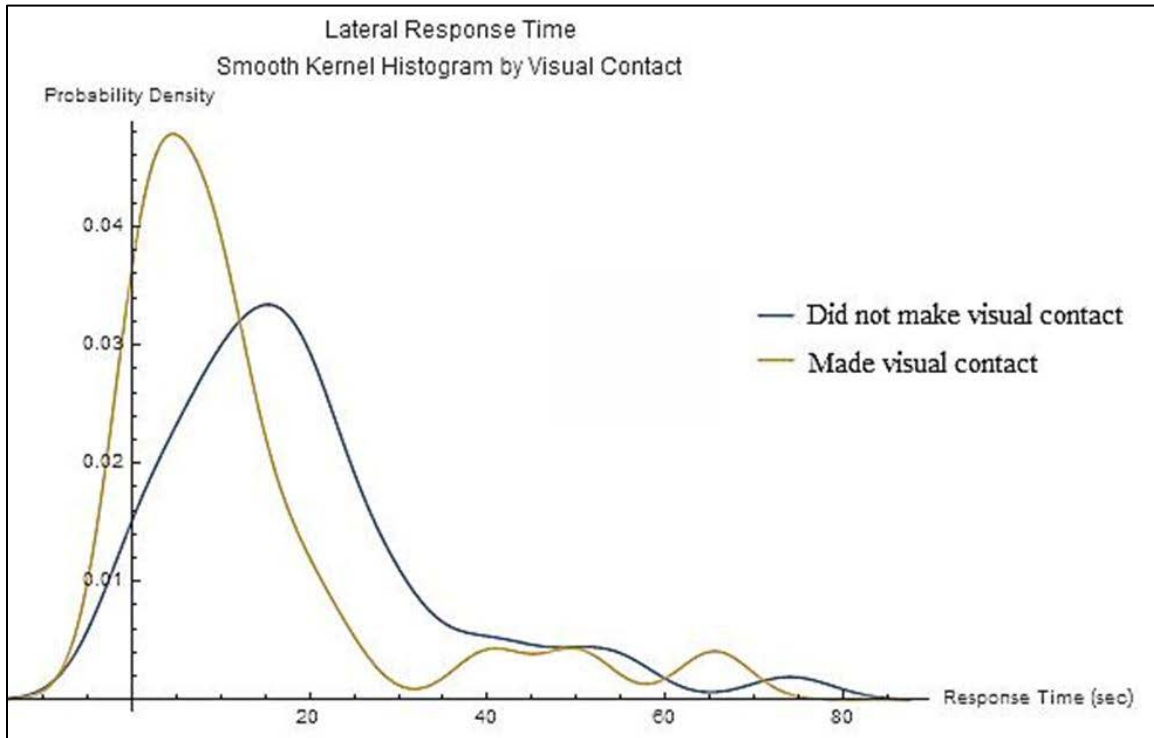


Figure 4-15: Lateral Response Time

Furthermore, we identified that the response times are substantially different in the go-around and continue approach cases. Due to the size of the continued approach dataset, which included only 15 approaches, the distribution used for modeling was fit to this dataset. This was a Johnson unbounded distribution with $\gamma = -270.2$, $\delta = 56.11$, $\mu = -384.4$, and $\sigma = 6.422$.

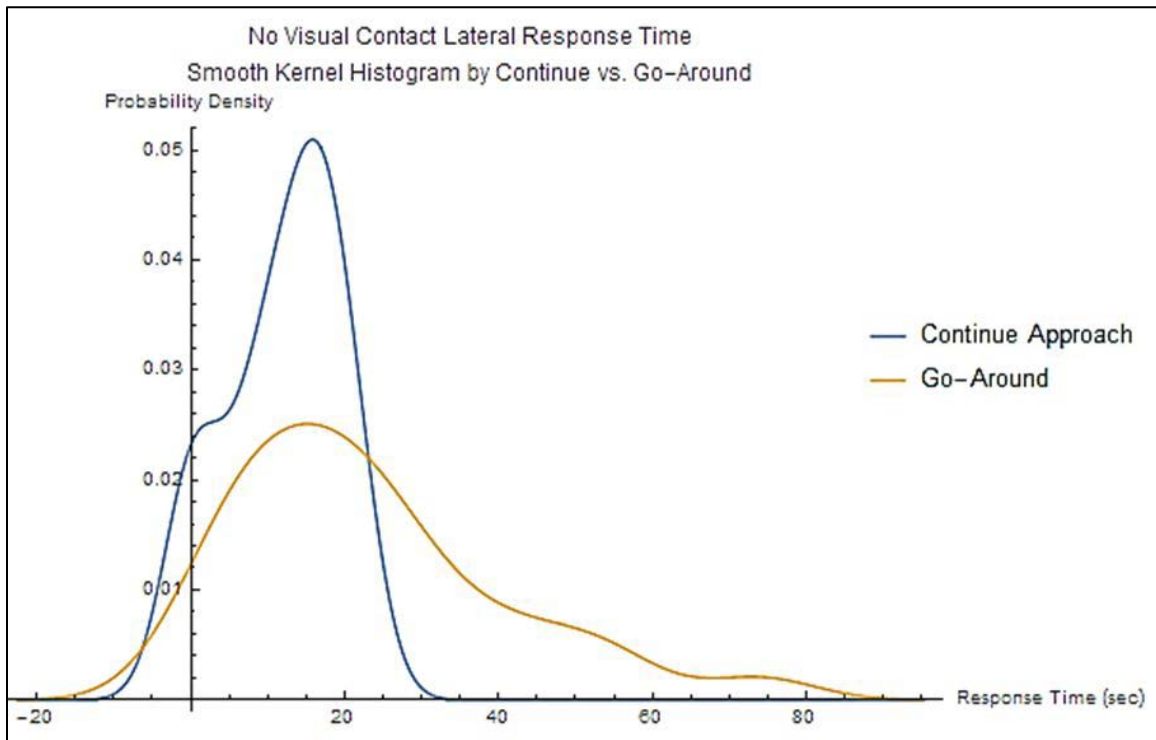


Figure 4-16: No Visual Contact Lateral Response Time

However, for the go-around dataset, the different failure types in the various simulators also impacted the distributions dramatically, see figure 4-17. To select the worst possible case, we fitted a distribution to the no VNAV, go-around, and no visual contact dataset for modeling. Only 20 approaches met these conditions. This was a Johnson unbounded distribution with $\gamma = -12.58$, $\delta = 2.698$, $\mu = -20.34$, and $\sigma = 0.8547$. This distribution will generate response times less than 86.74 seconds 99% of the time.

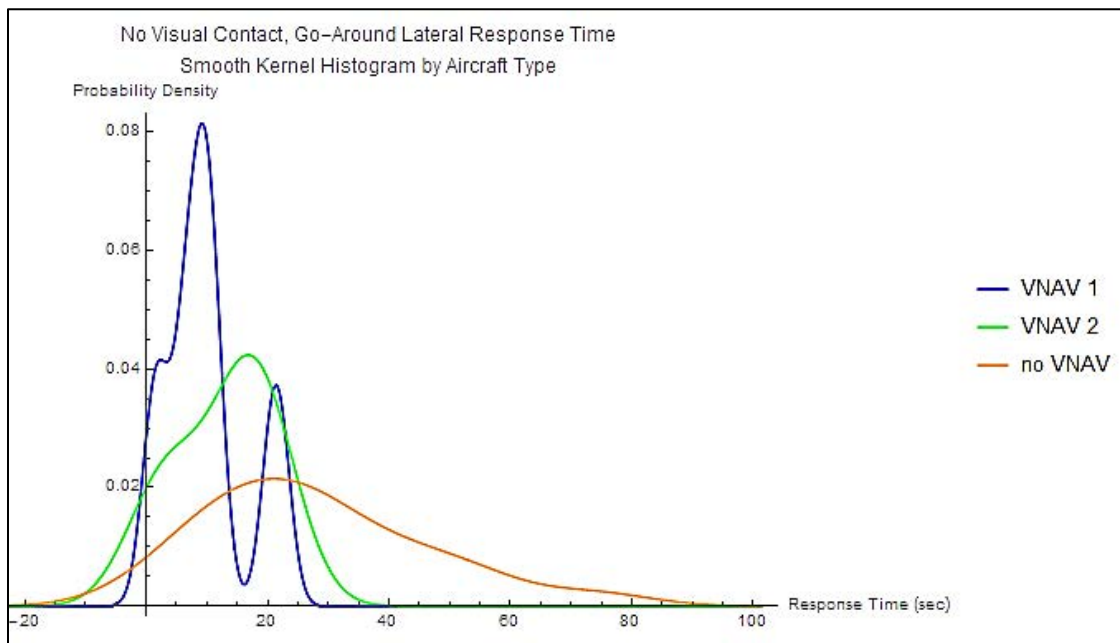


Figure 4-17: No Visual Contact, Go-Around Lateral Response Time

Each flight crew experienced four flight guidance malfunctions. Although we randomized scenarios and triggered failures in different positions, as described in section 4.1.2.3, pilots could have learned how to respond to the failures. After the first failure, 83% of approaches exhibited non-normal cross-track error, based on the filter described in section 4.3.2. Only 72% exhibited non-normal cross-track error on the second failure, 45% on the third failure, and, by the last flight guidance failure, only 31% of approaches exhibited non-normal cross-track error. When we analyzed only the approaches that exhibited non-normal cross-track error, we found no a significant difference between the reaction times measured from the first flight guidance failure and the reaction times measured from the last flight guidance failure. By comparing the two datasets with the Watson U^2 test, which yields a p-value of 0.12, we showed that there is one underlying distribution that can represent both datasets. Although flight crews were more likely to mitigate flight guidance failures with each successive malfunction, the filtered reaction times collected during the pilot HITL tests were not invalidated by an observable learning effect.

4.3.2.3 Vertical Responses during Failure Recovery

For the collision risk model, it was necessary to understand the position of the aircraft vertically to determine when aircraft could intersect. This required some understanding of the behavior of the aircraft vertically. When aircraft did not go-around, they generally did not experience large deviations. Aircraft that executed go-arounds tolerated larger lateral deviations and had highly varied vertical profiles. Using expert judgment and the following data, we assumed that aircraft attempting to capture a glideslope at some point would continue on the vertical profile needed to capture that glideslope, even as they experience a deviation. Figure 4-18 shows all flight guidance failure data collected for both left and right approaches superimposed on the left side of the figure and all nominal approaches for comparison on the right side. It plots the altitude of the aircraft by the distance from extended runway centerline to give some sense of vertical profiles during

the deviations, especially comparing the go-around, continued approach, and nominal datasets to both runways.

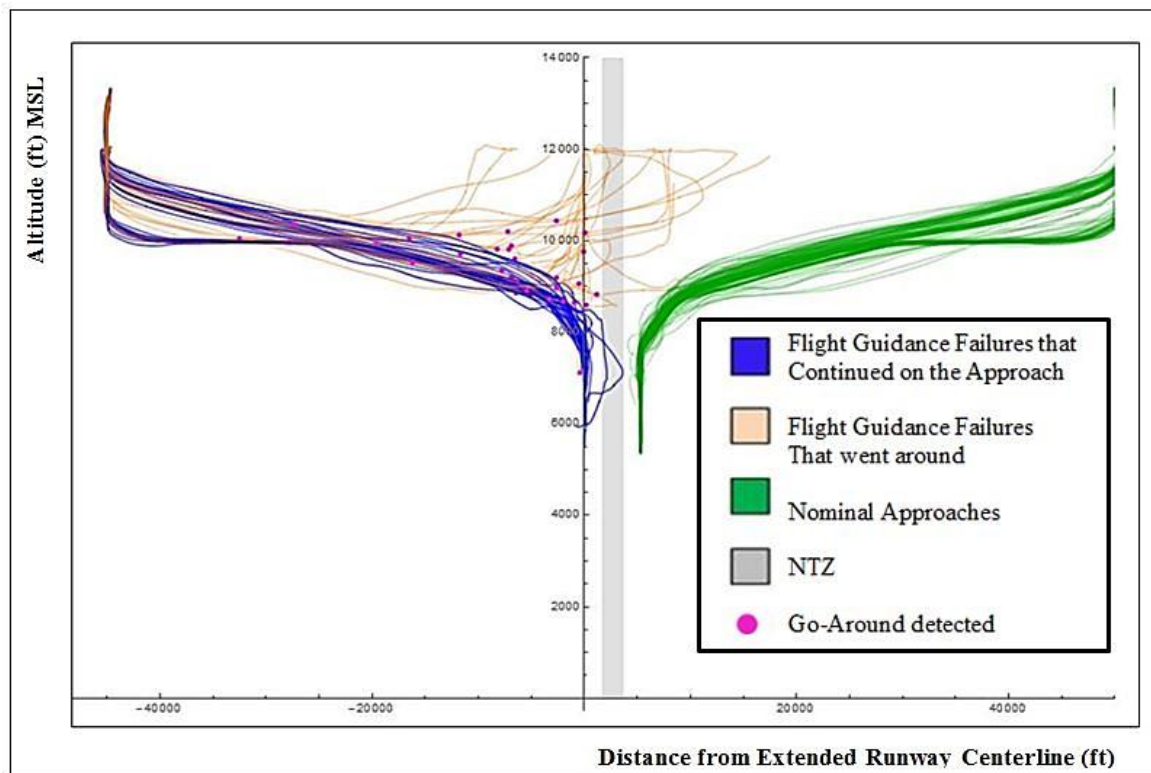


Figure 4-18: Distance from Extended Runway Centerline

One observation that analysts made while comparing the vertical data from the aircraft that experienced a lateral deviation, but continued the approach was that the standard deviation of the vertical error of the non-VNAV aircraft increased during the time that the flight crew experienced the lateral track deviation. The rate at which the standard deviation increased was 0.0065 ft for every foot of path length.

When the flight crews executed go-arounds, there was a large amount of variation. In particular, the Kolmogorov-Smirnov test with a p-value of 0.8 indicates that the time of the go-arounds relative to the time of lateral correction can be modelled by a normal distribution with mean equal to -25.52 seconds and standard deviation of 27.97 seconds. After approximately 3,500 ft along the EoR deviation path, the distribution of vertical angles while executing the go-arounds became reasonably stationary. We chose to model it using a normal distribution with a mean of 2.5° and a standard deviation of 1° which clearly represents most of the data, see figure 4-19.

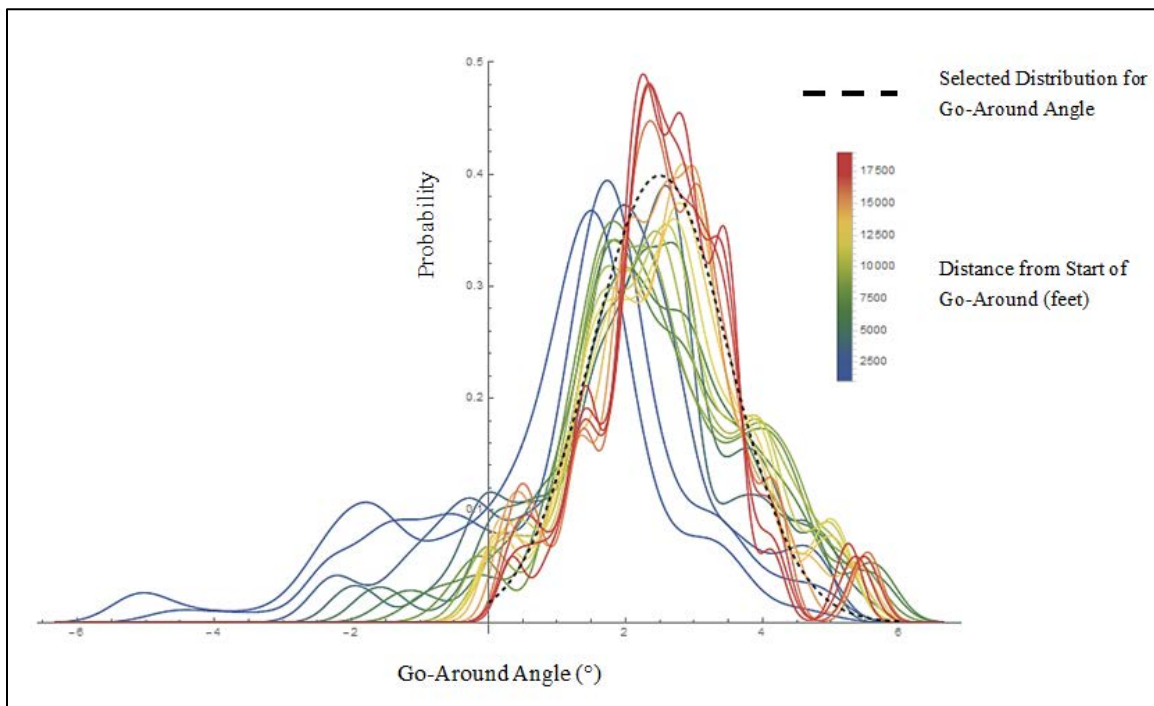


Figure 4-19: Height Above or Below the Glidepath by Distance from the Extended Runway Centerline

4.3.2.4 Flight Guidance Failure Human Factors Analysis

Flight crews reported the highest difficulty with increased workload and decreased comfort levels when responding to flight guidance failures, see figure 4-20. The VNAV1 crews scored better in all categories, suggesting either that the aircraft and flight crews were better equipped to handle the flight guidance failures or that the failure selected for the VNAV1 was less stressing.

Pilots regularly expressed confidence in the system and the ability of controllers to maintain separation. In aircraft with reduced flight deck display fidelity, flight crews expressed no discomfort despite some of the large lateral deviations that they experienced. Although flight crews were comfortable with the EoR operations, in some cases observers indicated that this was the result of poor situational awareness from reduced availability of error metrics in the flight deck displays.

As seen in section 4.3.2 and section 4.3.2.2, the non-VNAV crews had difficulty identifying lateral track deviations and taking corrective action. However, the non-VNAV subjective responses are not substantially different from those measured in the VNAV cases. This reflects the reduced position accuracy monitoring capabilities in the non-VNAV aircraft cockpit, see section 4.2.1.2.

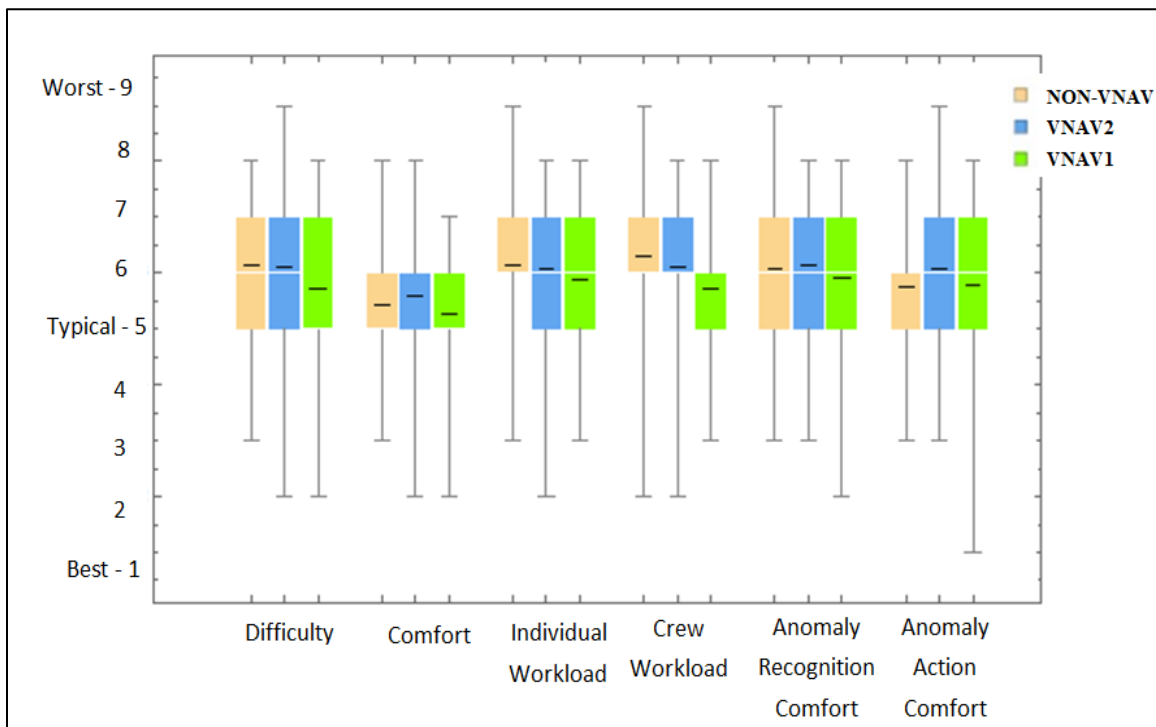


Figure 4-20: Questionnaire Responses to Flight Guidance Failures by Aircraft Type

More than half of flight crews first responded to a non-normal condition by contacting air traffic control while attempting to diagnose the situation. To enable the collection of pilot response data, non-subject controllers were only allowed to instruct aircraft to discontinue the approach, continue flying the RNAV track, and climb to a designated altitude. These instructions encouraged flight crews to attempt to return to course. Deviations that resulted from this situation could have been prevented by a controller who was allowed to vector a deviating aircraft away from parallel traffic upon first contact from the flight crew.

4.3.3 Wind and Turbulence Event Performance

Although the expectation going into the test was that high winds would generate some mismanagement of aircraft speed and, therefore, some overshoot, flight crews managed the gust well. In most cases the gust condition temporarily increased cross-track error slightly. It also increased the go-around rate in some aircraft. The high rate of go-arounds experienced in the VNAV1 aircraft, in conjunction with feedback from pilots involved in the test design, indicated that due to aircraft or simulator characteristics, the wind event was much more significant in the VNAV1 case, see table 4-3.

Table 4-3: Go-Arounds on Wind and Turbulence Approaches

	Go-Around	Total	Percent of Go-Arounds
VNAV1	10	32	31.25
VNAV2	0	32	0.00
Non-VNAV	1	36	2.77

4.3.3.1 Wind and Turbulence Event Lateral Performance

Direct observation of the ground tracks in figure 4-21 demonstrated that the lateral error during the wind and turbulence event is not much worse than that experienced in the nominal runs. Although the VNAV1 experienced higher go-around rates, it had lateral errors less than non-VNAV and VNAV2.

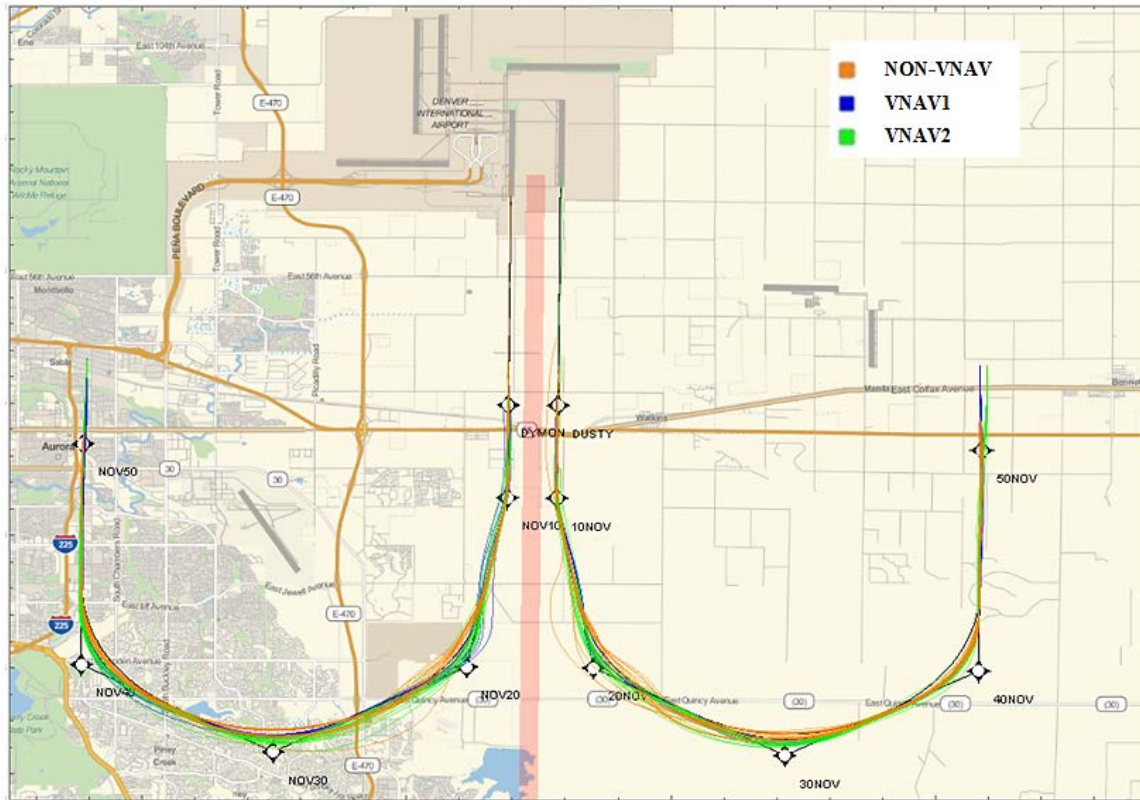


Figure 4-21: Wind and Turbulence Event Ground Tracks by Aircraft Type

Figure 4-22 directly compares the wind and turbulence total system error to the total system error during the nominal runs. While the variance of the tracks experiencing the wind event was larger, it did not significantly differ from the variance of the Gaussian distribution proposed to model normal operations. Therefore, we did not perform any additional risk analysis using the data from the wind event.

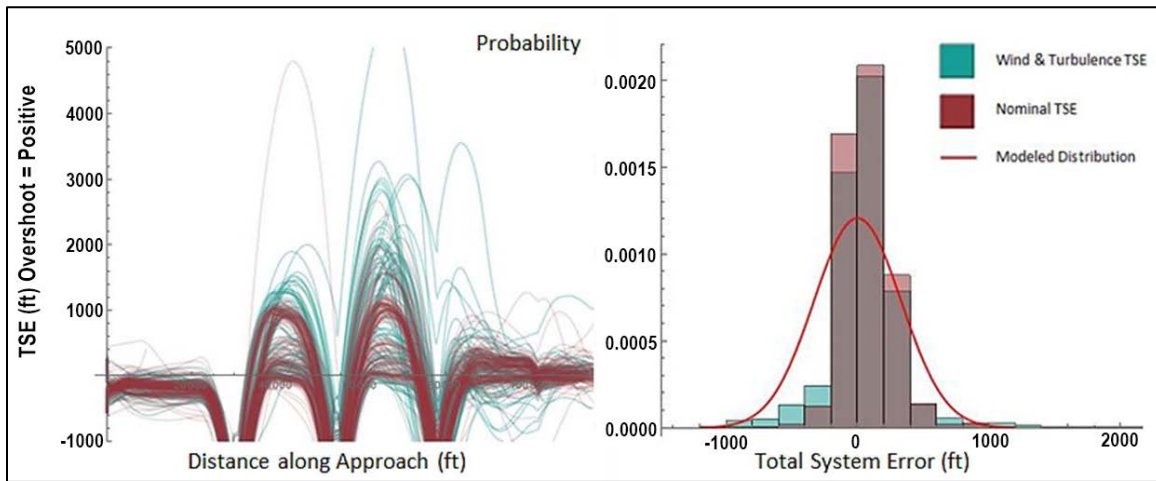


Figure 4-22: Total System Error Nominal versus Wind and Turbulence Event

4.3.3.2 Wind and Turbulence Event Human Factors Performance

Perceived subject pilot difficulty, comfort, and workload scores were substantially higher in the VNAV1 case than the same responses from the non-VNAV and VNAV2 cases, see figure 4-23. The VNAV1 case has the best objective performance data results, but the subjective responses indicate the worst experience. Operational experts theorized that this could be the result of differences in flight deck automation between VNAV1 and VNAV2. Another reason could be the differences in flight control feedback during wind or turbulence perturbations between VNAV1 and VNAV2. In both theories, the non-VNAV aircraft would be less likely to express discomfort and heightened workload because its normal operations are more often affected by wind and turbulence due to the aircraft weight. Further study would be required to validate either theory.

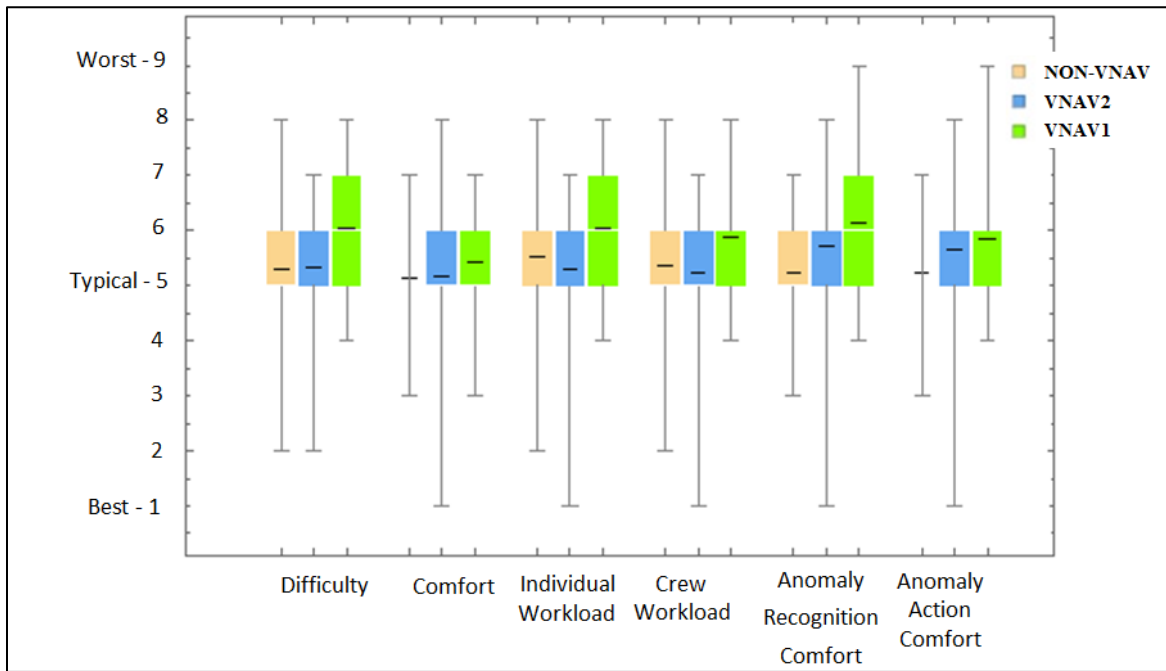


Figure 4-23: Questionnaire Responses for Wind Event

4.3.4 Controller Directed Breakout Performance

As discussed in section 4.1.2.5, an attention all users page was not provided in this test. During the test, observers noted a wide difference in methods for executing the breakout. The current FAA Simultaneous Close Parallel ILS/RNAV/GLS PRM approach breakout requires that the autopilot be turned off. [18] The autopilot was disconnected during 9 of 17 VNAV2 scenarios for a compliance rate of 53%. The VNAV1 had a compliance rate of 72% from 13 disconnections out of 18 scenarios. The increased rate may be due to the automatic autopilot disconnection in the TO/GA functionality. The non-VNAV case had a compliance rate of 78% from 14 disconnections out of 18 scenarios. This appeared to reflect an emphasis on annual breakout training reported by flight crews in the debrief. Given these compliance rates, it is clear that familiarity with the breakout varied among flight crews.

4.3.4.1 Breakout Initiation Performance

Pilot reaction times to controller directed breakout commands showed more variability than those observed in previous CSPO tests. Reaction times were calculated from the time that the controller pressed the push-to-talk button to issue the evasion command to the last time that the flight crew had a heading less than 3° offset from the final approach course. Although this method is different from those used in the most recent analysis on simultaneous independent operations by the CSPO program, this change was necessary because in these operations the evasion command sometimes occurred while the flight crew was executing the 10° heading change to turn to the final approach course. The methods used by the CSPO program involved identifying the first elevator, aileron, throttle, or TO/GA input to judge response time, which would be obscured by the turn in the procedure. However, the method used here produced more conservative results.

Due to reduced data collection capabilities in the non-VNAV simulator, this data only

included the VNAV aircraft. We collected scenarios in IMC and MVMC weather conditions as described in section 4.1.1. We also asked each flight crew whether they visually acquired the other traffic. During some of our IMC runs, the crews visually acquired the other traffic, resulting in pre-emptive breakouts. To collect the data most representative of the response to the controller, not the other traffic, we only used the data where the flight crew did not make contact with the other traffic, regardless of IMC or MVMC. Unfortunately, many flight crews observed the other traffic before the breakout, even during IMC conditions. This resulted in a limited dataset. Figure 4-24 depicts the data collected on pilot reaction times to controller directed breakouts.

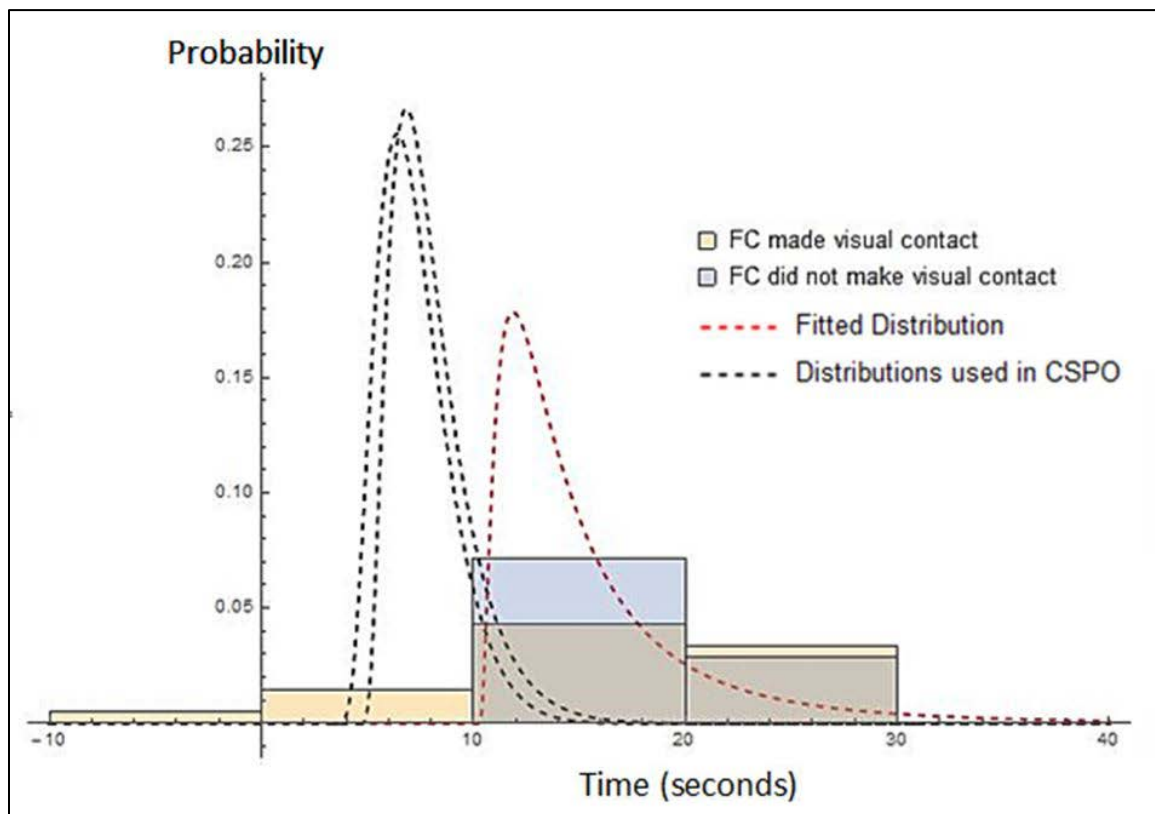


Figure 4-24: Pilot Reaction Time to Air Traffic Control Directed Breakout

4.3.4.2 Breakout Human Factors Analysis

Researchers received a variety of responses from VNAV crews when asked about their company breakout procedures. In general, pilots did not associate the tested procedure with an escape maneuver. They were not prepared to execute breakout procedures, and observers noted mixed urgency for disengaging the autopilot. During the debrief, some pilots stated that they did not believe this was a PRM type of procedure, so they did not equate an escape maneuver with the controller breakout command they received. Numerous crews expected the controller to provide a heading as part of the breakout command.

The use of a breakout maneuver is introduced to pilots as part of an operator-specific PRM certification process and in Part 121 recurrent training. VNAV pilots noted they rarely practice the breakout maneuver, while non-VNAV subject pilots noted they train for this maneuver every year. During the pre-briefing, flight crews were told that the

runways were 5,300 ft apart with a 2,000 ft NTZ, and they would have both a tower controller and final monitor. Six of the 9 non-VNAV crews and 5 of the 19 VNAV crews inquired about the EoR operations' similarity to PRM during the post flight debrief, but they were informed this was not a PRM operation. During the debrief, many pilots noted that an attention all users page would be appropriate if breakout maneuvers were part of the procedure. This demonstrated pilot association between PRM and breakouts.

For the pilot tests, we used the breakout phraseology as described in section 4.1.2.5. Interestingly, most crews did not recall any difference between the two phraseologies when asked during the crew debriefing. Of the few that did, they could not verify having heard "TRAFFIC ALERT". This was reflected in the measured reaction times as well. A Watson U² test indicated that the datasets were drawn from the same distribution with a p-value of 0.54. This indicated that breakout phraseology had a statistically insignificant impact on pilot reaction time. Note that test observers noted a few instances of incorrectly executed phraseologies by the non-subject controllers, which somewhat reduced our confidence in this result. The word "IMMEDIATELY" is a key word that controllers use to convey a sense of urgency during a breakout situation. Controller tone and voice inflection complement this sense of urgency. Pilot feedback indicated that the word "IMMEDIATELY", controller tone, and voice inflection were more effective at capturing pilot attention than the phrase "TRAFFIC ALERT".

4.3.5 Nominal to Off-Nominal Overview

For the sake of comparison, all wind events, flight guidance failures, go-arounds, and autopilot failures were combined into one group. All nominal approaches were compared against this group. Figure 4-25 shows a comparison of post-run questionnaire responses.

Pilots perceived the nominal approaches more favorably than off-nominal approaches. However, the difference between the means in each set is less than one unit on the Likert Scale. This suggests that, while perceived difficulty, workload, and comfort increase during off-nominal runs, this difference is not significant.

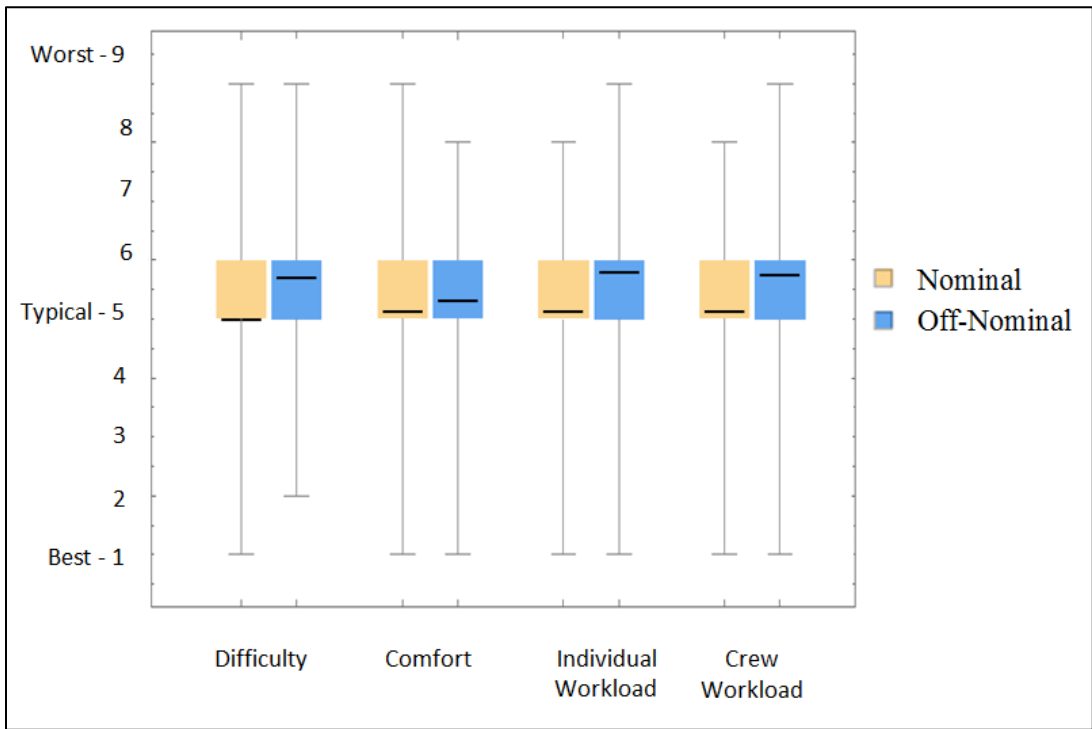


Figure 4-25: Nominal versus Off-Nominal Questionnaire Responses

5 Controller HITL Test

The test was conducted from February 18 through March 3, 2015. During the test we collected approximately 38 hours of simulated traffic monitored by certified professional controllers.

5.1 Test Design

The controller HITL test was designed to achieve the following objectives:

- Objective 1: Evaluate the time from the start of a deviation to the time a controller issues a breakout command; and
- Objective 2: Evaluate controller perception of comfort and workload while simulating an air traffic control environment that includes the EoR operations.

The following describes how we designed the test to achieve these objectives.

5.1.1 Test Environment

This test required a realistic simulation of the final monitor position at a generic TRACON facility with an airspace that included EoR operations. We used the FAA high fidelity ATC lab simulator for this test. This simulator was running a simulated airspace and radar display using the Simulation Model ATC Research and Training software. This software was configured to display a realistic airspace for the Denver TRACON environment.

The simulation was designed to allow the subject controllers to perform all of the actions typical to the final monitor position, including all communications to pilots and other controllers. This included non-subject controllers and non-subject pilots who helped simulate the airspace. The setup included a tower controller on the airport, who was regularly providing departure clearances and other activities suitable for the position. The final monitor controller was on the same frequency with override transmit and receive capabilities. On a separate frequency, a final controller at the TRACON cleared the aircraft for the approach procedure and transferred the aircraft to the tower frequency. In order to reduce pilot workload and minimize the potential for aircrew distraction, transfer of communications occurred on downwind after the aircraft passed the IAF and before the aircraft lost 3 NM or 1,000 ft vertical separation as currently required for simultaneous independent approaches. [17] From prior HITL tests for dependent EoR operations, we have learned that the transfer of communications from the final controller to the tower frequency can critically impact the safety of the operation. [4] Therefore, the transfer of communications with respect to the location of the aircraft on the approach procedure was carefully considered for this test.

This simulation also included the display and functionality of the FMA including a limited region where targets were displayed, called the active monitoring zone, and the NTZ, which provided alerts if violated. The video map also displayed ideal tracks for straight-in traffic as well as the TF legs for the EoR procedure. The final monitor positions were intended to monitor runways 35L and 35R at Denver International Airport.

Controller stations simulated an Airport Surveillance Radar-9 with a 4.8 second update rate, a Standard Terminal Automation Replacement System (STARS) FMA with a high resolution color monitor, visual and aural alerts, and a 3:1 aspect ratio. We selected a

3:1 aspect ratio to allow controllers to observe the entire downwind leg while maintaining an aspect ratio that maximized detection of aircraft deviating in the direction of the NTZ. Controller stations also displayed 10 second predicted track lines by default. These are solid lines that extend from the target in the direction of the velocity vector with a magnitude based on where the target is predicted to be in 10 seconds.

Simulated traffic was cleared to the EoR approach procedures and to the ILS extended final approach procedures. Because this test was not intended to address sequencing concerns, traffic from different approaches to the same runway was simulated to not cause sequencing difficulties. The test procedures used the same approaches and geometry as the pilot test, as described in section 4.1.1. The total system error experienced by the simulated aircraft on the EoR approach was randomly drawn from a normal distribution with a mean of zero and a standard deviation equal to 0.05447 NM. The nominal paths were based on typical turn radius calculations using a fleet mix of bank angles and varied speeds. We assumed that the total system error experienced by aircraft equipped to fly the proposed procedures would be equal to or better than this assumption. This assumption was demonstrated to be correct as discussed in section 4.2.1.2.

We requested certified professional controllers from NATCA. The controllers were from TRACON facilities that are equipped with STARS. NATCA provided a total of 21 controllers. Sixteen controllers came from facilities that run simultaneous independent operations and four controllers from facilities that run simultaneous dependent operations. We also used an instructor from the ATC Academy at the Mike Monroney Aeronautical Center.

A one hour briefing to all of the participating controllers was conducted at the beginning of each test day. The test consisted of six 45 minute shifts during which the controllers participated in a final monitor simulation. Two subject controllers were positioned in the ATC lab simulator per shift, and each pair of subject controllers worked the EoR approach traffic for three shifts. Air traffic control observers, knowledgeable in controller practices and procedures, were unobtrusively located behind the subject controllers to record behaviors and/or anomalies that were specific to this operation. Following each shift, a human factors specialist conducted a debriefing for the subject controllers.

Subject pilots and full flight simulators were not required for this controller HITL test. Instead, this test incorporated non-subject computer operators, or pseudo-pilots, who had been trained on appropriate phraseology for pilot and controller communications. The pseudo-pilots translated controller instructions into simulated aircraft behavior, and initiated appropriate communications to generate a realistic environment for the subject controllers.

5.1.2 Test Scenarios

Controller performance was observed utilizing two separate runway pairs with two different levels of traffic density. Low traffic density was simulated using the actual average arrival rate at Denver International Airport. High traffic density was simulated using the actual maximum arrival rate at Hartsfield-Jackson Atlanta International Airport. The traffic density was only varied when the shift changed. Appendix G shows the

controller test matrix used. Groups consisted of four controllers tested during each day. For example, group 1A was tested on Tuesday, and group 1B on Wednesday of that week. These are the only groups listed to indicate the random use of scenarios over the course of the three week test. Appendix G also lists the scenarios used sequentially from 1-15, and the associated traffic density, deviation side, and deviation type.

During each shift, each subject controller experienced two simulated aircraft that deviated non-normally. Each of these non-normal deviations was represented by one of the following types of events.

The first non-normal deviation introduced caused the simulated aircraft to experience a severe navigation system error with a track laterally translated toward the parallel approach, see figure 5-1.

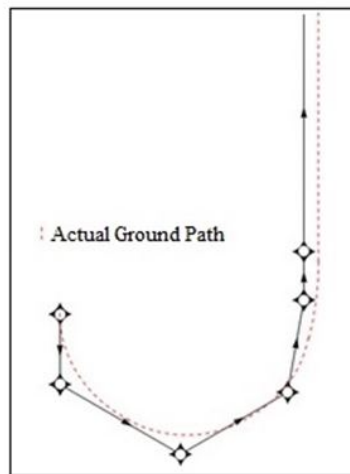


Figure 5-1: Scenario 1 – Navigation System Error

The second non-normal deviation caused the simulated aircraft to deviate from the approach course similarly to the deviations observed in the pilot HITL test, see figure 5-2. If the controller did not issue a return-to-course command, the simulated aircraft initiated a heading change to return to the approach course without controller intervention. This return-to-course correction was based on the results from the EoR pilot HITL test. If the controller issued a return-to-course command, the aircraft returned-to-course at a rate that reflected the rate observed in the pilot HITL test.

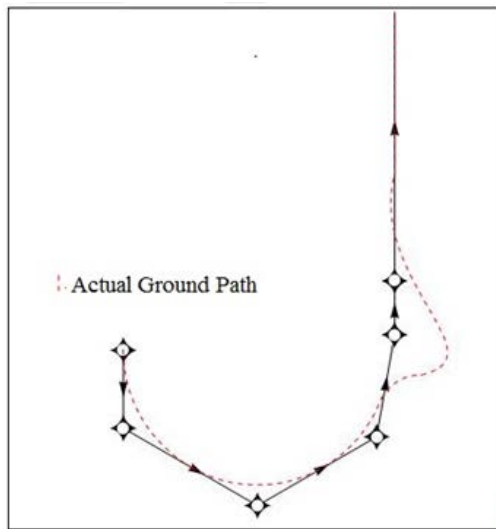


Figure 5-2: Scenario 2 – Course Deviation

To collect controller reactions to simulated aircraft that deviated from the approach course during go-around maneuvers, the non-subject pilot reported a landing gear malfunction as a reason to execute a go-around. Sample go-around deviation tracks from the pilot HITL test were used to simulate the deviation.

Some deviating simulated aircraft did not return to course (despite controller direction) until they achieved an NTZ violation. This was necessary to collect evasion reaction times from the controller monitoring the adjacent approach. Return-to-course corrections were based on the results from the EoR pilot HITL test.

The third non-normal deviation caused the flight crew to select a standard instrument approach procedure to another parallel runway at the airports see figure 5-3.

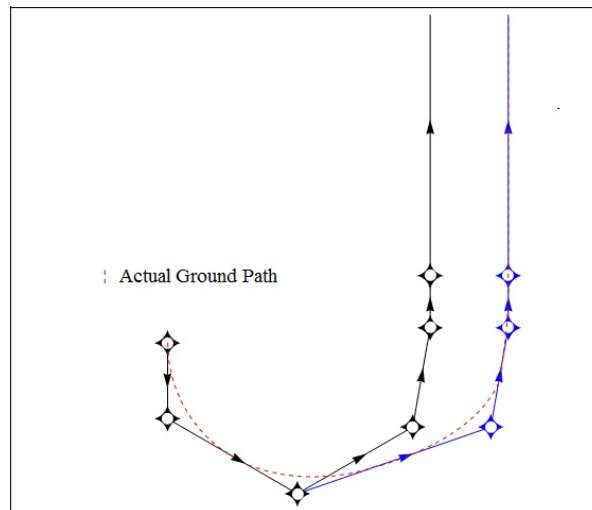


Figure 5-3: Scenario 3 – Wrong Runway Selection

These different types of deviations were based on various non-normal events. However, controllers did not know why the aircraft were deviating from the approach path. Any

other causes of aircraft path deviations or behaviors, such as database errors, would cause similar reactions to one of the three cases given above from the controllers' perspective.

5.1.3 Human Factors Data Collection

5.1.3.1 Post-Shift Questionnaires

Subjective performance measures included a post-shift questionnaire given at the end of each shift, see appendix H. A post-simulation debriefing questionnaire was given at the end of each day, see appendix I. Eight questions were included in the post-shift questionnaire to assess perceived sense of difficulty, comfort, and workload as well as controller sense of timeliness as it relates directly to their responses in given situations.

5.1.3.2 Direct Observations

Subjective data was collected in the ATC lab simulator utilizing one human factors observer and one controller observer per subject controller. The human factors specialist observed, interpreted, and captured the essential elements of individual controller and team interaction. The interactions were recorded to determine how they affected performance as well as potential comfort and workload changes.

All deviation scenarios were carefully scripted to modify controller activity. During periods in the shift when a flight crew had to perform non-normal functions, the observers monitored both primary and secondary task completion. During periods of heightened activity, workload, reaction times, latency of task completion, or task shedding may have changed. Primary task measures included all tasks associated with:

- Reacting to course deviations with arriving aircraft; and
- Coordination between paired controllers during non-normal situations.

Secondary task measures included all the other tasks that were part of a controller's normal routine.

5.1.3.3 Debriefing

The human factors observers administered a questionnaire and debriefing at the end of each day with the intent of soliciting each controller's and controller pair's overall perception of performance, see appendix I. The debriefing covered data collection execution, review of post-shift questionnaire responses and any issues that arose during the simulation. Open feedback and discussion from the controllers and between all members of the test team was encouraged.

Although there was some variation, major themes of questioning were consistent across all controllers. Besides some generic information regarding employment, experience, and training, we asked about the realism of the test, their comfort with the operations, changes in workload, comfort while controlling path deviations, and each controller's comfort with the breakout.

5.2 Human Factors Analysis

This operation and its geometry caused a shift in controller responsibilities. First, controllers indicated that the coincident altitude takes away one dimension of conflict resolution. In existing simultaneous independent operations, controllers are able to resolve proximity conflicts through vectoring, altitude separation, or a combination of both. For the EoR operations, aircraft did not require 1,000 ft vertical separation because

they were considered established on the approach before the 1st turn on. Subjective response data and post-evaluation debriefing comments indicated that this reduces the controller's capacity to resolve traffic conflicts. Second, many participants in this test were not comfortable with the simulated deviations. Their scan vigilance increased as their normal scan patterns accommodated a focus on the 3rd turn, the 50° turn. This caused some negative habit transfer. A corresponding increase in workload and decrease in comfort was observed, see figure 5-4. Based on controller debriefing remarks, many controllers were not comfortable in situations where they would have to be reactive. The focus on the 50° turn allowed them to be more proactive at that point in the approach.

Before they experienced any deviations, controller vigilance appeared to be at typical levels. If a deviation happened at the 50° turn and the controller was not focused on that turn when it happened, there was a significant chance that they would not be able to process the visual information, formulate a strategy, and successfully intervene quickly enough to keep the aircraft separated, see section 6.2.1. To account for this, controllers focused more on the portion of the approach around the 50° turn. While the impact on performance was not fully investigated, this is somewhat of a negative habit transfer that controllers felt affected their behavior. As this cognitive tunneling happens at the critical 50° turn, controller focus on the rest of the approach might be dismissed, leaving a gap in vigilance over those areas. The controllers' typical reference point for questions about the safety of this geometry or procedure originated from a standard separation viewpoint. This idea was clarified by a certified controller with the following comment: "When a controller feels there is not enough time to correct a potential conflict, it often means that standard separation (3 NM or 1,000 ft vertical) cannot be met" once an aircraft deviates from the approach path. This situation is exacerbated by proximity to the final approach course.

5.2.1 Aspect Ratio

Scopes for radar controllers who monitor simultaneous traffic can be set to scale the distance along the final approach course to one fourth of the distance perpendicular to the final approach course. This can assist in the detection of lateral deviations on the extended final approach course and it has regularly been required in prior tests of simultaneous independent operations. When applied to the EoR operations, however, the modified aspect ratio dampened the displayed cross-track error at the apex of the turn. A slightly reduced 3:1 aspect ratio was the default setting in the controller test, see section 5.1.1.

This 3:1 ratio was not familiar to all of the subject controllers and many of them expressed difficulty understanding the approach procedure with this setting. Many commented that it was strange to look at anything other than a 1:1 ratio, which was what many subject controllers used at their facilities. Test observers demonstrated the fundamentals of the aspect ratio and illustrated a comparison of the two ratios on the scope at the beginning of their first shift. Two controllers had FMA experience that allowed an easier transition to the 3:1 aspect ratio, though they both stated that they typically used 4:1 aspect ratio on straight-in approaches. Furthermore, they had never merged straight-in traffic with traffic from the downwind in anything other than a 1:1 ratio, because this merging was typically performed by the controller in the final position. They also noted that they were not allowed to vector aircraft using the 3:1 aspect ratio at

their current facility because they were using Multi Lat (PRM-A), and current facility policy required them to use a 4:1 aspect ratio. Several controllers recommended having a second scope with a 1:1 aspect ratio for monitoring EoR operations (i.e. a vector scope, as currently used in at least one TRACON with final monitor positions).

Although the 3:1 aspect ratio distorts spacing, closure rates, and angles, controllers became more comfortable as the testing progressed. Controllers stated that they used mental tie-points to determine spacing between EoR and straight-in traffic. Tie-points were also used to adjust for the distortion of the 3:1 aspect ratio. Although tie-points helped reduce the number of speed restrictions for most controllers, observers noted that some controllers continued to over-control speeds on final.

5.2.2 Phraseology

During the initial pre-brief, the subject controllers reviewed standard terminology as described in section 4.1.2.5. During the test, the phrase “TRAFFIC ALERT” was rarely used by the subject controllers although it is required in the standard phraseology. Those controllers who were experienced with simultaneous independent procedures believed the phrase was essential. They reported using this phraseology during breakouts. However, observation and audio data indicated that they did not in many cases. Instead, controllers generally used call sign first, followed by heading and/or altitude. To convey urgency to the command, controllers used the word “IMMEDIATELY”. A change of voice inflection also conveyed a heightened sense of urgency.

5.2.3 Controller Scan Pattern

The consensus among the subject controllers was that the 3rd turn (the 50° turn) would most likely be where “bad things” would happen. This resulted in the perception that this would be the spot on the approach that yielded a more limited margin of error and less reaction time to intervene, should a problem occur. Common verbal controller feedback indicated that 70-90% of controller time was spent scanning the 50° heading change.

5.2.4 Controller Comfort

Many subject controllers indicated that they were less comfortable while monitoring EoR operations than straight-in simultaneous arrivals. This is reflected in the post-shift questionnaire responses reported in figure 5-4. A few controllers commented that they were comfortable with the geometry until experiencing the first deviation. At that point, vigilance went up and scan patterns changed. Explanations centered on the feeling that they could not intercede in a timely enough manner if something critical happened at or near the 50° heading change. They strongly felt that the coincident altitude takes away a method of conflict resolution. Two typical comments were “the only tool in the toolbox is to vector” and “no plan B available to mitigate conflicts”.

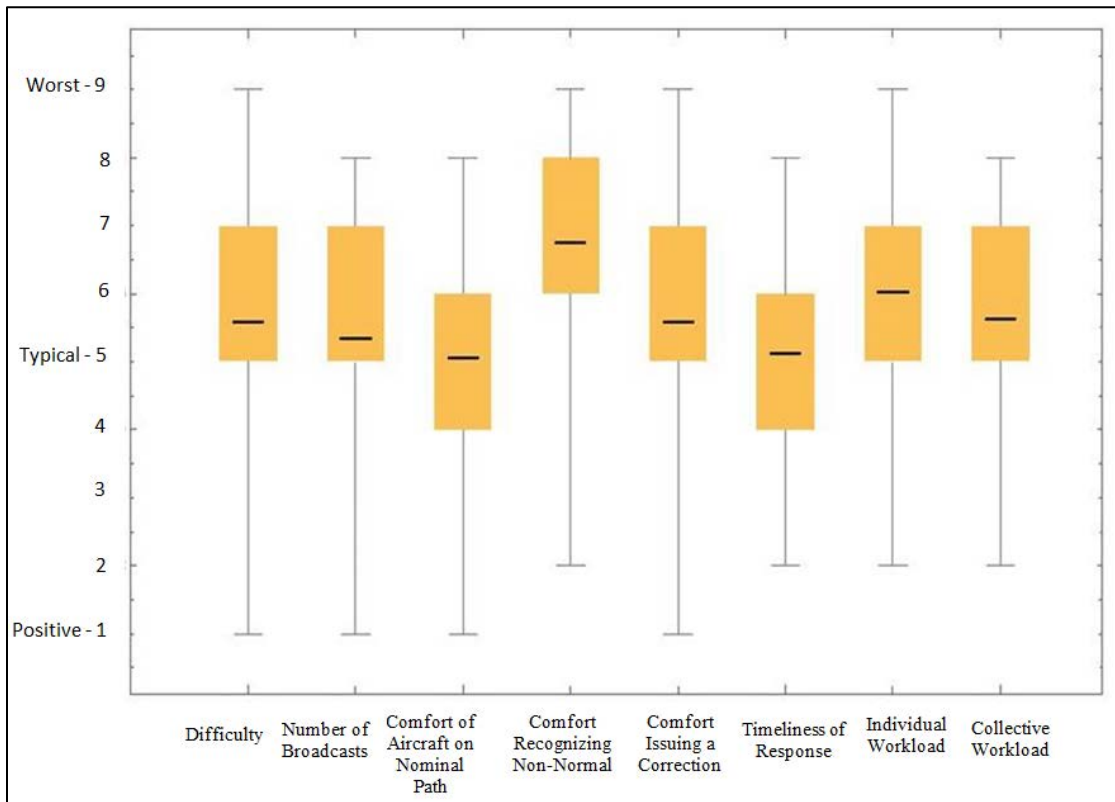


Figure 5-4: Post-Run Questionnaire Data

Most controllers commented that their comfort level would increase if the procedure included a stagger or vertical separation at the 50° heading change. A small number of subject controllers who generally came from busier facilities reported higher comfort levels. This may be due to their experience running similar simultaneous operations. Note that the subject controllers did not experience training typical for new operations before the HITL test.

Controllers indicated that they needed to maintain higher vigilance when the aircraft were head-to-head during the turn to the final approach course than if the turns were staggered. In head-to-head geometries with increased vigilance, controllers speculated that there might be more nuisance breakouts in response to any track deviations.

With the exception of the head-to-head, coincident altitude intercept, controllers appeared comfortable with the EoR concept. Three of the controllers had experience using curved RNP approaches and they were confident they could keep aircraft on final. Although this data suggests that eliminating the head-to-head, coincident altitude may increase controller comfort, this would not be considered a safety requirement.

5.3 Controller Response Time Analysis

While additional data could be extracted from this test, only one relatively simple metric was needed for the collision risk estimates that will be addressed in section 6. This metric was the amount of time that it takes for a controller to issue breakout instructions after a deviation occurs. In recent studies, we measured this reaction time from the time of the FMA caution alert (yellow) to the time when the controller has pressed the push-to-talk button. In every test, this measurement has resulted in instances where the controller corrects the deviation before the caution alert is activated. The controller reaction times with a negative value have conservatively been discarded from the data used to model the controller reaction time.

For this study, however, the nominal approach path has additional separation from the NTZ during the turn. If we were to apply the method used above, much of the data would be discarded. Therefore, we measured this controller reaction time from the start of the deviation, as determined by an algorithm in post-processing, to the time that controllers pressed push-to-talk to issue the correction. The algorithm used a combination of distance from the extended runway centerline and distances from specific waypoints to make this estimation. For more details on the algorithm, see appendix J. Using the data shown in figure 5-5, we modeled controller reaction times.

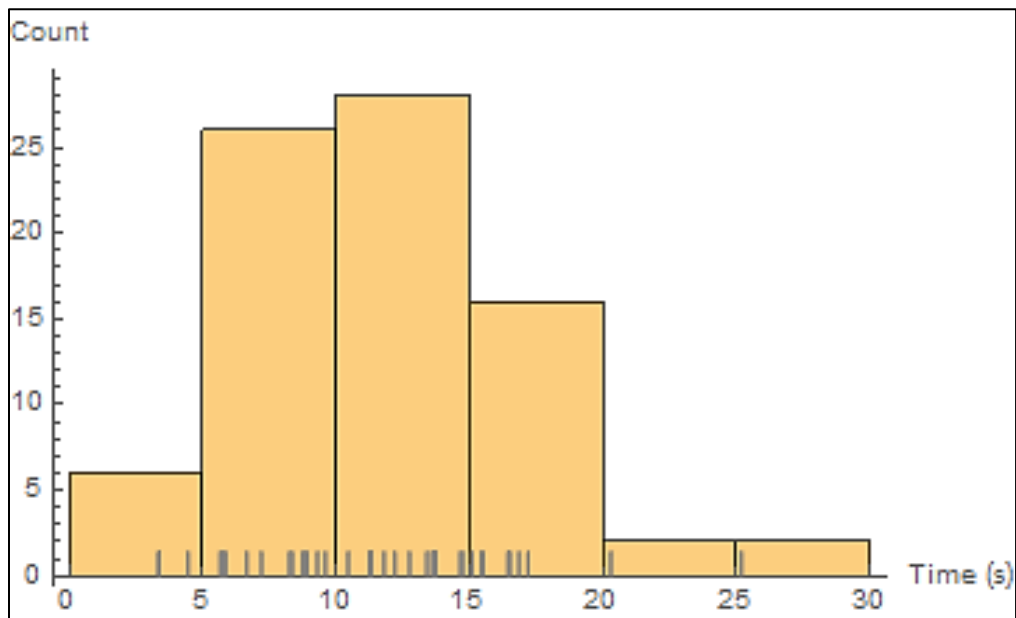


Figure 5-5: Histogram of Controller Response Times from Deviation Start

These controller responses were longer than those observed in prior controller HITL tests involving simultaneous independent closely spaced parallel operations. This may be due to the novelty of the EoR concept and the limited amount of familiarization prior to measurement of reaction time for this study.

6 Modeling and Simulation

This section presents the models and simulations used to estimate specific metrics for the EoR operations under this study. We estimated collision risk and the rate of several implementation barriers including nuisance FMA caution alerts and nuisance TCAS RAs. In section 4 and section 5, we described controlled experimental tests of the pilot-aircraft interface and the radar display-controller-pilot interface. During these tests, we collected quantitative measurements of human-machine performance. This section converts those results to actionable metrics used to assess collision risk, nuisance alerts, path length, and downwind path distance. Assessments of aircraft-to-aircraft collision risk will be evaluated to determine whether they meet the Safety Management System (SMS) target level of safety for catastrophic events, 10^{-9} . [19]

6.1 Normal Collision Risk

As stated in section 2, the primary objective of this study was to assess the aircraft-to-aircraft collision risk of EoR operations. To accomplish this, we estimated the rate at which aircraft-to-aircraft collisions occur during these operations. For ease of computation, we modeled the location of each aircraft's center of mass and considered a collision to be two aircraft that were separated by less than 265 ft laterally and 80 ft vertically. [20]

We split the collision risk into two cases for our analysis: normal and non-normal operations. Normal operations occurred when all aircraft and aircrews were operating as intended. Non-normal operations were the complement of the normal condition, and occurred when at least one pilot or aircraft was not operating as intended. With this partition, we can consider the overall collision risk to be:

$$P(\text{Collision}) = P(\text{Collision}|\text{Normal Operations}) \times P(\text{Normal Operations}) \\ + P(\text{Collision}|\text{Non-Normal Operations}) \times P(\text{Non-Normal Operations}) \quad (1)$$

Normal collision risk is usually calculated using statistical models of aircraft performance relative to the defined approach path. Generally, three types of performance are considered:

- Cross-track error: Error normal to the defined approach path;
- Vertical error: The difference between the altitude for any lateral position on the defined approach path and the intended altitude for that position; and
- Along-track performance: The aircraft position along the designed approach path.

For this analysis these errors are assumed to be independent.

Data was collected during the pilot tests that characterized aircraft performance while flying EoR procedures. The total system error distribution is a normal distribution centered on the designed approach path with a standard deviation of 0.05447 NM, see section 4.2.1.2. The test data exhibited some overshoot during the 1st, 2nd, and 3rd turns before the final turn onto the final approach course. We assume that the approach procedures will be designed to prevent these types of overshoots while turning onto the extended runway centerline. Furthermore, we observed from the pilot tests that all of the aircraft, including the non-VNAV aircraft, can be modeled with a constant angle descent. For more details regarding the data observed in the pilot tests, see section 4.

Although complex models of normal aircraft collision risk exist, we present a simplified model of normal collision risk to help illustrate how the collision risk is affected by each component of these models. One component of risk is the probability of lateral overlap. This is the probability that the aircraft lateral paths intersect or have a minimum distance of at least the radius of the collision volume. To illustrate this, assume that the cross-track error is constant, and there are two paths separated by some distance, say Δ . The random variable of the lateral separation of the two paths is the difference between the random variables of the cross-track error of one path and the cross-track error of the other path defined relative to the first path. The probability of horizontal overlap is equal to the probability that this random variable is between -265 ft and 265 ft. Mathematically, that is expressed:

$$P(\text{Horizontal Overlap}) = P(-265 \text{ ft} < Z < 265 \text{ ft}) \text{ where} \\ Z = X - Y \text{ and } X \sim N(\Delta, \sigma_X) \text{ and } Y \sim N(0, \sigma_Y) \text{ so } Z \sim N\left(\Delta, \sqrt{\sigma_X^2 + \sigma_Y^2}\right) \quad (2)$$

where Z is the random variable of the lateral separation of the two paths, X and Y are the random variables of the cross-track error, σ_X is the standard deviation of the cross-track error on one path and σ_Y is the standard deviation of the cross-track error on the other path. If we fix $\Delta = 2,600$ ft, $\sigma_X = 330$ ft, and $\sigma_Y = 330$ ft, we can visualize the new Gaussian distribution and the region of probability of horizontal overlap, see figure 6-1.

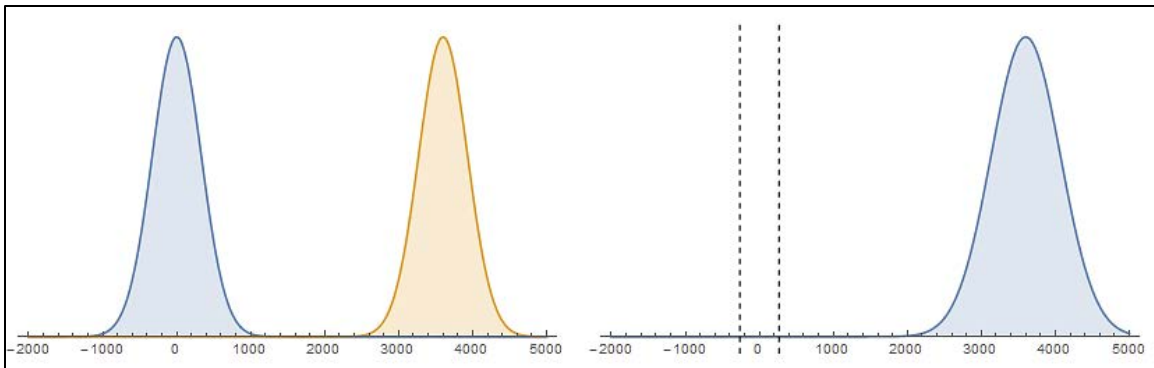


Figure 6-1: Lateral Separation Distribution and Region of Overlap

This assumes that the cross-track error is constant throughout the approach. Experts recognize that some portion of the aircraft error is time-dependent. Mathematical models use different methods to account for time-dependent cross-track error, but accounting for it generally increases the collision risk. However, the EoR approaches build on prior safety cases that have already demonstrated that the collision risk is acceptable during straight-in approach procedures. Therefore, the most significant normal collision risk occurs when the aircraft is turning onto the final approach course, but has not yet assumed the cross-track error characteristics of the straight-in approach. Due to the short period of interest, we assumed that we did not need to account for the effects of time-dependent error in the simplified model. Due to the turns, we considered $P(\text{Horizontal Overlap}) = P(Z < 265 \text{ ft})$ because the turning paths intersect if the errors are on the opposite sides.

Although the aircraft paths horizontally overlap, this does not mean that they are necessarily within ± 80 ft vertically. Using the same technique used in the lateral case, we

considered the difference between the vertical error random variables to determine the probability of vertical overlap.

$$P(\text{Vertical Overlap}) = P(-80 \text{ ft} < Z_V < 80 \text{ ft}) \text{ where}$$

$$Z_V = X_V - Y_V \text{ and } X \sim N(\Delta_V, \sigma_{X_V}) \text{ and } Y \sim N(0, \sigma_{Y_V}) \text{ so } Z \sim N(\Delta_V, \sqrt{\sigma_{X_V}^2 + \sigma_{Y_V}^2}) \quad (3)$$

where Z_V is the random variable of the vertical separation of the two paths, X_V and Y_V are the random variables of the vertical error, σ_{X_V} is the standard deviation of the vertical error on one path and σ_{Y_V} is the standard deviation of the vertical error on the other path. If we fix $\Delta_V = 0$, $\sigma_{X_V} = 55$ ft, and $\sigma_{Y_V} = 55$ ft, we can visualize the new Gaussian distribution and the region of probability of horizontal overlap as the blue distribution in figure 6-2. Furthermore, we can visualize how larger vertical errors would decrease the probability of overlap by considering the distribution with $\sigma_{X_V} = 192$ ft and $\sigma_{Y_V} = 192$ ft as seen in yellow in figure 6-2.

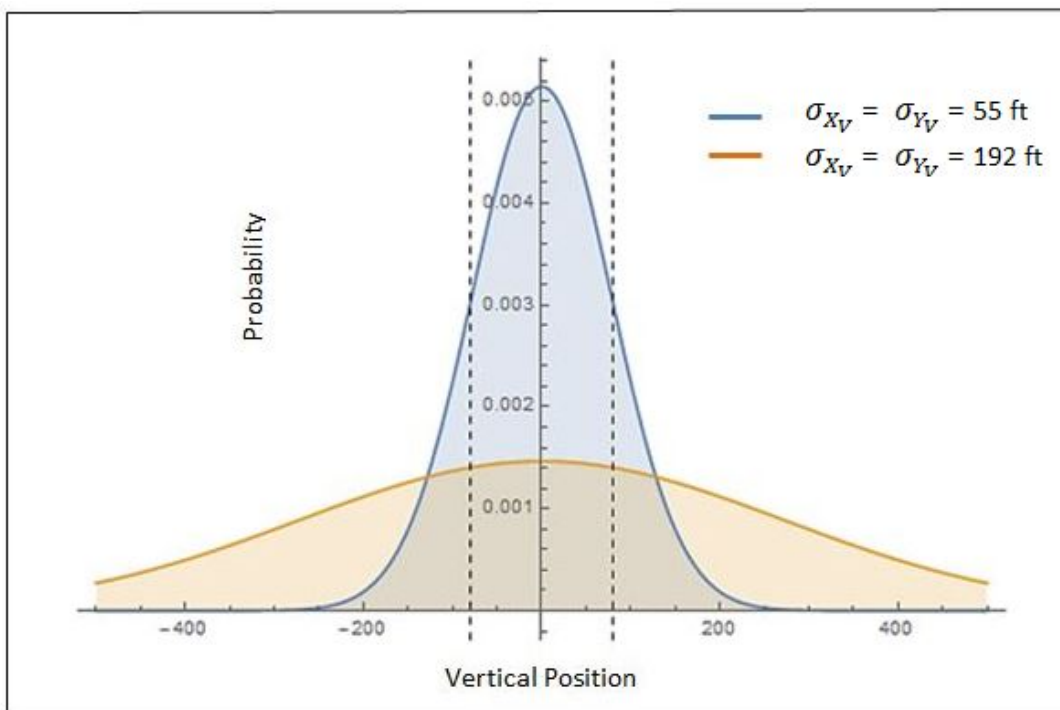


Figure 6-2: Distribution of Vertical Separation with Region of Overlap

For similar reasons as the lateral case, we did not account for time-dependent vertical error in this model. If we also accounted for the probability that the aircraft were positioned along the approach in a way that could result in a collision, we could reduce the probability further. However, this component of the collision risk can become complex as speed differences and time-dependent errors become more significant. Therefore, we assumed that the aircraft were always in the worst possible along-track configuration. Since we have assumed that vertical and lateral errors are independent, we can multiply the probability of horizontal overlap with the probability of vertical overlap to attain an estimate of collision risk, see tables 6-1 and 6-2.

Table 6-1: Simplified Model Collision Risks $\sigma_{Xv} = \sigma_{Yv} = 54.84$, as observed in VNAV equipped aircraft

	$\Delta_v = 0$ ft	$\Delta_v = 100$ ft	$\Delta_v = 200$ ft	$\Delta_v = 300$ ft	$\Delta_v = 400$ ft	$\Delta_v = 500$ ft
$\Delta = 2,000$ ft	7.3 E -5	4.1 E -5	6.4 E -6	2.4 E -7	1.9 E -9	3.2 E -12
$\Delta = 2,250$ ft	7.8 E -6	4.3 E -6	6.7 E -7	2.5 E -8	2.1 E -10	3.4 E -13
$\Delta = 2,500$ ft	6.3 E -7	3.4 E -7	5.4 E -8	2.0 E -9	1.7 E -11	2.8 E -14
$\Delta = 2,750$ ft	3.8 E -8	2.1 E -8	3.3 E -9	1.3 E -10	1.0 E -12	1.7 E -15
$\Delta = 3,000$ ft	1.8 E -9	9.9 E -10	1.6 E -10	5.8 E -12	4.7 E -14	7.8 E -17
$\Delta = 3,250$ ft	6.3 E -11	3.5 E -11	5.5 E -12	2.0 E -13	1.7 E -15	2.8 E -18
$\Delta = 3,500$ ft	1.7 E -12	9.3 E -13	1.5 E -13	5.4 E -15	4.4 E -17	7.3 E -20

Table 6-2: Simplified Model Collision Risks $\sigma_{Xv} = \sigma_{Yv} = 192.2$, as observed in aircraft not equipped with VNAV

	$\Delta_v = 0$ ft	$\Delta_v = 100$ ft	$\Delta_v = 200$ ft	$\Delta_v = 300$ ft	$\Delta_v = 400$ ft	$\Delta_v = 500$ ft
$\Delta = 2,000$ ft	2.4 E -5	2.3 E -5	1.9 E -5	1.3 E -5	8.5 E -6	4.7 E -6
$\Delta = 2,250$ ft	2.6 E -6	2.4 E -6	2.0 E -6	1.4 E -6	9.0 E -7	5.0 E -7
$\Delta = 2,500$ ft	2.1 E -7	1.9 E -7	1.6 E -7	1.1 E -7	7.2 E -8	4.0 E -8
$\Delta = 2,750$ ft	1.3 E -8	1.2 E -8	9.8 E -9	7.0 E -9	4.4 E -9	2.5 E -9
$\Delta = 3,000$ ft	5.9 E -10	5.5 E -10	4.5 E -10	3.3 E -10	2.1 E -10	1.1 E -10
$\Delta = 3,250$ ft	2.1 E -11	1.9 E -11	1.6 E -11	1.1 E -11	7.3 E -12	4.0 E -12
$\Delta = 3,500$ ft	5.5 E -13	5.2 E -13	4.2 E -13	3.0 E -13	1.9 E -13	1.1 E -13

We also have modified existing complex statistical models of collision risk on parallel and intersecting paths to assess the risk on EoR approaches. This statistical model uses fixed radius turns with 2.5 NM radii, 5 NM final approach lengths, and no nominal vertical separation. The results can be found in table 6-3. For further information on the definition of this model, see appendix L.

Table 6-3: Hsu-Anderson-Reich-Greenhaw Model of Normal Collision Risk Results

Runway Spacing (ft), Δ	Speed Difference = 0 knots	Speed Difference = 20 knots
2,000	1.09E-07	1.03E-06
2,200	1.22E-08	1.16E-07
2,400	1.11E-09	1.06E-08
2,600	8.24E-11	7.82E-10
2,800	4.96E-12	4.71E-11
3,000	2.42E-13	2.30E-12
3,200	9.62E-15	9.13E-14
3,400	3.1E-16	2.94E-15
3,600	8.12E-18	7.70E-17
3,800	1.73E-19	1.64E-18
4,000	2.98E-21	2.83E-20

These models indicate that runways separated by 3,600 ft or more have negligible normal collision risk when all aircraft are operating as intended.

6.2 Non-Normal Collision Risk

As stated above, non-normal operations are the complement of the normal condition and occur when at least one aircraft is not performing as intended. At some point during a

non-normal operation, one aircraft's lateral or vertical errors are no longer adequately characterized by normal performance models. Events that could cause non-normal errors include pilot errors, navigation system failures, aircraft failures, or extreme weather conditions. For a non-normal flight to pose a significant collision risk, it must include a significant deviation from the lateral path. FAA policies indicate that significant lateral path deviations are a major failure condition, and major risks are required to occur with a frequency of less than 1 in 100,000 operations, or 1×10^{-5} . [21, 22] Previous studies of the EoR concept have expressed concerns that a fault in the GPS system could cause this type of lateral deviation. [23, 24] On investigation, we determined that this failure type does not pose a significant collision risk.

Non-normal collision risk has previously assumed that only a radar controller would recognize an aircraft deviation from its intended path due to a non-normal error. However, subject matter experts have observed that pilots may also recognize a deviation from the intended path. These experts theorize that this may be an effective mitigation of collision risk in the non-normal case. In order to test pilot behavior during non-normal flight, we constructed scenarios that provided a representative sampling of events that would be expected to cause a non-normal path deviation. While these events may not have been the most severe events, our pretest coordination efforts allowed us to conclude that they consistently generated lateral path deviations without immediately requiring emergency procedures from the pilots. Based on industry collaboration, we believe that the flight guidance failures, controller-directed go-around, and wind events tested are representative of pilot behavior during non-normal operations. For more details on the testing, see section 4.

6.2.1 Dual Non-Normal Collision Risk Model Methodology

Pilot behavior during the tests varied drastically from flight crew to flight crew. Therefore, modeling pilot behavior proved somewhat difficult. Most failures that resulted in a major deviation had the following characteristics: (1) at some point following the failure, the flight crew failed to input the bank required to remain established on the procedure, and (2) following this, the flight crew mitigated the non-normal error by laterally returning to the approach path. In some instances, the pilots had a shallow bank angle prior to correcting back to course, but many flight crews appeared to momentarily fly wings level or nearly wings level prior to correcting back to the course. To simplify the model of non-normal collision risk, we made the assumption that when the aircraft enters non-normal flight, which can be anywhere along the designed approach path, the aircraft flies straight for some distance then assumes a constant bank to correct to the designed approach path. However, if the deviating aircraft crosses the other approach course and begins correcting, we do not believe that it will cross the other flight path a second time without first establishing altitude separation. Therefore, we only considered the deviation path as contributing to collision risk until the aircraft is parallel to the final approach.

To allow for wide application of these results, we attempted to construct this model to make as few assumptions about the approach procedure design as possible. To achieve this, we limited our analysis to cases where the deviation occurs adjacent to a straight-in approach procedure. This construction represents the most conservative case during non-normal conditions, assuming that the straight-in aircraft has the same error

If we consider the random variable \mathbf{S} to be based on a random variable of reaction time modeled by a Johnson unbounded distribution, we can consider the distribution of \mathbf{S} to be equal to the same distribution as the distribution used for the time, but multiplying the scale and location parameters by a groundspeed value. Thus we can consider the probability of lateral overlap to be equal to the probability that \mathbf{S} is greater than λ .

$$P(\text{Horizontal Overlap}) = \int_{\lambda}^{\infty} f_S(s) ds = 1 - F_S(\lambda)$$

$$\text{where } S \sim \text{Johnson } SU (\gamma_S = \gamma_t, \delta_S = \delta_t, \mu_S = gs \cdot \mu_t, \sigma_S = gs \cdot \sigma_t) \quad (6)$$

where γ_s , δ_s , μ_s , and σ_s are the Johnson parameters to model random variable \mathbf{S} and γ_t , δ_t , μ_t , and σ_t are the Johnson parameters that model the random variable for time of pilot correction of deviation. Furthermore, gs is the average groundspeed during the period of level flight.

As in the normal collision risk calculation, the probability of vertical overlap assumes that there is some mean vertical separation between aircraft at the time of the horizontal overlap and some normal vertical error for both aircraft. For simplicity, we represent the vertical errors as Gaussian distributions.

$$P(\text{Vertical Overlap}) = \int_{-80+\Delta_V}^{80+\Delta_V} f_Z(z) dz = F_Z(\Delta_V + 80) - F_Z(\Delta_V - 80)$$

$$\text{where } Z \sim \text{Gaussian}(\mu_Z = 0, \sigma_Z = \sqrt{\sigma_{X_V}^2 + \sigma_{Y_V}^2}) \quad (7)$$

where μ_Z and σ_Z are the mean and standard deviation of the Gaussian distribution of the random variable of difference in vertical position, \mathbf{Z} , and σ_{X_V} and σ_{Y_V} are the standard deviations of the random variable for the vertical errors for each aircraft. Furthermore, Δ_V is the vertical separation of the paths during the horizontal overlap. In this case, it is more appropriate to characterize this probability as the probability of vertical overlap given horizontal overlap. Therefore, we can assume that changes in vertical error are negligible in the brief period of lateral overlap.

To use these definitions to calculate a collision risk, we need to consider a few additional probabilities. First, we must consider the probability that an aircraft enters non-normal flight. As described above, this value is 1/100,000 or 10^{-5} per operation.

Additionally, EoR approach procedures do not exhibit new behavior for most of the operation. The time on the final segment of the approach is considered safe, based on prior studies of closely spaced parallel operations. Also, the area prior to the apex of the turn will have radar separation and the track and distance of the aircraft from the other approach contribute negligible collision risk. Therefore, we can consider the probability that a non-normal condition occurs during the portion of the procedure when the aircraft is not aligned on the final approach course and has a track that could result in an intersection with the parallel approach. This will vary between procedure designs, but dividing the path length of the area of interest by the total path length of a procedure with

a 5 NM final and a 2.5 NM radius turn of 180° results in a likelihood of approximately 30%.

We can also consider the probability that, even if the paths cross laterally and vertically, there might not be an aircraft positioned in the necessary along-track position. We can approximate this probability using the diameter collision volume by the along-track separation standard. That is, 530' (265'×2) divided by 3 NM. This estimate assumes that the position of the aircraft on the approach is uniformly distributed along the approach path and that the aircraft are travelling at approximately the same speed. Because the relative along-track spacing is independent of the location of the deviation and whether the non-normal event occurs, the resultant probability of 0.03 can then be multiplied by the other probabilities. Multiplying 10^{-5} , 0.3, and 0.03 yields 9×10^{-8} . Therefore, overall collision risk, without taking into account the vertical behavior during deviations, can be represented by:

$$P(\text{Collision}) = (9 \times 10^{-8}) \times P(\text{Horizontal Overlap}) \times P(\text{Vertical Overlap}) \quad (8)$$

This function can also be derived using mathematical models typically used for oceanic and enroute separation, similar to those used to calculate the normal collision risk in table 6-3. This derivation relies on the formula for lateral risk in the Reich model and it may augment understanding of this discussion, see appendix L. We now have a function for collision risk parameterized by the following variables:

- Johnson unbounded distribution for the amount of time spent in level flight before correction;
- The standard deviation of the vertical error of each approach path;
- The distance from the other approach laterally when the deviation starts;
- The angle that the deviation travels during the level segment relative to the other approach path;
- The radius of the correction;
- The average groundspeed of the aircraft during the level flight segment; and
- The mean vertical separation at the time of horizontal overlap.

Unfortunately, a function of so many parameters is difficult to visualize. For the sake of understanding the function in general, we selected certain variables that we believe represent a good baseline case for this portion of the analysis. First, we fixed the groundspeed to 260 knots, which is approximately 210 knots indicated airspeed at the altitude tested with average winds. Next, based on this value, we selected the correction turn radius based on a 25° bank at the selected groundspeed. We then used two baseline vertical error standard deviations: 55 ft for aircraft equipped with approved VNAV and 192 ft for aircraft without approved VNAV, based on the standard deviation of the vertical errors observed in our pilot test. Finally, for these illustrations, we used the correction time distribution fit that has not been filtered to any subset of reaction times. This provides us with a collision risk function of angle, distance, and mean vertical separation. In figure 6-4, graphs (a), (b), (c), and (d) illustrate the collision risk in four major cases.

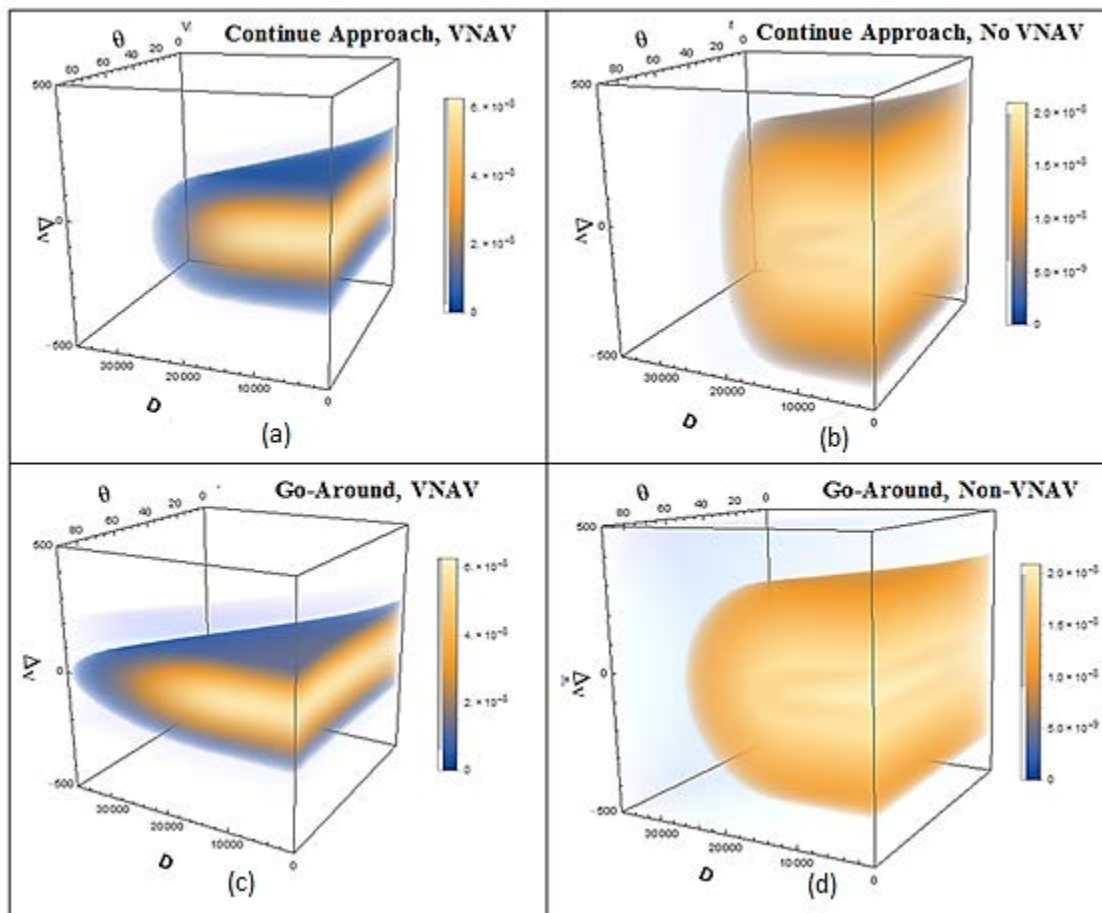


Figure 6-4: Collision Risk

Furthermore, if we set the mean vertical separation condition to the worst possible condition, zero vertical separation at the time of horizontal overlap, we can directly solve for the minimum distance required for each turn angle, which directly translates to an acceptable procedure design. However, without any account for vertical separation or other mitigations, the procedure design requirements are prohibitive. Figure 6-5 illustrates how a 9,000 ft runway spacing with a 10 NM fixed radius turn to final would seem to nearly meet the requirements given a lower vertical error assumption. Figure 6-5 also illustrates that a 5,500 ft runway separation with a 10 NM radius turn to final would work using the larger vertical error assumption. These illustrations indicate that depending on the turn radius selected and runway spacing, there is some specific region of turn angle that controls the lateral collision risk.

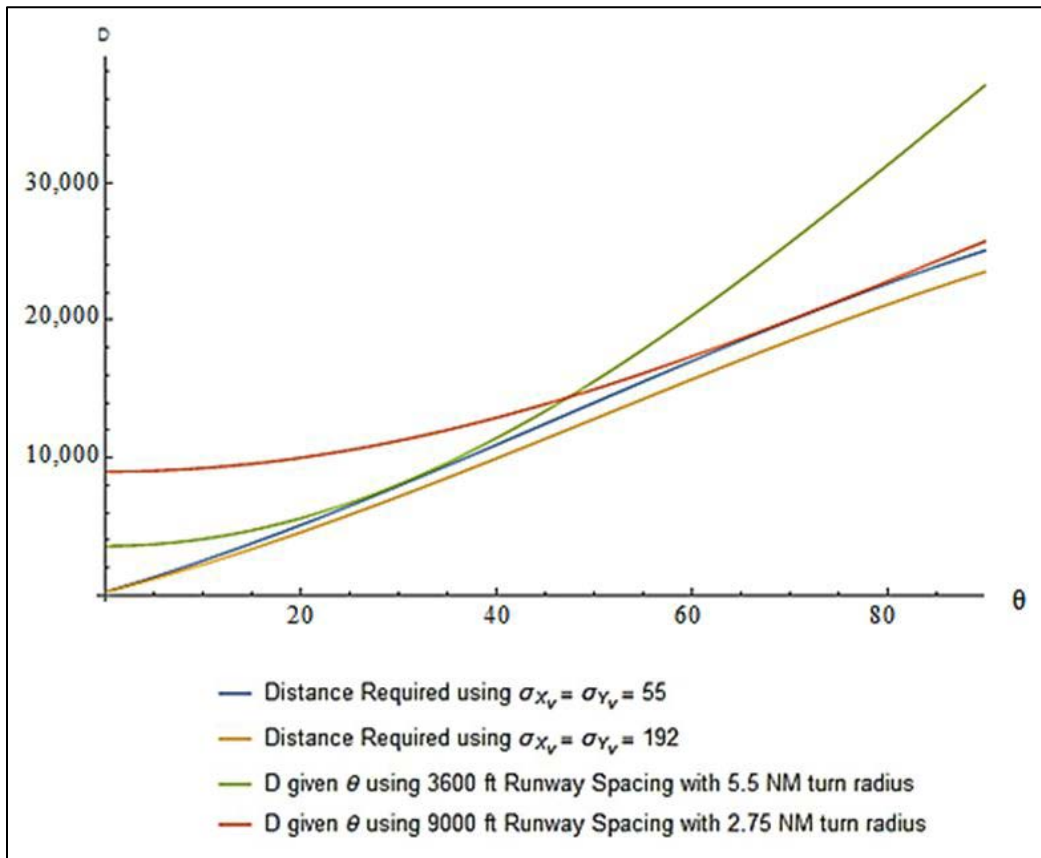


Figure 6-5: Distance Required to Maintain SMS Target Level of Safety Given a Lateral Path Deviation at Any Angle Relative to the Final Approach Course and Vertical Separation of 0 ft at Intersection

Figure 6-6 illustrates that, as vertical separation at the time of horizontal overlap is introduced, the higher standard deviation for vertical error becomes more demanding than the lower standard deviation for vertical error. Additionally, the runway spacing and procedure design requirements become less extreme.

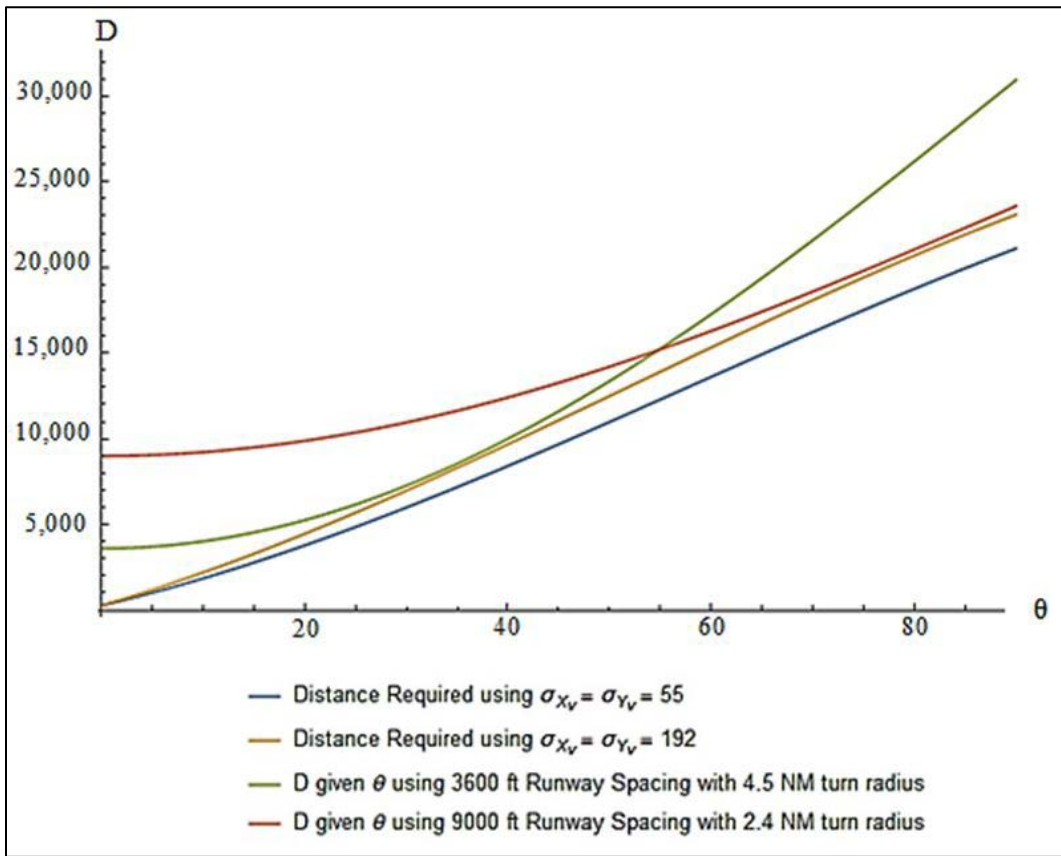


Figure 6-6: Distance Required to Maintain SMS Target Level of Safety Given a Lateral Path Deviation at Any Angle Relative to the Final Approach Course and Vertical Separation of 200 ft at Intersection

Based on our analysis of the track data, we have two reaction time distributions: one for aircraft that continue the approach after the malfunction and another for those who initiate a go-around.

Furthermore, we have two vertical error models: one for aircraft with VNAV and another for those without it, as shown in table 6-4. Setting the vertical separation for all 4 cases to 0, we can see that only the go-around response times with the VNAV error characteristics present a collision risk 3 times higher than 10^{-9} . This is not a concern because with 150 ft of vertical separation at the time of intercept that collision risk falls below 10^{-9} . We can expect the mean vertical separation to be greater than 150 ft if the flight crew executes a go-around.

Table 6-4: Collision Risk during the 10° Turn without Vertical Separation at Intersection

	Continue Approach	Go-Around
VNAV	7.24×10^{-14}	2.84×10^{-9}
No Approved VNAV	2.40×10^{-14}	9.46×10^{-10}

This collision risk model is dependent on the mean vertical separation during horizontal overlap. The intention of this study is to define the deviation angles and distances

relative to the parallel approach procedure by informing the instrument approach procedure design. Mean vertical separation at the point of horizontal overlap does not inform which altitudes are safest for the approach procedure. To inform instrument approach designs including the vertical separation, we will need to make a few additional assumptions. In the pilot test, the approach procedure tested joined the final approach course using a 10° leg. This leg did not experience overshoot during the test, but some other TF fly-by turns in the test did. It is therefore necessary to require a 10° intercept of the final approach course. Furthermore, we demonstrated above that deviations with a track less than 10° relative to the other approach do not pose a substantial collision risk. With this in mind, we will fix a 10° heading change joining a final approach course at some runway spacing. As shown in figure 6-7, we will calculate D and V based on θ and the length of the straight segment between the 10° leg and the turn to final. Furthermore, we will assume that the altitude difference at the points f and g is some fixed value.

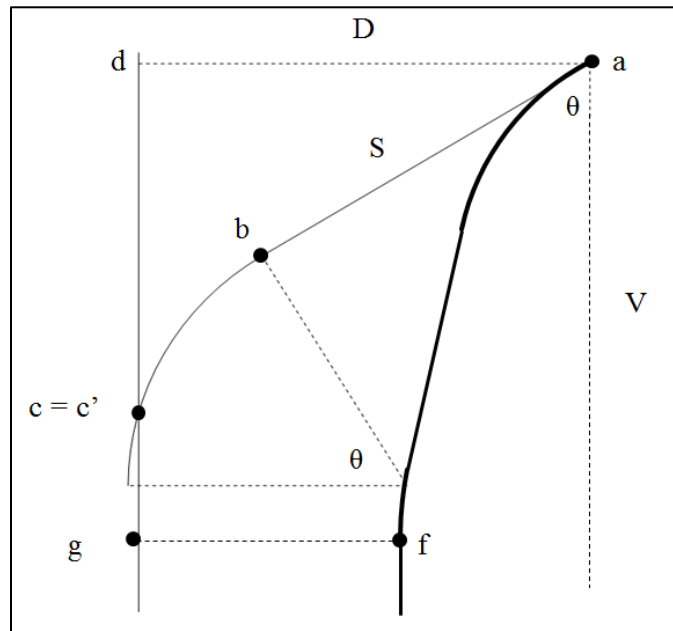


Figure 6-7: 10° Heading Change Joining a Final Approach Course

Using this geometric model, we will be able to get the straight-in aircraft's altitude at c relative to f by taking into account the altitude difference between f and g , then adding the altitude lost from c to g . Then we get the deviating aircraft's altitude at c by considering the altitude lost from a to f and subtracting the altitude lost from a to c . If we consider $A(x,y)$ to be the difference in altitude between the point x and the point y , $P(x,y)$ to be the path length between two points in the above geometric model, and c' to be the location of point c on the EoR approach procedure, then the equation for the altitude separation can be expressed as follows:

$$\begin{aligned}
\Delta_V &= A(c, c') = A(f, c') - A(f, c) \\
&= (A(f, a) - A(a, c')) - (A(f, g) + A(g, c)) \\
&= -P(a, f) \tan \varphi_1 + A(g, f) + P(a, c') \tan \varphi_1 + P(c, g) \tan \varphi_2 \quad (9)
\end{aligned}$$

However, since we are considering \mathbf{S} to be a random variable, the deviation path is composed of a straight segment and a turning segment. The path length varies depending on the length of \mathbf{S} . To illustrate this, if \mathbf{S} is such that the deviation intersects the normally performing aircraft's path at its endpoint, then the path length includes the entire circle segment. However, if the value of \mathbf{S} is very large, the deviation path intersects the other approach during the straight segment, which has a different path length. Geometrically, the path length functions can be expressed as the following piecewise equation:

$$\begin{aligned}
P(a, c) &= \begin{cases} S + \theta R & S \leq \frac{D - R + R \cos \theta}{2} \\ S + R(\theta - \psi) & \frac{D - R + R \cos \theta}{2} < S < \frac{D}{\sin \theta} \\ D/\sin \theta & S \geq \frac{D}{\sin \theta} \end{cases} \\
V - P(c, g) = P(d, c) &= \begin{cases} S \cos \theta + R \sin \theta & S \leq \frac{D - R + R \cos \theta}{2} \\ S \cos \theta + R \sin \theta - R \sin \psi & \frac{D - R + R \cos \theta}{2} < S < \frac{D}{\sin \theta} \\ D/\tan \theta & S \geq \frac{D}{\sin \theta} \end{cases} \\
\text{where } \psi &= \cos^{-1} \left(\frac{D + R \cos \theta - S \sin \theta}{R} \right) \quad (10)
\end{aligned}$$

Although these variables are a function of \mathbf{S} , we can visualize the regions where mean vertical separation is more likely by taking the minimum of the function along \mathbf{S} and varying the other parameters, as seen in figure 6-7. We also fixed φ_2 to -3° , which represents a typical glidepath angle. Each plot is labeled using an ordered pair of $(\mathbf{A}(\mathbf{a}, \mathbf{d}), -\varphi_1)$. The x-axis is the angle of the deviation, and the y-axis is the distance from the normally performing path at the start of the deviation. Figure 6-8 demonstrates that depending on the specific conditions of the deviation, there are clear descent angles and positions that increase the likelihood that the aircraft will not have vertical separation at the time of horizontal overlap.

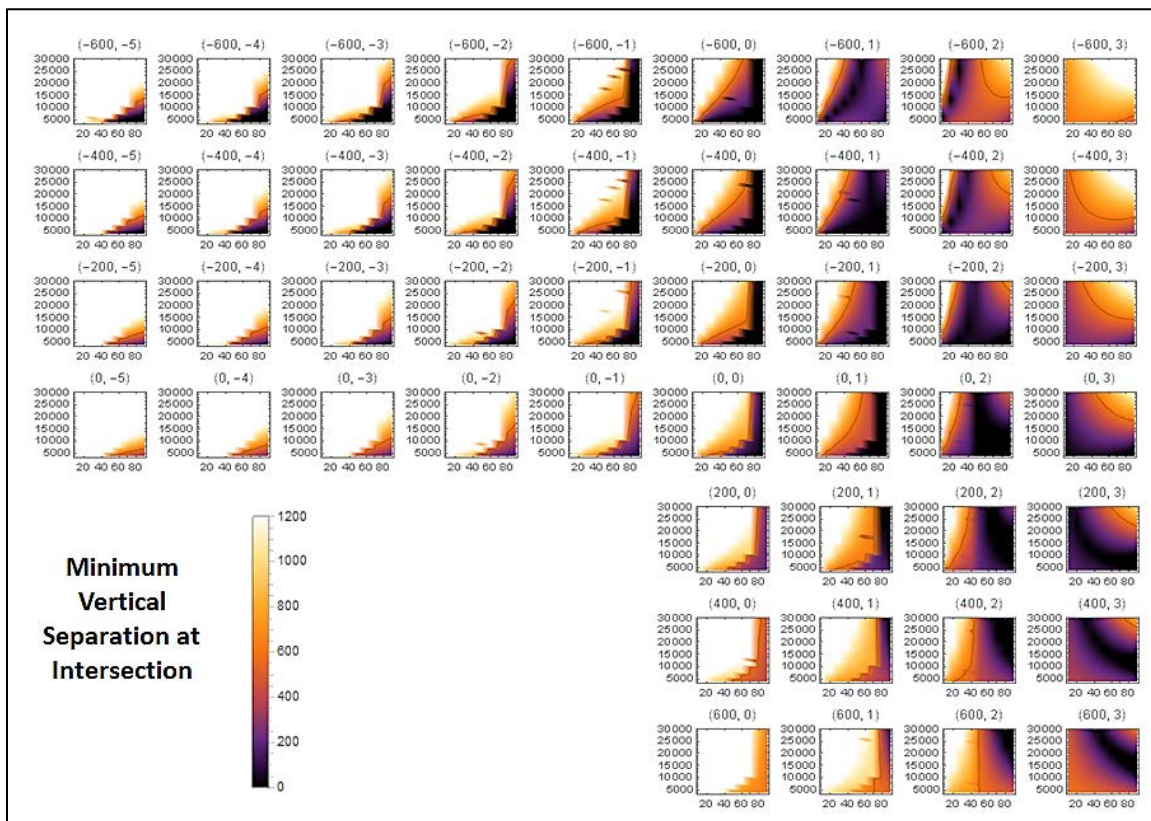


Figure 6-8: Minimum Vertical Separation

However, these simple equations of vertical separation only apply in the case where the aircraft continues on the approach. If the lateral path deviation results in the flight crew executing a go-around, the probability of vertical overlap changes. The starting point for this calculation is the result from the altitude separation function defined above. However, the time of the go-around relative to the time of the lateral correction and the angle of the climb used to execute the go-around are random variables. Both of these random variables were determined to be normally distributed based on the data from the pilot tests with a mean of 2.5° and a standard deviation of 1° for the climb angle and a mean of -25.52 seconds and a standard deviation of 27.97 seconds for the time of the go-around. For details on the test results, see section 4.3.2.3.

In the cases where the go-around occurs after the lateral paths intersect, the probability of lateral overlap is the same as if the aircraft did not go-around. This results in a probability mass in the distribution of vertical overlap. The vertical separation random variable involves taking the tangent of the climb angle distribution and multiplying it with the go-around time distribution transformed by groundspeed and the path length along the deviation path. This random variable is somewhat complicated. In order to capture an estimate via modeling, we can make some simplifying assumptions. First, the angles in the tangent function are very small; therefore, the tangent function can be reasonably approximated via the first term of its Taylor series expansion, which is the random variable itself. Second, the product random variable is symbolically complicated to evaluate. However, the effect of the angles on the variability is relatively small compared to the distance in most of the cases under consideration. Therefore, the random

variable of the angles introduces relatively small changes in the higher order moments of the resultant distribution. For computational ease, we will instead model the vertical separation distribution using only the mean and variance of the product distribution. Finally, in the case when the deviation is above the other approach at the time of lateral overlap, we consider all of the aircraft that went around before the lateral intersection to have no collision risk at the time of lateral overlap.

In figure 6-9, the time of the lateral correction is represented by the blue point and the altitude of the victim aircraft is represented by the red point. The mean position of the go-around is represented by the green point and the green dashed line represents the climbing path. The orange dashed lines represent the 10th and 90th quantile go-around times and angles. This model does not include the aircraft aerodynamics required to accurately generate an entire go-around track. However, the go-around characteristics measured were based on the times when the aircraft began behaving as if they were flying a constant angle. It would be approximately equivalent to saying that the vertical profile given below represents a track that initiates a go-around before the point, but does not assume a constant climb until the vertical profile is characterized by the dashed line. The collision risk in this case has two parts: (1) the probability that the go-around occurs after the red point multiplied by the probability of vertical overlap given that the aircraft continues the approach, and (2) the probability that the deviating aircraft is within ± 80 ft from the red point, given the distribution of go-around times, angles, and normal error characteristics.

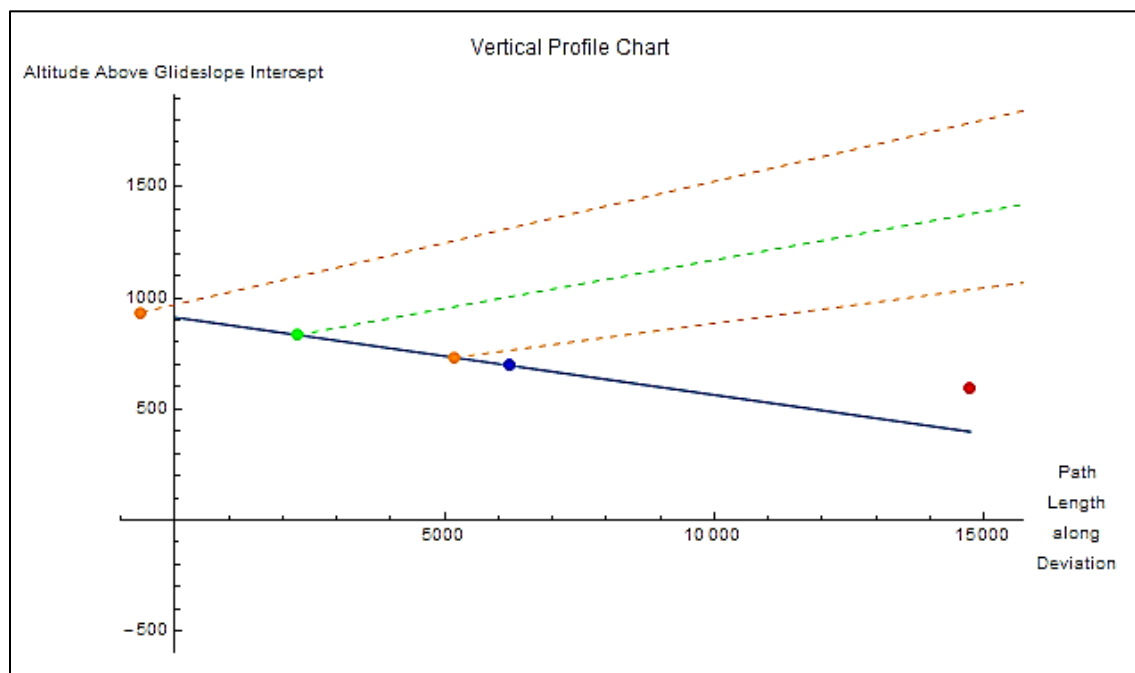


Figure 6-9: Vertical Profile

However, these modifications to the model eliminate one of our fundamental assumptions: that the horizontal overlap event and the vertical overlap event are independent. This is no longer the case because the probability of vertical overlap is a function of vertical separation, which is a function of S , but S is the random variable used to calculate horizontal overlap. Since we have assumed that the distributions are

independent except with respect to S , we can consider each probability given S to be independent.

Figure 6-10 shows one example of how the conditional probabilities of horizontal and vertical overlap given S can be multiplied with each other to attain the probability of collision given S . This can then be multiplied by $f(S)$ and integrated over S to attain collision risk.

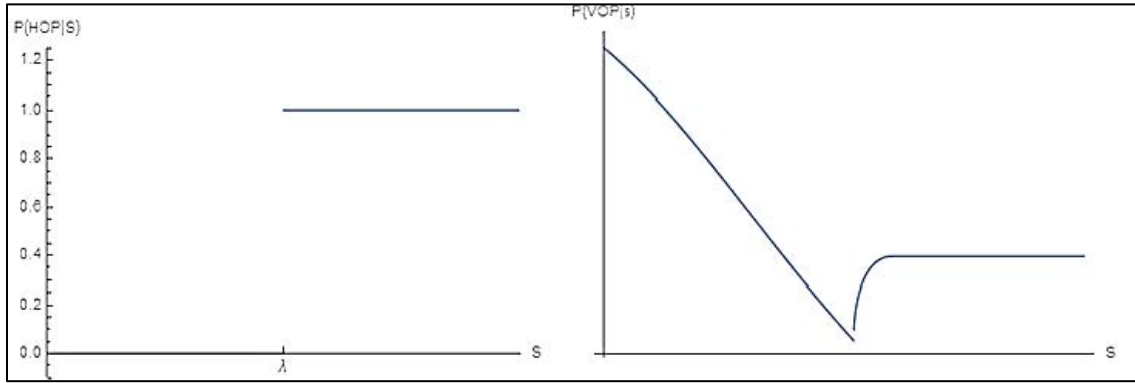


Figure 6-10: Horizontal and Vertical Overlap Given S

Since $P(\text{Horizontal Overlap} | S)$ is binary, $P(\text{Horizontal Overlap} \cap \text{Vertical Overlap} | S) = P(\text{Vertical Overlap} | S)$ when $S > \lambda$. So after making this correction, collision risk can be expressed as the following equation. The definition of $P(\text{Vertical Overlap} | S)$ is the difference of two error functions whose location varies as a function of S and $f(S)$ is the probability density function of the response time distribution. This combination of variables cannot be symbolically integrated, but evaluating it using numerical integration toolsets in Mathematica yields a collision risk value given specific parameters.

$$P(\text{Collision}) = \int_{\lambda}^{\infty} P(\text{Vertical Overlap} | S) * f(S) dS \quad (11)$$

To calculate the collision risk with controller monitoring and intervention, we also calculated the same results using a shortened response time distribution, which represents the minimum of the pilot response to a deviation without controller intervention and the sum of the controller response to a deviation and the pilot response to a controller command.

There are several major variables that impact collision risk results. Rather than profile the entire large probability space, operational experts have selected a baseline approach procedure that they believe represents the most viable implementation of an EoR approach. This baseline approach procedure involves:

- 60°-60°-50°-10° heading change configuration;
- 2° descent angle on the EoR approach;
- Groundspeed equal to 210 indicated airspeed at Denver International Airport’s altitude with the average wind speed at the turn altitude;
- 3,600 ft runway spacing; and
- An altitude separation at f and g as if the EoR approach was on a 2° descent for 1 NM while the other approach was at 3° over that distance.

In the baseline case, the collision risk without controller intervention was 4.6×10^{-10} and 9.4×10^{-11} with controller intervention.

6.2.2 Triple Non-Normal Collision Risk Model Methodology

The methodology used to calculate the collision risk between an EoR operation and an approach along the extended final approach course can be easily extended to triple operations. Triple operations are a common application of simultaneous independent approaches at high traffic airports. These operations are similar to the tested EoR operations, except that the outboard EoR approaches are separated by at least 7,800 ft and a third parallel runway is located between the EoR instrument approach procedures separated from each one by 3,900 ft, see figure 6-11. Using the assumptions historically used to evaluate triples operations in AFS-400, the collision risk of triple operations can be separated into the probability of multiple dual operations. [25] There are two cases to be considered: first, that the center aircraft blunders towards one of the outboard aircraft; second, that one of the outboard aircraft blunders towards the center aircraft and the other outboard aircraft.

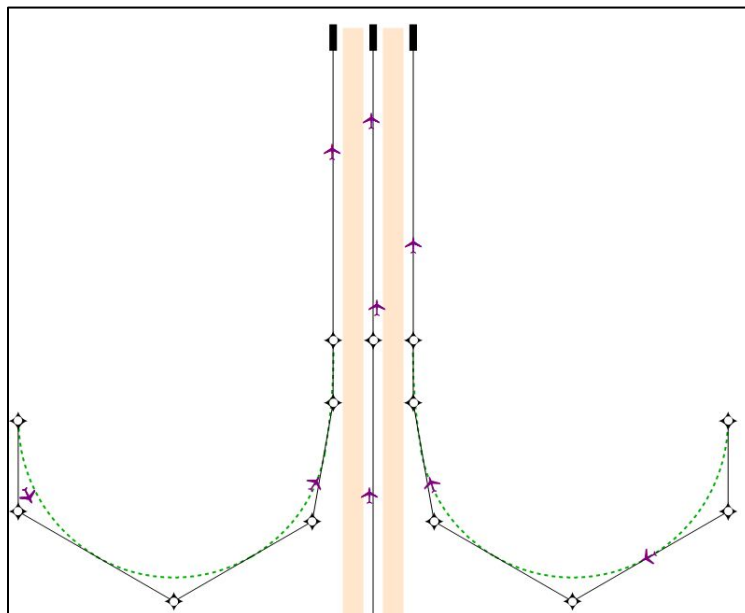


Figure 6-11: Triple Approach Concept

The first case, where the center aircraft blunders towards one of the outboard aircraft, is not applicable to the analysis methodology for EoR. This study has not considered any lateral path deviations that originate on a straight portion of an approach procedure. Furthermore, this case is quite similar to the original CSPO evaluation, excepting that there is additional space between the EoR aircraft and the center approach for much of the length of the center instrument approach procedure. Due to its dissimilarity to the collision risk calculated for EoR operations and that this case has already been shown to be safe, we will assume that this case contributes negligible collision risk when runways are spaced greater than 3,900 ft.

The second case, where an outboard aircraft blunders toward the center approach, can be separated into two duals cases with a few assumptions. First, we assume that the evading

center aircraft does not pose any significant collision risk to the evading outboard aircraft. This assumption is reasonable because the controllers monitoring those two aircraft typically sit at adjacent scopes and coordinate during non-normal situations. Second, we assume that the probability of collision is linear. That is, the collision risk of an outboard blunder with an aircraft on approach to a center runway 3,900 ft from the outboard runway or with an aircraft on approach to the other outboard runway 7,800 ft away is the same as the collision risk of the outboard with the center plus the collision risk of the outboards, see equation 12. This assumption is conservative because, while the collision with an aircraft on approach to the center runway has the same geometry as the dual operation, the outboard collision geometry would involve a much earlier FMA alert and a lateral deviation crossing over another approach path. It seems reasonable to assume that this would trigger a shorter response time than in the dual case with runways spaced 7,800 ft.

$$P_{Collision}(Runways\ 3,900\ ft + Runways\ 7,800\ ft) = P_{Collision}(Runways\ 3,900\ ft) + P_{Collision}(Runways\ 7,800\ ft) \quad (12)$$

This is the same as saying that the collision risk of the operation seen in figure 6-11 is equal to the collision risk of the operation seen in figure 6-12 (a) plus the collision risk of the operation seen in figure 6-12 (b). Furthermore, the above discussion demonstrates that the collision risk in figure 6-12 (b) is assumed to be less than or equal to the collision risk of the operation seen in figure 6-12 (c).

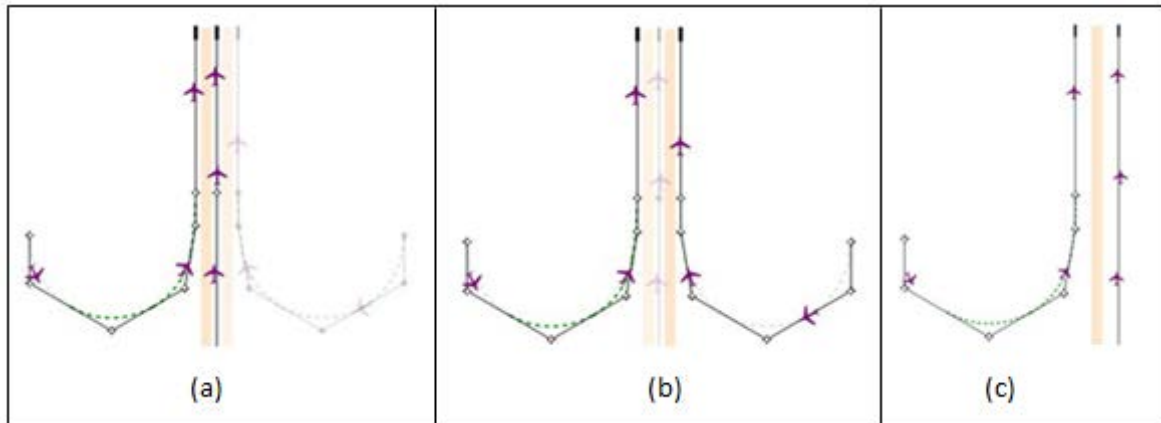


Figure 6-12: Sample Triple Geometries

From prior research, confirmed by the results seen in figure 6-13, we know that collision risk strictly decreases as runway spacing increases. Knowing this, we can establish a few inequalities around equation 12. In particular, we know that:

$$P_{Collision}(Runways\ 3,900\ ft) > P_{Collision}(Runways\ 7,800\ ft) \quad (13)$$

This implies:

$$2 * P_{Collision}(Runways 3,900 ft) > P_{Collision}(Runways 3,900 ft) + P_{Collision}(Runways 7,800 ft) \quad (14)$$

In general, this also implies that the collision risk of a generic runway spacing of ρ can be bounded by:

$$P_{Collision}(Runways \rho ft + Runways (2 * \rho) ft) < 2 * P_{Collision}(Runways \rho ft) \quad (15)$$

Based on this inequality, we see that the triple runway operations collision risk is less than two times the dual runway collision risk. If the dual runway operations do not exceed half the SMS target level of safety, triple runway operations with the same parameters will not exceed the SMS target level of safety. Since neither baseline value in the duals case is greater than 5×10^{-10} , we can conclude that for the baseline case triples operations would meet the SMS target level of safety. Furthermore, any collision risk value that is lower than 5×10^{-10} would be acceptable for use in triples operations. Some values higher than this value may be acceptable; however, this threshold is met with controller intervention for all EoR operations, see section 6.2.3.

6.2.3 Sensitivity Analysis

In the following discussion, we vary from this baseline by each major variable that contributes to collision risk to explore the relative impact on collision risk. Note that in all of the sensitivities explored, the EoR collision risk is less than 10^{-9} . Most of these sensitivities, therefore, do not impose restrictions on the development of EoR operations but they should be considered during implementation of EoR operations.

These results are based on an assumption that the 3rd turn (50°) introduces the majority of the collision risk. This is supported by the analysis without vertical navigation that suggests that the 4th turn (10° in the test procedure) is safe. This is also supported by assuming that the 2nd turn (apex in the test procedure) is designed such that the aircraft have sufficient separation and it does not introduce substantial collision risk. Some variable combinations may result in a collision risk higher than 10^{-9} ; however, when we combine these results, the collision risk is always less than 10^{-9} . For more details, see appendix M.

The label *Triple SMS Target Level of Safety* in figures 6-13 through 6-19 does not indicate that triple runway operations require an alternate target level of safety. Instead, it represents half of the SMS target level of safety. If dual runway operations meet this threshold, triple runway operations with the same configuration will meet the SMS target level of safety threshold, see section 6.2.2.

CSPO generally uses runway spacing to mitigate collision risk. As the runway spacing increases from 3,600 ft to 9,000 ft, the collision risk without controller intervention decreases by approximately one order of magnitude, see figure 6-13. The collision risk with controller intervention decreases by almost four orders of magnitude over the same interval.

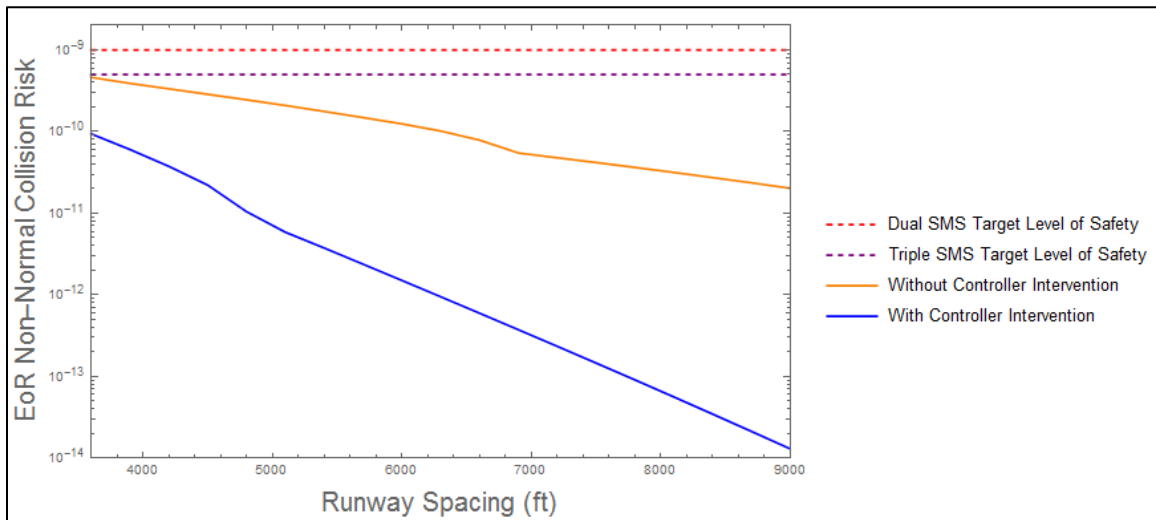


Figure 6-13: Sensitivity to Runway Spacing

Historical closely spaced parallel analysis has demonstrated that blunders of 10° do not contribute substantial safety risk to parallel operations. This is also demonstrated by the above analysis without considering vertical separation. Therefore, a similar mitigation to collision risk is extending the length of the 10° leg, see figure 6-14. By adding 3 NM to the minimum length of the 10° leg, the collision risk without controller intervention is reduced by approximately the same amount as it would be if we increased the runway spacing by 5,400 ft. Over the interval from 0 ft to 18,000 ft the collision risk decreases by a little less than an order of magnitude without controller intervention. With controller intervention, the collision risk decreases by approximately 2.5 orders of magnitude.

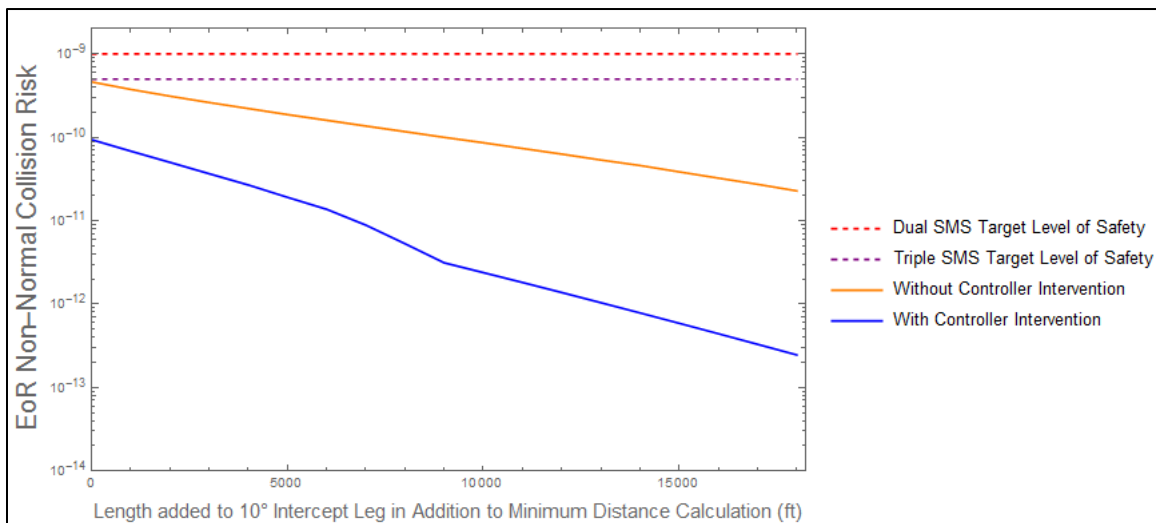


Figure 6-14: Sensitivity to Extra Length Added to Leg

Other possible mitigations of collision risk include varying glidepath angle used to calculate the fix altitudes on the EoR approach, see figure 6-15. For the baseline design select, which has the EoR approach joining the glideslope below the other aircraft by 106 ft, the shallower glidepaths contribute higher risk. This is mainly a result of the

go-around cases and the cases where the other aircraft captures the glideslope at the same time as the non-normal approach.

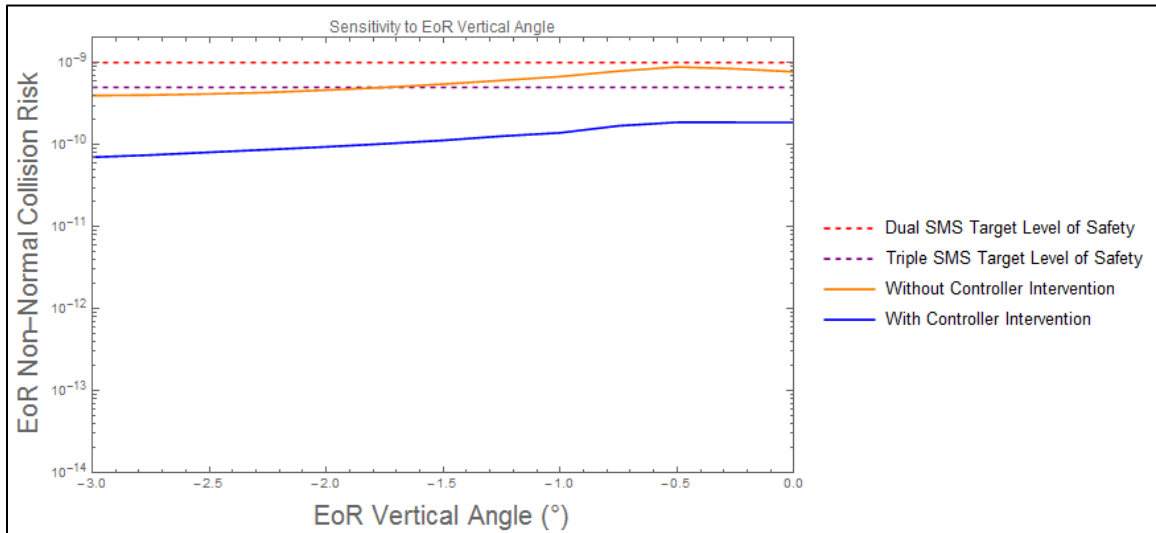


Figure 6-15: Sensitivity to EoR Vertical Angle

Another possible mitigation to collision risk involves using altitude to modify the glideslope intercept such that the EoR approach intercepts at a different altitude than the other aircraft, see figure 6-16. This can be done by introducing level segments on approach procedures and it happens when runway thresholds are offset. If the EoR approach is at a lower altitude than the adjacent traffic, then the increased collision risk when the deviating aircraft executes a go-around cancels out any reduction in the collision risk in cases where the aircraft continues the approach. If the EoR approach is above the other approach by at least 300 ft, the collision risk with and without controller intervention decreases by approximately 2 orders of magnitude.

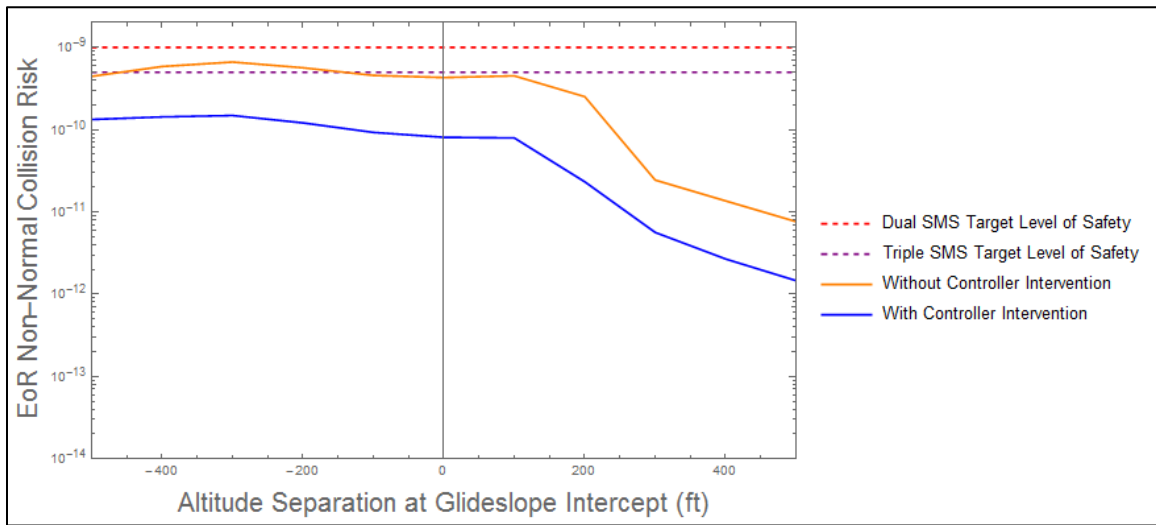


Figure 6-16: Sensitivity to Altitude Separation at Glideslope Intercept

Restricting the turn angles in the procedure design is another possible mitigation. This assumes that the next turn angle is sufficiently offset to make its contribution to the collision risk negligible. When the 3rd turn angle is very small, then this would need to be very long. Between a 90°-80°-10° configuration and an 80°-60°-30°-10° configuration, the collision risk without controller intervention is reduced by about 1 order of magnitude, see figure 6-17. Over the same interval, the collision risk with controller intervention decreases by approximately 2 orders of magnitude.

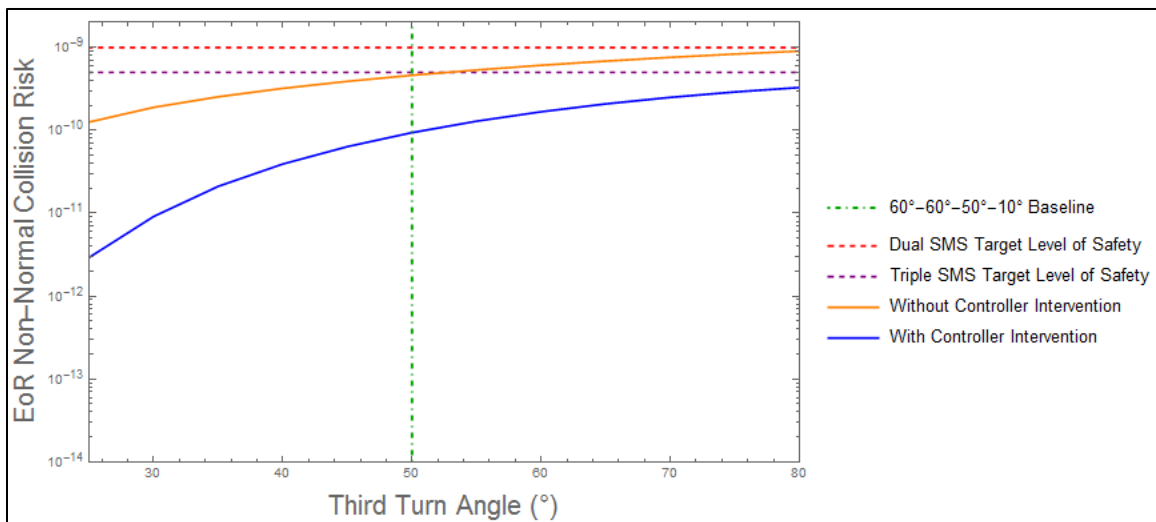


Figure 6-17: Sensitivity to Third Turn Angle

The next two sensitivities do not explore possible mitigations as much as the validity of our assumptions. One assumption is groundspeed. Groundspeed impacts the model in multiple ways: how far the aircraft goes during the deviation, the radius of the correction, and the starting position of the aircraft (changing the assumed procedure design), see figure 6-18. Although this complex relationship results in an interesting curve, the

overall collision risk is not changed as groundspeed changes by more than an order of magnitude.

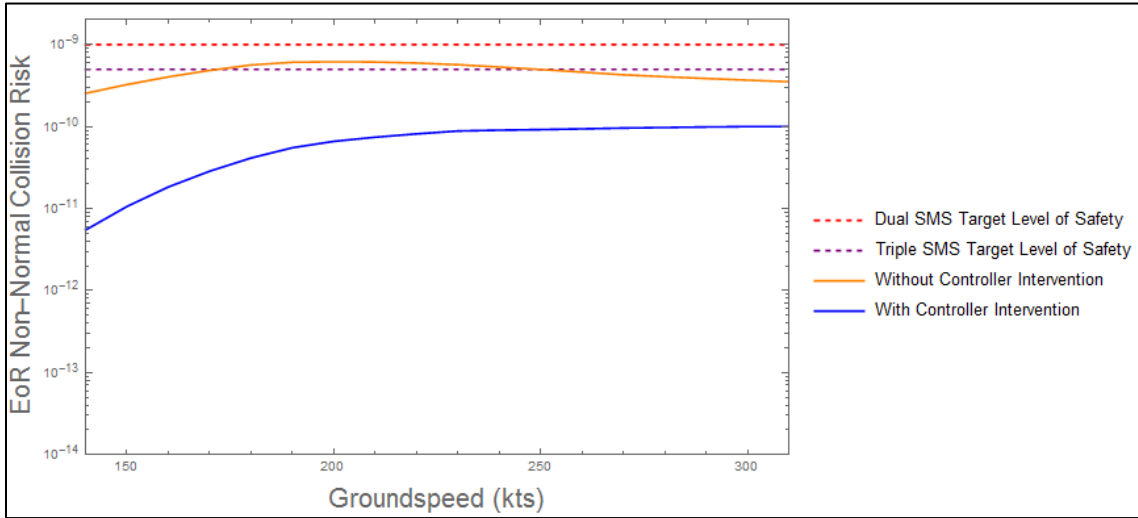


Figure 6-18: Sensitivity to Groundspeed

Another assumption was that the aircraft would correct any deviation using the maximum bank for instrument procedure design, 25°, see figure 6-19. Many pilots would command a bank greater than this if they felt threatened, up to 30°. It is possible that pilots could also have a serious loss of situational awareness, not understand the severity of their deviation, and bank less than 25°. However, over the region of plausible bank angles, the collision risk without controller intervention varies by less than an order of magnitude. The collision risk with controller intervention varies by one order of magnitude over the same interval.

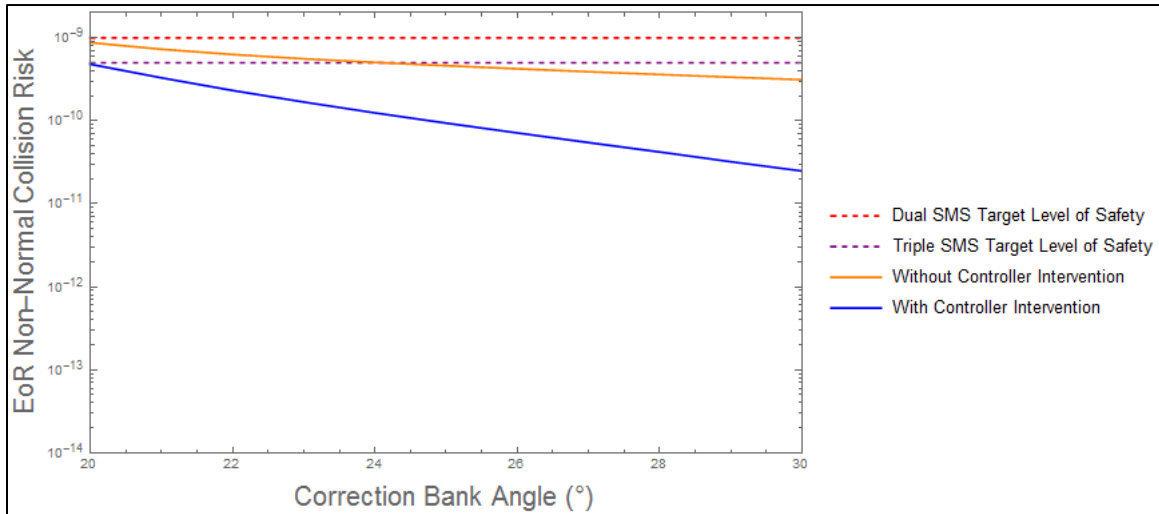


Figure 6-19: Sensitivity to Correction Bank Angle

6.2.4 Controller Directed Breakout

A risk mitigation that has not been considered in detail to this point is action by the final monitor controllers upon detecting a deviation from course. Historically, many studies

have been performed to examine controller reactions to deviations (blunders) from simultaneous parallel approach operations where both aircraft are flying straight-in paths to parallel runways. Most of these operations involved final monitor controllers handling individual streams of traffic, similar to the envisioned EoR operations. However, direct application of those historical results to this operation would be of questionable validity due to the recognition issues associated with detecting deviations from a straight course with an expected track over the ground versus a TF fly-by turn with a track affected by airspeed, wind, avionics, and other factors. The controller test that was performed as part of this study was intended to answer some of the questions about those recognition issues, but it still left many issues unresolved (as well as raising a few new questions). There were also questions about pilot response times considering the differences between being on a stable straight-in constant descent approach and being in a relatively high bank turn with potentially no vertical guidance.

Data from the HITL tests seemed to bear out the concerns. Pilot response times, which were measured from the controllers' push-to-talk input to the aircraft making a detectable corrective maneuver, were much longer by 10 to 20 seconds. Whether this delay was entirely due to additional aircraft configuration time or some other factor(s) will require further study. Controller response times were measured from the start of the deviation to controller push-to-talk inputs and were generally much longer than in parallel approach tests. Several response times in excess of a minute were detected. Given that in most cases the controllers had never seen this operation before and didn't really have a preconceived idea on what the tracks should look like, this was not totally unexpected, but it does make it difficult to determine what an appropriate value for the response time to use in any modeling should be.

Using the geometry in the figure 6-20 (c) as a reference, the time it takes an aircraft deviating from the 3rd turn to intercept the parallel approach is related to the angle θ , the runway separation, the length of the 10° leg, and the airspeed. The descent angle has a small effect, but for the purposes of this discussion, we are going to fix that at -2°. Images (a), (b), and (c) in figure 6-20 depict this time as a function of airspeed and runway separation for track headings at 10°, 50°, and 80° from the runway bearing. The non-linearity is created by the turning distance being proportional to the square of the speed rather than linear (so that as the speed doubles, the distance the aircraft is in the turn increases by a factor of four) and the trigonometry of the θ . At 10°, the speed effect is almost negligible because the increase in the lateral distance needed to complete the turn is almost all along-track whereas at 80°, it is almost perpendicular to the track, which increases the distance the aircraft has to fly.

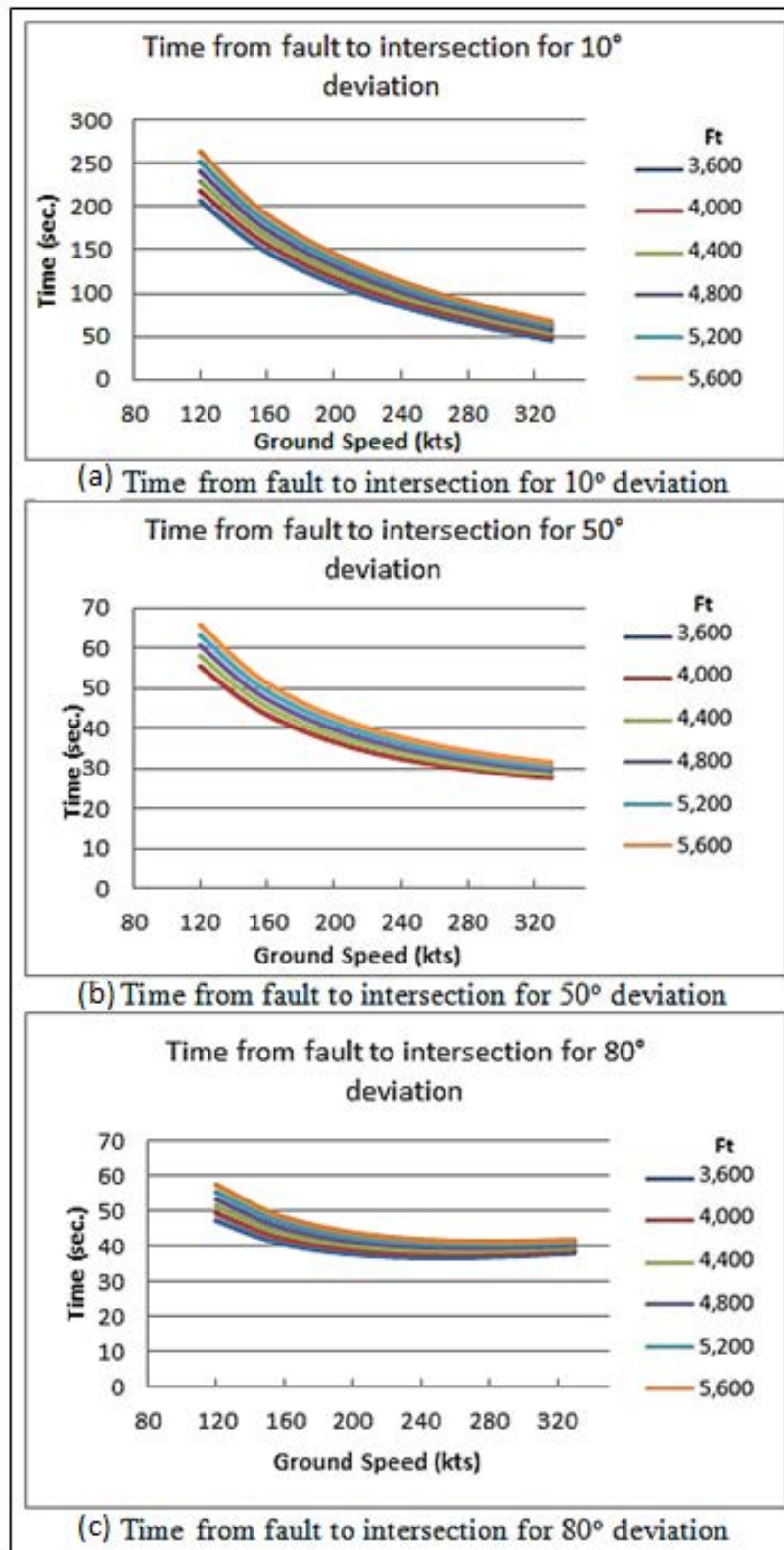


Figure 6-20: Time from Fault to Intersection

If we look at the most likely approach speeds, between 180 and 240 knots, and subtract out the time required to change the heading back to the approach course (assuming 3° per second turn rate), the required combined controller and pilot response time is shown in table 6-5. While the times required to resolve the 10° deviation appear to be easily handled even with the increased response times shown during the testing, the other two deviation angles examined would be more problematical. Trained and experienced controllers and pilots should be able to meet the 50° case, but the limiting 80° case would require additional study and does not seem achievable.

Table 6-5: Required Air Traffic Control and Pilot Response Time

Deviation Angle (°)	Required ATC and Pilot Response Time (sec.)
10	81-156
50	16-29
80	10-18

Note that this analysis does not factor in the possibility of vertical separation nor does it consider the likelihood of longitudinal alignment or the probability of a deviation in the first place. It is also possible that in some circumstances there may be operationally superior resolutions to turning the deviating aircraft back onto course. Another resolution that is probably more long term is the provision of a modified final monitor alert algorithm that could issue an alert sooner than the current configuration when EoR operations are being performed.

6.2.5 Vertical Navigation Considerations

When the original multiple parallel approach program studies of CSPO were accomplished back in the late 1980's and 1990's, all of the tests assumed the approaches were being flown to fully operational ILS facilities, with a localizer for lateral guidance and a glideslope for vertical. In the absence of any data to support operations without vertical guidance, it was decided not to allow such operations until additional studies could be performed.

An early commercial aviation safety team analysis showed that approaches without vertical guidance had a significantly higher risk than those with a glideslope. Even though these results had no real bearing on simultaneous approach operations, they were used as supporting evidence in not allowing CSPO approaches without vertical guidance, though the FAA continued to allow single straight-in approaches without vertical guidance.

From numerous discussions throughout the years, and with all other factors being equal, the collision risk associated with two parallel approaches that are both on a glideslope should be higher than a case where one aircraft is on the glideslope and the other is performing a dive and drive approach technique as the vertical alignment is significantly reduced in the latter case. However there was much anecdotal evidence that pilots flying an ILS would have lower flight technical error or deviations from the desired course than pilots flying a course deviation indicator for lateral guidance and dealing with the workload associated with the dive and drive technique. In August 2011, a safety report was published based on a series of simulator tests that examined this question. [30] The

data indicated there was an increase in flight technical errors when line pilots used the dive and drive technique versus flying the full ILS. Most of the pilots used in the tests very seldom, if ever, used the dive and drive technique, and several of them worked for airlines that would not allow such a procedure, so it was not clear that those results would hold for pilots that had dive and drive experience. Most modern aircraft use onboard vertical error data such as barometric altimetry-based vertical navigation (baro-VNAV) to calculate a smooth vertical path even when a glideslope is not available.

A fast-time simulation comparing ILS-ILS to ILS-localizer only approaches using the data produced from the simulator studies showed a very small increase in risk (approximately 2%), but did not consider the very low likelihood of a localizer only dive and drive approach being flown.

Data from the EoR pilot phase 2 HITL looking at non-VNAV regional jets provided some relevant data for a re-evaluation of the question. Although the test scenarios terminated shortly after the aircraft joined the final approach course, there was enough data collected during that period to estimate a vertical distribution. Numerous fast-time simulations were performed using the wider vertical distributions and the results were compared to previous work done with ILS glideslopes and representative RNAV vertical guidance. Although the lateral tracking errors that were seen in the non-VNAV EoR test did not show any significant increase over the VNAV case, the previous 2011 report indicated that there could be up to a 33% increase. [30] However, this data was based on localizer only performance, which is substantially different than the lateral navigation provided by GPS. Considering the increased errors observed in the 2011 test and the lack of increased error during the non-VNAV test, we tested the sensitivity of the collision risk by simulating additional scenarios where the cross track error distribution was increased by 20%.

The standard blunder scenario used for numerous previous safety studies was run on our fast time simulation system. Table 6-6 shows results for a near sea-level runway pair separated by 3,600 ft with no stagger. Both approaching aircraft were non-VNAV. A fleet mix of 50% heavy and 50% large aircraft was used to be extra conservative. The non-VNAV vertical error was modeled with a Gaussian distribution with a mean of 0.0 and a standard deviation of 175 ft based on the EoR non-VNAV test data. The base case modeled lateral error using a Gaussian distribution with 95% containment within 0.080 NM and the 20% greater case used the same distribution with 95% containment within 0.096 NM. Since the EoR operation is intended to shorten the length of the final approach course, the risk was only evaluated from 2 NM to 10 NM from threshold versus the usual 2 NM to 14 NM.

Table 6-6: Near Sea-Level Runway Pair/3,600 ft Separation/No Stagger

Field Elevation (ft)	ILS Risk	RNAV (w/ VNAV)	RNAV (non-VNAV)	RNAV (non-VNAV and +20% lateral)
2,000	7.00E-10	7.93E-10	6.67E-10	6.83E-10
1,000	6.68E-10	7.50E-10	6.29E-10	6.52E-10
15	6.21E-10	7.03E-10	5.99E-10	6.16E-10

In summary, there is no compelling evidence to support that vertical navigation should be required for closely spaced simultaneous approach operations. The historical restriction on such operations has not been studied. A preliminary study has now been performed considering actual test data and indicates that the collision risk is lower for aircraft without vertical navigation. [31] Note that this study does not address the risk associated with controlled flight into terrain which was the primary risk identified by the commercial aviation safety team study mentioned above.

6.3 Implementation Risks

Experts recognize that current national airspace safety systems and FAA policy may not be designed to accommodate EoR operations. In the following section, we discuss two systems that may generate false alarms during the new operations. We also address some of the concerns regarding instrument procedure design criteria and EoR operations.

6.3.1 Nuisance Final Monitor Aid Caution Alerts

When a facility is approved to run independent closely spaced parallel operations, they are required to have special monitoring of the aircraft. This monitoring often takes the form of a special radar controller position at the TRACON assigned to each parallel approach. These special positions are called final monitors and they are assigned to watch the traffic on the parallel approaches to help detect potential deviations. To support these positions, the STARS has a functionality called the FMA. This functionality defines a region called an active monitor zone and aircraft in this region are subject to additional alerting. In particular, the FMA defines regions between the extended runway centerlines of parallel runways called NTZs. If an aircraft in the active monitor zone enters the NTZ, it triggers an aural and visual alert called an FMA warning. This alert causes the target and datablock of the offending aircraft to flash red. To help trigger a faster reaction time from controllers, the FMA also calculates a predicted aircraft position in 10 seconds using the target position and velocity; if this predicted position enters the NTZ, it triggers an aural and visual alert called an FMA caution. This alert causes the target and datablock of the offending datablock to flash yellow.

Due to the assumption that the aircraft is travelling along the extended runway centerline, the 10 second prediction algorithm does not assume that an aircraft turning next to the NTZ would continue turning. Instead, the algorithm predicts that the aircraft continue tangentially from their current position for 10 seconds. This means of prediction can prove problematic for the implementation of EoR because these operations intercept of the extended runway centerline next to the NTZ. Especially when considering radar errors, this can cause frequent FMA caution alerts that do not correspond to a real collision risk event. A frequent, unnecessary alert could be frustrating for controllers and it could cause desensitization to the alert – eliminating its benefit as a safety mitigation. To support implementation of this operation we modeled the behavior of the FMA on the STARS platform to predict the rate of caution alerts during normal operations to inform the selection of implementation sites. Furthermore, we checked the results attained from its radar and automation simulation capabilities with results from scenarios run at a training implementation of STARS adapted to Denver International Airport. For more information on the model and for details on the verification test conducted, see appendix K.

There are several variables that impact the FMA results. Additionally, the current rate of false FMA alerts at TRACONs that run simultaneous independent operations is unknown to us at this time. Without considering radar error, the 10 second predictor overshoots the other approach by the amounts given in the contours below, see figure 6-21.

Figure 6-21 (a) provides the value if the aircraft performs an entire turn using a particular groundspeed and turn radius adjacent to the NTZ. Figure 6-21 (b) provides the same information, but only assumes that the aircraft performs the last 10° of the turn sufficiently close to the NTZ to cause a caution alert. The 10° restriction dramatically reduces the amount of overshoot experienced, as explained in figures 6-21 (c and d).

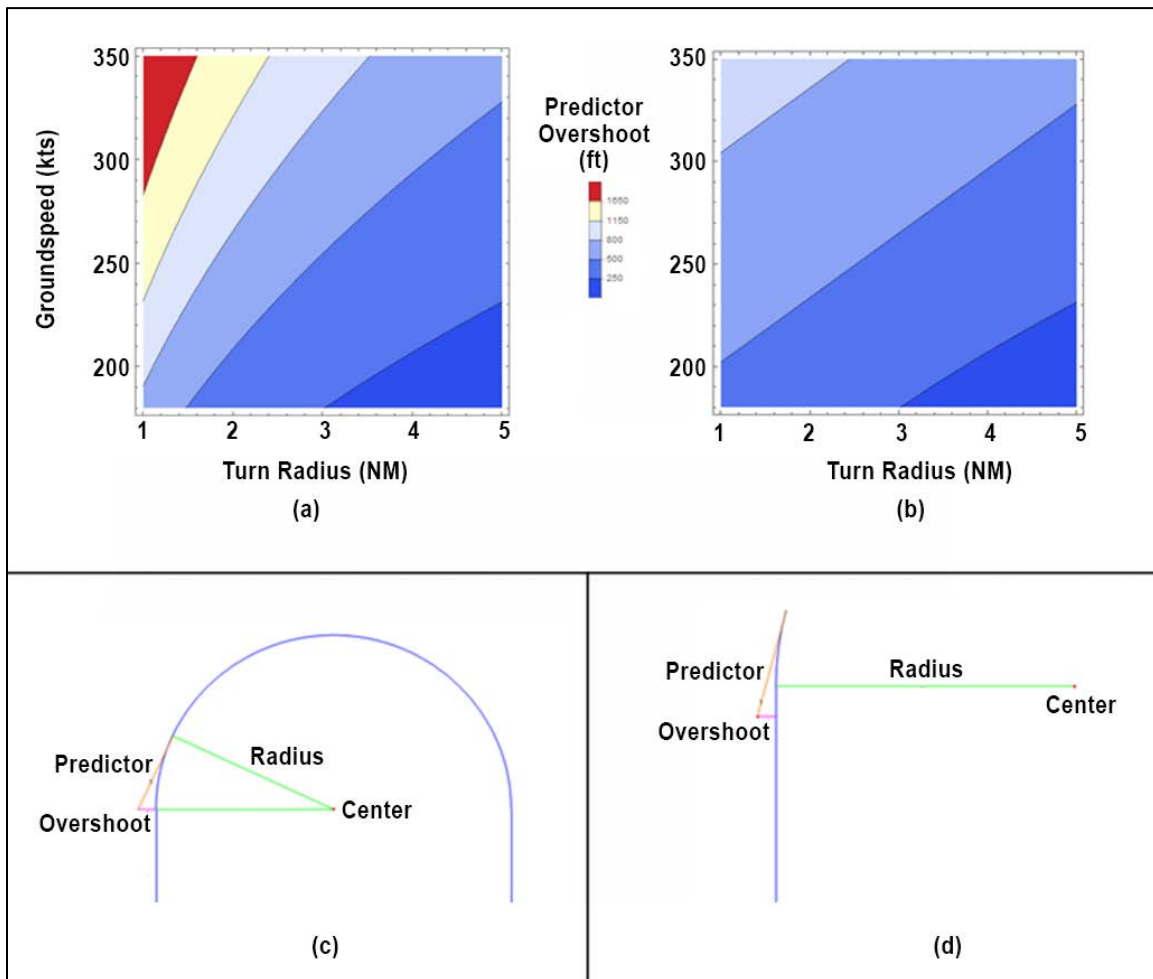


Figure 6-21: FMA 10 Second Predictor Overshoot Towards NTZ Geometry

Figure 6-22 depicts contour plots of the results including radar errors. It is clear that the 10° final approach course interception helps mitigate the rate of alerts substantially. Given the 10° intercept, it is still difficult to determine what runway spacing would result in a rate of nuisance alerts that any facility would accept. For example, if a facility where the aircraft regularly had a groundspeed of 250 knots when turning onto the final approach course wanted to keep the nuisance FMA alert rate below 1 in 1,000, they would need to have runways spaced 4,800 ft or more. If they could accept a rate of 1 nuisance alert for every 100 approaches, a runway pair spaced 4,200 ft or more would

be acceptable. Some relief from this may be provided by modifying the predictor length to less than 10 seconds, but it is unclear how much relief this would provide.

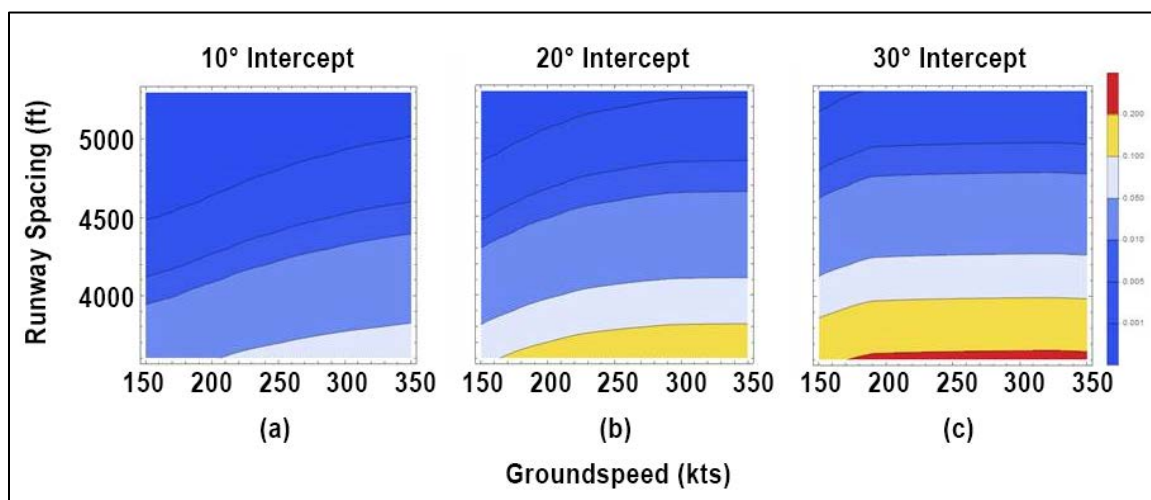


Figure 6-22: Nuisance Alert Rates (# of Nuisance Alerts / # of EoR Approaches)

6.3.2 Traffic Alert and Collision Avoidance System

TCAS is an aircraft system that identifies nearby converging traffic independently from the ground-based air traffic control system. It was designed to increase cockpit awareness of proximate aircraft and to serve as an advisory system for the prevention of mid-air collisions. TCAS provides flight crews with two types of advisories. Indications to the flight crew that a particular intruder is a potential threat are called traffic advisories, while indications that command an aircraft maneuver to provide separation from the threat are called RAs.

During an RA, evasion instructions are provided to the flight crew that should be complied with in a timely manner. If an RA is encountered during an approach procedure, the aircraft that receives the RA may require re-sequencing in order to fly the approach procedure again. The impact of receiving an RA while flying an EoR approach procedure would reduce the track miles benefits and could increase collision risk depending on the circumstances. For this reason, we evaluated the rate of nuisance TCAS RAs. Many potential mitigations of nuisance TCAS RAs were evaluated including: extending the length of the 10° leg, adding runway stagger, using RF turns, using only EoR operations adjacent to approaches along the extended final approach course, and requiring wider runway separations. Furthermore, TCAS alerts at different closure rates depending on altitude of the aircraft above ground level. When the altitude is below 2,350 ft and above 1,000 ft relative to the ground, the aircraft is in sensitivity level 3. When the aircraft is above 2,350 ft, but less than 5,000 ft above ground level, the aircraft is in sensitivity level 4.

Since TCAS was set to traffic alert-only during the pilot HITL tests, the nuisance TCAS RA rate evaluation was conducted separately. Our researchers teamed with the MITRE Center for Advanced Aviation System Development to determine what conditions could result in TCAS RAs. For each condition tested, we designed an instrument approach procedure using MITRE's Terminal Area Route Generation Evaluation and Traffic

Simulation tool. These procedures were packed by a General Electric navigation database program and flown using the CAE A320 FMS test bench. The tracks generated by the test bench were then evaluated against a validated TCAS 7.0 model to determine where RAs could occur during pairs of those operations.

An example of the location of TCAS alerts observed under one set of variables can be observed in figure 6-23 (a). The black lines depict the tracks generated by the test bench software and the blue arrows indicate the location of the TCAS alert where the line begins at the position of the victim aircraft and the arrowhead ends at the position of the intruding aircraft. Each position along each path was then converted to a distance from touchdown and, by subtracting the intruding aircraft's distance from touchdown from the victim aircraft's distance from touchdown, we calculated the relative along-track spacing at the time of the TCAS alert, plotted as blue dots in figure 6-23 (b). This means that if each aircraft receives the TCAS alert at the same distance from touchdown, whether at the apex of the turn or on the final approach course, they are considered to have zero relative along-track spacing and would be head-to-head at the time of the turn-on (removing speed variations). The TCAS RA positions were generated by the TCAS model releasing the aircraft pairs at various times, with 1 second increments for the time variation. To account for this time variation, we selected a distance of 250 ft as a value sufficient to convert the discrete observed TCAS RAs to a region of high TCAS RA risk. Each identified TCAS alert location with the 250 ft buffer can be seen as red line segments in figure 6-23 (b). By dividing the length of the high risk region by the total possible number of positions for along-track spacing, we estimate the nuisance TCAS RA rate. The risk region at the top of figure 6-23 (b), which results from the union of the segments under it, is plotted in figure 6-23 (c) adjacent to an orange line segment representing all equally likely along-track configurations given standard along-track separation. This captures the intuitive understanding that a head-to-head pair will most likely generate a TCAS RA, but a pair with 1 NM dependent stagger is not likely to generate a TCAS RA. With this analysis, we estimate how close to a head-to-head configuration aircraft need to be to generate nuisance TCAS RAs.

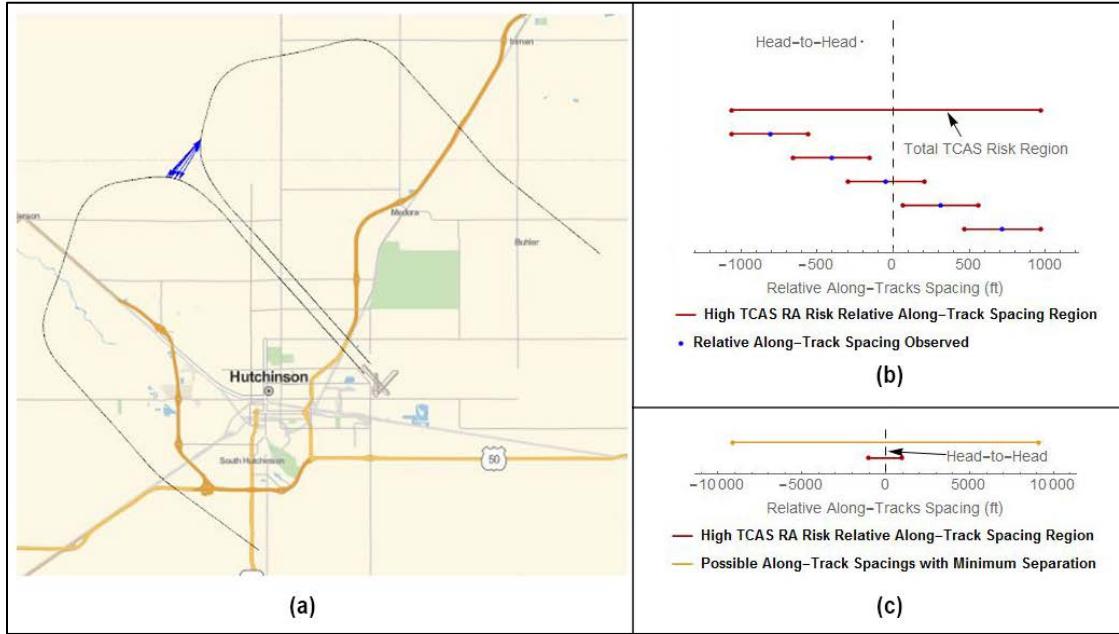


Figure 6-23: TCAS Rate Calculation Method

Previous studies have identified that TCAS RA rates in excess of 3% can significantly reduce expected capacity gains at airports that support simultaneous independent operations. [13] The nuisance TCAS RA rate observed in practice across the National Airspace System may vary with differing runway spacings and airport elevations. [26] Table 6-7 shows that adding length to the 10° intercept leg reduces the TCAS RA rate, but RAs should not be generated for safe runway spacings if the aircraft flies the 50° turn below 2,350 ft above ground level. Note that in all of these tables, there is a substantial amount of error in the TCAS RA rate due to variations in aircraft speeds during track generation. Readers should avoid over-interpreting small variations that are contrary to the overall trends observed in the tables.

Table 6-7: 10° Interception Added Leg Length TCAS RA Rate; Sensitivity Level 3

Added 10° Leg Length (NM)	Runway Spacing 0 ft	Runway Spacing 500 ft	Runway Spacing 1,000 ft	Runway Spacing 1,500 ft	Runway Spacing 2,000 ft	Runway Spacing 2,500 ft	Runway Spacing 3,000 ft	Runway Spacing 3,500 ft
0	51.8%	47.6%	43.6%	39.4%	35.1%	28.6%	20.3%	0.0%
1	37.5%	35.4%	23.9%	19.9%	0.0%	0.0%	0.0%	0.0%
2	26.6%	26.9%	22.3%	15.7%	0.0%	0.0%	0.0%	0.0%
3	28.8%	26.7%	22.2%	18.0%	0.0%	0.0%	0.0%	0.0%

Table 6-8 demonstrates the key behavior associated with extending the 10° intercept demonstrates the key behavior associated with extending the 10° intercept leg. The row where the length added to the 10° interception leg is 0 generates RAs when the aircraft is on the 50° turn. If that leg is extended by 1 NM, the rates drop drastically as the location where RAs occur changes to the 10° interception. In summary, if the procedure is designed to turn on to the final approach above 2,350 ft above ground level, that is when

TCAS is in sensitivity level 4, then there must be at least 1 NM of extra length added to the 10° leg to prevent RAs when the runway spacing is less than 7,000 ft.

Table 6-8: 10° Interception Added Leg Length TCAS RA Rate; Sensitivity Level 4

Added 10° Leg Length (NM)	Runway Spacing 1,000 ft	Runway Spacing 2,000 ft	Runway Spacing 3,000 ft	Runway Spacing 4,000 ft	Runway Spacing 5,000 ft	Runway Spacing 6,000 ft	Runway Spacing 6,500 ft	Runway Spacing 7,000 ft
0	74.5%	65.6%	57.3%	48.6%	39.9%	20.0%	4.84%	0.0%
1	56.9%	41.2%	28.4%	27.4%	0.0%	0.0%	0.0%	0.0%
2	60.3%	55.4%	22.5%	0.0%	0.0%	0.0%	0.0%	0.0%
3	61.5%	52.7%	33.5%	0.0%	0.0%	0.0%	0.0%	0.0%

Similar to the 10° interception extension case, the procedure stagger at sensitivity level 3, seen in table 6-9, always falls below 3,600 ft. However, the general effect of procedure stagger is clear: staggers help reduce TCAS RAs.

Table 6-9: Procedure Stagger TCAS RA Rate; Sensitivity Level 3

Procedure Stagger (NM)	Runway Spacing 0 ft	Runway Spacing 500 ft	Runway Spacing 1,000 ft	Runway Spacing 1,500 ft	Runway Spacing 2,000 ft	Runway Spacing 2,500 ft	Runway Spacing 3,000 ft	Runway Spacing 3,500 ft
0	51.8%	47.6%	43.6%	39.4%	35.1%	28.6%	20.3%	0.0%
0.6	47.8%	45.8%	41.6%	37.5%	33.2%	24.5%	7.21%	0.0%
0.9	64.4%	60.6%	50.0%	5.12%	0.0%	0.0%	0.0%	0.0%
1.2	58.3%	55.8%	49.9%	36.9%	8.85%	0.0%	0.0%	0.0%

Table 6-10 shows the same pattern; however, it also shows that small staggers can somewhat increase the nuisance TCAS rate. This analysis indicates that adding two or more NM of procedure stagger would reduce the RA rate such that a 3,500 ft or 4,000 ft runway spacing would have an acceptably low RA rate, even if the procedure was designed to turn on above 2,350 ft above ground level.

Table 6-10: Procedure Stagger TCAS RA Rate; Sensitivity Level 4

Procedure Stagger (NM)	Runway Spacing 1,000 ft	Runway Spacing 2,000 ft	Runway Spacing 3,000 ft	Runway Spacing 3,500 ft	Runway Spacing 4,000 ft	Runway Spacing 5,000 ft	Runway Spacing 5,500 ft	Runway Spacing 6,000 ft
0	74.5%	65.6%	57.3%	48.6%	39.9%	4.84%	0.00%	0.0%
0.5	83.1%	74.4%	57.1%	45.6%	39.1%	28.2%	19.9%	0.0%
0.75	72.5%	67.5%	55.3%	41.4%	34.7%	20.4%	2.74%	0.0%
1	74.6%	68.2%	57.6%	37.0%	28.3%	0.0%	0.0%	0.0%
2	61.1%	50.4%	30.6%	21.1%	0.0%	0.0%	0.0%	0.0%
3	59.6%	53.3%	31.4%	18.3%	0.0%	0.0%	0.0%	0.0%

Other results indicated that introducing vertical stagger between the turn-ons made no difference unless the vertical stagger was 600 ft or larger, in which case no TCAS RAs

were observed. Runway staggers or level segments would have to exceed 1.88 NM to introduce the necessary amount of vertical separation.

In short, extending the 10° intercept leg, ensuring that the turn on occurred when the aircraft was below 2,350 ft above ground level (sensitivity level 3 or below), or staggering the procedure turn-ons by at least 2 NM was effective for eliminating nuisance TCAS RAs.

6.3.3 Instrument Approach Procedure Design

A prototype procedure design was developed for these tests. The FAA conducted several outreach meetings with industry and considered several operational factors in developing the prototype procedure design. The selected design used four fly-by turns to transition from the downwind initial approach segment to the aligned final approach segment: a 60° turn (1st), a second 60° turn (2nd), a 50° turn (3rd), and a final 10° turn (4th). The 10° turn was selected to improve the effectiveness of the collision risk mitigations and improve compatibility with existing traffic alerting systems. Based on accepted procedure design practices and stakeholder feedback, the prototype procedure design included an at or below 210 knot speed restriction at the IAF and an at or below 180 knot speed restriction at the 10° turn waypoint. The test EoR configuration used symmetric, head-to-head, and co-altitude approach procedures as it was assumed to represent the worst-case scenario for test purposes, see figures B-2 and B-3 in appendix B.

As stated in section 3, this procedure design also compared the current tracks at all qualifying airports to confirm that it was compatible with the existing ground tracks. Part of the initial design was to mimic an RF turn with consecutive TF fly-by turns. From January through April 2014, the Area Navigation Visual Flight Procedures program at Hartsfield-Jackson Atlanta International Airport provided an initial operational demonstration of the EoR concept. [27] This information aided the selection of a TF turn procedure with the additional goal to maximize fleet participation.

Creation of the procedure utilized the Instrument Procedures Development System Version 2.0.6 software which implements criteria from the FAA 8260.54A order, *The United States Standard for Area Navigation*, with modifications from the FAA 8260.58 order, *United States Standard for Performance Based Navigation (PBN) Instrument Procedure Design*. [28, 29] The FAA currently utilizes the Instrument Procedures Development System software tool to produce all RNAV (GPS) procedures. This software was used to generate the shortest feasible path for an RNAV (GPS) procedure using TF legs without resulting in a failure on obstacle evaluation area construction. Adjustments in procedure speeds, bank angles, and winds will adjust the turn distance of turn anticipation and obstacle evaluation area construction. This method of route construction is as close to publishable as possible, in order to achieve more representative test data.

The length of the final 10° leg was calculated to provide minimum path length. In the final implementation it can be adjusted to mitigate a variety of additional risk and acceptance factors. TCAS, FMA, and downwind leg distance are major acceptance factors for procedure implementation and are all directly affected by this leg length.

The downwind leg distance, which is the perpendicular distance from the final approach course to the downwind leg, is a factor in operational acceptance. If the final procedure

design does not overlay with existing downwind legs, then additional environmental surveys may be required to implement an EoR operation. Site specific implementations can take advantage of local effects to better match to existing procedure designs. In cooperation with MITRE, we looked at in-service flight data of airports with parallel runways to determine where existing downwind legs were located and estimated where the test procedure's downwind leg distance may be a problem. MITRE was tasked to investigate this data and provided downwind leg distance distributions. Figure 6-24 shows where implementation problems may occur as a result of this data. The downwind estimates represented by the black lines in figure 6-24 may be optimistic because they only use the minimum leg length calculations in FAA Order 8260.58, but they do not consider any additional restrictions on minimum leg length from obstacle evaluation area construction. [29] This evaluation of the obstacle evaluation area construction was substantially more complex and, at the time of the study, it could only be evaluated by manually building the approach procedure in the Instrument Procedures Development System.

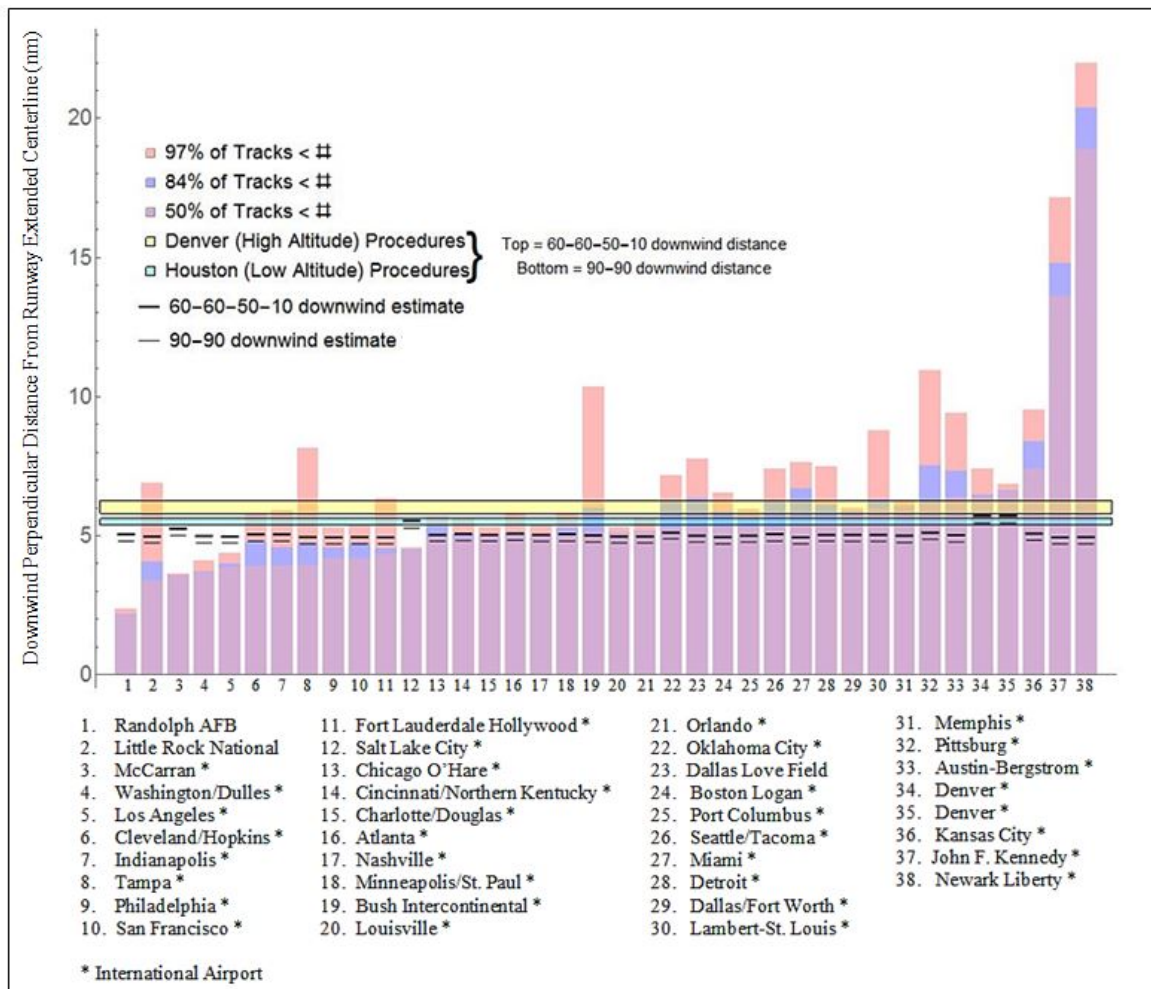


Figure 6-24: Downwind Leg Distance Acceptance Estimation

The vertical axis represents the downwind perpendicular distance from the runway extended centerline. The horizontal axis is binned by each airport surveyed. The colored

vertical bars represent the quantile of tracks that were at a particular downwind distance. The horizontal boxes show estimates of downwind procedure distances, as well as the lines in each of the bars. This visually shows where procedure designs may be problematic for overlaying with existing procedures, noting that the final procedure design may be different from the test procedure design.

For example, in figure 6-24 you can see that at Tampa International Airport (8th bar from the left), 84% of downwind distances are at or below 4.5 NM, which is below all the estimated procedure downwind distances, but 97% of the downwind distances are at or below approximately 8 NM, which is a few miles farther out than the estimated procedure design. If the 84% matches the true downwind leg, then the procedure design is unlikely to cause implementation problems. If the 97% matches the true downwind leg distance, then the procedure design is likely to cause implementation problems.

7 Key Findings and Conclusions

For the runway and approach geometries analyzed, the EoR operations meet the FAA acceptable level of collision risk of 1×10^{-9} per operation for dual parallel runway configurations spaced 3,600 ft or greater, and for triple parallel runway configurations spaced 3,900 ft or greater. EoR operations to runways spaced 9,000 ft or less require an FMA with an NTZ, while operations to runways spaced more than 9,000 ft meet the acceptable level of collision risk without an FMA. Dual EoR operations based on RNAV (GPS) procedures require a 10° intercept of the extended final approach course, and may also be performed adjacent to a straight-in procedure to one of the runways. Triple EoR operations require the 10° intercept on either or both outside runways, and a straight-in approach to the center runway. These results apply to GPS based RNAV and RNP aircraft with or without vertical guidance using TF fly-by turn procedure design, and may be combined with ILS or GLS straight-in approaches. In addition to this conclusion, the following key findings should be considered:

- A 10° intercept of the final approach course and an at-or-below 210 knot speed restriction on the downwind leg are required to prevent consistent overshooting of the extended runway centerline;
- Extending the length of the 10° intercept leg, decreasing the angle of the turn prior to the 10° intercept leg, or increasing the runway spacing are effective methods to further reduce collision risk;
- An aircraft should not be considered established on an approach unless the procedure is designed such that the controller can verify that the flight crew is flying the approach for which they were cleared;
- RNP of 1 NM is acceptable for the turn to the final approach segment, provided GPS and autopilot or flight director are required;
- VNAV capability may reduce crew workload;
- Publishing an “at altitude” restriction near the apex of the EoR turn can improve operational performance and slightly reduce collision risk if this simulates a descent angle between 2° and 3° . Compatibility with aircraft automation may impact the suitability of altitude restrictions;
- Controller intervention is a more effective mitigation when the heading change of the turn immediately preceding the 10° intercept leg is 50° or less;
- An aspect ratio of 3:1, used in less than 4,300 ft parallel approach operations, may not be appropriate for curved operations such as EoR;
- Modifying the FMA and displays to more closely match the EoR operating concept may considerably improve the controller reaction time;
- Controller interventions may better maintain aircraft-to-aircraft separation by issuing a specific heading when directing a go-around, rather than flying the published lateral track;
- Head-to-head configurations may not be compatible with TCAS, particularly at close runway spacings, and were not preferred by the controllers;
- FMA and TCAS may generate nuisance alerts especially if the length of the 10° intercept leg is not sufficient to keep high convergence areas separated; and
- Extending the 10° intercept leg, ensuring that the turn-on occurred when the aircraft was below 2,350 ft above ground level (sensitivity level 3 or below), or staggering the procedure turn-ons by at least 2 NM were effective for eliminating nuisance TCAS RAs on EoR approaches.

Some of the deviations that we experienced in our pilot test were a product of the non-subject controllers instructing the pilots to return to the RNAV path. The rate of significant lateral path deviations during the implemented EoR operations may be further reduced if controllers consistently vector aircraft that report non-normal conditions instead of relying on pilots to return to the approach.

The collision risk in this study does not incorporate the risk of wrong runway selection. The risk of a pilot flying the wrong approach can be eliminated through procedure design alone by ensuring an aircraft is on a path that is unique to the intended landing runway prior to being considered established on the approach. Procedure designs that do not incorporate this concept will invalidate the collision risks presented in this report unless mitigations are evaluated and validated via a safety assessment involving all stakeholders.

This study focused on the risk of aircraft-to-aircraft collision. Operational considerations due to FMA, TCAS, and controller workload were included to consider their impact on the implementation of this operation. No other safety risks, such as controlled flight into terrain or wake vortex encounter, were evaluated. This study did not evaluate the collision risk of instrument approach procedures that include radius-to-fix legs.

8 References

1. FAA Performance Based Navigation Simultaneous Independent Established on RNP Concept of Operations, Final Version 1.0, Prepared by Digital iBiz, August 22, 2014. (draft)
2. PARC RNP Benefits Sub-Team “RNP Established – Parallel Approach”, Prepared by the Performance-Based operations Aviation Rulemaking Committee, January 10, 2011.
3. TORP 1294/Task Order 8 Greener Skies i2 Final Report, Revision Version 1.0, Prepared by Boeing SE2020 Task Order 8/TORP 1294 Team, March 31, 2014.
4. FAA Report DOT-FAA-AFS-400-89, Established on Required Navigation Performance Human in the Loop Data Collection for Dependent Simultaneous Operations with Runways Spaced 2,500’ at Seattle, Washington, prepared by the Flight Systems Laboratory, May 2014.
5. Waiver to FAA JO 7110.65 Paragraphs 5-9-6a.1 and 5-9-6b.1, Seattle TRACON Simultaneous Dependent Approaches, August 21, 2014.
6. FAA Memorandum 14-0314-54799, Required Navigation Performance Authorization Required Curved Path Approaches to Widely Spaced Runways, June 24, 2014.
7. FAA Memorandum, Request for Waiver to FAA Order JO 7110.65, Simultaneous Independent Approaches to Widely Spaced Parallel Runways without Final Monitors, for Denver Airport Traffic Control Tower (DEN ATCT) and Denver Terminal Radar Approach Control (D01 TRACON), your request dated November 19, 2014, March 11, 2015.
8. Established on Required Navigation Performance (RNP) Concept Research and Analysis Plan, Identification of Implementation Challenges and Corresponding Mitigation Strategies, and a Simulation Methodology to Assess the Impact of Each, Prepared by The MITRE Corporation, December 2014.
9. Established on RNP (EoR) Utilization Modeling Methodology and Validation, Prepared by The MITRE Corporation, June 2015.
10. Methodology for Established on Required Navigation Performance (RNP) Concept Validation for a Widely Spaced Parallel Runway Operation, A Plan for Assessing the Impact of an Established on RNP (EoR) Operation throughout the National Airspace System (NAS) with Particular Focus on Denver as a Development Site, Prepared by The MITRE Corporation, revised May 2015.
11. Methodology for Established on Required Navigation Performance (RNP) Concept Validation for a Dependent Parallel Runway Operation, A Plan for Assessing the Impact of an Established on RNP (EoR) Operation throughout the National Airspace System (NAS) with Particular Focus on Seattle as a Development Site, Prepared by The MITRE Corporation, revised May 2015.
12. DOT/FAA/RD-91/5, Precision Runway Monitor Demonstration Report, Precision Runway Monitor Program Office, ARD-300, February 1991.

13. FAA Report DOT-FAA-AFS-450-69, Simultaneous Independent Close Parallel Approaches – High Update Radar Not Required, Prepared by the Flight Systems Laboratory, September 2011.
14. NASA Contractor Report 191549, Volume 1, Parallel Runway Requirement Analysis Study, December 1993.
15. RTCA DO-236C, Minimum Aviation System Performance Standards: Required Navigation Performance for Area Navigation, appendix B, June 19, 2013.
16. FAA Advisory Circular 90-105, Approval Guidance for RNP Operations and Barometric Vertical Navigation in the U.S. National Airspace System, January 23, 2009.
17. FAA JO 7110.65W, Air Traffic Control, U.S. Department of Transportation/Federal Aviation Agency/Air Traffic Organization Policy, December 2015.
18. DOT FAA Aeronautical Information Manual, section 5-4-16 Simultaneous Close Parallel ILS/RNAV/GLS PRM Approaches (Independent) and Simultaneous Offset Instrument Approaches (SOIA), paragraph d Attention All Users Page (AAUP) 2 (e) (4) (f) (3). April 3, 2014.
19. Safety Management System Manual Version 4.0, Air Traffic Organization, May 30, 2014.
20. FAA Report DOT-FAA-AFS-450-63, Geometrical Models for Aircraft in Terminal Area Risk Analyses, prepared by the Flight Systems Laboratory, April 2011.
21. FAA Advisory Circular 25.1309-1A, System Design and Analysis, June 21, 1988.
22. FAA Advisory Circular 20-138D, Airworthiness Approval of Positioning and Navigation Systems, March 28, 2014.
23. “Typical Error and Atypical Error of GNSS Aircraft and the PBN RNP Navigation Performance Requirements”, by Dr. Geoffrey Aldis and Robert Butcher, Australia, Separation and Airspace Safety Panel, 20th Meeting, Montreal, Canada, May 14-25, 2012.
24. “GPS Accuracy Based on Q-Routes in the Gulf of Mexico”, by Richard Greenhaw and Madison Walton, FAA, Separation and Airspace Safety Panel, 18th Meeting, Brussels, Belgium, November 8-19, 2010.
25. FAA Report DOT-FAA-AFS-400-85, Separation Requirements for Triple Simultaneous Independent Close Parallel Approaches – High Update Rate Surveillance Not Required, prepared by the Flight Systems Laboratory, September 2014.
26. TOPA Report #12: October 2013 – September 2014, Massachusetts Institute of Technology Lincoln Laboratory, December 31, 2014.
27. "Characterizations of navigation performance in terminal performance-based navigation operations," in Digital Avionics Systems Conference (DASC), by Mayer, R.H.; Zondervan, D.J.; Hudak, T.B., 2014 IEEE/AIAA 33rd , vol., no., pp.3E3-1-3E3-11, 5-9, October 2014.

28. FAA Order 8260.54A, United States Standard for Performance Based Navigation (PBN) Instrument Procedure Design.
29. FAA Order 8260.58, United States Standard for Performance Based Navigation (PBN) Instrument Procedure Design.
30. FAA Report DOT-FAA-AFS-450-73, Comparative Evaluation of Lateral Flight Technical Error for Instrument Landing System and Localizer Only Approaches, prepared by the Flight Systems Laboratory, August 2011.
31. FAA Report DOT/FAA/AFS400/2016/R/02, Vertical Navigation Requirement for Simultaneous Independent Parallel Instrument Approaches to Closely Spaced Parallel Runways, prepared by Flight Systems Laboratory, June 2016. (Awaiting Publication)

Appendix A: Flight Crew Demographics

Appendix A includes two tables on flight crew demographics. The first table lists data for the pilot phase 1 HITL test and the second table lists data for the pilot phase 2 HITL test. Each table shows the crew number, the aircraft type, and the flight crew's hours, broken down into captain and first officer flight hours.

Table A-1 depicts the demographic data for 10 VNAV1 and 9 VNAV2 flight crews. The captain in crew 3 and the first officer in crew 5 were experienced in a VNAV2 variant (A320 vs A330, for example). There were some differences in the VNAV2 aircraft simulator operation and performance that did not negatively affect the data collected.

Due to last minute cancellations, an FAA substitute pilot was used to complement the aircrew. The captain position for crew 7 was filled in this manner as well as the first officer position on crews 13 and 14. Some flight crews did not provide their flight hours, as noted by the "No Info" double dashed line for the captain's position in crews 11, 12, and 18, and the first officer's position in crews 4, 11, 12, and 15.

Table A-2 is complete with all requisite information for the non-VNAV flight crews.

Table A-1: Pilot Test Phase 1

***A320 Current **FAA Substitute Pilot --No Info**

Crew #	Aircraft Type	Captain Hours	First Officer Hours
1	VNAV2	3000	7000
2	VNAV2	8500	5000
3	VNAV2	*	400
4	VNAV2	300	--
5	VNAV2	5000	10000*
6	VNAV2	4000	6000
7	VNAV2	**	490
8	VNAV2	650	1700
9	VNAV2	1000	1000
10	N/A	N/A	N/A
11	VNAV1	--	--
12	VNAV1	--	--
13	VNAV1	9500	**
14	VNAV1	2100	**
15	VNAV1	4300	--
16	VNAV1	9000	865
17	VNAV1	10000	6600
18	VNAV1	--	6500
19	VNAV1	3500	2200
20	VNAV1	10000	2100

Table A-2: Pilot Test Phase 2

Crew #	Aircraft Type	Captain Hours	First Officer Hours
1	Non-VNAV	8300	2400
2	Non-VNAV	10000	500
3	Non-VNAV	4000	2000
4	Non-VNAV	5500	3300
5	Non-VNAV	10000	2000
6	Non-VNAV	2500	3700
7	Non-VNAV	8200	1500
8	Non-VNAV	5200	300
9	Non-VNAV	3000	6600

Appendix B: Scenario Matrix List for Phase 1 Pilot Test

This appendix describes the elements of the 26 simulator runs that each flight crew flew in the simulator for the phase 1 pilot test. The simulator runs were split evenly between the captain and first officer. The first two runs were warm-up flights for the captain and the first officer to become acquainted with the EoR procedure. The remaining 12 runs for each flight crew member were flown to runway 35L or 35R, with 9 runs in IMC and 3 in MVMC. The 12 runs were divided equally using autopilot and flight director for flight guidance.

There were five scenarios flown that included malfunctions, breakouts, and go-arounds. The malfunctions were categorized as flight guidance failures (MAL1) or energy management issues (MAL2). Each of these scenarios occurred at points along the approach track called event positions. Figure B-1 shows the event positions as A, B, C, or D. MAL1 events occurred at positions B or D, whereas MAL2 events occurred somewhere between positions B-A or D-B.

The scenarios used were:

- Nominal (no malfunctions): Runs 3, 4, 5, 6, 15, 16, 17, and 18. An alternate airspeed profile was directed by controllers on runs 5 and 17, and flight crews were directed to fly 210 knots from when they checked-in for the approach until point A. Controllers used the command, “INCREASE AIRSPEED TO 210 UNTIL FURTHER ADVISED”;
- MAL1 failure: Autopilot failure occurred on run 7 at point D, and run 8 at point B. A flight director failure occurred on run 19 at point D and run 20 at point B;
- MAL2 energy management problems: A wind gust up to 105 knots and increased turbulence was introduced in runs 9 and 21 from position B to A, and on runs 10 and 22 from position D to B;
- Breakout: Breakout instructions were issued by controllers in runs 11 and 23 at point A, and in runs 12 and 24 at point C. Breakout instructions were given in two different phraseologies and are noted in the table as P1 and P2:
 - P1: “TRAFFIC ALERT, (call sign), TURN (left/right) IMMEDIATELY HEADING (degrees), CLIMB AND MAINTAIN (altitude)”;
 - P2: “(Call sign), TURN (left/right) IMMEDIATELY HEADING (degrees), CLIMB AND MAINTAIN (altitude).”

Additionally in run 23, an alternate speed profile of 210 knots was assigned by the controller from initial check-in to point A; and

- Go-around: Controllers directed flight crews to go-around on runs 13 and 25 at point A, and on runs 14 and 26 at point C. Controllers used the phraseology: “(call sign), CANCEL APPROACH CLEARANCE, FLY THE RNAV TRACK. CLIMB AND MAINTAIN ONE ZERO THOUSAND.” Additionally in run 13, an alternate speed profile of 210 knots was assigned by the controller from initial check-in to point A.

To read table B-1, which is the scenario matrix list used during the phase 1 pilot test, here are two examples:

- Run 9 was flown using scenario 3 by the captain on autopilot in IMC to runway 35L. A MAL2 (energy management) problem was given to the flight crew between point B and point A; and

- Run 23 was flown using scenario 4 by the captain on flight director in IMC to runway 35L. An alternate speed profile was assigned and a breakout was directed at point A using phraseology P2.

Table B-1: Scenario Matrix List for Phase 1 Pilot Test

Run	Scenario	Pilot Flying (PF)	Autopilot / Flight Director (AP/FD)	Weather Conditions	RWY	Alt Speed Profile	Nominal	MAL1: Flight Guidance	MAL2: Energy Management	Breakout	Go-around
1	Warm-up	Captain (CA)		IMC	RWY35L						
2	Warm-up	First Officer (FO)		MVMC	RWY35R						
3	1	CA	AP	IMC	RWY35R		X				
4	1	FO	AP	MVMC	RWY35L		X				
5	1	CA	AP	IMC	RWY35L	X	X				
6	1	FO	AP	IMC	RWY35R		X				
7	2	CA	AP	MVMC	RWY35R			D			
8	2	FO	AP	IMC	RWY35L			B			
9	3	CA	AP	IMC	RWY35L				B-A		
10	3	FO	AP	IMC	RWY35R				D-B		
11	4	CA	AP	IMC	RWY35R					A P1	
12	4	FO	AP	MVMC	RWY35L					C P2	
13	5	CA	AP	IMC	RWY35L	X					A
14	5	FO	AP	IMC	RWY35R						C
15	1	CA	FD	IMC	RWY35L		X				
16	1	FO	FD	IMC	RWY35R	X	X				
17	1	CA	FD	IMC	RWY35R		X				
18	1	FO	FD	MVMC	RWY35L		X				
19	2	CA	FD	IMC	RWY35L			D			
20	2	FO	FD	IMC	RWY35R			B			
21	3	CA	FD	IMC	RWY35R				B-A		

22	3	FO	FD	MVMC	RWY35L				D-B		
23	4	CA	FD	IMC	RWY35L	X				A P2	
24	4	FO	FD	IMC	RWY35R					C P1	
25	5	CA	FD	IMC	RWY35R						A
26	5	FO	FD	MVMC	RWY35L						C

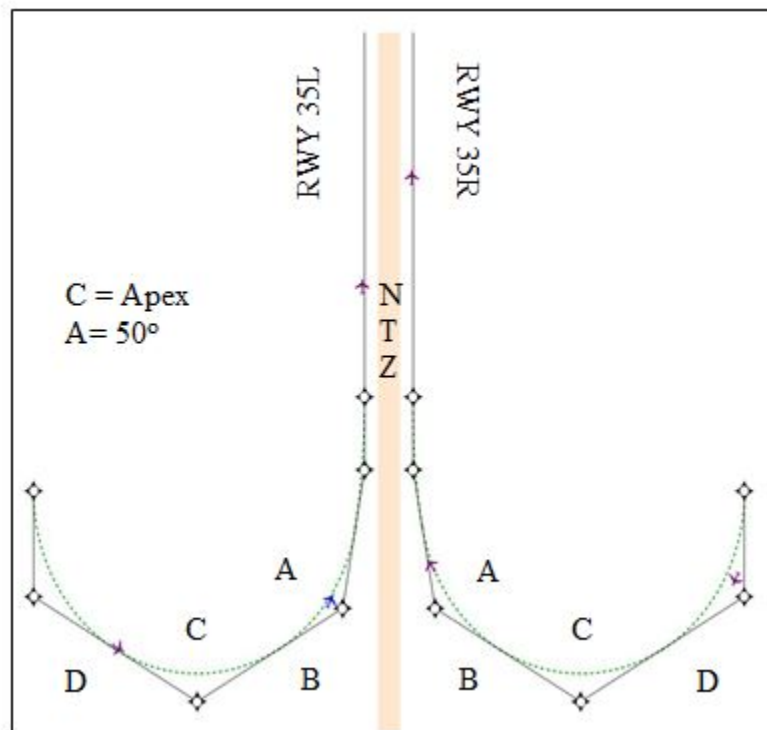
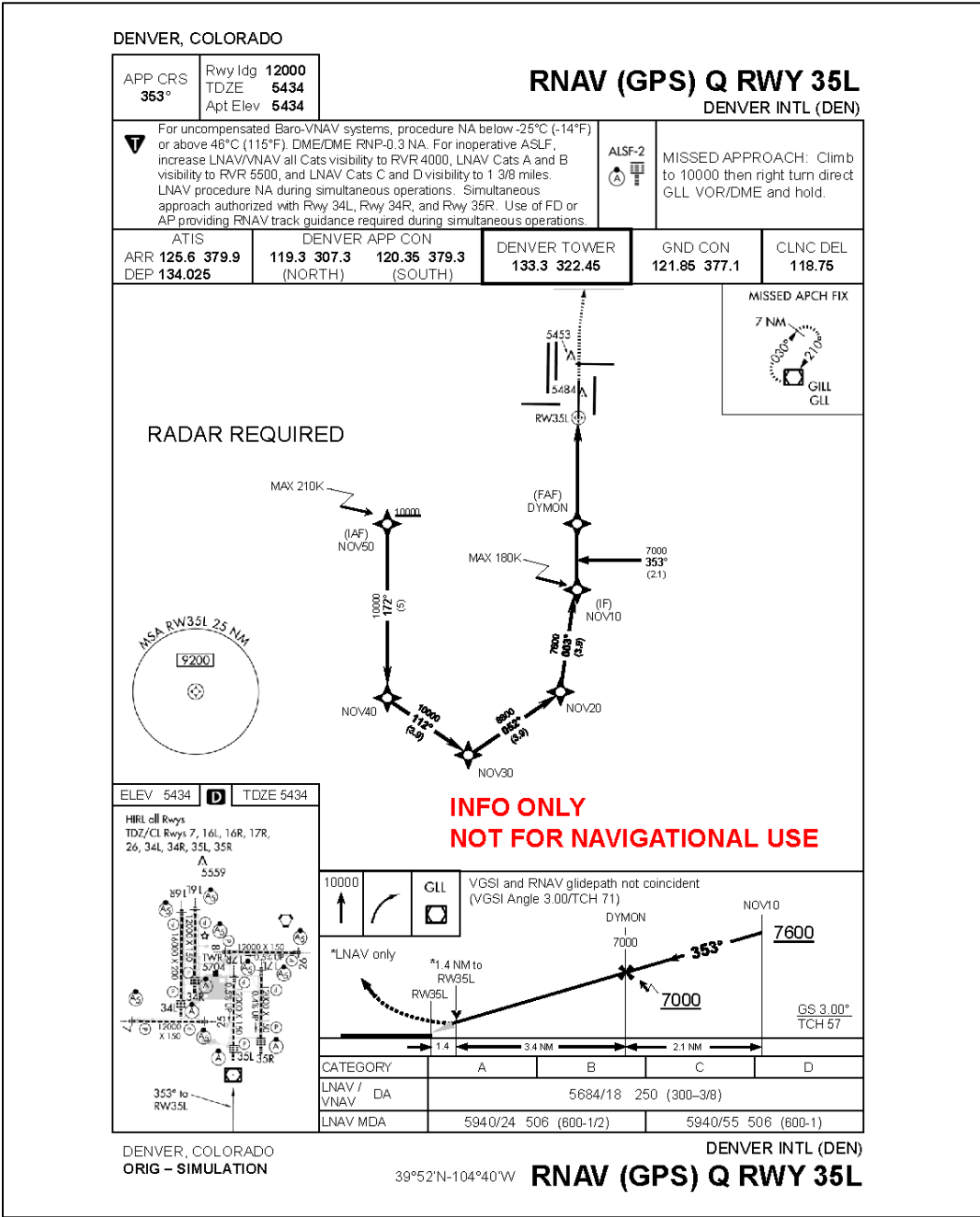


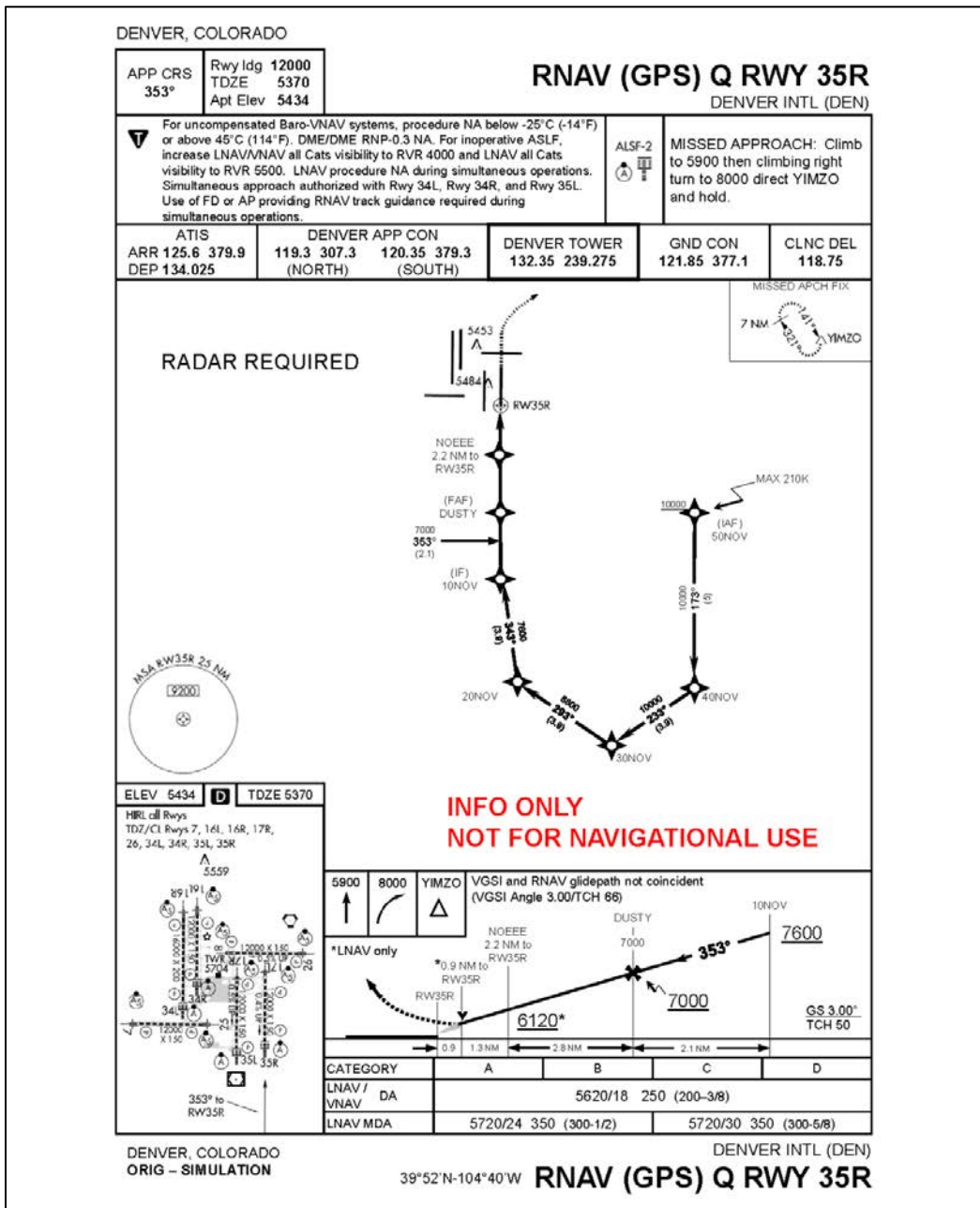
Figure B-1: Event position

Figures B-2 and B-3 are full size HITL test approach plates that describe the EoR approach procedures and the coordinates for the waypoints.



Waypoint	Latitude	Longitude
NOV50 (IAF)	39°44'04.699" N	104°49'20.142" W
NOV40 (IAF)	39°39'04.461" N	104°49'22.993" W
NOV30 (IAF)	39°37'05.785" N	104°45'01.873" W
NOV20 (IAF)	39°39'01.120" N	104°40'39.263" W
NOV10 (IF)	39°44'57.470" N	104°39'42.897" W
DYMON (LNAV/VNAV)	39°44'57.470" N	104°39'41.390" W
DYMON (LNAV - PFAF)	39°44'57.470" N	104°39'41.390" W
RWY35L	39°49'41.926" N	104°39'37.984" W

Figure B-2: Runway 35L Approach Plate and Waypoint Coordinates



Waypoint	Latitude	Longitude
50NOV (IAF)	39°43'55.863" N	104°28'56.423" W
40NOV (IAF)	39°38'55.636" N	104°29'00.835" W
30NOV (IAF)	39°37'00.752" N	104°33'24.769" W
20NOV (IAF)	39°38'59.872" N	104°37'45.545" W
10NOV (IF)	39°42'51.373" N	104°38'35.338" W
DUSTY (LNAV/VNAV)	39°44'56.980" N	104°38'33.800" W
DUSTY (LNAV - PFAF)	39°44'56.980" N	104°38'33.800" W
RWY35R	39°49'55.271" N	104°38'30.155" W

Figure B-3: Runway 35R Approach Plate and Waypoint Coordinates

Appendix C: Scenario Matrix for Phase 2 Pilot Test

This appendix lists the 26 simulator runs that each flight crew flew in the simulator for the phase 2 pilot test. This appendix can be read similar to appendix B.

Table C-1: Scenario Matrix for Phase 2 Pilot Test

Run	Scenario	Pilot Flying (PF)	Flight Director (AP/FD)	Weather Conditions	RWY	Air Speed Profile	Nominal	AHRS Failure	A/P Fail	Energy Management	Break-out	Go-around
1	Warm-up	CA		IMC	RWY 35L							
2	Warm-up	FO		MVMC	RWY 35R							
3	1	CA	AP	IMC	RWY 35R		X					
4	1	FO	AP	MVMC	RWY 35L		X					
5	1	CA	AP	MVMC	RWY 35L	X	X					
6	1	FO	AP	IMC	RWY 35R		X					
7	2	CA	AP	MVMC	RWY 35R			D				
8	2	FO	AP	IMC	RWY 35L			B				
9	3	CA	AP	IMC	RWY 35L					B-A		
10	3	FO	AP	IMC	RWY 35R					D-B		
11	4	CA	AP	IMC	RWY 35R						A	
12	4	FO	AP	IMC	RWY 35L						A	
13	2	CA	AP	IMC	RWY 35L				A			
14	2	FO	AP	MVMC	RWY 35R				C			
15	1	CA	FD	IMC	RWY 35L		X					
16	1	FO	FD	MVMC	RWY 35R	X	X					
17	1	CA	FD	MVMC	RWY 35R		X					
18	1	FO	FD	IMC	RWY 35L		X					
19	2	CA	FD	IMC	RWY 35L			D				
20	2	FO	FD	MVMC	RWY 35R			B				
21	3	CA	FD	IMC	RWY 35R					B-A		
22	3	FO	FD	IMC	RWY 35L					D-B		
23	4	CA	FD	IMC	RWY 35L	X					A	

24	4	FO	FD	IMC	RWY 35R							A	
25	5	CA	FD	IMC	RWY 35R								A
26	5	FO	FD	IMC	RWY 35L								C

Appendix D: Post-Run Questionnaire for Pilot Tests

DATE: _____ CREW #: _____ RUN: _____ SCENARIO: _____ PF/PM

1. Compared to your typical approach, rate the level of difficulty performing this operation.

Much Easier		Somewhat Easier		Same as Typical Approach		Somewhat More Difficult		Much More Difficult
1	2	3	4	5	6	7	8	9

2. How comfortable were you while flying a simultaneous independent parallel approach with no required vertical separation with an aircraft on the adjacent approaches compared to a typical approach?

Much More Comfortable		Somewhat More Comfortable		Same as Typical Approach		Somewhat More Uncomfortable		Much More Uncomfortable
1	2	3	4	5	6	7	8	9

3. Compared to your typical approach, how comfortable were you after recognizing an anomaly has occurred?

Much More Comfortable		Somewhat More Comfortable		Same as Typical Approach		Somewhat More Uncomfortable		Much More Uncomfortable
1	2	3	4	5	6	7	8	9

4. Compared to an approach without an anomaly, how comfortable were you with having to react to an anomaly and/or adjust your flight profile?

Much More Comfortable		Somewhat More Comfortable		Same as Typical Approach		Somewhat More Uncomfortable		Much More Uncomfortable
1	2	3	4	5	6	7	8	9

5. Compared to your typical approach, rate your perceived level of individual workload for this procedure from the standpoint of communication, coordination, and procedural habit patterns throughout the approach.

Much Lower Workload		Somewhat Lower Workload		Same as Typical Approach		Somewhat Higher Workload		Much Higher Workload
1	2	3	4	5	6	7	8	9

6. Compared to your typical approach, rate your perceived level of crew workload for this procedure from the standpoint of communication, coordination, and procedural habit patterns throughout the approach.

Much Lower Workload		Somewhat Lower Workload		Same as Typical Approach		Somewhat Higher Workload		Much Higher Workload
1	2	3	4	5	6	7	8	9

7. Did you see any aircraft on the other approach during this approach? Yes/No

Appendix E: Re-engagement of Managed NAV Algorithm for Pilot Test

One scenario in the pilot HITL test for aircraft equipped with approved VNAV involved controllers requesting a go-around during the 3rd (50°) turn. In one aircraft simulator, this scenario could result in a situation where the flight management computer could provide lateral guidance towards the other approach path. When the TO/GA switch was engaged, the flight management computer would no longer provide LNAV guidance for the original instrument approach procedure, but attempt to follow a track averaged from the last several seconds of flight. Pilot training prepares flight crews that may experience this problem to engage LNAV again after engaging TO/GA. Some of our flight crews failed to properly or quickly execute the procedure. In either case, this is an interesting measure of the amount of time that it takes a flight crew to identify and correct a lateral deviation. It is especially informative because the remedy is a single button press.

We recorded the time in the simulator that TO/GA was engaged, but the time that LNAV was re-engaged was not recorded in the simulator output. Therefore, we will estimate that time using the algorithm described in this section. Not every flight crew elected to go-around using the TO/GA functionality. In fact, only 20 out of 32 approaches engaged TO/GA to go-around. Those that did not use TO/GA either manually controlled the aircraft to climb or selected the target altitude using the altitude selector on the flight control unit. Many of those that used TO/GA also used the correct procedure and, therefore, experienced normal path keeping. Identifying whether the flight crews experienced a major deviation required an initial algorithm. We called this the existential algorithm.

The existential algorithm starts by calculating the track at each position in the aircraft path. The simulator output recorded aircraft position at a rate of 5 Hz and the track time-series preserves this rate. The algorithm then calculates segments where the track is less than 0.5° per second (a typical turn rate is approximately 3° per second). For one example, these level segments are indicated by the green regions in figure E-1. If there is at least one level segment whose mean track is more than ±5° from one of the tracks where aircraft are supposed to level during the TF fly-by turns and that level segment starts within 10 seconds from the time that TO/GA was engaged, then the algorithm indicates that the flight crew experienced non-normal flight during the sample approach. In the example shown in figure E-1, this means that if the average heading is outside of the red regions, which are the TF fly-by turn tracks, and it starts less than 10 seconds after the vertical green dashed line, which is when TO/GA is engaged, then that track is marked as experiencing a TO/GA issue.

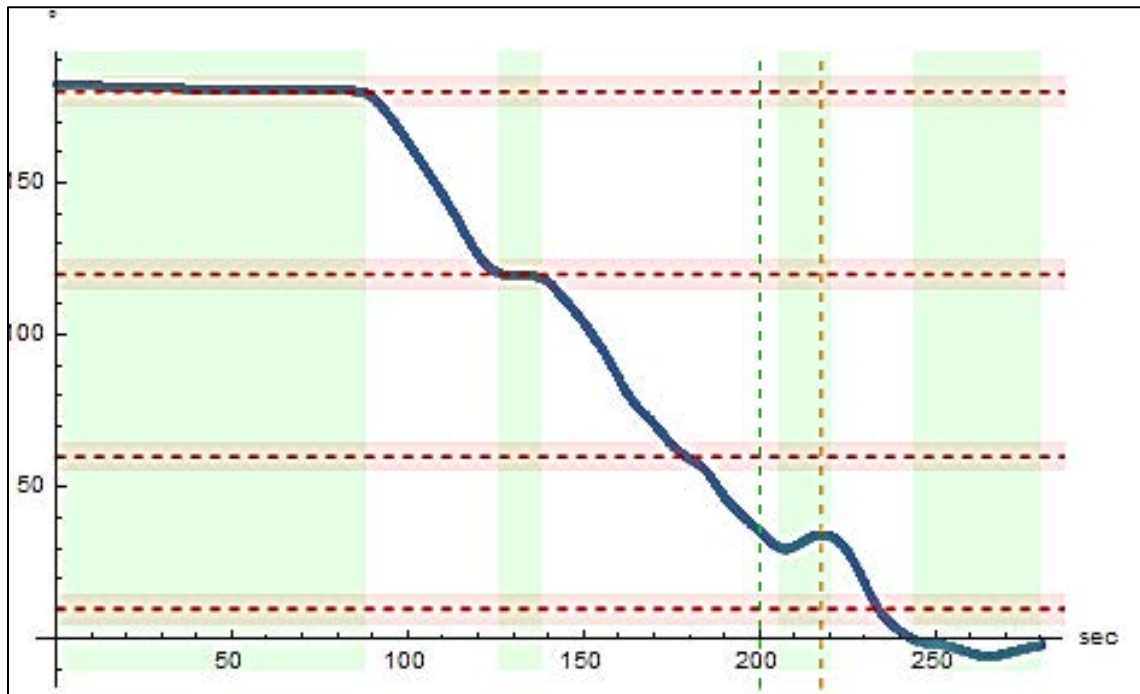


Figure E-1: Track Time Series and Existential Algorithm Example

If a track experienced a TO/GA issue, we needed to identify when they began correcting back to the approach path, typically by re-engaging LNAV. The algorithm used to identify this time was called the value algorithm. The targeted event is best identified using the bank time-series. Because the selected track is based on an average of several seconds prior to the time of engaging TO/GA, the guidance initially commands a bank in the opposite direction required for the turn. The bank time-series was extremely consistent during the approaches where autopilot was engaged. Pilot input introduced additional noise in the time-series during the hand-flown approaches with flight director guidance. To remove the noise from these approaches, we smoothed the bank time-series with a Gaussian filter with a radius of 8° . Then we identified the first local minimum after TO/GA was engaged, and the first maximum after that. The minimum is the time when the most bank was applied to achieve the averaged track. The maximum is the time when the most bank was applied to return to the approach path. Therefore, we know that the time that LNAV was engaged falls between these two times. If the flight crew did not re-engage LNAV, the aircraft may have had some positive bank if the system attaining the path was under-damped. On the other hand, if the LNAV is re-engaged while the flight crew is in the negative bank, it would be unnoticeable. Therefore, it is somewhat ambiguous when the flight crew engaged the LNAV. We thought a reasonable assumption would be that the positive bank experienced during the turn-on would be relatively negligible. Therefore, a conservative time for LNAV re-engagement can be calculated as the first unsmoothed bank measurement before the maximum bank of the same sign required to correct back to course.

Figure E-2 is an example of the bank time-series for one of the deviations during an autopilot approach. The time-series starts when the TO/GA is engaged. At this time, the aircraft was in an approximately 5° bank. After a two second delay, the bank rapidly and consistently decreased to approximately -8° , which indicated that the aircraft was turning

in the opposite direction needed for the turn. This position is shown as the leftmost red dot in figure E-2. Then the bank increased from -8° to approximately 10° , back towards the intended approach path. The maximum is shown as the rightmost red dot in figure E-2. The algorithm selects the region of the unsmoothed time-series from the second red dot to the start of the time-series, reverses it, and selects the point before the first one that is negative. This time is indicated by the dashed green line in figure E-2.

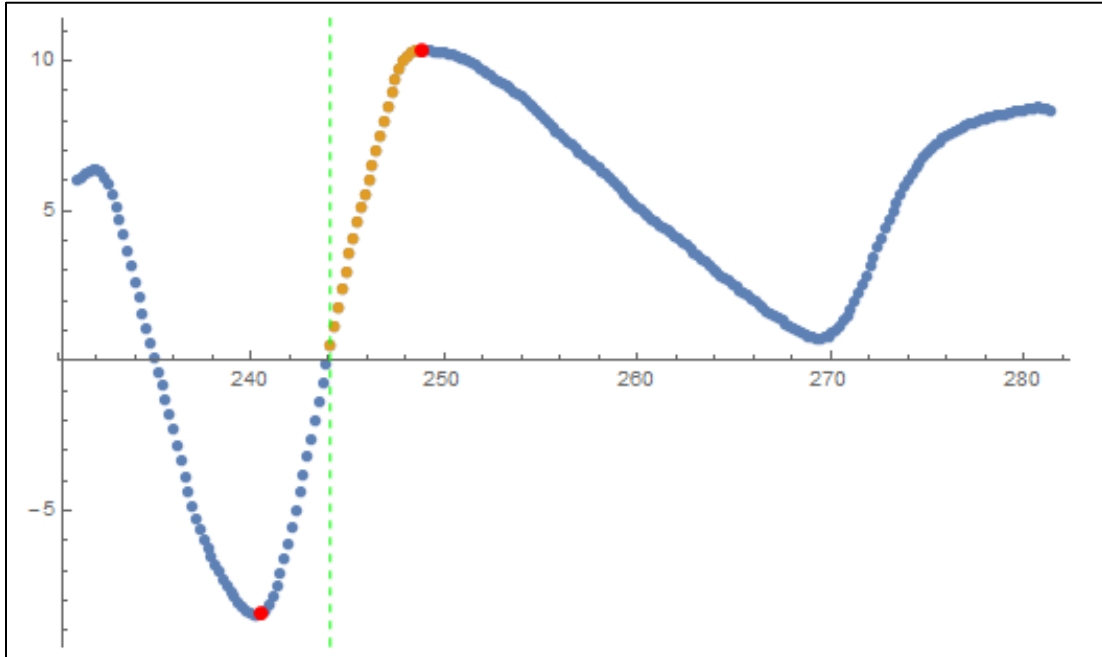


Figure E-2: Bank Angle Time-Series

Appendix F: Failure Recovery Initiation Reaction Time for Pilot Test

This appendix describes 10 pilot reaction times during the phase 1 and phase 2 HITL tests. It shows the five most interesting reaction times for two categories: go-around responses and continue approach responses. Each scenario is depicted in a figure that shows the flight track. The figure is accompanied by a table indicating the event list which includes the timing in seconds of specific events relevant to the flight path flown and a table that lists the flight profile details. The second table in each scenario indicates a “false” reading for the speed event. This indicates that there were no 210 knot speed restrictions applied in the scenario, which, for some aircraft, pushed them off course. In some scenarios, an altitude flight profile figure is also shown to add perspective to the vertical path of the aircraft as well as the lateral path. Table F-1 lists the acronyms used in the tables.

Table F-1: Key

Abbreviation	Word
CA	Captain
FO	First Officer
AP	Autopilot: AP1 = CA; AP2 = FO
FD	Flight Director: FD1 = CA; FD2 = FO
IMC	Instrument Meteorological Conditions
VMC	Visual Meteorological Conditions
MVMC	Marginal Visual Meteorological Conditions
TO/GA	Take Off/Go-Around
AHRS	Altitude Heading Reference System
NTZ	No-Transgression Zone

Go-around Responses:

Go-around 1: Crew 24, Run 9, Scenario 19

Figure F-1 shows that an AHRS failure occurred between waypoints NOV40 and NOV30. As the aircraft flew by the apex (NOV30) on the approach, it continued on a straight path, deviating far right of the track. Tower asked the pilot to state his intentions, and the pilot requested a go-around. As he initiated his recovery he crossed the NTZ into the other parallel approach path before correcting back onto the original runway heading while executing a missed approach.



Figure F-1: Crew 24, Run 9, Scenario 19 Track

Table F-2 lists the event time and the associated category with pilot actions. The captain was flying using the flight director. The flight director failed 103.4 seconds into the scenario. The captain delayed transferring control of the aircraft to the first officer while he analyzed the problem. The first officer was eventually given control and was hand-flying the aircraft until both flight directors were engaged at 165.4 seconds. At 166.0 seconds, a go-around was initiated. The pilot reaction time of 177.4 seconds indicates the initial course correction back to track. The go-around altitude was achieved at the 264.0 second elapsed time mark.

Table F-2: Crew 24, Run 9, Scenario 19 Event List

Event Time (sec)	Event Category	Event Details
0.0	Scenario start	CA flying FD
103.4	Malfunction start	FD1 fail
161.2	Hand-flying	FO hand-flying
162.4	Flight guidance	FD2 engaged
165.4	Flight guidance	Both FD engaged
166.0	Go-around	Start climb
177.4	Pilot reaction	Initiation of recovery
264.0	Go-around	Stop climb

Table F-3 lists the scenario details. The captain was flying a non-VNAV aircraft using the flight director in IMC conditions on the EoR approach to runway 35L. The speed event was false, meaning that a 210 knot speed restriction was not applied. The elapsed time to the malfunction time and pilot reaction time in seconds, when added together, gives the total elapsed time from scenario start to pilot initial course correction. In this

case, the malfunction time (103.4 seconds) + reaction time (74.0 seconds) equals 177.4 seconds of elapsed time.

Table F-3: Crew 24, Run 9, Scenario 19 Details

Aircraft	Pilot Flying	Flight Guidance	Weather	Runway	Speed Event	Malfunction Time (sec)	Reaction Time (sec)
Non-VNAV	CA	FD	IMC	35L	False	103.4	74.0

The observer noted that this flight crew was slow to recognize and then act on the AHRS failure. The captain did not immediately transfer control to the first officer, which extended the deviation off course. Compounding the problem, when control of the aircraft was transferred, the first officer had difficulty assessing why the flight director was not activating. When prompted by the captain to activate NAV, the first officer completed the activation of the flight director. This explains the 57.8 second lapse between the malfunction start (103.4 seconds) and the transfer of control to the first officer (161.2 seconds). The flight crew initially asked for vectors back to course, but accepted the tower's direction to follow the RNAV track. The aircraft corrected back to the RNAV track and reestablished on course after it had passed the final approach fix.

Go-around 2: Crew 17, Run 7, Scenario 18

In figure F-2, a flight director failure occurred prior to the apex (30NOV). The pilot requested a go-around after passing the apex. The flight crew did not transfer control of the aircraft. The captain recognized and informed the first officer that he was deviating left of the track after the apex. The first officer corrected back towards course, initiated TO/GA, and flew inside of 20NOV (50° waypoint). The aircraft then flew outside of course while on the 50° leg. Then the aircraft turned parallel to the 10° leg, remaining inside of the course, correcting back onto course at the final approach fix.

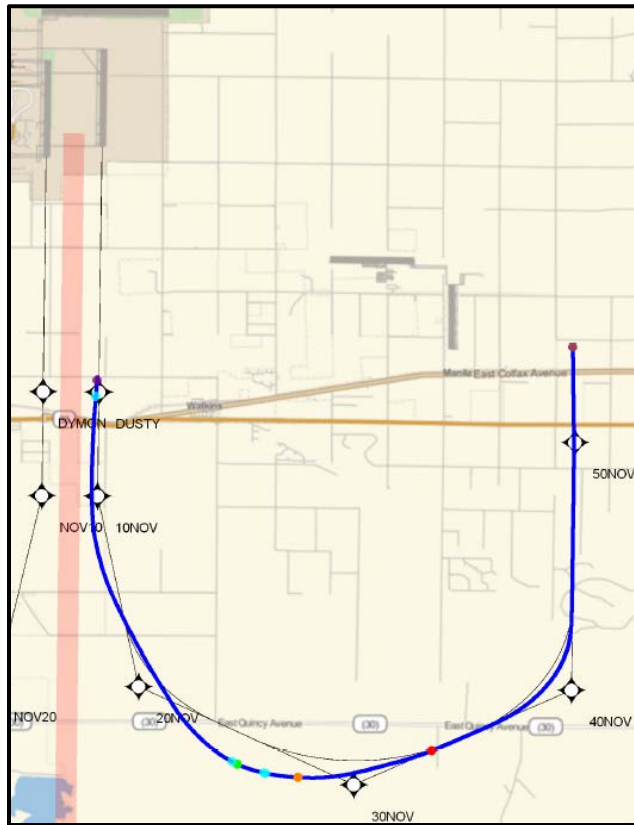


Figure F-2: Crew 17, Run 7, Scenario 18 Track

Table F-4 indicates the flight director failed at the 152.8 second mark. Though his reaction time was 21.4 seconds, the pilot made the decision to go-around, initiating TO/GA at 191.4 seconds, 16 seconds after he began his turn back towards the approach course (174.18 seconds). The aircraft began to climb at 199.4 seconds and achieved go-around altitude at the 297.0 second mark.

Table F-4: Crew 17, Run 7, Scenario 18 Event List

Event Time (sec)	Event Category	Event Details
0.0	Scenario start	FO flying FD
152.8	Malfunction start	FD2 failure
174.2	Pilot reaction	Initiation of recovery
191.4	Go-around	TO/GA actuated
199.4	Go-around	Start climb
297.0	Go-around	Stop climb

Table F-5 shows the first officer was flying a VNAV1 aircraft using flight director in IMC on the EoR approach to runway 35R. There was no speed restriction directed. The malfunction initiated at 152.8 seconds and the pilot initiated lateral correction 21.4 seconds later.

Table F-5: Crew 17, Run 7, Scenario 18 Details

Aircraft	Pilot Flying	Flight Guidance	Weather	Runway	Speed Event	Malfunction Time (sec)	Reaction Time (sec)
VNAV1	FO	FD	IMC	35R	False	152.8	21.4

Go-around 3: Crew 1, Run 7, Scenario 6

In figure F-3, an autopilot failure occurred prior to the apex (NOV30). The aircraft continued to deviate right of course after the failure. The first officer transferred control of the aircraft to the captain. The captain made a correction back to course, engaged the autopilot, and then requested a go-around.

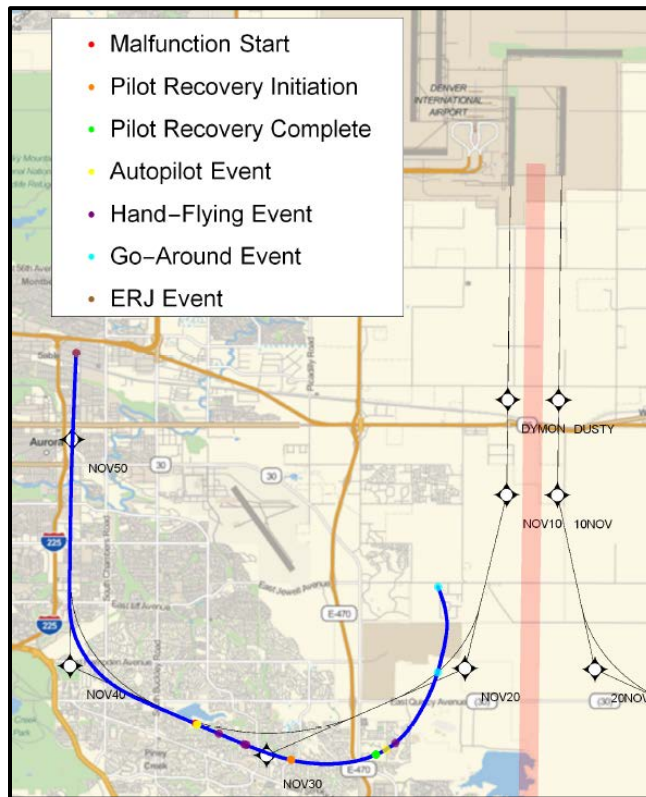


Figure F-3: Crew 1, Run 7, Scenario 6 Track

Figure F-4 shows the descent profile for this scenario. The pilot leveled off after the malfunction, but then descended as he was correcting back to course. He leveled off again as he was correcting back to course before executing the go-around.

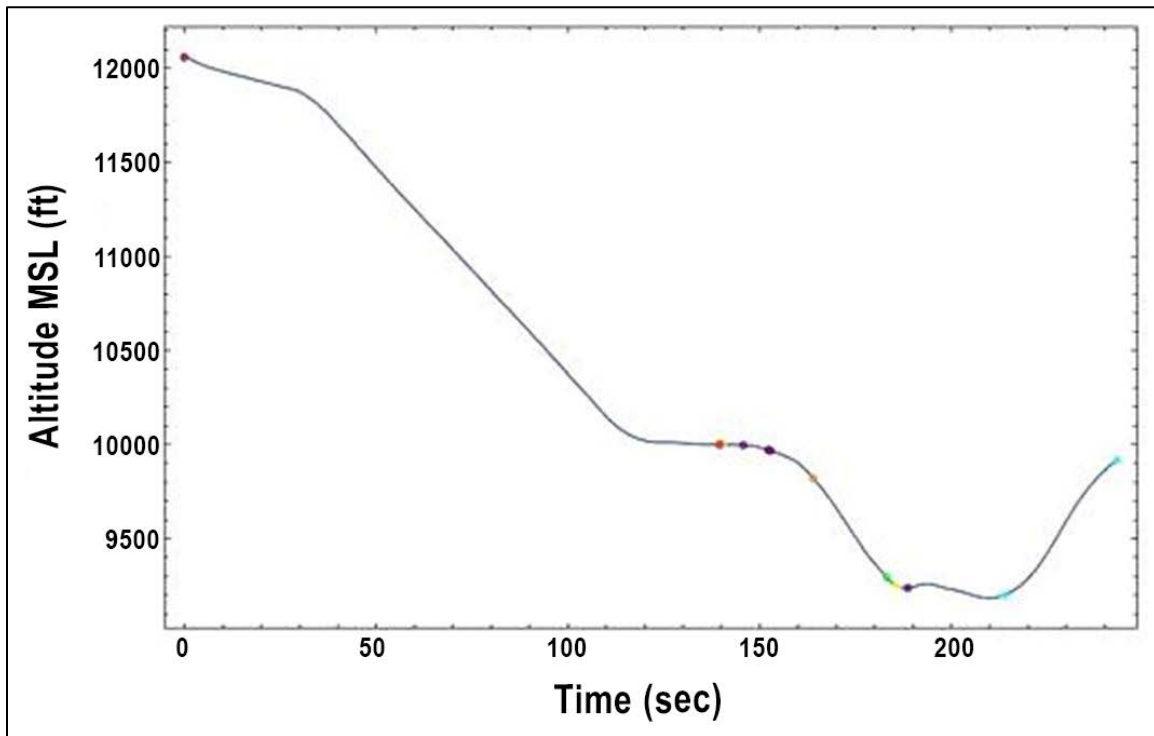


Figure F-4: Crew 1, Run 7, Scenario 6 Altitude Profile

In table F-6, the first officer began hand-flying the aircraft at the 145.7 second mark. The transfer of control of the aircraft to the captain occurred at 152.8 seconds. The captain initiated the recovery back to course at 159.2 seconds. Autopilot 1 was engaged at 185.9 seconds. The pilot requested a go-around at 213.8 seconds and began to climb.

Table F-6: Crew 1, Run 7, Scenario 6 Event List

Event Time (sec)	Event Category	Event Details
0.0	Scenario start	FO flying AP
139.6	Malfunction start	AP2 failure
145.7	Hand-flying	FO hand-flying
152.8	Hand-flying	CA hand-flying
159.2	Pilot reaction	Initiation of recovery
185.9	Flight guidance	AP1 engaged
213.8	Go-around	Start climb

Table F-7 shows the first officer was flying a VNAV2 aircraft with autopilot in IMC on the EoR approach to runway 35L. There were no speed restrictions in place. The malfunction occurred at the 139.6 second mark and the reaction time was 19.6 seconds. The go-around was initiated late.

Table F-7: Crew 1, Run 7, Scenario 6 Details

Aircraft	Pilot Flying	Flight Guidance	Weather	Runway	Speed Event	Malfunction Time (sec)	Reaction Time (sec)
VNAV2	FO	AP	IMC	35L	False	139.6	19.6

Go-around 4: Crew 22, Run 5, Scenario 7

In figure F-5, an AHRS failure occurred prior to the apex (30NOV). The aircraft flew straight through the apex and continued heading straight, left of course. The pilot requested a heading vector and then initiated his turn late. The aircraft crossed over the NTZ while correcting back to course and executing a go-around.

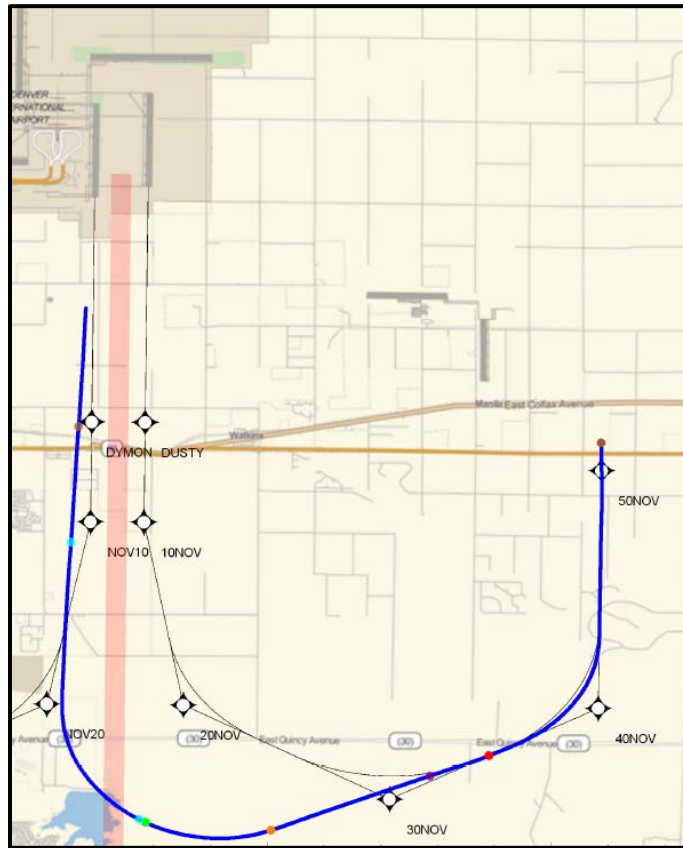


Figure F-5: Crew 22, Run 5, Scenario 7 Track

Figure F-6 shows the altitude profile for this scenario. The flight crew continued to descend and then leveled off after the first officer began hand-flying. The aircraft remained in near level flight as the first officer initiated the correction back to track, prior to requesting and then initiating a go-around.

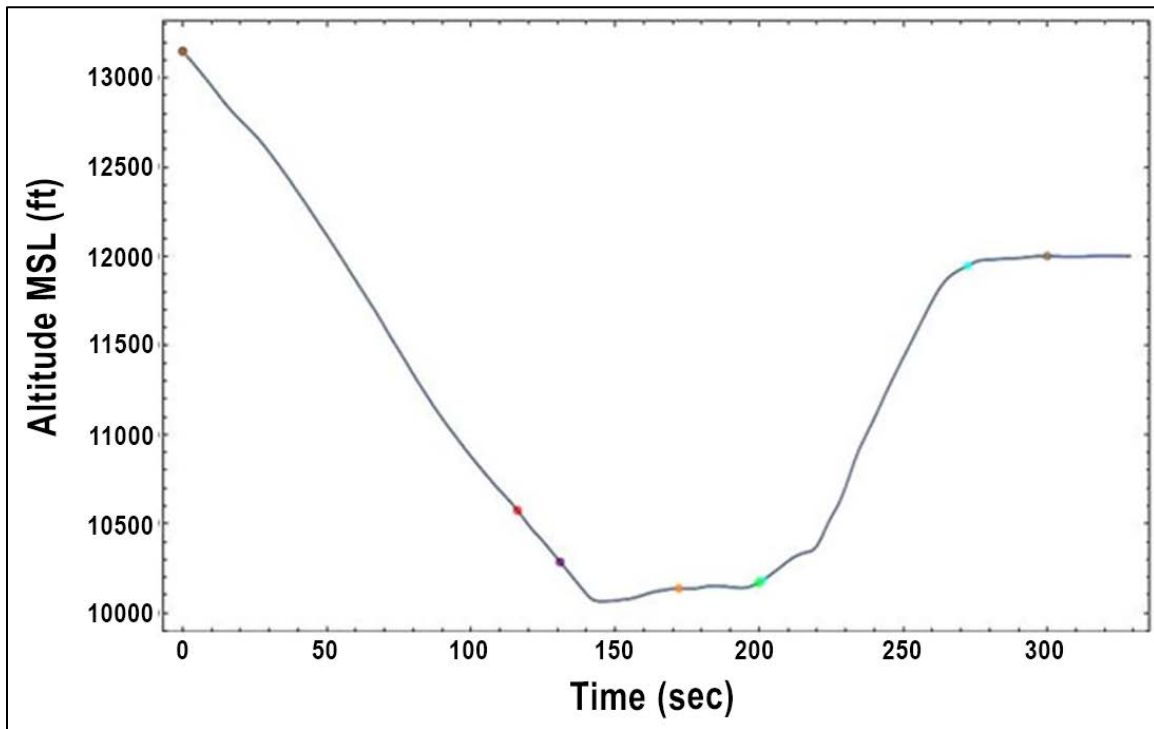


Figure F-6: Crew 22, Run 5, Scenario 7 Altitude Profile

Table F-8 shows the autopilot failed at the 116.2 second mark. The captain transferred control to the first officer at the 131.0 second mark and delayed coupling of the autopilot to the first officer’s side. The captain requested a heading from the controller and then began to troubleshoot the failure with the AHRS. The first officer initiated a turn back to course at 171.4 seconds and then requested a go-around. The aircraft began climbing at 201.2 seconds and achieved altitude at 272.4 seconds. The pilot was able to clear the problem by pressing the reversionary panel AHRS button at the 300.0 second mark.

Table F-8: Crew 22, Run 5, Scenario 7 Event List

Event Time (sec)	Event Category	Event Details
0.0	Scenario start	CA flying AP
116.2	Malfunction start	AP1 failure
131.0	Hand-flying	FO hand-flying
171.4	Pilot reaction	Initiation of recovery
201.2	Go-around	Start climb
272.4	Go-around	Stop climb
300.0	Non-VNAV only	AHRS reversion actuated

Table F-9 shows the captain was flying a non-VNAV aircraft on autopilot in MVMC on an EoR approach to runway 35R. No speed restrictions were applied. The flight crew’s reaction to the malfunction took 55.2 seconds.

Table F-9: Crew 22, Run 5, Scenario 7 Details

Aircraft	Pilot Flying	Flight Guidance	Weather	Runway	Speed Event	Malfunction Time (sec)	Reaction Time (sec)
Non-VNAV	CA	AP	MVMC	35R	False	116.2	55.2

Go-around 5: Crew 25, Run 3, Scenario 19

In figure F-7, an AHRS failure occurred prior to the apex (NOV30). The pilot leveled the aircraft and flew inside of the apex, deviating right of the track. The pilot requested a heading and was given “TURN LEFT, HEADING 355.” The aircraft crossed over the NTZ as it was correcting back while executing a go-around.

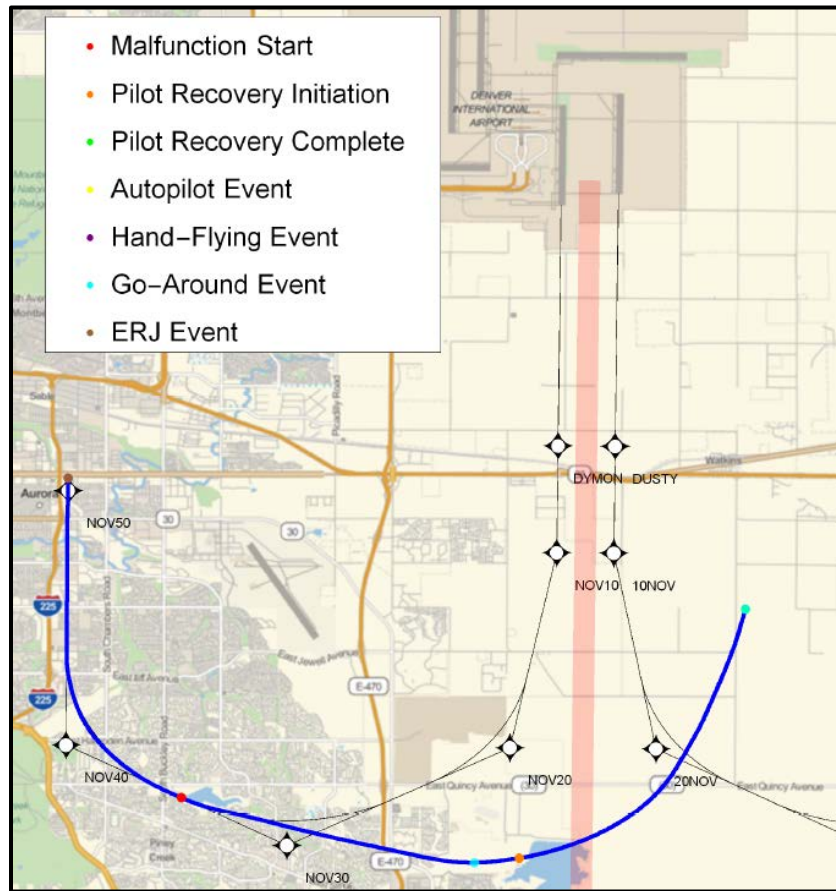


Figure F-7: Crew 25, Run 3, Scenario 19 Track

Table F-10 shows the AHRS failing at the 103.8 second mark. The captain did not transfer control of the aircraft and directed the first officer to request vectors or divert-to-alternate instructions from the controller. The controller issued instructions to fly the RNAV track. The crew responded they were unable and requested a vector. The controller issued a heading of 355. The captain initiated the turn at the 156.6 second mark and requested a go-around. The climb began at 165.0 seconds and altitude was achieved at the 246.6 second mark.

Table F-10: Crew 25, Run 3, Scenario 19 Event List

Event Time (sec)	Event Category	Event Details
0.0	Scenario start	CA flying FD
103.8	Malfunction start	FD1 failure
156.6	Pilot reaction	Initiation of recovery
165.0	Go-around	Start climb
246.6	Go-around	Stop climb

Table F-11 shows the captain flying with flight director in IMC on the EoR approach to runway 35L. No speed restrictions were made. The flight crew's reaction time to the malfunction was 52.8 seconds later.

The observer on the flight deck noted that the flight crew never attempted to fly the RNAV track on the missed approach. This was the only crew that reacted in this manner.

Table F-11: Crew 25, Run 3, Scenario 19 Details

Aircraft	Pilot Flying	Flight Guidance	Weather	Runway	Speed Event	Malfunction Time (sec)	Reaction Time (sec)
Non-VNAV	CA	FD	IMC	35L	False	103.8	52.8

Continue Approach Responses:

Continue Approach 1: Crew 24, Run 17, Scenario 8

Figure F-8 shows an AHRS failure occurred prior to the 50° turn (NOV20). The aircraft deviated right of track past the 50° turn. The aircraft corrected back to course and was able to continue the approach.



Figure F-8: Crew 24, Run 17, Scenario 8 Track

Table F-12 lists the malfunction start time at the 150.6 second mark when the flight director failed. The first officer initially was hand-flying the aircraft at the 151.8 second mark until he transferred control of the aircraft to the captain at 159.8 seconds. The captain initiated a turn back to course at the 172.2 second mark and was able to continue the approach.

Table F-12: Crew 24, Run 17, Scenario 8 Event List

Event Time (sec)	Event Category	Event Details
0.0	Scenario start	FO flying FD
150.6	Malfunction start	FD2 failure
151.8	Hand-flying	FO hand-flying
159.8	Hand-flying	CA hand-flying
172.2	Pilot reaction	Initiation of recovery

Table F-13 shows the first officer flying a non-VNAV aircraft on flight director in IMC on an EoR approach to runway 35L. There were no speed restrictions. The flight crew's reaction time was 21.6 seconds and enabled the approach to continue.

Table F-13: Crew 24, Run 17, Scenario 8 Details

Aircraft	Pilot Flying	Flight Guidance	Weather	Runway	Speed Event	Malfunction Time (sec)	Reaction Time (sec)
Non-VNAV	FO	FD	IMC	35L	False	150.6	21.6

Continue Approach 2: Crew 21, Run 20, Scenario 19

Figure F-9 shows an AHRS failure occurred prior to the apex (NOV30). The captain leveled the aircraft and continued straight to the apex, initiated a left turn at the apex, and continued to deviate right of course. The captain selected the MFD on the reversionary panel, which did not work, so he transferred control to the first officer. The captain then selected the AHRS button, bringing the flight data back to his MFD. The first officer corrected back to course and flew slightly inside of the 50° turn (NOV20) to continue the approach.

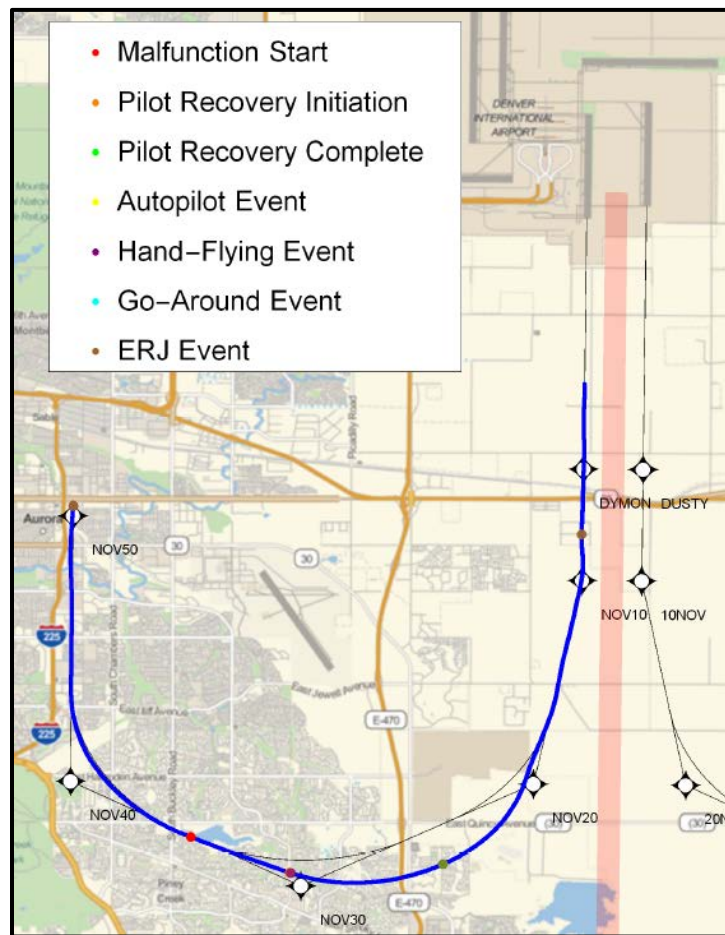


Figure F-9: Crew 21, Run 20, Scenario 19 Track

Table F-14 shows the flight director failed at the 104.0 second mark. The first officer initiated a correction back to course at the 124.6 second mark as he was hand-flying the aircraft. The AHRS reversion was activated at 154.8 seconds, restoring flight data back to his instrument panel.

Table F-14: Crew 21, Run 20, Scenario 19 Event List

Event Time (sec)	Event Category	Event Details
0.0	Scenario start	CA flying FD
104.0	Malfunction start	FD1 failure
124.6	Pilot reaction	Initiation of recovery
125.4	Hand-flying	FO hand-flying
154.8	Non-VNAV only	AHRS reversion actuated

Table F-15 shows that the captain was flying a non-VNAV aircraft with flight director in IMC on an EoR approach to runway 25L. No speed restrictions were in place. The reaction time was quick, registering at 20.6 seconds, enabling the flight crew to continue the approach.

Table F-15: Crew 21, Run 20, Scenario 19 Details

Aircraft	Pilot Flying	Flight Guidance	Weather	Runway	Speed Event	Malfunction Time (sec)	Reaction Time (sec)
Non-VNAV	CA	FD	IMC	35L	False	104.0	20.6

Continue Approach 3: Crew 24, Run 22, Scenario 7

Figure F-10 shows an AHRS failure occurred prior to the apex (30NOV). The aircraft flew past the apex heading left of course. The pilot initiated a turn and corrected back to course, flying outside of the 50° waypoint (20NOV) and intercepted the course, continuing on the approach.

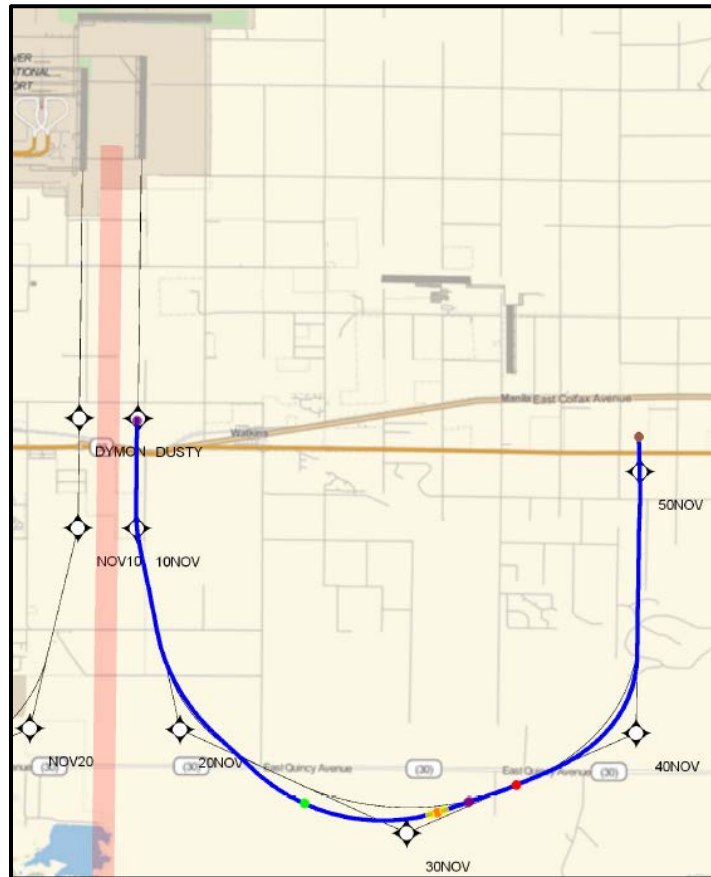


Figure F-10: Crew 24, Run 22, Scenario 7 Track

Table F-16 shows the autopilot failure occurring at the 120.6 second mark. The captain immediately transferred control to the first officer who was hand-flying the aircraft. The autopilot was disengaged at the 137.6 second mark and the first officer began correcting back to course at the 139.0 second mark. Shortly thereafter at 140.8 seconds, autopilot 1 was engaged to maintain the approach.

Table F-16: Crew 24, Run 22, Scenario 7 Event List

Event Time (sec)	Event Category	Event Details
0.0	Scenario start	CA flying AP
120.6	Malfunction start	AP failure
132.0	Hand-flying	FO hand-flying
137.6	Flight guidance	AP disengaged
139.0	Pilot reaction	Initiation of recovery
140.8	Flight guidance	AP1 engaged

Table F-17 indicates that the captain was flying a non-VNAV aircraft on autopilot in MVMC on an EoR approach to runway 35R. No speed restrictions were in place. A rapid control transfer and quick reaction time of 18.4 seconds aided in the flight crew's ability to continue the approach. Additionally, they were aided by the MVMC condition as the field was visible at times while flying the approach.

Table F-17: Crew 24, Run 22, Scenario 7 Details

Aircraft	Pilot Flying	Flight Guidance	Weather	Runway	Speed Event	Malfunction Time (sec)	Reaction Time (sec)
Non-VNAV	CA	AP	MVMC	35R	False	120.6	18.4

Continue Approach 4: Crew 23, Run 17, Scenario 8

Figure F-11 shows an AHRS failure occurred prior to the 50° waypoint (NOV20). The aircraft flew past NOV20 and slightly inside of the 50° leg track, but corrected back to course and continued on the approach.

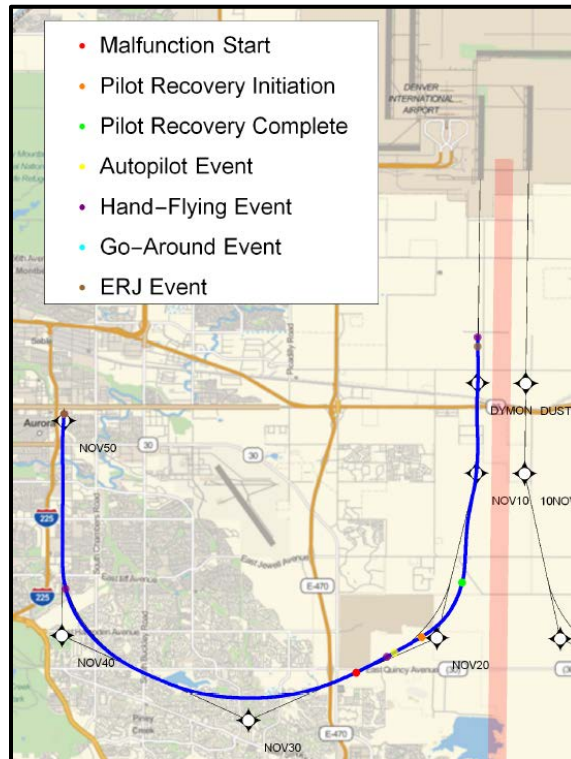


Figure F-11: Crew 23, Run 17, Scenario 8 Track

Figure F-12 depicts the altitude profile during this scenario. The aircraft was descending and then leveled off briefly following the captain's turn back to course.

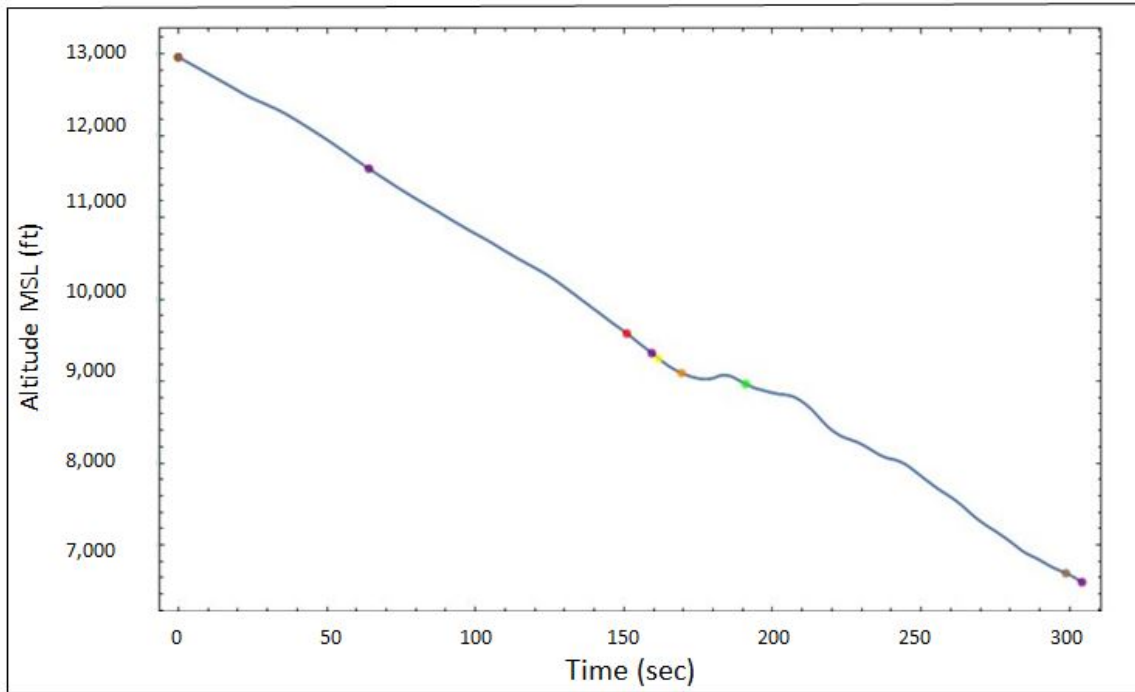


Figure F-12: Crew 23, Run 17, Scenario 8 Altitude Profile

Table F-18 shows the autopilot failed at the 151.0 second mark. The first officer immediately transferred control to the captain, who was hand-flying the aircraft. The autopilot was disengaged at the 161.6 second mark, followed by the captain making a course correction at 168.6 seconds. An AHRS reversion was actuated at the 298.8 second mark. The expedient transfer of control and rapid reaction time of 17.6 seconds by this flight crew enabled the approach to be continued.

Table F-18: Crew 23, Run 17, Scenario 8 Event List

Event Time (sec)	Event Category	Event Details
0	Scenario start	FO flying AP
151.0	Malfunction start	AP failure
159.4	Hand-flying	CA hand-flying
161.6	Flight guidance	AP disengaged
168.6	Pilot reaction	Initiation of recovery
298.8	Non-VNAV only	AHRS reversion actuated

Table F-19 shows the first officer was flying a non-VNAV aircraft with autopilot in IMC on an EoR approach to runway 35L. There were no speed restrictions. The flight crew's reaction time to the malfunction was 17.6 seconds.

Table F-19: Crew 23, Run 17, Scenario 8 Details

Aircraft	Pilot Flying	Flight Guidance	Weather	Runway	Speed Event	Malfunction Time (sec)	Reaction Time (sec)
Non-VNAV	FO	AP	IMC	35L	False	151.0	17.6

Continue Approach 5: Crew 8, Run 18, Scenario 6

Figure F-13 shows an autopilot failure occurred prior to the apex (NOV30). The first officer continued on heading past the apex and then began correcting with a left turn. The first officer reacquired the course at the 50° turn (NOV20), and was able to continue the approach.



Figure F-13: Crew 8, Run 18, Scenario 6 Track

Figure F-14 shows the altitude profile for this scenario. The malfunction occurred while the aircraft was in level flight. The first officer began to descend shortly after he corrected back to the approach course.

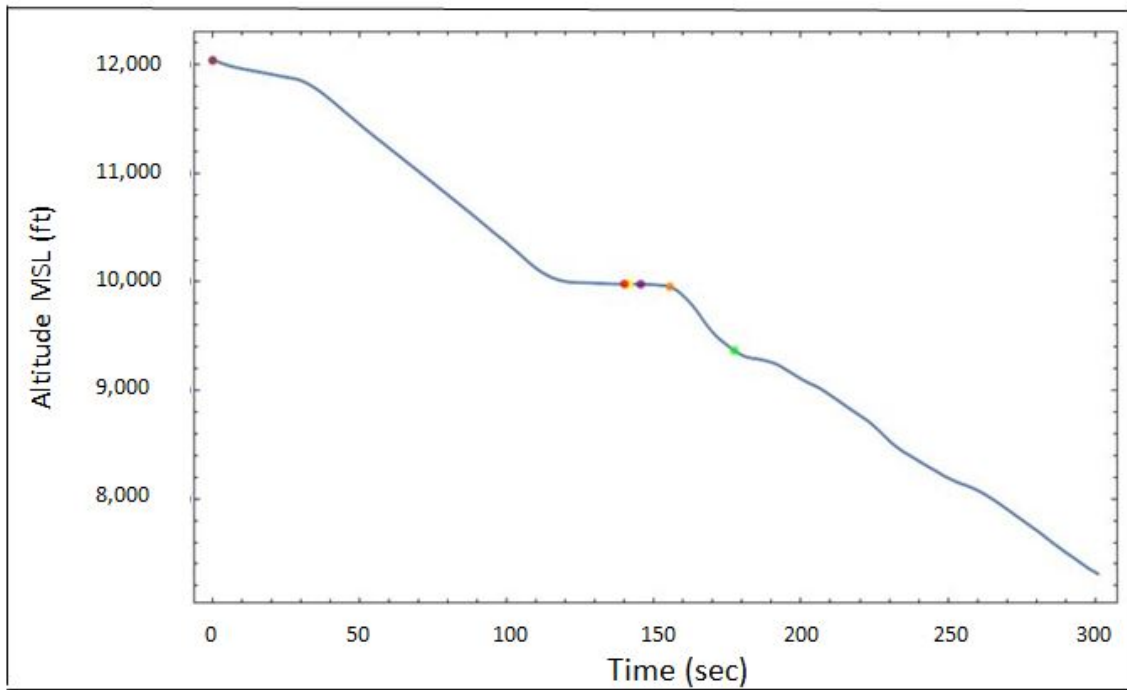


Figure F-14: Crew 8, Run 18, Scenario 6 Altitude Profile

Table F-20 shows the malfunction occurred at 140.0 seconds. The autopilot was disengaged at 141.6 seconds and the flight director 1 engaged at the same time. The first officer was hand-flying the aircraft after the failure and made a course correction back to the approach course at the 154.6 second mark.

Table F-20: Crew 8, Run 18, Scenario 6 Event List

Event Time (sec)	Event Category	Event Details
0.0	Scenario start	FO flying AP
140.0	Malfunction start	AP failure
141.6	Flight guidance	AP disengaged
141.6	Flight guidance	FD1 engaged
145.5	Hand-flying	FO hand-flying
154.6	Pilot reaction	Initiation of recovery

Table F-21 shows the first officer was flying a VNAV 2 aircraft on autopilot in IMC on an EoR approach to runway 35L. No speed restrictions were applied. The rapid reaction time of 14.6 seconds enabled the flight crew to continue the approach.

Table F-21: Crew 8, Run 18, Scenario 6 Details

Aircraft	Pilot Flying	Flight Guidance	Weather	Runway	Speed Event	Malfunction Time (sec)	Reaction Time (sec)
VNAV2	FO	AP	IMC	35L	False	140.0	14.6

Appendix G: Controller Test Matrix

This appendix shows the test parameters used for the controller HITL test. Groups consisted of 4 controllers tested during each day, and 21 controllers participated. The controller groups were utilized over the course of three weeks. Groups 1A and 1B were tested on different days during week 1. Groups 2A, 2B, and 2C were tested on separate days during the second week, and group 3A was tested during week 3. For brevity, groups 1A and 1B are depicted to show the random use of scenarios. The remaining groups were tested randomly, similar to groups 1A and 1B. Runway spacing used for all groups was 5,300 ft.

Table G-1 lists the random scenario plan for controller group 1A, and table G-2 lists the random scenario plan for controller group 1B. Each day, there were six shifts that lasted 45 minutes each. Each controller pair completed three shifts. The traffic density was either low or high, with aircraft arriving at a slow or faster pace. Low density was simulated using the actual average arrival rate at Denver International Airport. High density traffic was simulated using the actual maximum arrival rate at Hartsfield-Jackson Atlanta International Airport. The deviation side is synonymous with runways 35L (left) or 35R (right). This is the side where a non-normal deviation type was injected into the simulation.

There were three types of non-normal deviations:

1. Navigation system error: The simulated aircraft experienced a severe navigation system error with a track laterally translated toward the parallel approach;
2. Course deviation: The simulated aircraft deviated from the approach course similar to the deviations observed in the pilot HITL test; and
3. Wrong runway selection: The flight crew was simulated selecting a standard instrument approach procedure to another parallel runway at the airport.

The scenario number is the column on the right side of tables G-1 and G-2. Table G-3 shows the scenarios in numerical order with the associated traffic density, deviation side, and deviation type. Scenarios 13 and 14 included non-normal deviation type 2, course deviation. It also included a request by the flight crew to go-around. Scenario 15 also used non-normal deviation type 2, and included a temporary no radio (NORDO) situation, where communication was temporarily lost with the pilot.

To read the table, here are two examples.

- In table G-1, during the first shift #2 with controller pair #2, traffic density was high and the deviation side was on the right. The deviation type was 2, a course deviation, with a temporary NORDO situation. The scenario used was 15; and
- In table G-2, during the 3rd event for shift #1, controller pair #1, where traffic density was low and the deviation side was on the left, scenario 13 was used. The deviation type 2, a course deviation, was injected with a go-around.

Table G-1: Controller Group 1A

Shift #	Controller Pair #	Traffic Density	Deviation Side	Deviation Type	Scenario #
1	1	Low	Right	1	1
1	1	Low	Left	2- Go-Around	13
1	1	Low	Right	3	3
2	2	High	Right	2-Temp NORDO	15
2	2	High	Left	1	10
2	2	High	Right	3	9
2	2	High	Left	2	11
3	1	High	Left	1	10
3	1	High	Right	2	8
3	1	High	Right	1	7
3	1	High	Left	3	12
4	2	Low	Right	2	2
4	2	Low	Left	1	4
4	2	Low	Left	3	6
4	2	Low	Right	1	1
5	1	Low	Right	3	3
5	1	Low	Left	2	5
5	1	Low	Left	1	4
5	1	Low	Right	2	2
6	2	High	Left	3	12
6	2	High	Right	1	7
6	2	High	Right	3	9
6	2	High	Left	2- Go-Around	14

Table G-2: Controller Group 1B

Shift #	Controller Pair #	Traffic Density	Deviation Side	Deviation Type	Scenario #
1	1	Low	Left	3	6
1	1	Low	Right	1	1
1	1	Low	Left	2- Go-Around	13
1	1	Low	Right	3	3
2	2	Low	Right	2	2
2	2	Low	Right	1	1
2	2	Low	Left	1	4
2	2	Low	Left	3	6
3	1	Low	Right	2	2
3	1	Low	Left	2	5
3	1	Low	Left	1	4
3	1	Low	Right	3	3
4	2	High	Right	2-Temp NORDO	15
4	2	High	Left	2	11
4	2	High	Left	1	10
4	2	High	Right	3	9
5	1	High	Right	2	8
5	1	High	Right	1	7
5	1	High	Left	1	10
5	1	High	Left	3	12
6	2	High	Left	3	12
6	2	High	Right	3	9
6	2	High	Left	2- Go-Around	14
6	2	High	Right	1	7

Table G-3: Controller Scenarios

Scenario #	Traffic Density	Deviation Side	Deviation Type
1	Low	Right	1
2	Low	Right	2
3	Low	Right	3
4	Low	Left	1
5	Low	Left	2
6	Low	Left	3
7	High	Right	1
8	High	Right	2
9	High	Right	3
10	High	Left	1
11	High	Left	2
12	High	Left	3
13	Low	Left	2-Go-Around
14	High	Left	2-Go-Around
15	High	Right	2-Temp NORDO

Appendix H: Post-Shift Questionnaire for Controller Test

This was originally titled: "Post-Session Questionnaire".

DATE: _____ CONTROLLER #: _____ SHIFT #: _____

1. As compared to straight-in simultaneous arrivals to runways 35L and 35R, rate your overall difficulty level working this traffic with dual simultaneous independent RNAV (GPS) track-to-fix procedures:

		Somewhat		Same as Typical	Somewhat More		Much More	
Much Easier		Easier		Operation	Difficult		Difficult	
1	2	3	4	5	6	7	8	9

2. As compared to straight-in simultaneous arrivals to runways 35L and 35R, in your opinion, was the number of broadcasts required:

		Somewhat		Same as Typical	Somewhat			
Much Lower		Lower		Operation	Higher		Much Higher	
1	2	3	4	5	6	7	8	9

3. As compared to straight-in simultaneous arrivals, rate your level of comfort at the following phases of the simulation:

- a. While observing the aircraft on its nominal flight path

		Somewhat		Same as Typical	Somewhat		Much More	
Very Comfortable		Comfortable		Operation	Uncomfortable		Uncomfortable	
1	2	3	4	5	6	7	8	9

- b. After recognizing that an aircraft did not respond as expected to your instructions or deviated from its intended flight path

		Somewhat		Same as Typical	Somewhat		Much More	
Very Comfortable		Comfortable		Operation	Uncomfortable		Uncomfortable	
1	2	3	4	5	6	7	8	9

- c. Issuing a control instruction to correct the problem

		Somewhat		Same as Typical	Somewhat		Much More	
Very Comfortable		Comfortable		Operation	Uncomfortable		Uncomfortable	
1	2	3	4	5	6	7	8	9

4. As compared to straight-in simultaneous operations, rate how timely you felt your corrective instructions were, based on your recognition of a problem:

		Somewhat		Same as Typical	Somewhat			
Much Faster		Faster		Operation	Slower		Much Slower	
1	2	3	4	5	6	7	8	9

5. As compared to straight-in simultaneous arrivals, rate your perceived level of individual workload, from the standpoint of mental demand (e.g. looking, searching, thinking, deciding, communicating etc.) for this operation:

		Somewhat		Same as Typical	Somewhat			
Much Lower		Lower		Operation	Higher		Much Higher	
1	2	3	4	5	6	7	8	9

6. As compared to straight-in simultaneous arrivals, rate the collective workload (all controllers; tower and final) for this operation:

Much Lower		Somewhat Lower		Same as Typical Operation	Somewhat Higher		Much Higher	
1	2	3	4	5	6	7	8	9

Appendix I: Post-Simulation Debriefing Questionnaire for Controller Test

Date: _____ Controller Pair: _____

1. Were you comfortable with the Established on RNP geometry and procedures that you were exposed to during this evaluation? _____
Why?/Why Not? _____

2. As compared to straight-in simultaneous arrivals to runways 35L and 35R, what additional mental or physical requirements, if any, were imposed on you with dual simultaneous independent RNAV (GPS) track-to-fix procedures? _____

3. Which part of the simulation was most difficult (in trail spacing, traffic density, course deviation, and coordination/communication)?
Why? _____

- Were you comfortable giving instructions to aircraft that did not respond as expected to your directions or deviated from its intended flight path?

4. What was your reaction to those deviations and were you comfortable with them? _____

5. Is it more important to ensure the phraseology specified by JO 7110.65V is used, or is it more important to transmit a call as soon as possible regardless of the wording? _____

6. What is the optimal phraseology for the breakout? If different from JO 7110.65V, please explain your rationale.

7. Rate the realism of these components of the simulator (if unrealistic say why: e.g., inconsistent, jerky, etc.):
 - a. Video Display _____
 - b. Display of track movement _____
 - c. Audio _____
 - d. What, if anything, would make the system more realistic?

8. Do you have any other comments about anything you observed during the simulation?

9. Do you have any suggestions for the use of phraseology in the future?
Breakouts? Go-Arounds?

Appendix J: Deviation Recognition Algorithm for Controller Test

This appendix explains the method used to compute the start of a deviation for computing controller reaction times from the controller HITL test. Section 5.3 details the definition of controller reaction time, restated here: “This metric is the amount of time that it takes for a controller to issue breakout instructions after a deviation occurs”. The time of an issued breakout instruction comes from the time a controller presses push-to-talk. This is recorded in the SMART data. A meaningful starting time for a deviation is not recorded; therefore we must post-process the data and make a standard metric for each scenario.

There are three off-nominal scenarios detailed in section 5.1.2:

- Navigation system scenario (figure 5-1) is a slow constant deviation from flight path;
- Course deviation scenario (figure 5-2) is an overshoot before the 10° turn at NOV20, and a correction to course; and
- Wrong runway selection scenario (figure 5-3) is an approach to the wrong runway, which is similar to an offshoot from between the apex at NOV30 and 50° turn at NOV20.

Each of these scenarios requires different assumptions to compute the start of a deviation. In order to make the determination of the reaction time clear, we chose to use two simple geometric algorithms:

1. Time of crossing a line parallel to the extended runway centerline, shown in figure J-1;

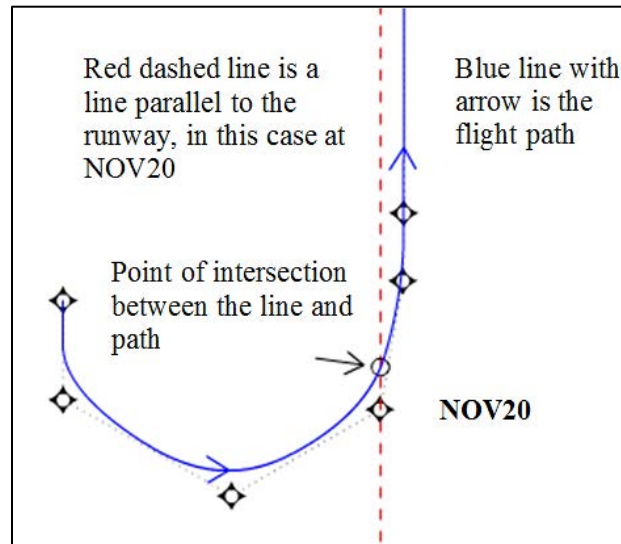


Figure J-1: Time of Crossing a Line Parallel to the Extended Runway Centerline

2. Time at closest point of approach to a point or waypoint, shown in figure J-2.

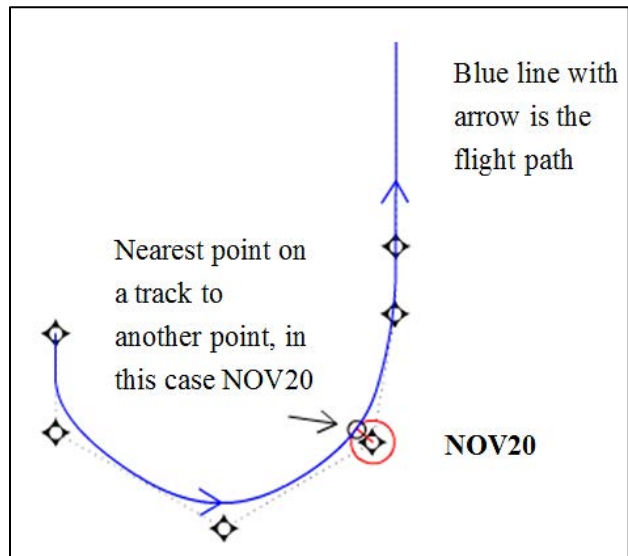


Figure J-2: Time at Closest Point of Approach to a Point or Waypoint

With these tests, we can reasonably estimate the starting time of the deviation. The assumptions used per scenario are as follows:

Navigation System Scenario

As this is a slow, gradual offset there are two reasonable measures for the start of a deviation, shown in figure J-3:

- a) Crossing the NOV20/20NOV parallel; and
- b) Crossing the NOV10/10NOV parallel.

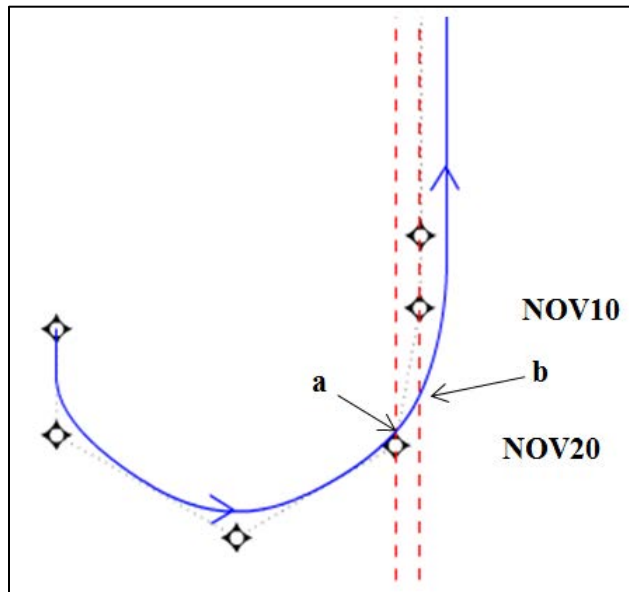


Figure J-3: Navigation System Scenario

Course Deviation Scenario

This is a direct path towards the centerline before correcting, so we can estimate it with two tests for the start of the deviation, shown in figure J-4:

- a) Crossing the NOV20/20NOV parallel;
- b) Nearest distance to NOV20.

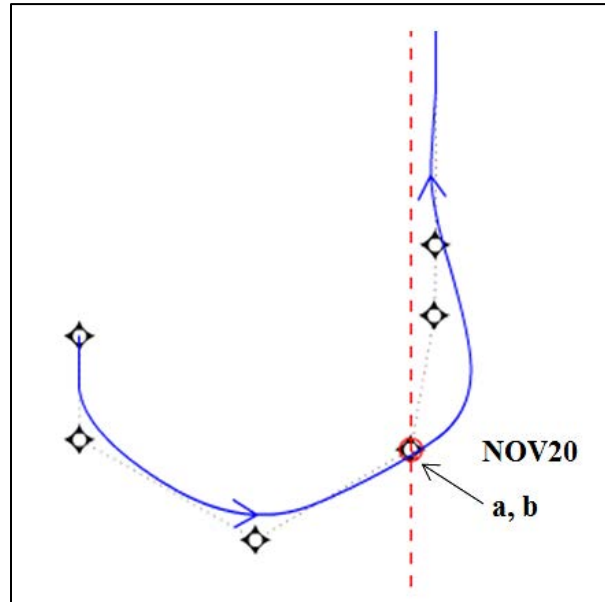


Figure J-4: Course Deviation Scenario

Wrong Runway Selection Scenario

Since the deviation occurs near the apex of the turn, we use an interpolated point between NOV30 and NOV20 to detect the nearest distance. It is possible for the deviation to be detected at NOV30 depending on the flight path. The perpendicular distance to NOV20 is fairly conservative and the deviation is likely to be noticed at or before this point, as shown in figure J-5:

- a) Nearest distance to point halfway between NOV20 and NOV30; and
- b) Crossing the NOV20 parallel.

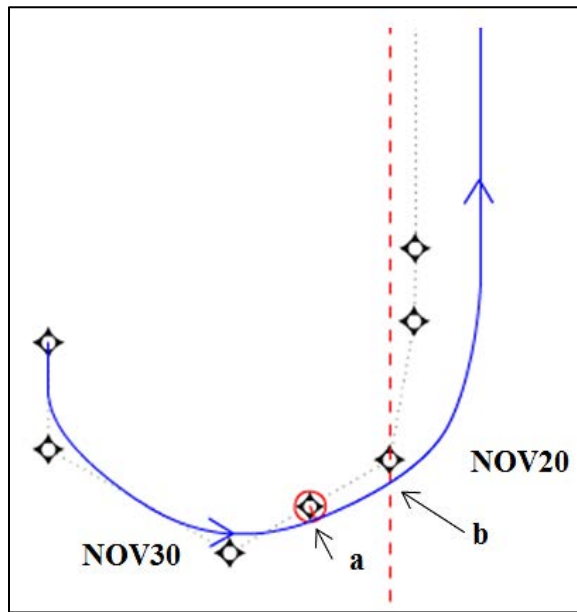


Figure J-5: Wrong Runway Selection

From these post-processed events and times, we can then compute the difference from the controller response of hitting push-to-talk and the computed start of deviation. As stated in section 5.3, it is common for controllers to react well before these standard positions, and any negative times were discarded. Expert opinion indicated that the longer of the two reaction times measured from the course deviation scenarios were most applicable to the collision risk analysis methodology.

Appendix K: Final Monitor Aid Model Description

While studying EoR operations, we determined that the primary safety system used to maintain separation between aircraft on parallel simultaneous independent operations spaced by less than 4,300 ft, the FMA with NTZ, could generate nuisance caution alerts during normal operations. To understand the impact of this on EoR operations, we developed a model to estimate the rate of nuisance caution alerts. The most fundamental metric associated with the nuisance caution alert is the amount that the 10 second predictor, whose entry into the NTZ triggers the caution alert, overshoots the extended runway centerline. The geometry of this based on an idealized flight track flying a constant radius turn with a constant velocity is fairly straight forward, see figure K-1.

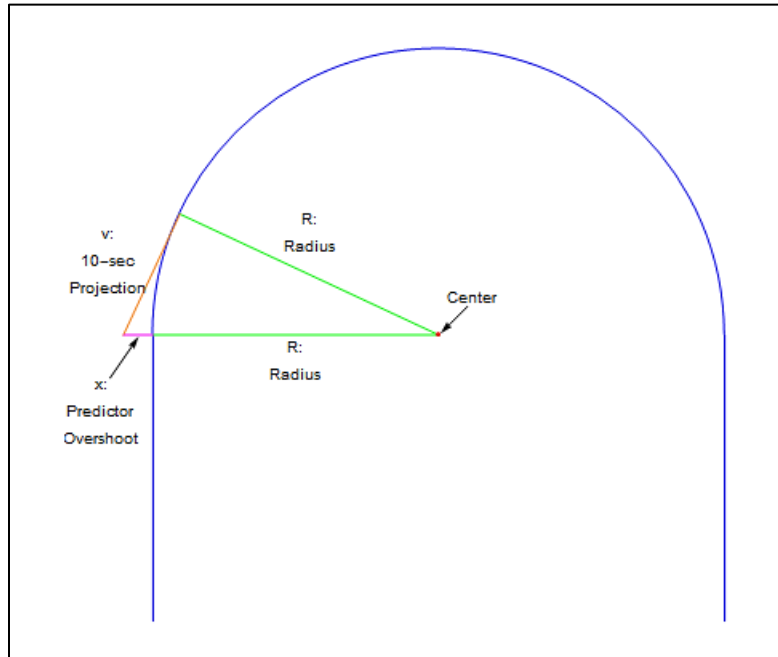


Figure K-1: Base Geometry Full Turn

This maximum overshoot is attained when the direction of the predictor overshoot is entirely directed towards the parallel approach, or orthogonal to the extended runway centerline. The length of v is the groundspeed of the aircraft in knots multiplied by 10 seconds / 3,600 seconds per hour. The amount of overshoot, x , is solved by using the Pythagorean Theorem to solve for the hypotenuse (the length from the center of the arc to the endpoint of the 10 second predictor) and subtracting the length of the radius, R :

$$x = \sqrt{R^2 + v^2} - R \quad (K1)$$

However, in this EoR study, we did not evaluate radius-to-fix turns. Instead, we reviewed fly-by TF turn transitions. These are characterized by turns that fall within a theoretical transition area that allows for various turn radii, based on aircraft speed and bank, with straight segments preceding and following. If we only consider the last turn, the worst case overshoot position would continue to occur at the point described above if the turn amount is sufficiently large to allow that position to exist. If it does not, then the maximum overshoot occurs at the start of the turn, see figure K-2.

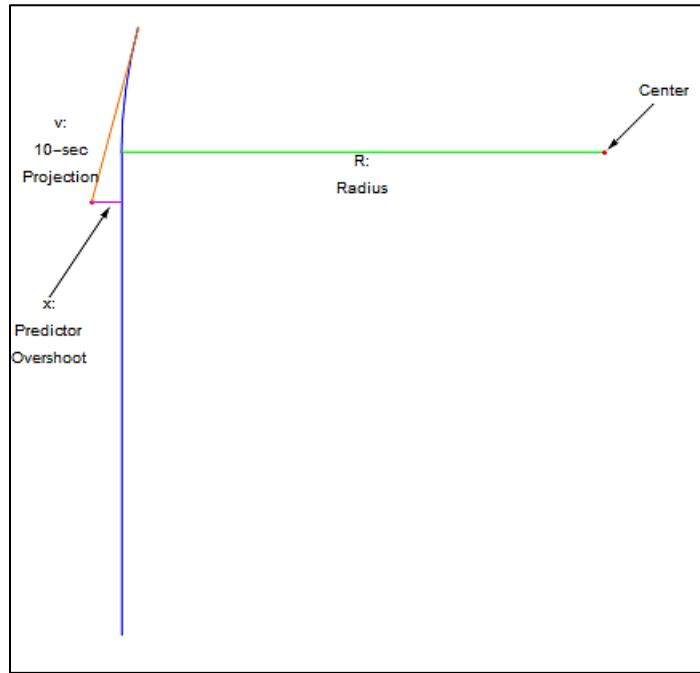


Figure K-2: Maximum Overshoot in Restricted Turn Amount Case

While the other variables are the same as above, β represents the amount of heading change in degrees associated with the turn. This geometry results in the following piecewise function that uses the worst-case overshoot when β is sufficiently large, but multiplies the sine of the start angle of the projection by the length of v discounted by the amount of the projection that does not exceed the extended runway centerline.

$$x = \begin{cases} \sin(\beta) \left(v - R \tan \frac{\beta}{2} \right) & \beta < \tan^{-1} \frac{v}{R} \\ \sqrt{R^2 + v^2} - R & \beta \geq \tan^{-1} \frac{v}{R} \end{cases} \quad (\text{K2})$$

However, this representation of the 10 second projection as an instantaneous projection off of the flight path is an oversimplification of reality. The 10 second prediction is based off of targets calculated based off radar returns measuring the position of a flight path. Fundamentally, these systems only measure the aircraft position every 4.8 seconds with additional latency for processing and display. Furthermore, the radar introduces substantial noise while measuring the aircraft position. To determine the effects of this noise and latency, we used fast-time simulation capabilities that include aircraft position simulation and simulation of the radar measurement and automation platform. These simulations entailed aircraft flying the paths shown in figures K-1 and K-2 parameterized by a constant groundspeed, a constant radius, and the number of degrees of turn. We tested 44 variable combinations with speeds between 150 knots and 240 knots, radii between 1.113 NM and 4.5 NM, and heading changes between 10° and 180° , see table K-1.

Table K-1: Simulation List

Radius	Speed	Heading Change
1.454	165	10
1.454	165	12.5
1.454	165	15
1.454	165	17.5
1.454	165	50
1.454	165	90
1.454	210	10
1.454	210	12.5
1.454	210	15
1.454	210	17.5
1.454	210	20
1.454	210	25
1.454	210	90
1.454	240	10
1.454	240	12.5
1.454	240	15
1.454	240	17.5
1.454	240	20
1.454	240	22.5
1.454	240	25
1.454	240	30
1.454	240	50
1.454	240	90
2.25	165	10
2.25	165	12.5
2.25	165	90
2.25	240	10
2.25	240	12.5
2.25	240	15
2.25	240	17.5
2.25	240	50
2.25	240	90
3	240	10
3	240	12.5
3	240	90
3	210	180
3	240	180
3	150	180
1.454	240	180

1.113	190	180
1.113	210	180
1.113	150	180
4.5	210	180

These simulations introduced no error on the path of the aircraft, but shifted the entire flight path by a certain number of feet from the NTZ. Some tracks, therefore, turned onto a final approach course that was on the boundary of the NTZ and others turned onto a final approach course 2,000 ft from the NTZ. The maximum 2,000 ft case would be equivalent to a 6,000 ft runway spacing. When we binned the data by this distance from extended runway centerline to the NTZ, it yields an interesting function that is always one when the distance is zero and decreases monotonically as the distance increases, eventually equaling zero. Due to noise in the simulation, however, the individual data points may not always decrease monotonically, see figure K-3.

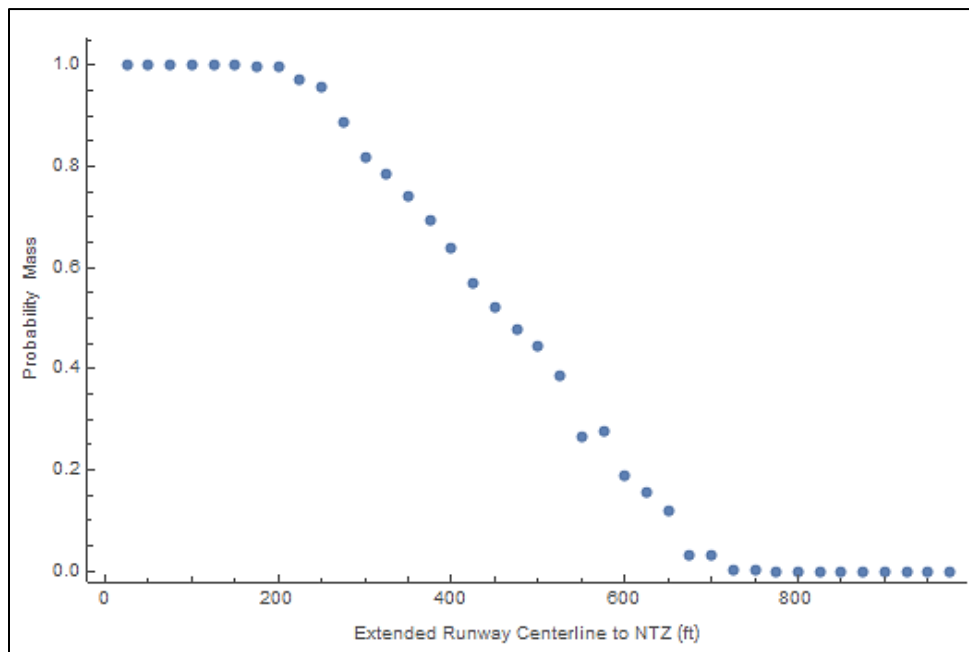


Figure K-3: Example Function of False Caution Alert Probability per distance between NTZ and Extended Runway Centerline

This function is clearly related to a survival function, $S(x)$, which is defined by the probability density function, $P(x)$, of any probability distribution and also decreases from one to zero over the domain of the function, see equation K3. Using the survival function of a highly parameterized bounded distribution like the Johnson bounded distribution, we are able to model the results attained by the simulation. However, these models are parameterized by four values, which are not easily ordered. Fortunately, the fitted models all seem to have very similar shapes and the only significant difference is the location where the probability begins to decrease, see figure K-4. Figure K-5 demonstrates that when models of interest are plotted with the same location parameter, the variation is less than 100 ft.

Therefore, we reduce the parameterization on these models to the location parameter and an average of the most relevant shape and scale parameters for all of the models.

$$S(x) = Prob(X > x) = \int_x^{x_{max}} P(x_0) dx_0 \quad (K3)$$

$$F(x) + S(x) = Prob(X > x) + Prob(X \leq x) = 1$$

where $F(x)$ is the cumulative density function.

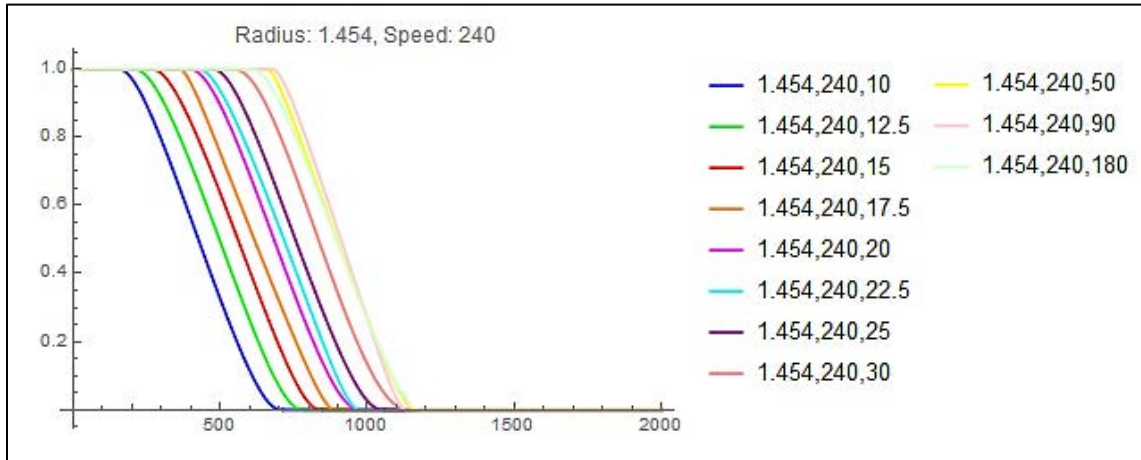


Figure K-4: Example Fitted Models

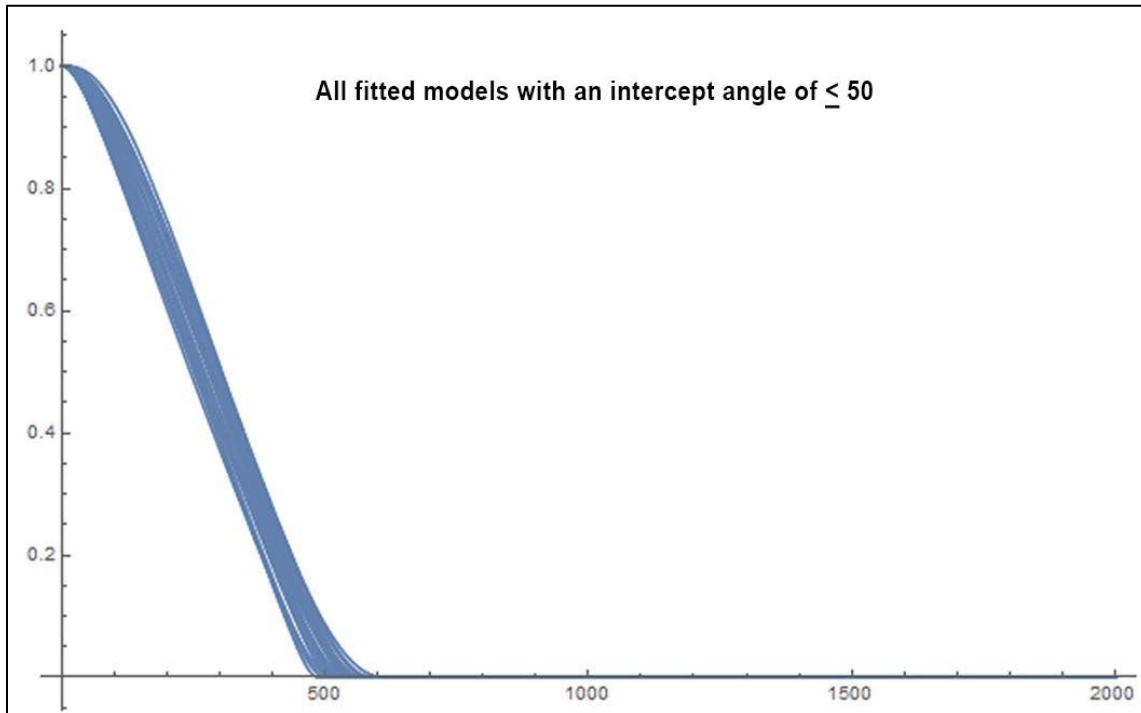


Figure K-5: Independent Models Plotted with Location Set to Zero

Ultimately, this results in a model of the probability of each of these cases described by a single parameter. From the discussion of the overshoot geometry, we are able to calculate a single, reasonable metric that we believed would correlate with the simulation

results. Unfortunately, the correlation is strong, but there is too much variation to predict the collision risk with sufficient accuracy, see figure K-6. Most of the variation is clearly associated with the cases where the heading change is less than 50°.

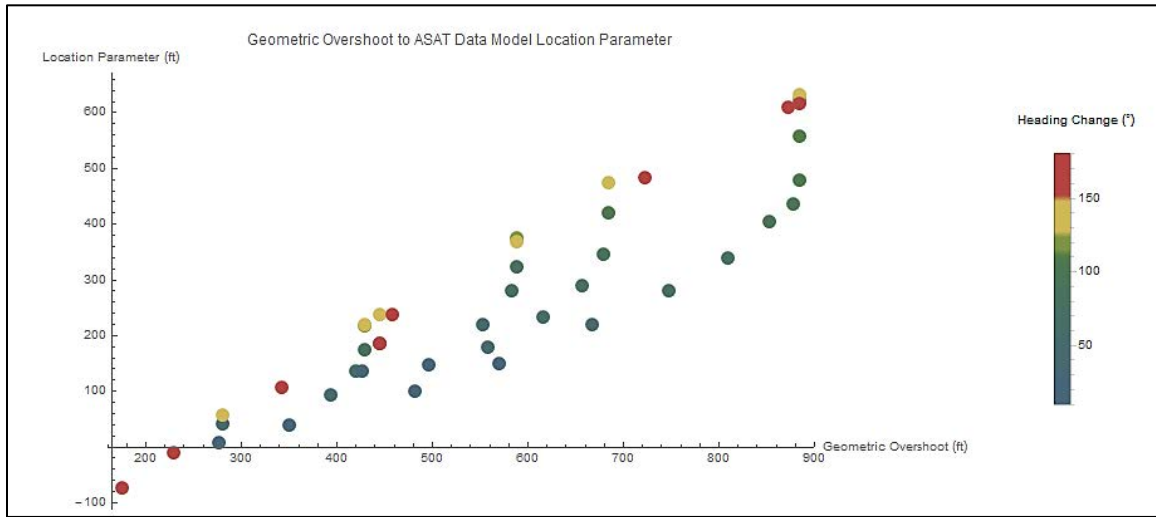


Figure K-6: Scatter Plot of Location Parameter by Geometric Overshoot

After careful examination of the effect of the heading change on the location of probability model for nuisance caution alerts, it became clear that this was a function of all of the variables in the geometry calculation. Since this was the case, we attempted to correlate the residuals of the initial model with the derivative of the worst-case only overshoot, see equation K4. This was successful, but only if an additional parameter was incorporated into the value of β used in equation K4 to tune the scale of the impact of the heading change variable, see equation K5. Based on simulation of various this tuning variable was set to 59.

$$x' = \begin{cases} \frac{-v \cos(\beta) + 360R \sin(\beta)}{v \sin(\beta) + 360R \cos(\beta)} & \beta \leq 90 \text{ and } \cos(\beta) \left(\frac{v}{360} - R \tan\left(\frac{\beta}{2}\right) \right) \geq R \tan\left(\frac{\beta}{2}\right) \quad (\text{K4}) \\ 0 & \text{Else} \end{cases}$$

$$\beta = \beta_0 - \frac{2v\xi}{3600R} \quad (\text{K5})$$

Using the worst-case geometric overshoot calculation and the tuned overshoot derivative calculation, we were able to fit a 2-dimensional parabolic model that estimates the parameters of the survival function that describes the probability of attaining a nuisance alert based on the speed, radius, and heading change, see figure K-7. The residuals of this model are all within ± 50 ft.

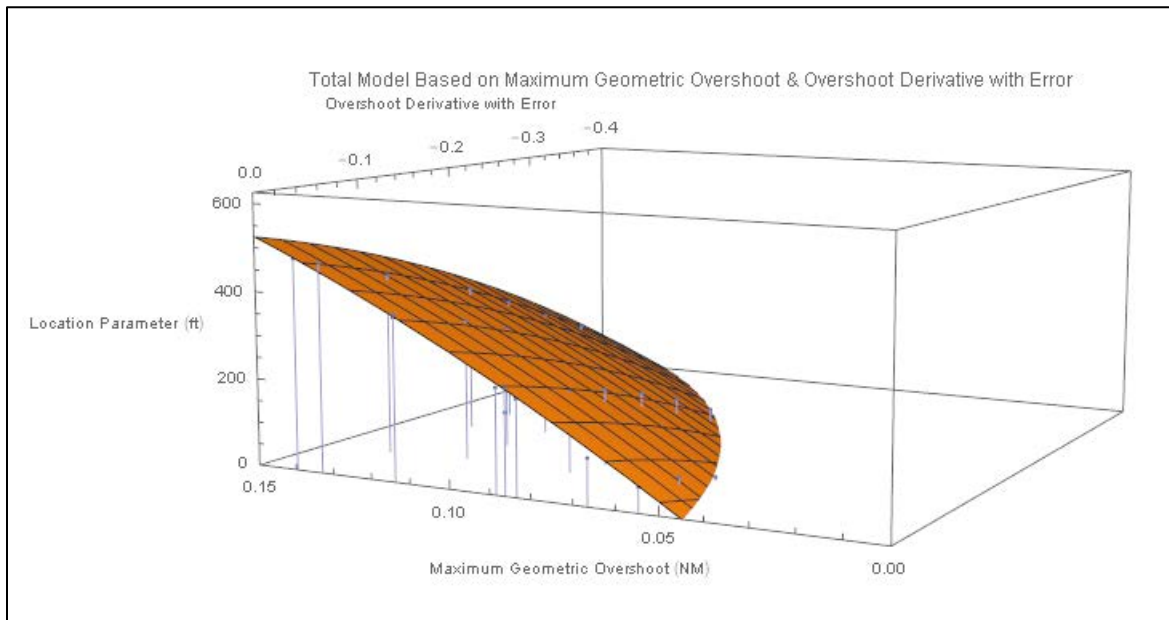


Figure K-7: Fitted Model of Location Parameter by Worst-Case Geometric Overshoot and Tuned Overshoot Derivative

However, to convert this model to a generic function that calculates the nuisance caution rate based on a specific TF-TF fly-by turn procedure design, additional functions must be composed with this model. The full functions that need to be composed are diagramed in figure K-8.

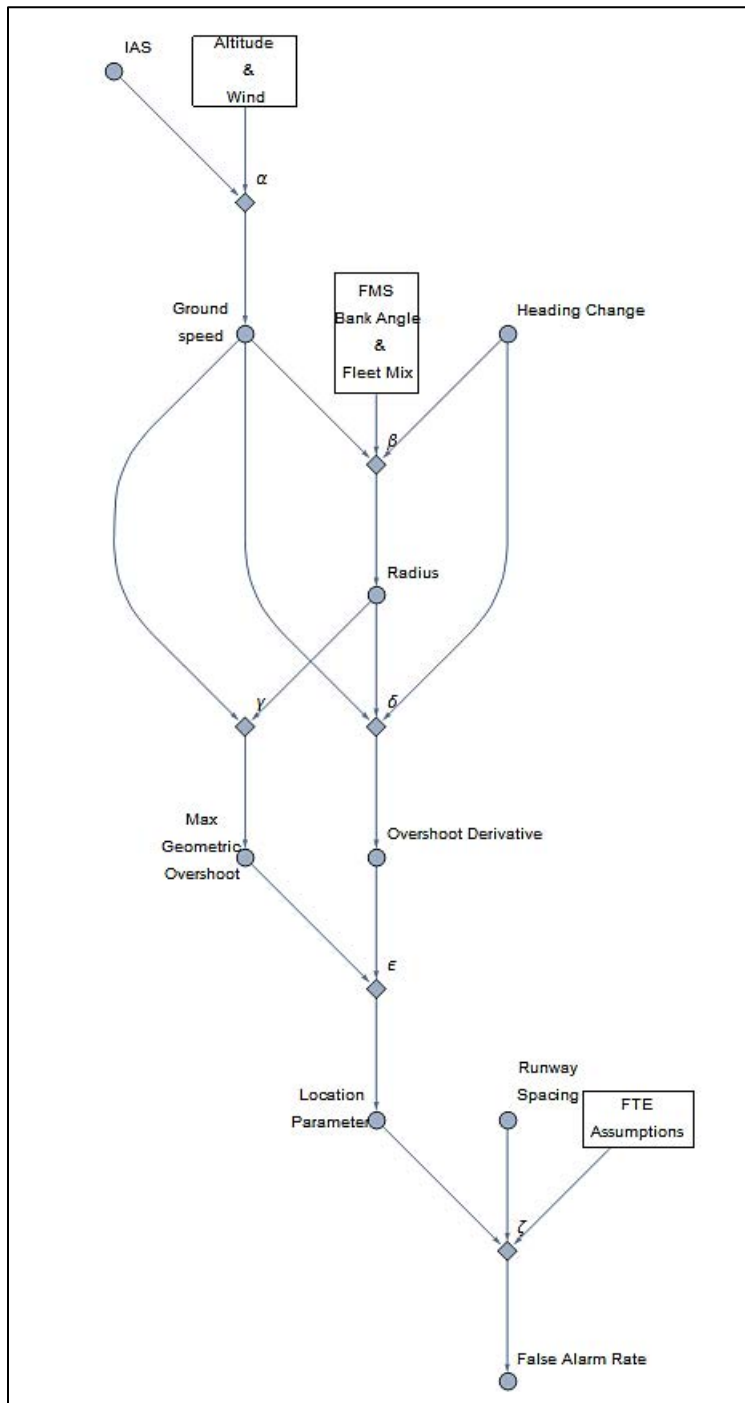


Figure K-8: Function Composition Diagram

Having derived the functions denoted by γ , δ , and ϵ in figure K-8, we still need to define those functions indicated by α , β , and ζ . The α function can be found by convolving two functions used in instrument approach procedure design criteria. [24] For this equation, we have defined v to be the groundspeed in knots, u to be indicated airspeed in knots, A to be the altitude at the turn in feet mean sea level, and w to be the speed of the tailwind during the turn in knots.

$$v = \frac{171233u \sqrt{303 - 0.00198A}}{(288 - 0.00198)^{2.628}} + w \quad (K6)$$

The β function is also reliant on an equation from FAA Order 8260.58 that converts a groundspeed and bank angle to a turn radius, see equation K6. [24] However, for TF-TF fly-by turns, the bank angle is dependent on FMS logic. MITRE Center for Advanced Aviation System Development surveyed the logic in FMS software that represents 83% of the active fleet. The probabilities associated with each given turn radius were then weighted by the percentage of the fleet that has FMS logic that would result in that turn radius.

$$R = \frac{v^2}{68625.4 \tan(\phi)} \quad (K7)$$

Finally, we need a function, labeled ζ in figure K-8, to convert the survival function to a probability given a specific runway separation and path keeping error assumption. To get this, we need to understand that the survival function is actually the probability of receiving a caution alert given a distance between the final approach course and the NTZ. With a specific runway spacing and an assumption that the cross-track error is constant throughout one turn-on and can be modeled by a normal distribution, we can then determine that the probability that any particular distance occurs. By multiplying the probability of caution alert given a distance by the probability of a distance, we are able to get a function of the probability of a caution alert and distance. Integrating this numerically over all distances yields the probability of a caution alert. The results shown in figure 6-22 are given numerically below, see table K-2. It is difficult to say which runway spacings are acceptable at any given airport because this will vary based on the facility attitude toward nuisance alerts as well as local factors including winds, fleet mix, and turn elevation.

Table K-2: 10° Intercept Nuisance FMA Alerts by Runway Spacing and Groundspeed

Ground Speed (knots)	RWY Spacing 3,600 ft	RWY Spacing 3,700 ft	RWY Spacing 3,800 ft	RWY Spacing 3,900 ft	RWY Spacing 4,000 ft	RWY Spacing 4,100 ft	RWY Spacing 4,200 ft	RWY Spacing 4,300 ft	RWY Spacing 4,400 ft
150	3E-2	2E-2	2E-2	1E-2	8E-3	5E-3	4E-3	2E-3	1E-3
160	3E-2	3E-2	2E-2	1E-2	9E-3	6E-3	4E-3	3E-3	2E-3
170	4E-2	3E-2	2E-2	1E-2	1E-2	7E-3	4E-3	3E-3	2E-3
180	4E-2	3E-2	2E-2	2E-2	1E-2	7E-3	5E-3	3E-3	2E-3
190	4E-2	3E-2	2E-2	2E-2	1E-2	8E-3	6E-3	4E-3	2E-3
200	5E-2	4E-2	3E-2	2E-2	1E-2	9E-3	6E-3	4E-3	3E-3
210	5E-2	4E-2	3E-2	2E-2	1E-2	1E-2	7E-3	5E-3	3E-3
220	6E-2	4E-2	3E-2	2E-2	2E-2	1E-2	8E-3	6E-3	4E-3
230	6E-2	4E-2	3E-2	2E-2	2E-2	1E-2	9E-3	6E-3	4E-3
240	6E-2	5E-2	4E-2	3E-2	2E-2	1E-2	1E-2	7E-3	5E-3
250	6E-2	5E-2	4E-2	3E-2	2E-2	1E-2	1E-2	8E-3	5E-3
260	7E-2	5E-2	4E-2	3E-2	2E-2	2E-2	1E-2	8E-3	6E-3
270	7E-2	5E-2	4E-2	3E-2	2E-2	2E-2	1E-2	9E-3	6E-3
280	7E-2	6E-2	4E-2	3E-2	2E-2	2E-2	1E-2	9E-3	7E-3
290	7E-2	6E-2	4E-2	3E-2	3E-2	2E-2	1E-2	1E-2	7E-3
300	8E-2	6E-2	5E-2	4E-2	3E-2	2E-2	1E-2	1E-2	8E-3
310	8E-2	6E-2	5E-2	4E-2	3E-2	2E-2	2E-2	1E-2	8E-3
320	8E-2	6E-2	5E-2	4E-2	3E-2	2E-2	2E-2	1E-2	9E-3
330	8E-2	6E-2	5E-2	4E-2	3E-2	2E-2	2E-2	1E-2	9E-3
340	8E-2	7E-2	5E-2	4E-2	3E-2	2E-2	2E-2	1E-2	9E-3
350	8E-2	7E-2	5E-2	4E-2	3E-2	2E-2	2E-2	1E-2	1E-2

Ground Speed (knots)	RWY Spacing 4,500 ft	RWY Spacing 4,600 ft	RWY Spacing 4,700 ft	RWY Spacing 4,800 ft	RWY Spacing 4,900 ft	RWY Spacing 5,000 ft	RWY Spacing 5,100 ft	RWY Spacing 5,200 ft	RWY Spacing 5,300 ft
150	9E-4	6E-4	3E-4	2E-4	1E-4	7E-5	4E-5	2E-5	1E-5
160	1E-3	6E-4	4E-4	2E-4	1E-4	7E-5	4E-5	2E-5	1E-5
170	1E-3	7E-4	4E-4	3E-4	2E-4	9E-5	5E-5	3E-5	1E-5
180	1E-3	8E-4	5E-4	3E-4	2E-4	1E-4	6E-5	3E-5	2E-5
190	2E-3	1E-3	6E-4	4E-4	2E-4	1E-4	7E-5	4E-5	2E-5
200	2E-3	1E-3	7E-4	4E-4	3E-4	2E-4	9E-5	5E-5	3E-5
210	2E-3	1E-3	9E-4	5E-4	3E-4	2E-4	1E-4	7E-5	4E-5
220	2E-3	2E-3	1E-3	7E-4	4E-4	2E-4	1E-4	9E-5	5E-5
230	3E-3	2E-3	1E-3	8E-4	5E-4	3E-4	2E-4	1E-4	6E-5
240	3E-3	2E-3	1E-3	9E-4	6E-4	3E-4	2E-4	1E-4	7E-5
250	4E-3	2E-3	2E-3	1E-3	6E-4	4E-4	2E-4	1E-4	9E-5
260	4E-3	3E-3	2E-3	1E-3	7E-4	5E-4	3E-4	2E-4	1E-4
270	4E-3	3E-3	2E-3	1E-3	8E-4	5E-4	3E-4	2E-4	1E-4
280	5E-3	3E-3	2E-3	1E-3	9E-4	6E-4	4E-4	2E-4	1E-4
290	5E-3	3E-3	2E-3	2E-3	1E-3	7E-4	4E-4	3E-4	2E-4

300	5E-3	4E-3	3E-3	2E-3	1E-3	7E-4	5E-4	3E-4	2E-4
310	6E-3	4E-3	3E-3	2E-3	1E-3	8E-4	5E-4	3E-4	2E-4
320	6E-3	4E-3	3E-3	2E-3	1E-3	9E-4	6E-4	4E-4	2E-4
330	6E-3	4E-3	3E-3	2E-3	1E-3	9E-4	6E-4	4E-4	2E-4
340	7E-3	5E-3	3E-3	2E-3	2E-3	1E-3	7E-4	4E-4	3E-4
350	7E-3	5E-3	3E-3	2E-3	2E-3	1E-3	7E-4	4E-4	3E-4

The realism of the simulation of the FMA logic was validated in an effort where we collaborated with the FAA Academy (AMA-421) by using ATCoach to simulate aircraft tracks that entered the NTZ as implemented on the actual STARS platform, collected the recorded data, and inspected it to ensure that similar alert times were generated by our simulated FMA as the actual FMA.

Appendix L: Hsu-Anderson Reich Greenhaw Model

The nominal collision risk of two aircraft on proximate approach paths can be calculated by means of a generalization of the Hsu-Anderson model. The details of such a calculation are presented in the two equations below and the associated table of parameters, table L-1.

$$CR(t_0, t_1) = 2 \times NP \int_{t_0}^{t_1} HOP(t) \times P_z(h_z(t)) \times \left(\frac{2V_{rel}}{\pi\lambda_{xy}} + \frac{|\dot{z}|}{2\lambda_z} \right) dt \quad (L1)$$

Where,

$$HOP(t) \approx \pi\lambda_{xy}^2 \int_a^c \int_c^a f_A(S_x(t) + a \cos(\theta(t)) - c \sin(\theta(t))) f_A(a) f_C(S_y(t) + a \sin(\theta(t)) + c \cos(\theta(t))) f_C(c) dc da. \quad (L2)$$

Table L-1: Parameters Used to Calculate Collision Risk from Equations (L1) & (L2)

Parameter Symbol	Parameter Description	Value Used
$CR(t_0, t_1)$	Collision Risk during time interval (t_0, t_1)	Calculated
NP	Number of Aircraft Pairs	1
$HOP(t)$	Horizontal Overlap Probability at time t	Calculated
$h_z(t)$	Nominal vertical separation at time t	0
$P_z(h_z(t))$	Vertical Overlap Probability with given vertical separation at time t	1.0
V_{rel}	Relative horizontal approach speed of the two aircraft	20 knots, 0 knots
$ \dot{z} $	Relative vertical approach speed of the two aircraft	1.5 knots
λ_{xy}	Radius of the cylinder modelling aircraft	0.030 NM
λ_z	Height of the cylinder modelling aircraft	0.015 NM
a	Along-track error	Variable
f_A	Along-track error distribution function	Uniform
c	Cross-track (lateral) error	Variable
f_C	Cross-track error distribution function	Gaussian based on RNP 0.1 ($\sigma=0.051$)
$S_x(t)$	Nominal longitudinal separation at time t	Based on model, see Equations (L5)
$S_y(t)$	Nominal lateral separation at time t	Based on model, see Equations (L5)
$\theta(t)$	Angle at time, t , between the tangents to the two curves defining the two routes	Based on model, see Equation (L6)
V	Nominal ground speed of aircraft along path	200 knots
r	Radius of nominal RF turn	2.5 NM
y_0	Half the runway spacing	1000 to 2000 feet

Figure L-1 illustrates the geometry of the scenario used. The lower route is a mirror image of the upper one, and each is the concatenation of an RF turn of radius, r , and a straight approach segment that is a distance y_0 from the x -axis. For normal operations, it was determined that evaluating RF would be substantially easier to evaluate and provide sufficiently similar results. Two proximate aircraft are assumed to fly a constant

velocity, V , starting at the same nominal distance out on their respective routes, points P_1 and P_2 at time $t_0 = 0$. The nominal lateral distance between the aircraft at time, t , will be $S_y(t)$.

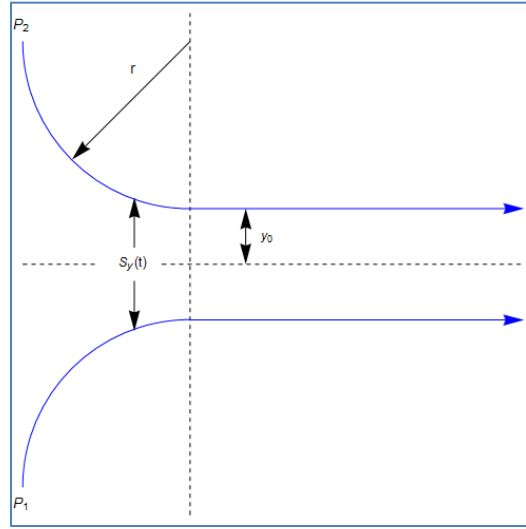


Figure L-1: Typical EoR Geometry for Two Adjacent Routes Involving Proximate Aircraft

Based on this EoR geometry, the nominal positions of the two aircraft at time t , $(x_{N1}(t), y_{N1}(t))$ and $(x_{N2}(t), y_{N2}(t))$ can be described as:

$$x_{N1}(t) = \begin{cases} \left(r - r \cos\left(\frac{tV}{r}\right) & 0 \leq t \leq \frac{\pi r}{2V} \right) \\ \left(V\left(t - \frac{\pi r}{2V}\right) + r & \frac{\pi r}{2V} < t \right) \end{cases} \quad (L3)$$

$$y_{N2}(t) = \begin{cases} \left(-\sqrt{r^2 - (r - X_{N1})^2} + r + y_0 & 0 \leq t \leq \frac{\pi r}{2V} \right) \\ \left(y_0 & \frac{\pi r}{2V} < t \right) \end{cases} \quad (L4)$$

And, therefore, the nominal lateral and longitudinal separations can be described as:

$$S_y(t) = y_{N2}(t) - y_{N1}(t) = 2y_{N2}(t), \quad S_x(t) = x_{N2}(t) - x_{N1}(t) = 0. \quad (L5)$$

Where the angle between the tangents to the two curves defining the two routes at time, t , is:

$$\theta(t) = \begin{cases} \left(2t \frac{V}{r} - \pi, 0 \leq t \leq \frac{\pi r}{2V} \right) \\ \left(0, \frac{\pi r}{2V} < t \right) \end{cases} \quad (L6)$$

Besides using these models for fault-free, or normal, aircraft-to-aircraft collision risk, they can also be used to describe the mathematical model used for faulted, or non-normal, collision risk. The Reich model describes a collision using multiple types of overtakes;

however, the non-normal condition required for a collision in this case is a significant path deviation. Therefore, the lateral risk seen in equation L7 is the most related term in the Reich collision risk equation.

$$\frac{\# \text{ Collisions}}{\text{Flight Hour}} = N_x \frac{2\lambda_x}{V_x} \left(P_y \frac{V_y}{2\lambda_y} \right) P_z \quad (\text{L7})$$

In this equation, N_x is the longitudinal overtake frequency per hour, λ_x is the size of a box representing the aircraft's volume in the longitudinal direction, and V_x is the relative velocity in the longitudinal direction. Thus the term $(2\lambda_x)/V_x$ represents the duration of a longitudinal overlap in hours. Furthermore, P_y is the probability of entry into lateral overlap, V_y is the lateral relative velocity, λ_y is the size of a box representing the aircraft's volume in the lateral direction, and P_z is the probability of vertical overlap. Note that the term $P_y(V_y/2\lambda_y)$ represents the rate of entry into lateral overlap per hour.

The SMS process requires that terminal operations be evaluated based on the number of collisions per operation, rather than per flight hour. If we let h_x be the number of hours per operation, we can convert the above formula into collisions per operation, see equation L8.

$$\frac{\# \text{ Collisions}}{\text{Operation}} = N_x h_x \frac{2\lambda_x}{V_x h_x} \left(P_y \frac{V_y h_x}{2\lambda_y} \right) P_z \quad (\text{L8})$$

Now $(2\lambda_x)/V_x h_x$ is the length of longitudinal overlap per operation and $P_y(V_y h_x/2\lambda_y)$ is the rate of entering into horizontal overlap per operation. This corresponds to equation 8 in section 6. The probability of failure in the appropriate part of the event, which is the condition for the non-normal collision risk, are not represented in equation L8, but the rate of the longitudinal positions allowing for a possible collision is calculated as 0.03 and is multiplied by the other two terms to get to the 9×10^{-8} coefficient. This corresponds to the $(2\lambda_x)/V_x h_x$ term in L8. The $P_y(V_y h_x/2\lambda_y)$ term then corresponds to equation L8's probability of horizontal overlap and P_z corresponds to the probability of vertical overlap.

Appendix M: Sensitivity Analysis Details

Extra Length in 10° Leg

Figure M-1 displays the relationship between collision risk and length of the 10° leg of the EoR procedure. As the length of the leg increases above the minimum leg length (0-18,000 ft shown), the collision risk decreases beyond 5.0×10^{-4} . Figures M-1 through M-4 clearly depict a decrease in collision risk as the length of the 10° leg increases measured in feet.

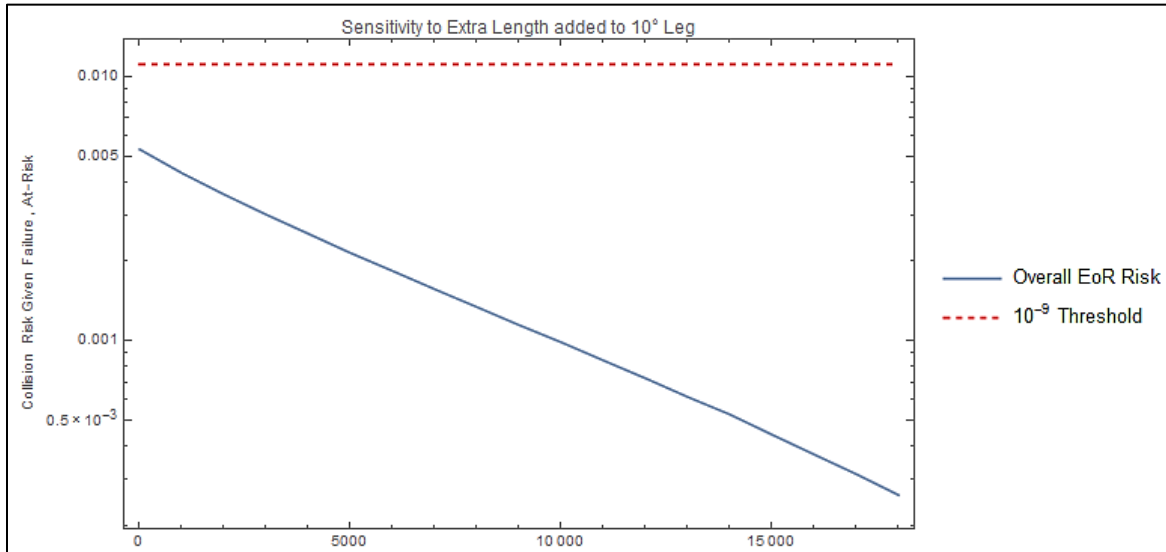


Figure M-1: Collision Risk versus 10° Leg Length

Figure M-2 displays the collision risk as it relates to the extra length added to the 10° leg. There are eight total cases under consideration: four nominal aircraft with and without VNAV equipment continued the approach to capture the glideslope or were in level flight; four nominal aircraft with and without VNAV equipment had captured the glideslope or were in level flight and conducted a go-around. As the leg length increases in feet (0-18,000 ft shown) the collision risk decreases based on aircraft configurations. In this graph, the best case shown is a VNAV-equipped nominal aircraft that has captured the glideslope and is continuing the approach. The worst case shown is a nominal aircraft with no approved VNAV equipment, executing a go-around that has captured the glideslope. Note: the horizontal (red) line depicts the 10^{-9} threshold.

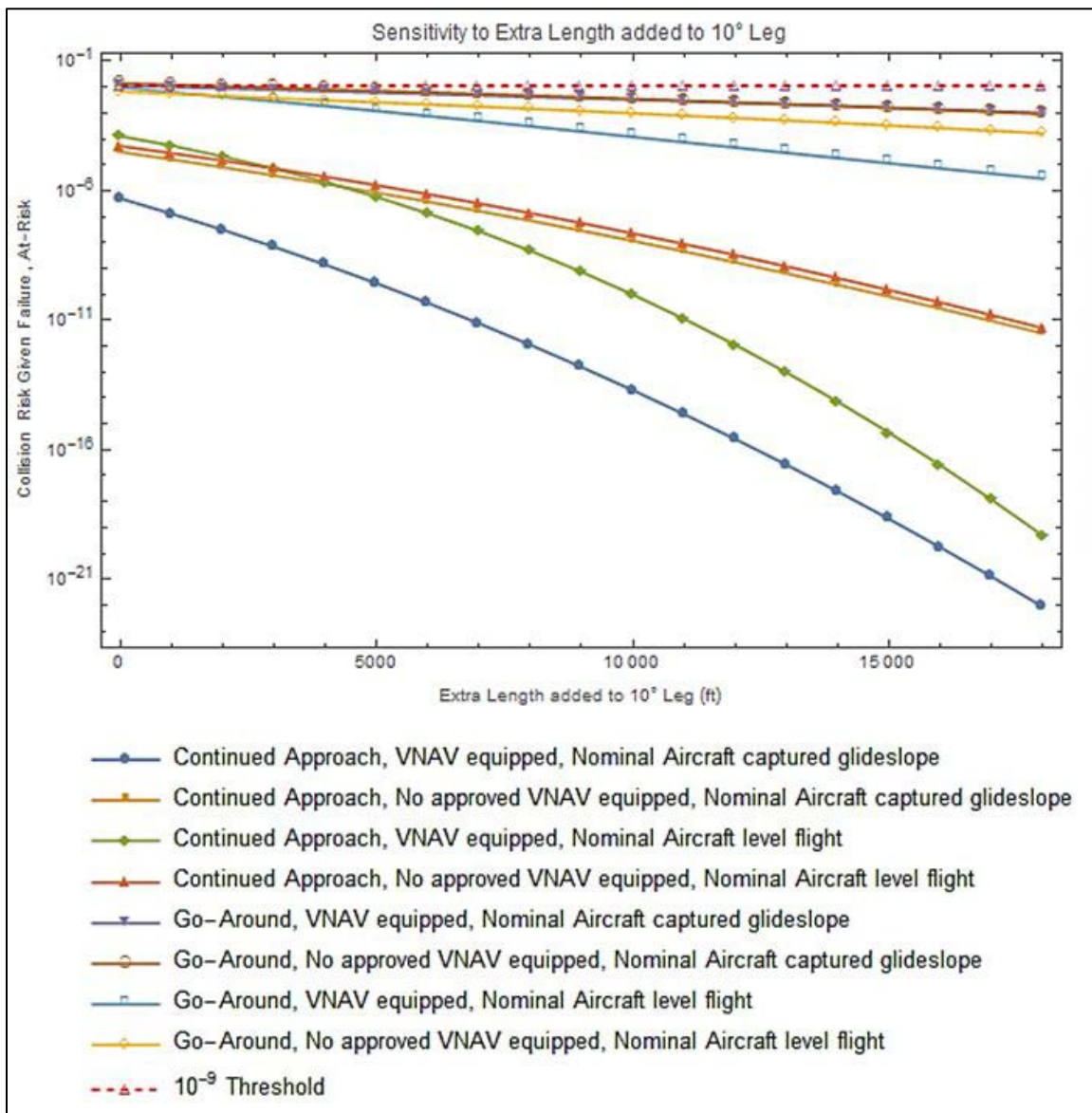


Figure M-2: Collision Risk versus Sensitivity to Extra Length added to 10° Leg

Figure M-3 further breaks down the data presented in figure M-2. In this figure, there are four cases of nominal aircraft that continued approaches with and without VNAV equipment that either captured the glideslope or were in level flight. The extra 10° leg length in feet is plotted against the track angle relative to the ILS, with associated collision risk. The darker shade (blue) that is visible in each graph indicates a decrease in collision risk as the length of the 10° leg is increased. The concentration of the data graphed indicates that the level of risk increases at that angle shown. For example, graphs (a) and (b) indicate an increase in risk at the 50° track and the 90° track relative to the ILS based on that aircraft configuration. Graphs (c) and (d) indicate an increase in risk at the 90° track relative to the ILS, based on that aircraft configuration.

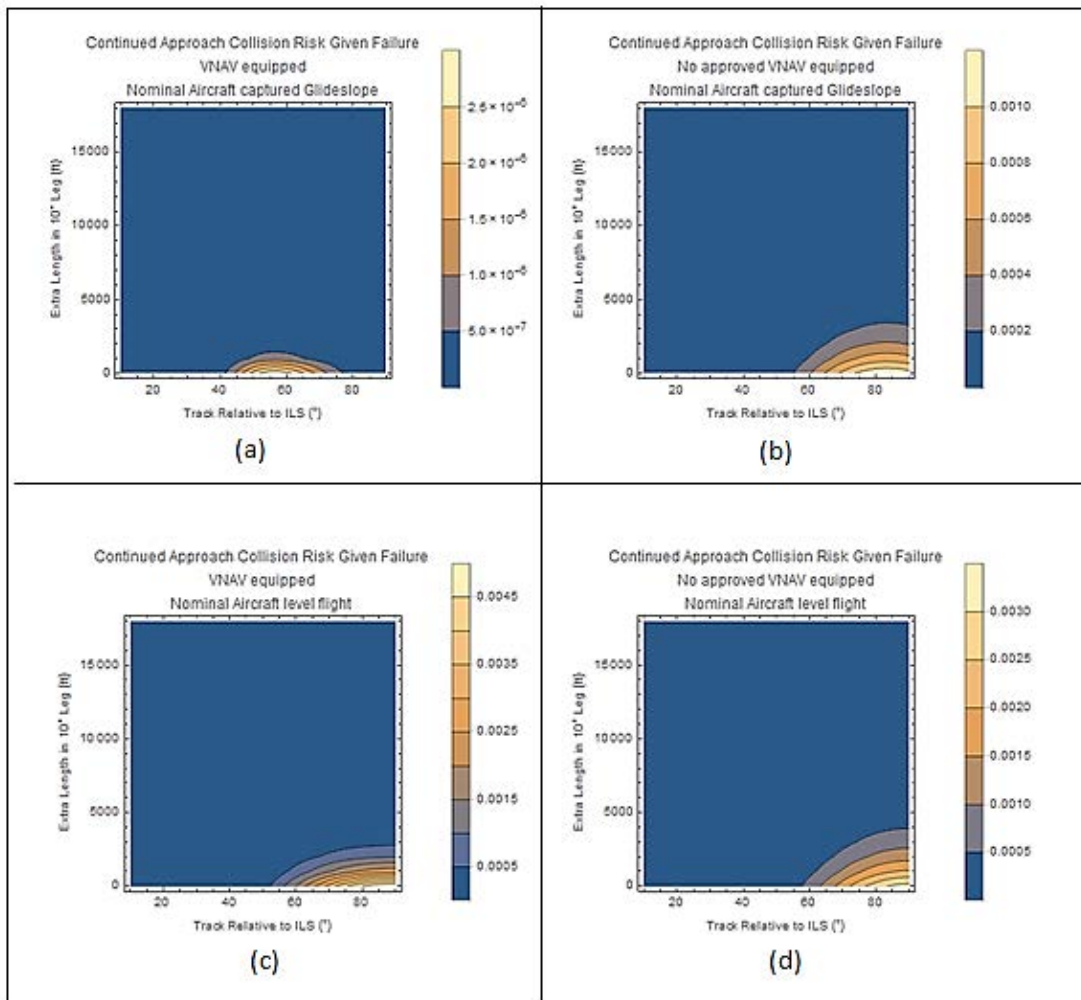


Figure M-3: Collision Risk for Nominal Aircraft with and without VNAV Equipment with Captured Glideslope and in Level Flight

Figure M-4 breaks down the data presented in figure M-2 just as described above. In this figure, there are four cases of nominal aircraft that executed go-arounds with and without VNAV equipment that either captured the glideslope or were in level flight. The extra 10° leg length in feet is plotted against the track angle relative to the ILS, with associated collision risk. The darker shade (blue) that is visible in each graph indicates a decrease in collision risk as the length of the 10° leg is increased. The concentration of the data graphed indicates that the level of risk increases at that angle shown. For example, graphs (a) and (b) indicate an increase in risk at the 80° track and the 70° track relative to the ILS based on that aircraft configuration. Graphs (c) and (d) indicate an increase in risk at the 30° and 50° tracks respectively relative to the ILS, based on that aircraft configuration.

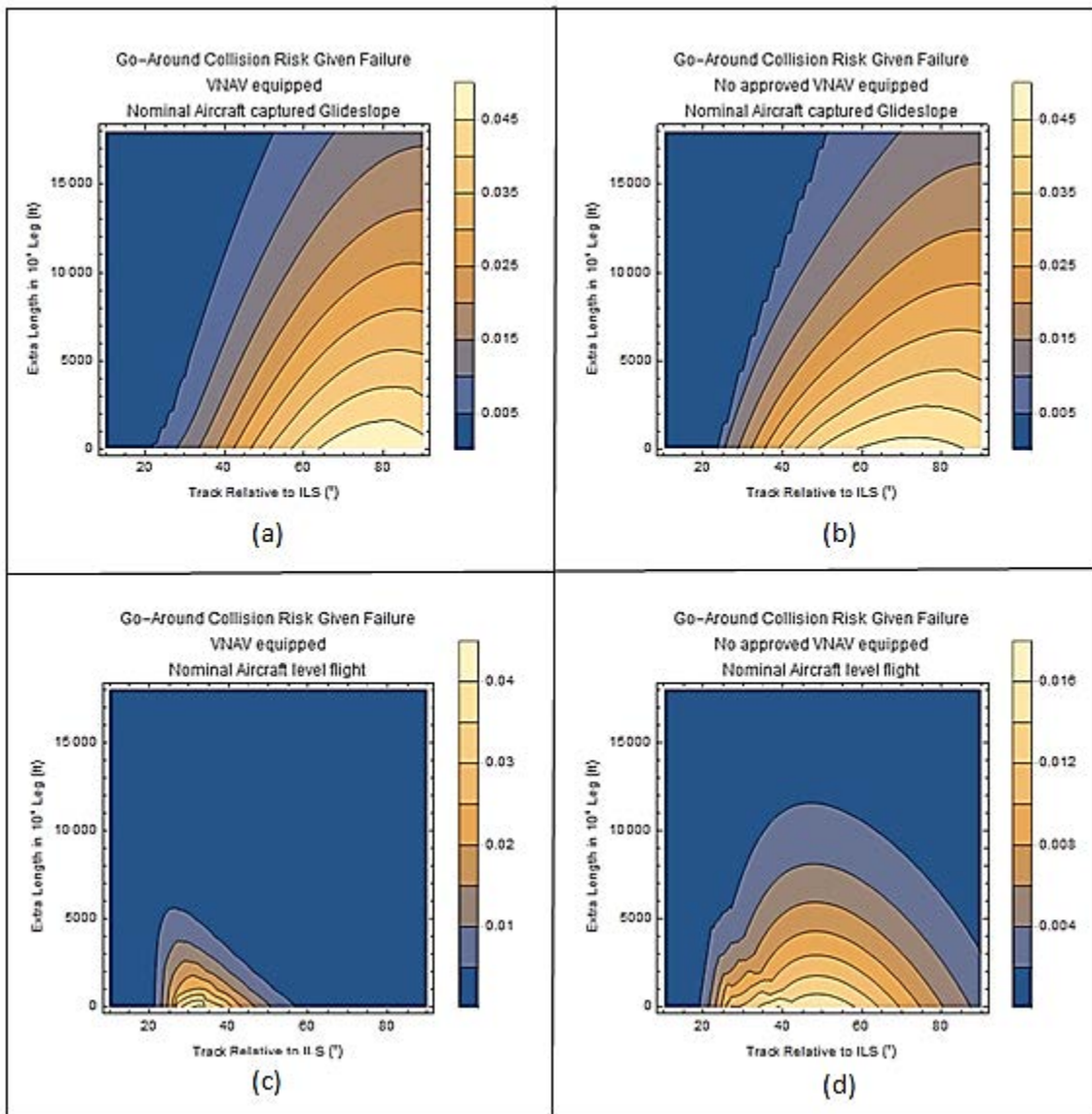


Figure M-4: Collision Risk for Nominal Aircraft Executing a Go-around with and without VNAV Equipment with Captured Glideslope and in Level Flight

Runway Spacing

Similar to how increasing the length of the 10° leg reduces collision risk, the same can be said about increasing the distance between parallel runways. In figure M-5, the dashed (red) line indicates the 10^{-9} threshold for collision risk. The overall EoR collision risk decreases from 3,600 ft to 9,000 ft runway separation, well below the threshold.

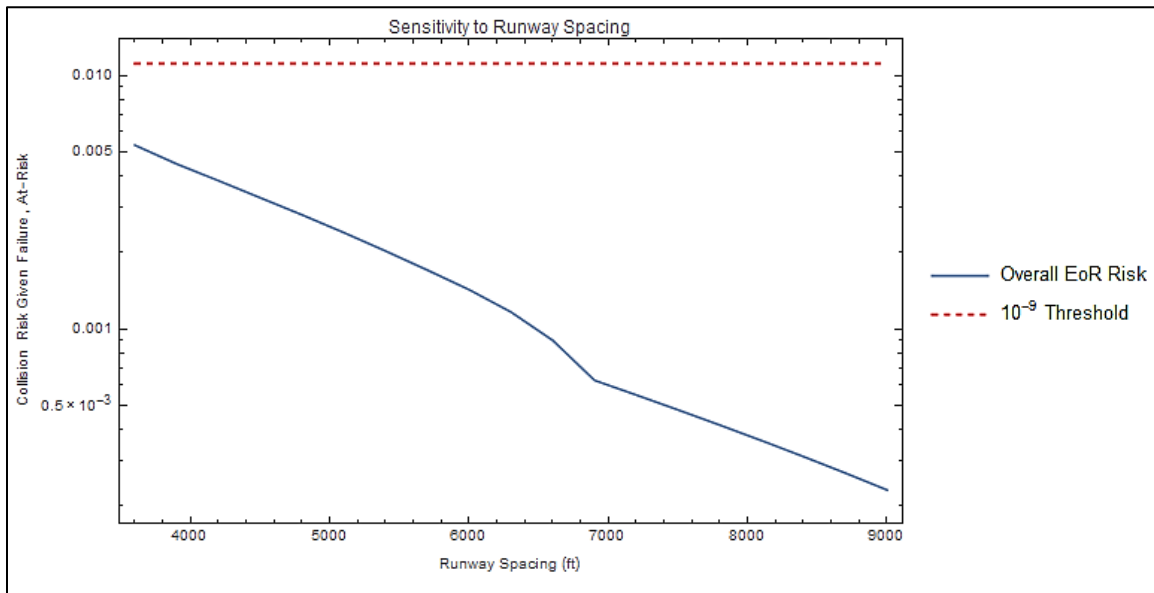


Figure M-5: Sensitivity of Collision Risk versus Runway Spacing in Feet

Figure M-6 displays the sensitivity of collision risk as it relates to runway spacing in feet. Once again the eight cases under consideration are depicted. As the runway spacing distance increases in feet (3,600-9,000 ft shown) the collision risk decreases based on aircraft configurations. In this graph, the best case shown is a VNAV-equipped nominal aircraft that has captured the glideslope and is continuing the approach. The worst case shown is a nominal aircraft with VNAV equipment, executing a go-around in level flight. Note: the horizontal (red) line depicts the 10^{-9} threshold.

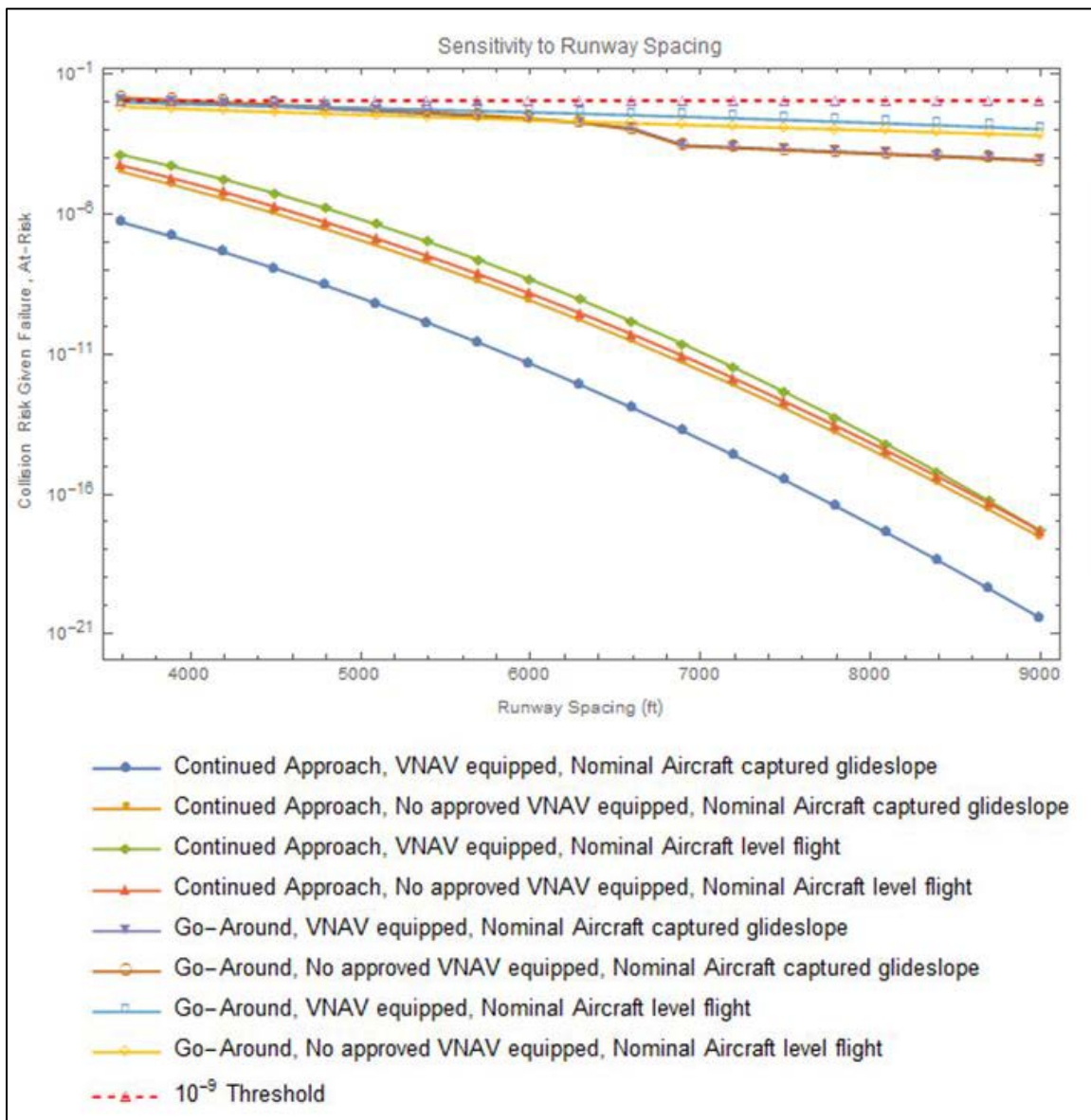


Figure M-6: Sensitivity of Collision Risk versus Runway Spacing in Feet

Figure M-7 further breaks down the data presented in figure M-6. As previously discussed, there are four cases of nominal aircraft that continued approaches with and without VNAV equipment that either captured the glideslope or were in level flight. The runway spacing length in feet is plotted against the track angle relative to the ILS, with associated collision risk. The darker shade (blue) that is visible in each graph indicates a decrease in collision risk as the runway spacing distance is increased. The concentration of the data graphed indicates that the level of risk increases at that angle shown. For example, graphs (a) and (b) indicate an increase in risk at the 55° track and the 80° track relative to the ILS based on that aircraft configuration. Graphs (c) and (d) indicate an increase in risk at the 90° track relative to the ILS, based on that aircraft configuration.

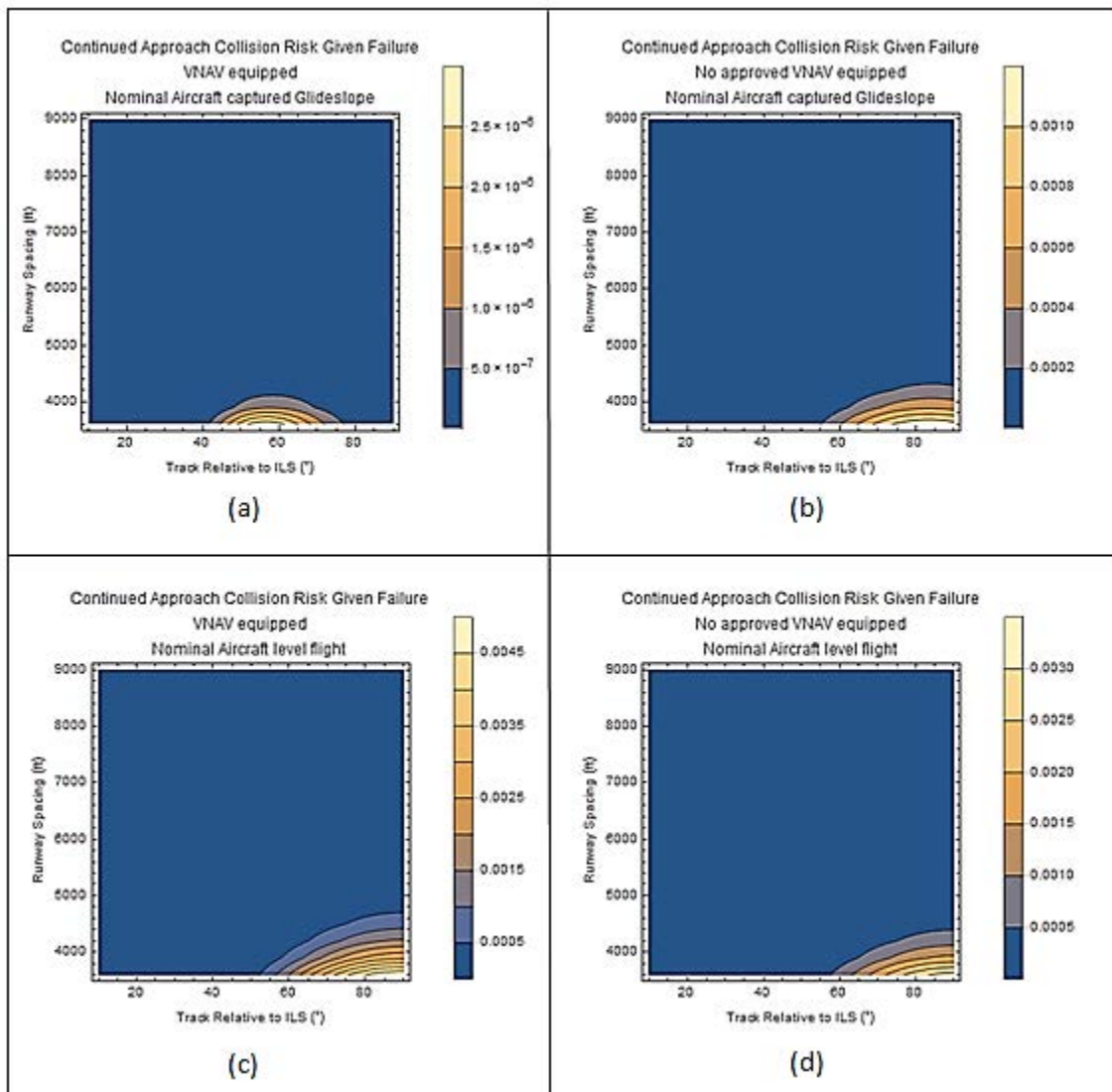


Figure M-7: Collision Risk of Runway Spacing for Nominal Aircraft with and without VNAV Equipment with Captured Glideslope and in Level Flight

Figure M-8 breaks down the data presented in figure M-6 just as described above. Depicted are the four cases of nominal aircraft that executed go-arounds with and without VNAV equipment that either captured the glideslope or were in level flight. The runway spacing length in feet is plotted against the track angle relative to the ILS, with associated collision risk. The darker shade (blue) that is visible in each graph indicates a decrease in collision risk as the length of the runway spacing is increased. The concentration of the data graphed indicates that the level of risk increases at that angle shown. For example, graphs (a) and (b) indicate an increase in risk at the 80° track and the 70° track relative to the ILS based on that aircraft configuration. Graphs (c) and (d) indicate an increase in risk at the 30° and 45° tracks respectively relative to the ILS, based on that aircraft configuration.

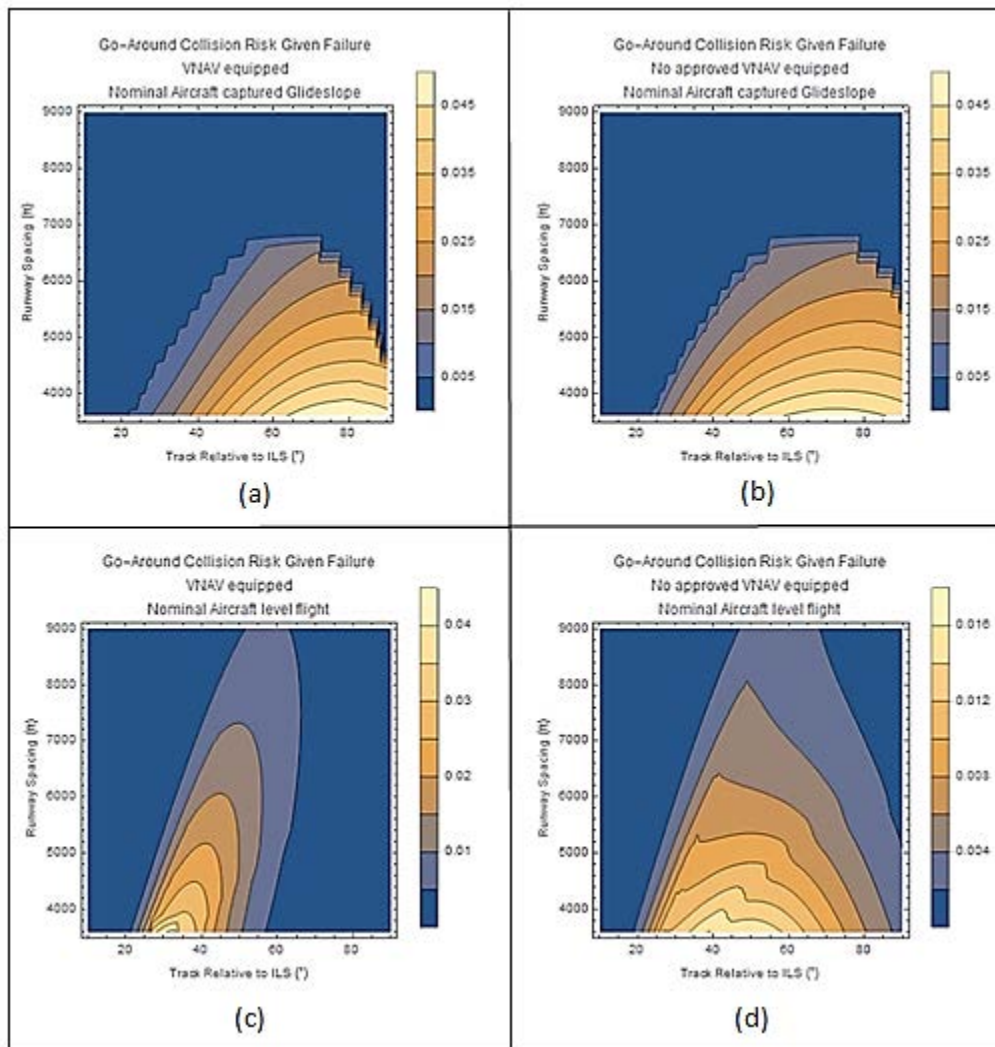


Figure M-8: Collision Risk of Runway Spacing for Nominal Aircraft Executing a Go-around with and without VNAV Equipment with Captured Glideslope and in Level Flight

EoR Vertical Angle

Figure M-9 represents the collision risk sensitivity to the EoR vertical angle. The 10^{-9} threshold is the dashed (red) line. As the vertical angle decreases from -3.0 to 0.0 in the graph, the collision risk increases until it peaks at -0.5, and then begins to decrease once again.

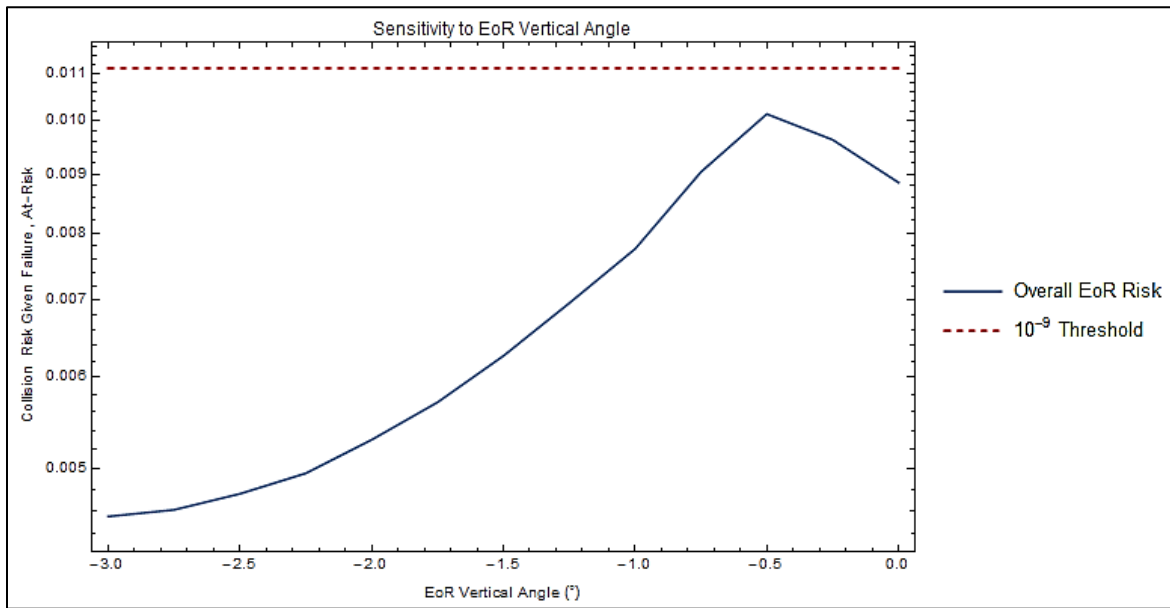


Figure M-9: Sensitivity of Collision Risk to Vertical Angle

Figure M-10 shows the eight cases under consideration. The best case depicted is the nominal aircraft that continued the approach with VNAV equipment and a captured glideslope, well below the threshold. Two cases exceed the threshold level at different angles. The nominal VNAV-equipped aircraft in level flight executing a go-around exceeds the threshold at approximately -1.7 vertical angle. The nominal non-VNAV-equipped aircraft in level flight executing a go-around exceeds the threshold at approximately -1.0 vertical angle. A third case rides slightly above to barely below the threshold for the entire data set collected. This nominal aircraft was executing a go-around, was not VNAV-equipped, and had captured the glideslope.

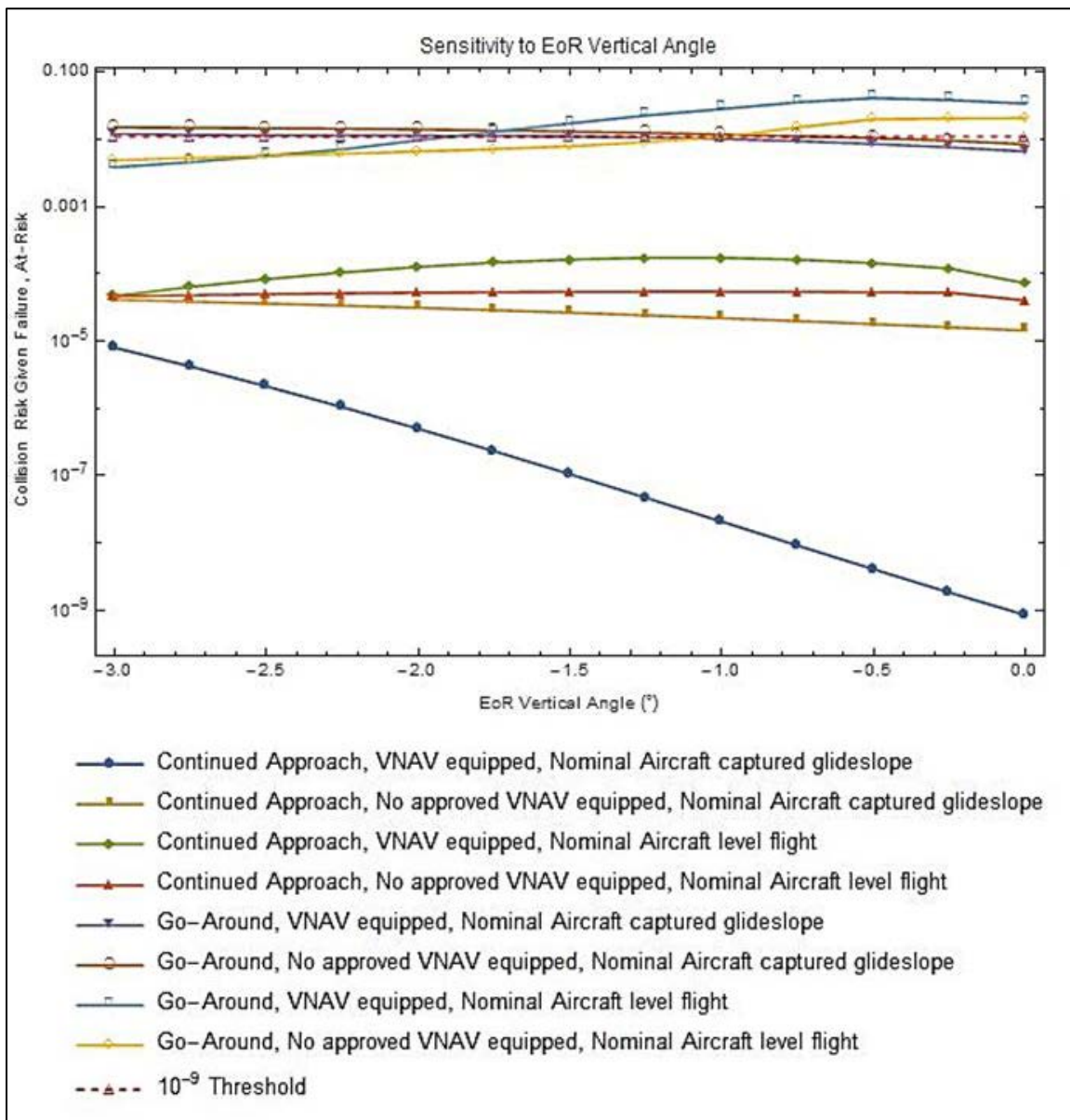


Figure M-10: Collision Risk Sensitivity to EoR Vertical Angle

Graph (a) in figure M-11 shows collision risk is minimally evident at the 65° track relative to the ILS. It becomes more prominent at the 85° track in graph (b). In both of these cases the aircraft is continuing the approach and has captured the glideslope. In graphs (c) and (d), both aircraft are continuing the approach in level flight. In the VNAV equipped aircraft (graph (c)), the collision risk is centered on the 90° track and -0.8 vertical angle. The non-VNAV-equipped aircraft in graph (d) shows a considerable level of collision risk on the 90° track and centered between 0.0 and -0.5.

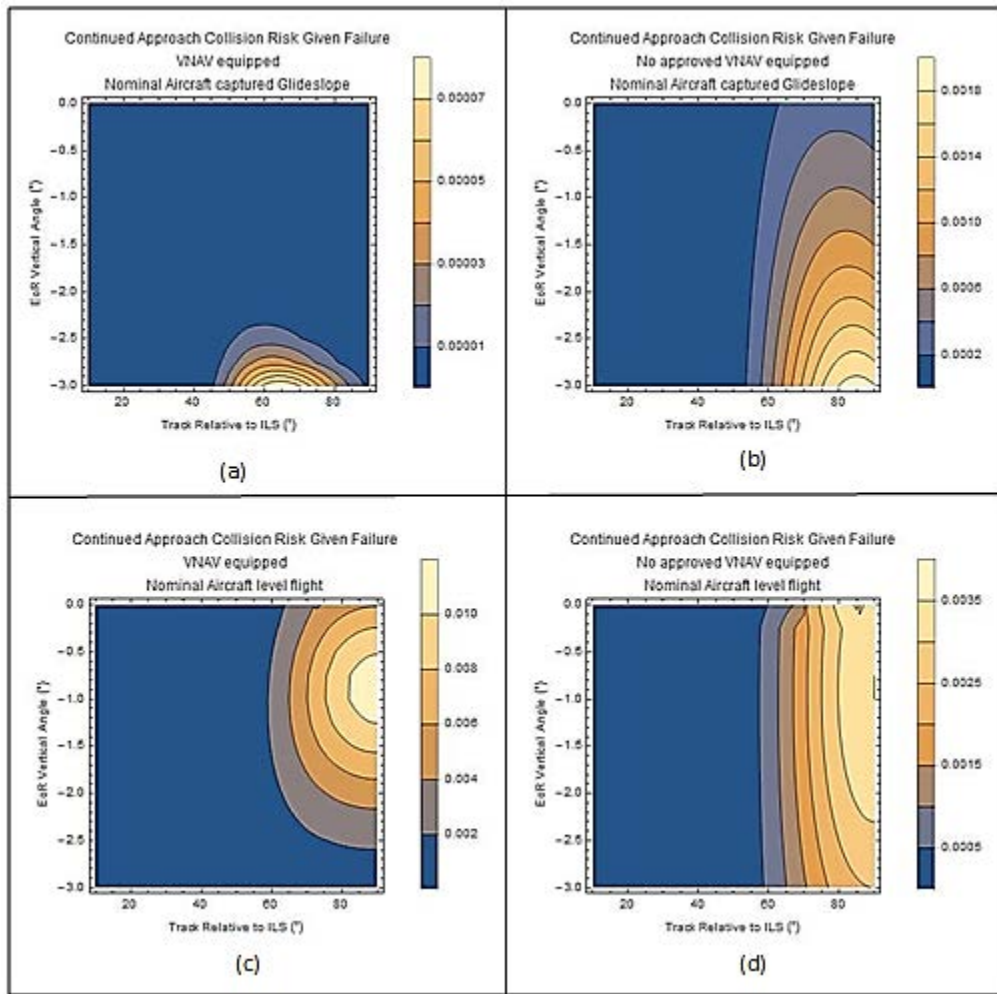


Figure M-11: Collision Risk Sensitivity to EoR Vertical Angle for Aircraft Continuing Approach with Captured Glideslope and in Level Flight

In figure M-12, collision risk for nominal aircraft executing a go-around with a captured glideslope is depicted in graphs (a) and (b). In graph (a), the aircraft shows collision risk at the -1.4 vertical angle at the 90° track. Graph (b) shows a significant increase in collision risk at the -3.0 vertical angle and 90° track. The difference between the two nominal aircraft is VNAV-equipped versus non-VNAV-equipped. Graphs (c) and (d) show the nominal aircraft in level flight. Graph (c) indicates the greatest collision risk occurs at the -0.3 vertical angle at the 55° track. This aircraft is VNAV-equipped. Graph (d) shows a non-VNAV-equipped aircraft, where the collision risk is prominent at 0.0 vertical angle and at the 65° track.

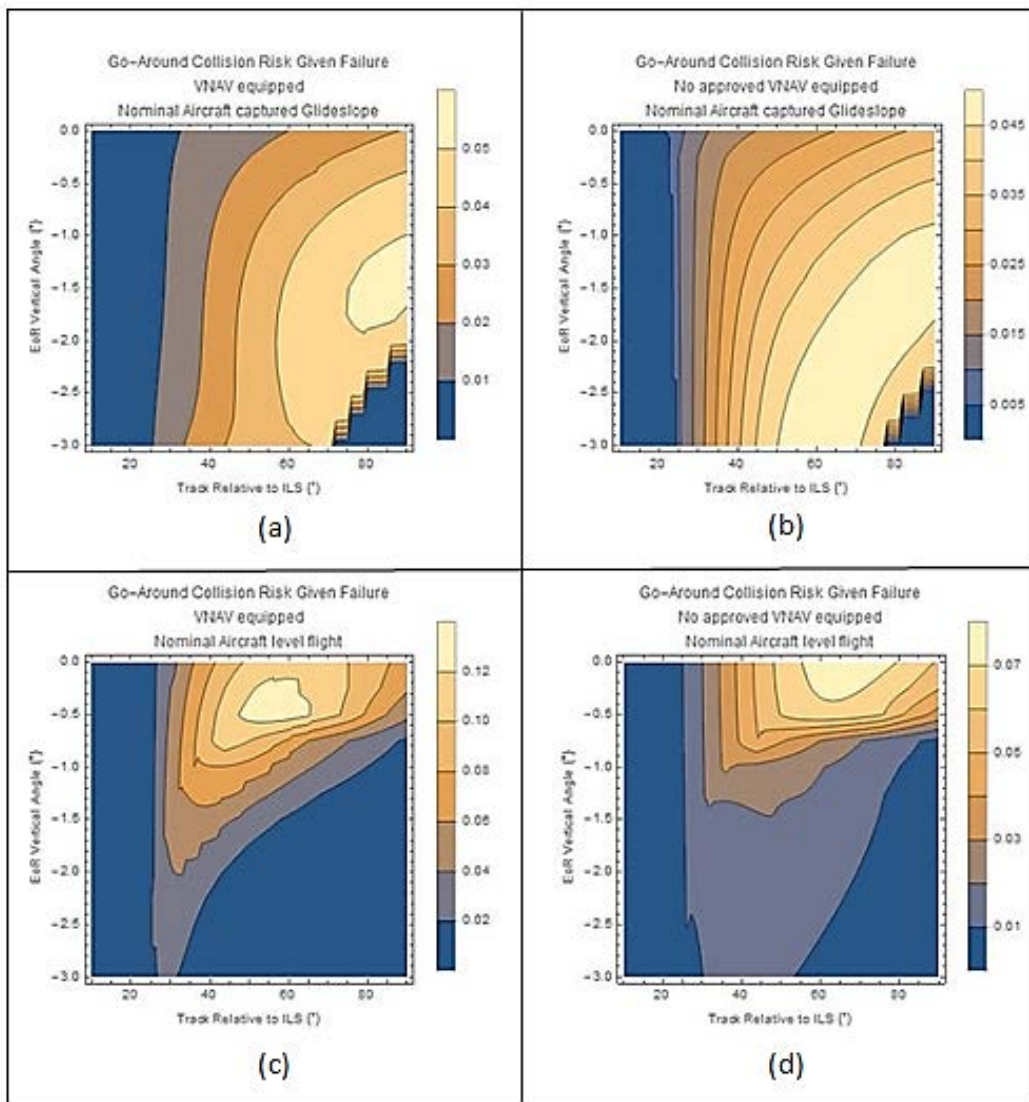


Figure M-12: Collision Risk Sensitivity to EoR Vertical Angle for Aircraft Executing a Go-around with Captured Glideslope and in Level Flight

Altitude Separation

Figure M-13 shows collision risk sensitivity to altitude separation at glideslope intercept altitude. The dashed (red) line is the collision risk threshold. Collision risk fluctuates somewhat between 0.005 – 0.008 as the altitude decreases from -400 to +100. Then it decreases rapidly beyond +200 ft.

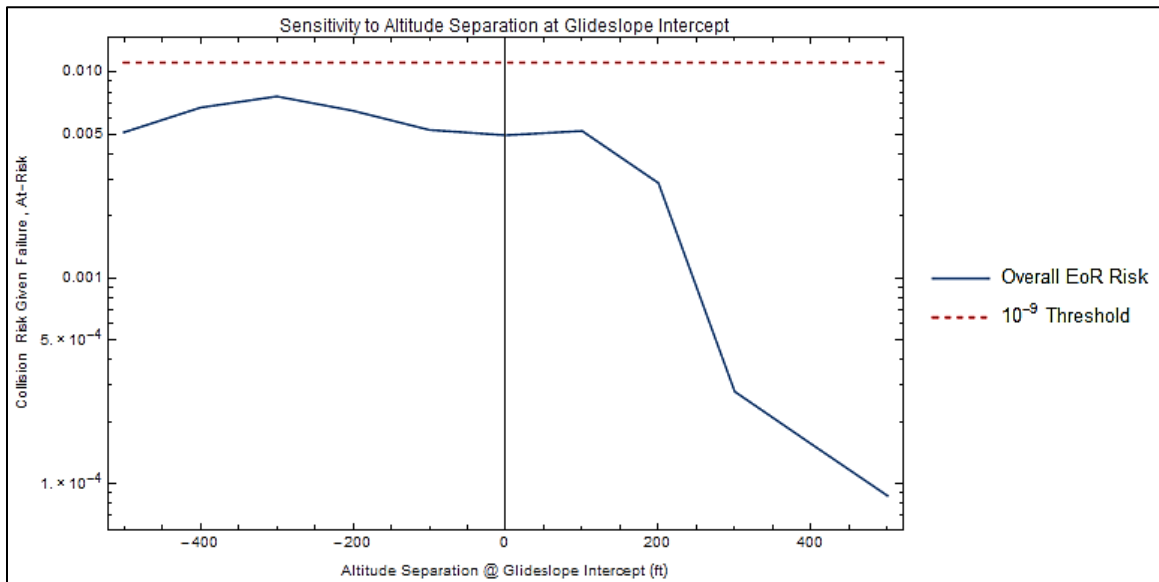


Figure M-13: Collision Risk Sensitivity to Altitude Separation at Glideslope Intercept

Figure M-14 plots the eight aircraft configuration cases with collision risk sensitivity to altitude separation at glideslope intercept. Three of the eight cases exceed the dashed (red) collision risk threshold. The nominal VNAV-equipped aircraft executing a go-around in level flight goes below the threshold at -100 foot separation. The nominal non-VNAV-equipped aircraft executing a go-around in level flight gradually goes below the threshold at -150 foot altitude separation. The nominal non-VNAV-equipped aircraft rides the threshold until the +100 ft separation altitude.

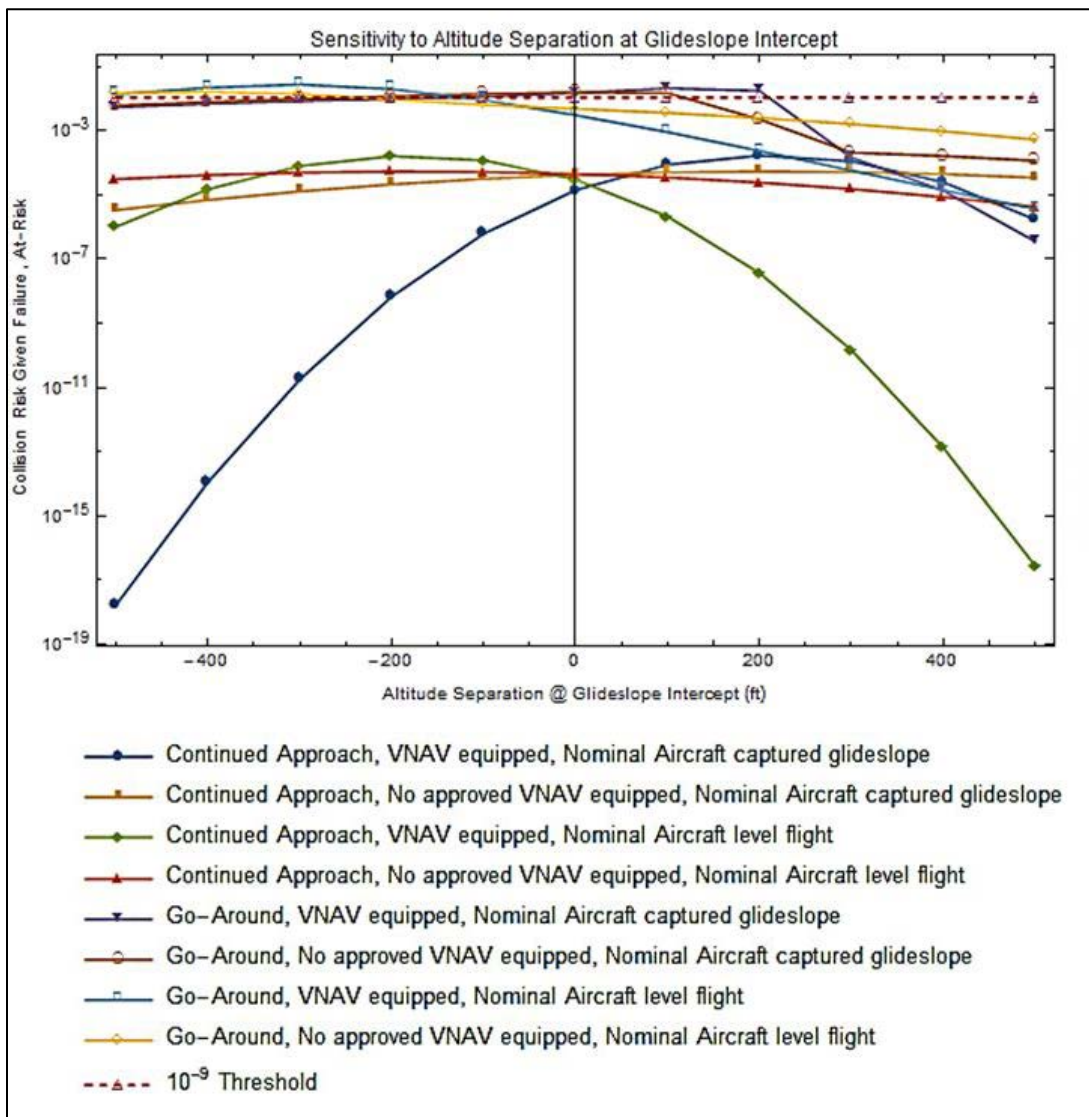


Figure M-14: Collision Risk Sensitivity to Altitude Separation at Glideslope Intercept for Nominal VNAV and Non-VNAV Equipped Aircraft

Figure M-15 depicts nominal aircraft that continued the approach with a captured glideslope and in level flight. Graphs (a) and (b) show the aircraft that have captured the glideslope, and graphs (c) and (d) show aircraft in level flight. In each case, the collision risk is elevated at the 90° track relative to the ILS. Graph (a) shows an increased collision risk at the +350 ft altitude separation, and graph (b) shows increased collision risk at the +400 ft altitude separation. Graphs (c) and (d) indicate increased collision risk at the -200 ft altitude separation. The major difference between graphs (a), (b), (c), and (d) is captured glideslope versus level flight.

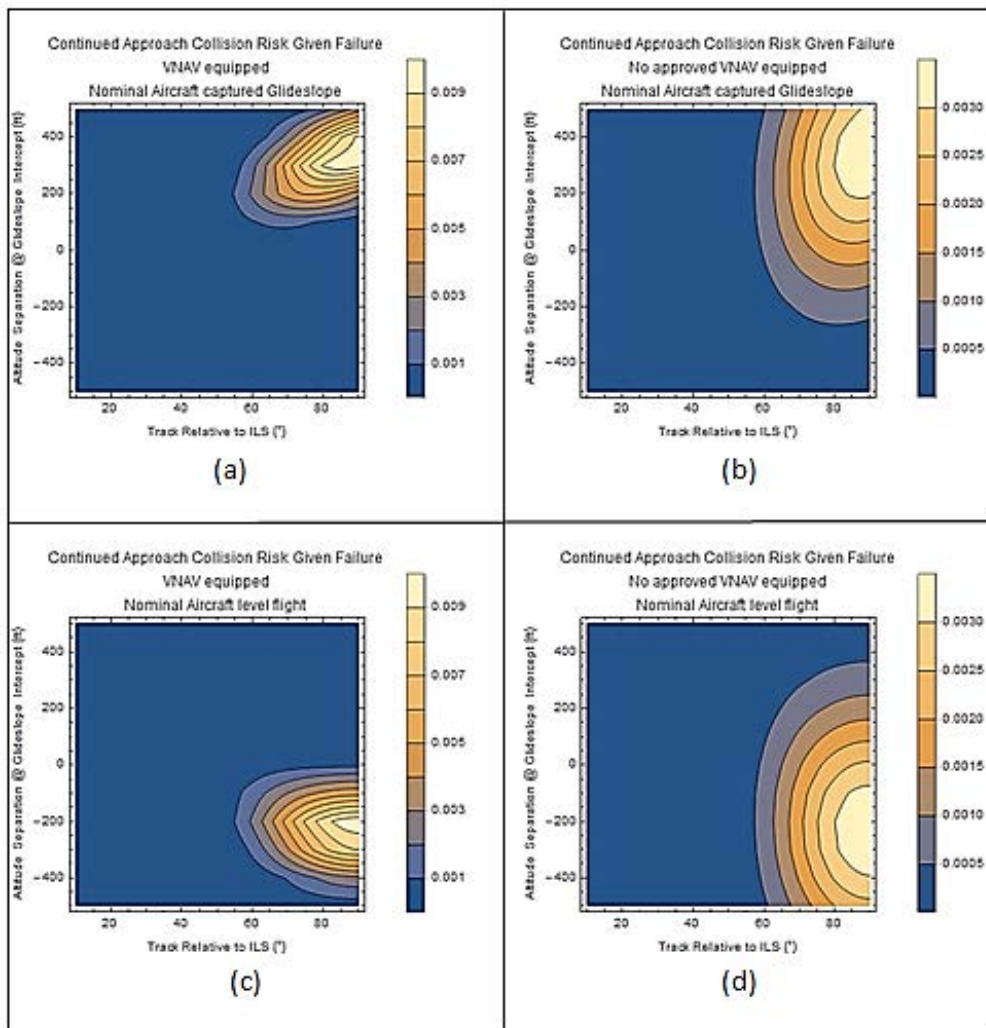


Figure M-15: Collision Risk for Nominal Aircraft Continuing on Approach with Captured Glideslope and in Level Flight

Figure M-16 depicts nominal aircraft that executed a go-around with a captured glideslope and in level flight. Graphs (a) and (b) show the aircraft that have captured the glideslope, and graphs (c) and (d) show aircraft in level flight. Graph (a) shows an increased collision risk at the +200 ft altitude separation at the 45° track, and graph (b) shows increased collision risk at the +100 ft altitude separation at the 70° track. Graphs (c) and (d) indicate increased collision risk at the greater than -400 ft altitude separation at the 60° track. The major difference between graphs (a), (b), (c), and (d) is captured glideslope versus level flight.

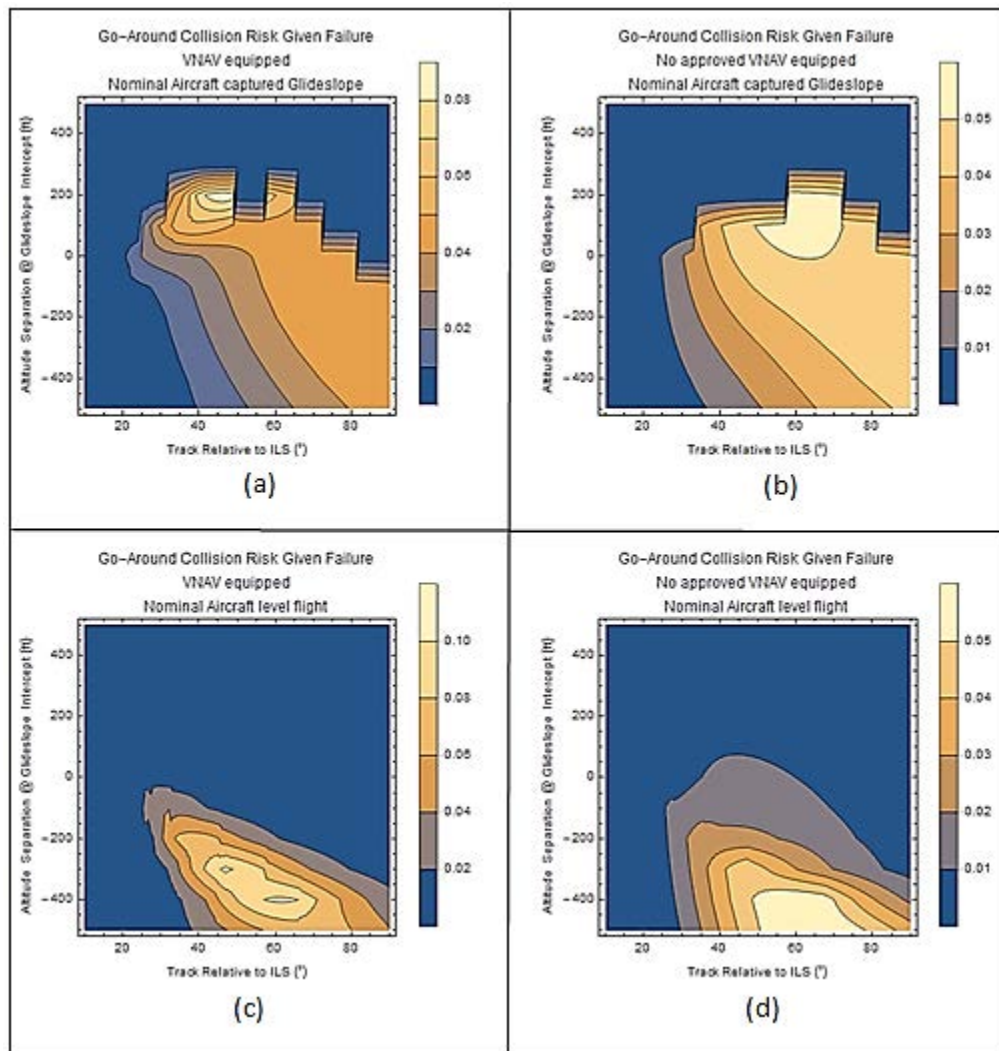


Figure M-16: Collision Risk for Nominal Aircraft Executing a Go-around with Captured Glideslope and in Level Flight

Second Turn Angle

Figure M-17 graphs the collision risk sensitivity to second turn angle. As the turn angle increases from 10° up to 80°, the collision risk increases and approaches the dashed (red) threshold line.

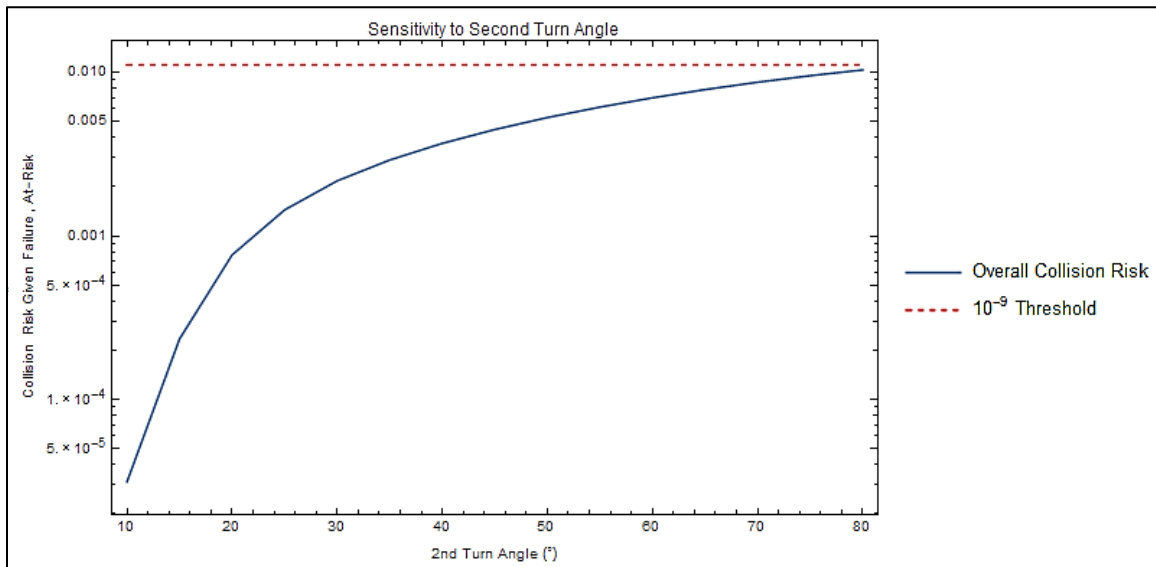


Figure M-17: Collision Risk Sensitivity to Second Turn Angle

In figure M-18, four of the considered cases ride or go above the collision risk threshold. The two cases where the aircraft is VNAV and non-VNAV-equipped with captured glideslope executing a go-around, and the two cases where the aircraft is VNAV and non-VNAV-equipped executing a go-around in level flight all exceed the collision risk threshold.

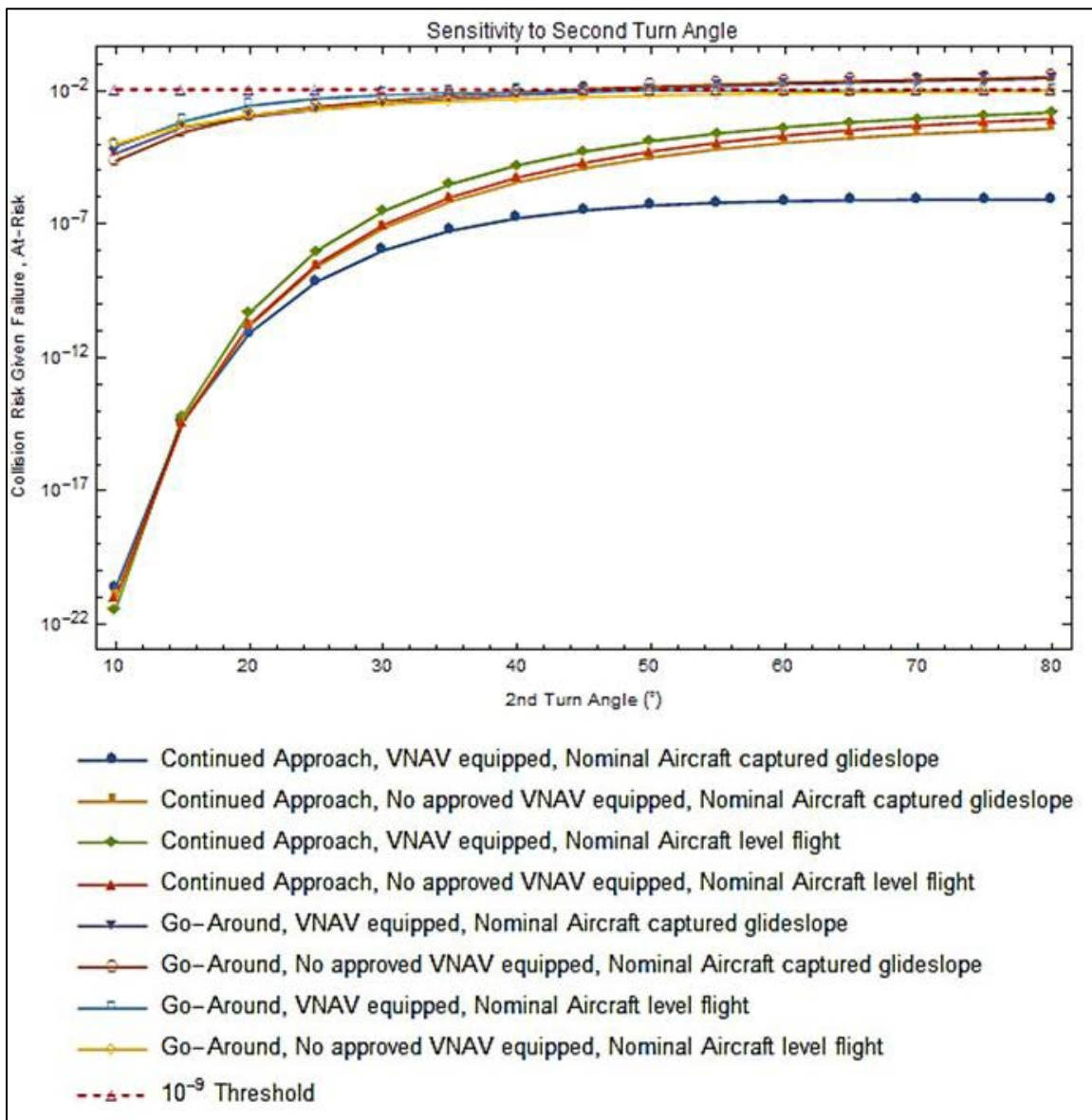


Figure M-18: Collision Risk Sensitivity to Second Turn Angle

Figure M-19 shows the collision risk sensitivity to groundspeed. This figure demonstrates that as groundspeed increases from 140 to 210 knots the collision risk increases and approaches the threshold (red-dashed line). The overall collision risk is not changed as groundspeed changes by more than an order of magnitude.

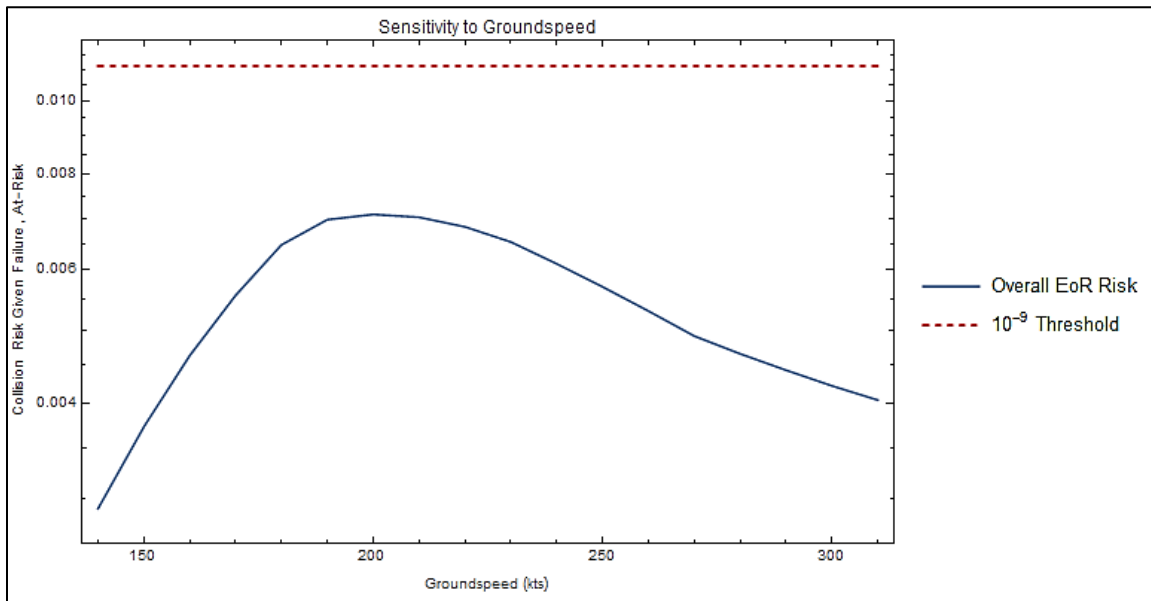


Figure M-19: Collision Risk Sensitivity to Ground Speed

In figure M-20, four of the considered cases ride or go above the collision risk threshold. The two cases where the aircraft is VNAV and non-VNAV-equipped with captured glideslope executing a go-around, and the two cases where the aircraft is VNAV and non-VNAV-equipped executing a go-around in level flight all exceed the collision risk threshold at lower groundspeeds.

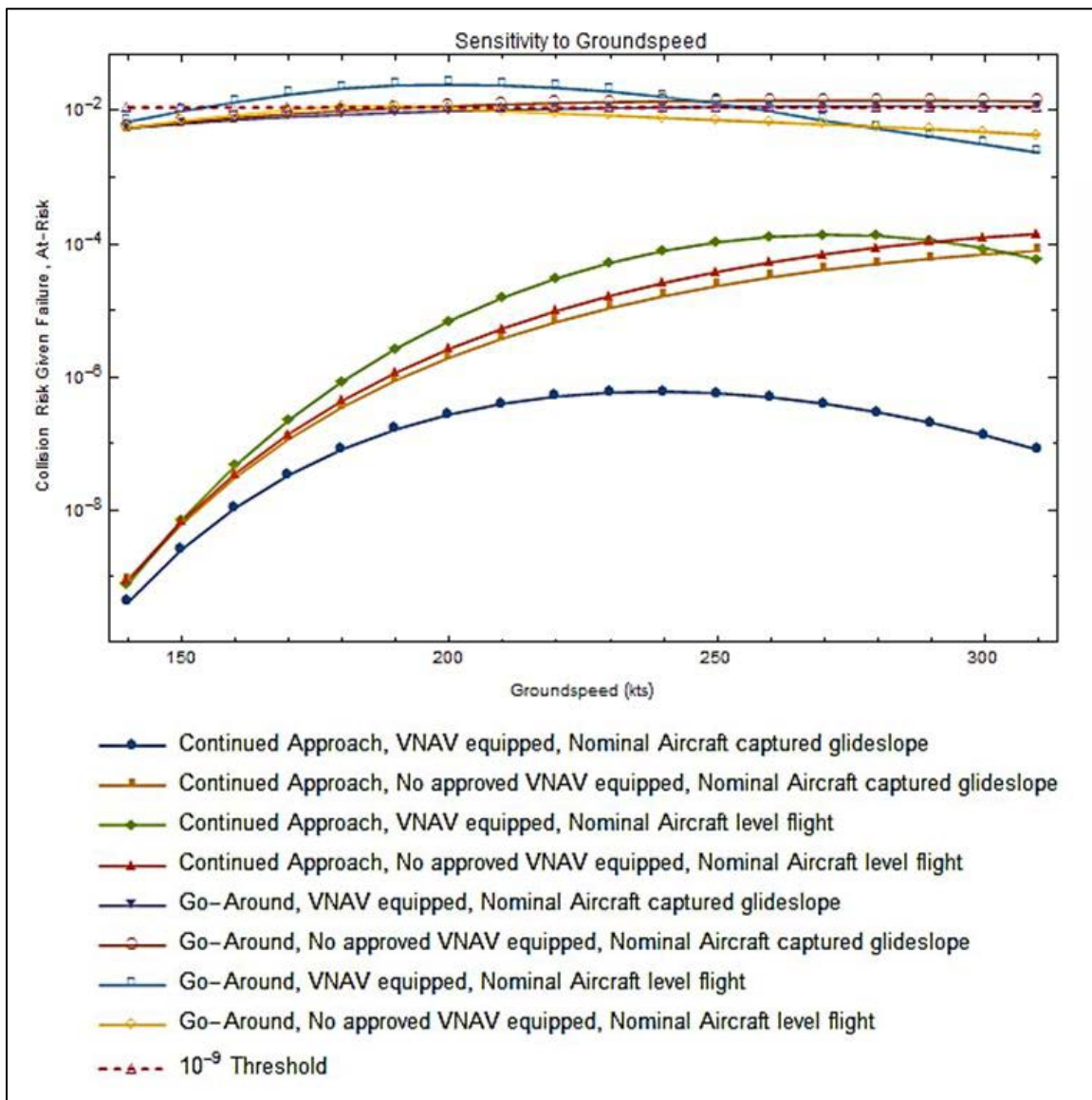


Figure M-20: Collision Risk Sensitivity to Groundspeed for Nominal Aircraft with Captured Glideslope and in Level Flight

Figure M-21 depicts nominal aircraft that continued the approach with a captured glideslope and in level flight. Graphs (a) and (b) show the aircraft that have captured the glideslope, and graphs (c) and (d) show aircraft in level flight. Graph (a) shows an increased collision risk at the 220 knot groundspeed at the 65° track, and graph (b) shows increased collision risk at the 300 knot and above groundspeed at the 85° track. Graphs (c) and (d) indicate increased collision risk at the 250 knot and at or above 300 knot groundspeed at the 90° track.

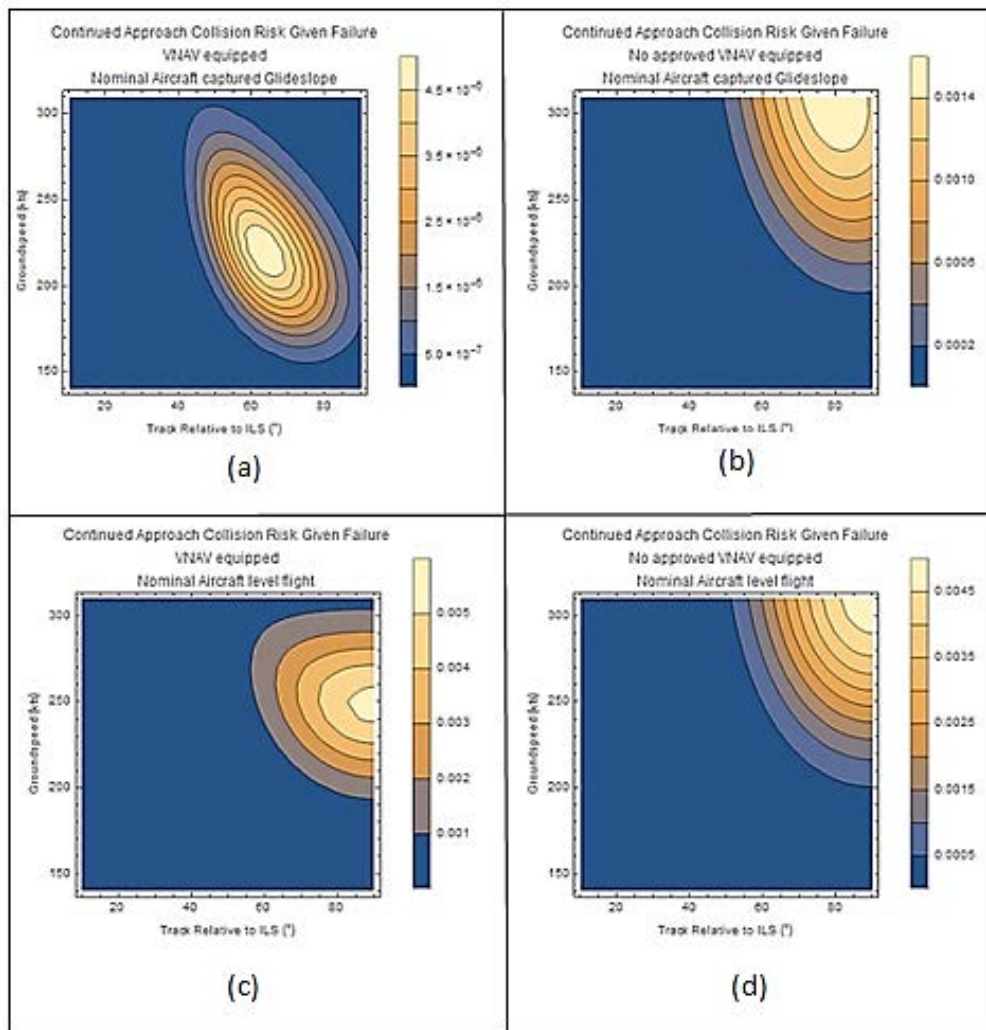


Figure M-21: Collision Risk Sensitivity to Groundspeed for Nominal Aircraft Continuing on Approach with Captured Glideslope and in Level Flight

Figure M-22 depicts nominal aircraft that executed a go-around with a captured glideslope and in level flight. Graphs (a) and (b) show the aircraft that have captured the glideslope, and graphs (c) and (d) show aircraft in level flight. Graph (a) shows an increased collision risk at the 230 knot groundspeed at the 85° track, and graph (b) shows increased collision risk at the 230 knot groundspeed at the 75° track. Graphs (c) and (d) indicate increased collision risk at lower groundspeeds, 170 knots, and at the 70° track.

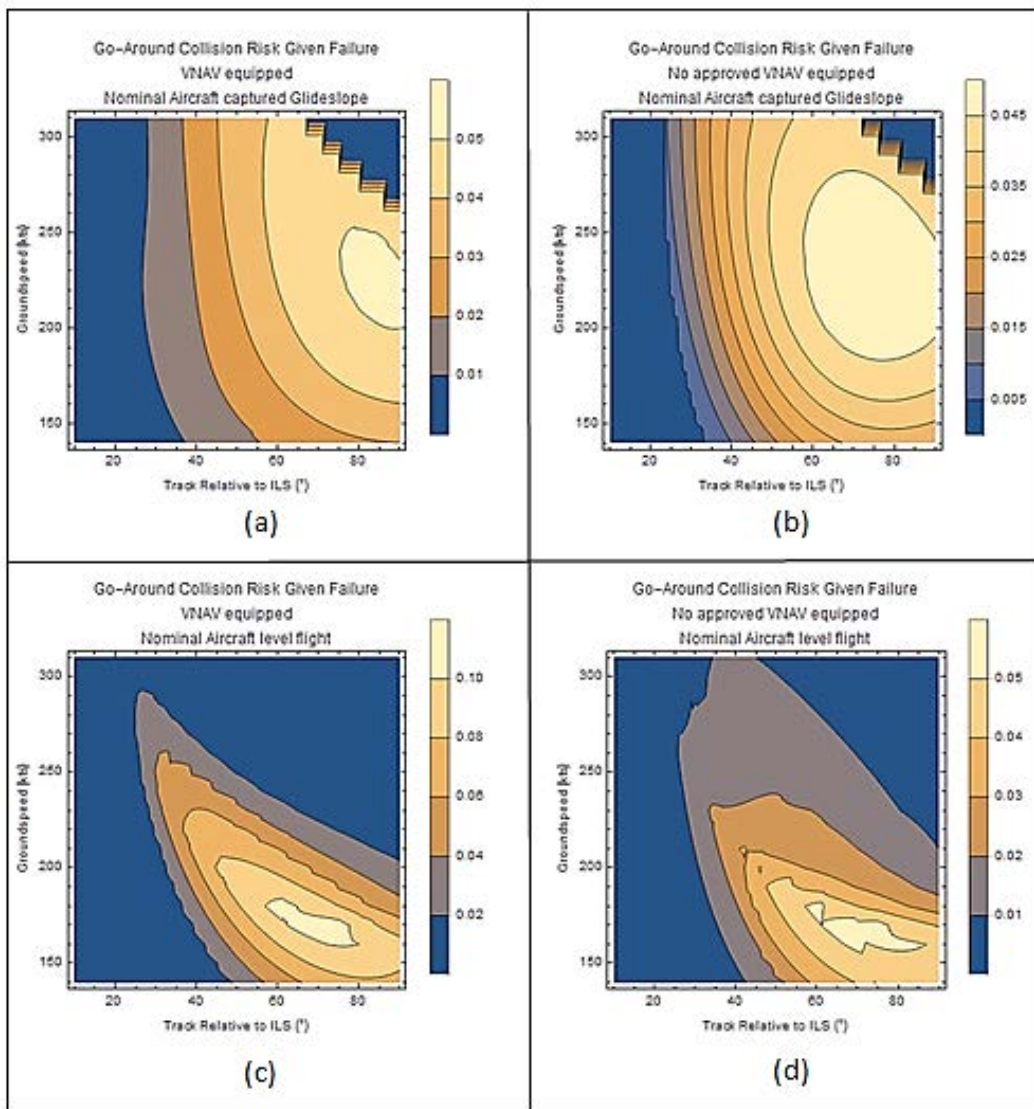


Figure M-22: Collision Risk Sensitivity to Groundspeed for Nominal Aircraft Executing a Go-around with Captured Glideslope and in Level Flight Bank Angle for Correction

In figure M-23, the collision risk sensitivity to correction bank angle is depicted. The collision risk decreases as the bank angle increases from 20° to 30°, and correspondingly decreases to well below the dashed (red) threshold line.

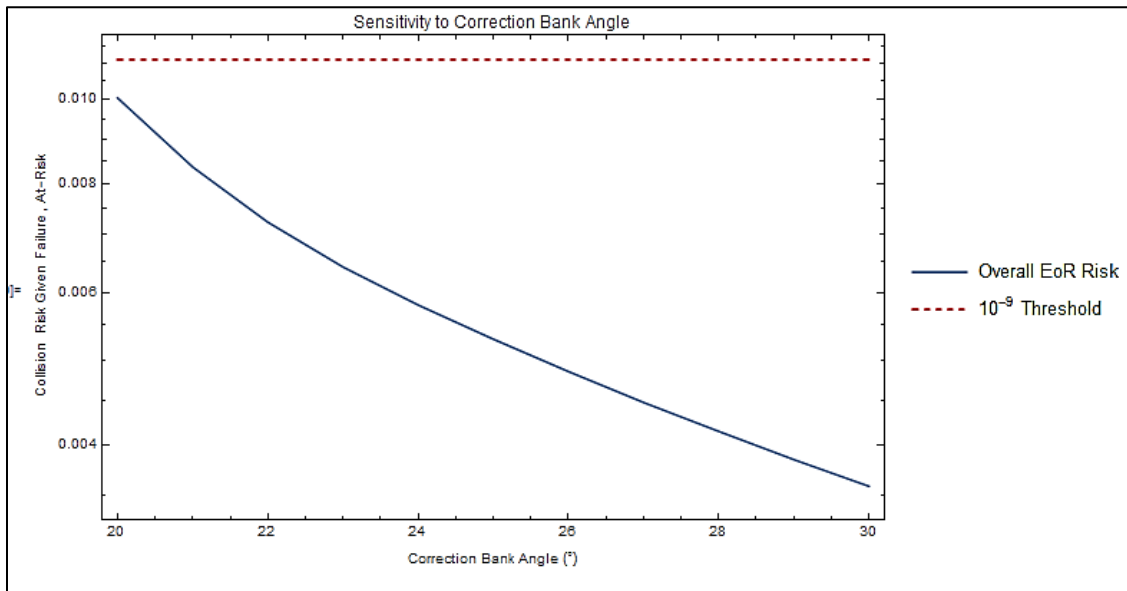


Figure M-23: Collision Risk Sensitivity to Correction Bank Angle for Nominal Aircraft with Captured Glideslope and in Level Flight

In figure M-24, four of the considered cases ride or gradually decrease to below the collision risk dashed (red) threshold as bank angle increases. The two cases where the aircraft is VNAV and non-VNAV-equipped with captured glideslope executing a go-around, and the two cases where the aircraft is VNAV and non-VNAV-equipped executing a go-around in level flight all exceed the collision risk threshold starting at the 20° bank angle, and gradually go slightly below by the 30° bank angle. The other four cases dramatically show reduced collision risk as the bank angle increases from 20° to 30°.

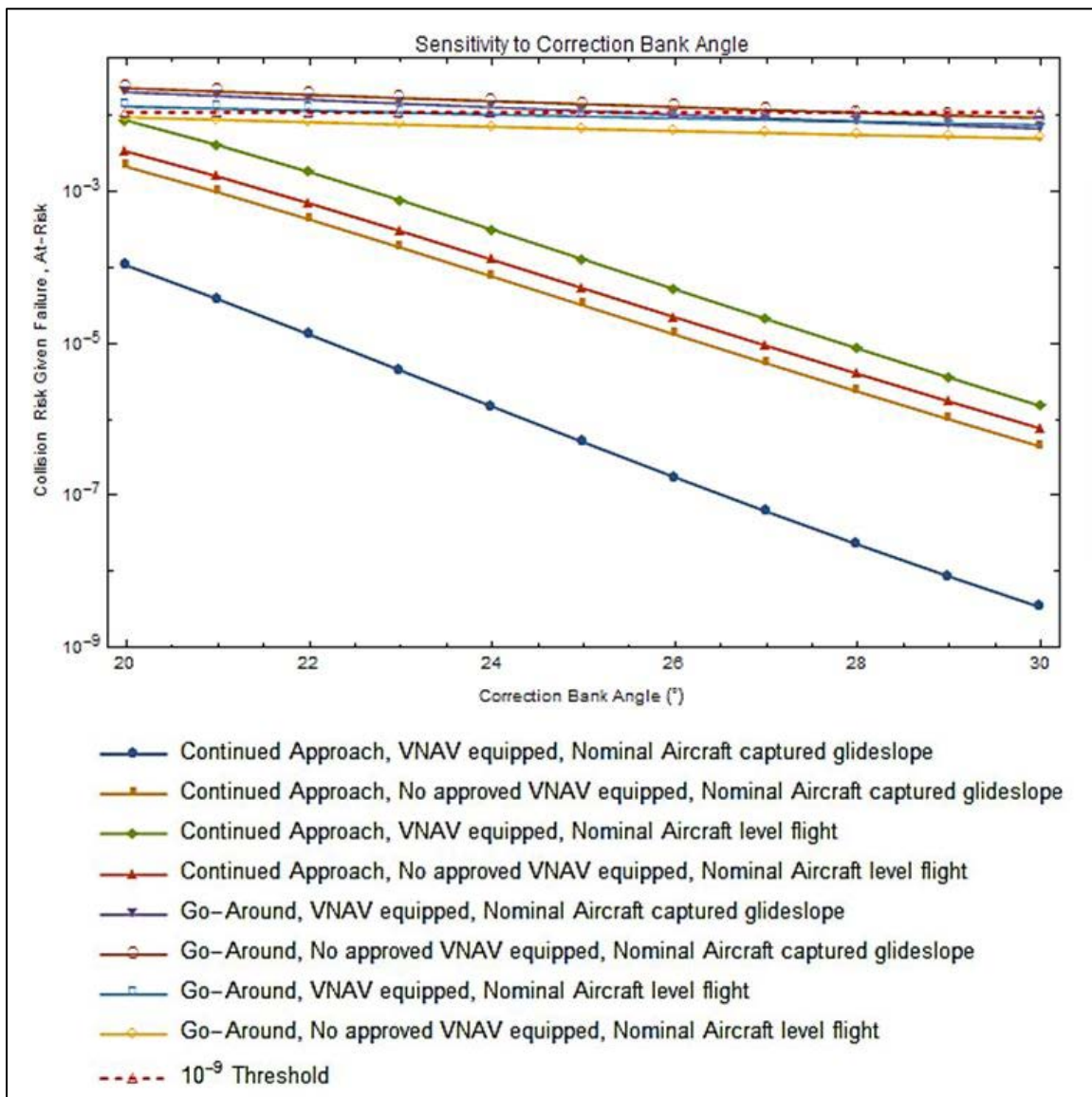


Figure M-24: Collision Risk Sensitivity to Correction Bank Angle for Nominal Aircraft with Captured Glideslope and in Level Flight

Figure M-25 depicts nominal aircraft that continued on the approach with a captured glideslope and in level flight. Graphs (a) and (b) show the aircraft that have captured the glideslope, and graphs (c) and (d) show aircraft in level flight. Graph (a) shows an increased collision risk at the 20° angle of bank at the 60° track, and graph (b) shows increased collision risk at the 20° angle of bank at the 85° track. Graphs (c) and (d) indicate increased collision risk at the 20° angle of bank at the 80° and 90° tracks.

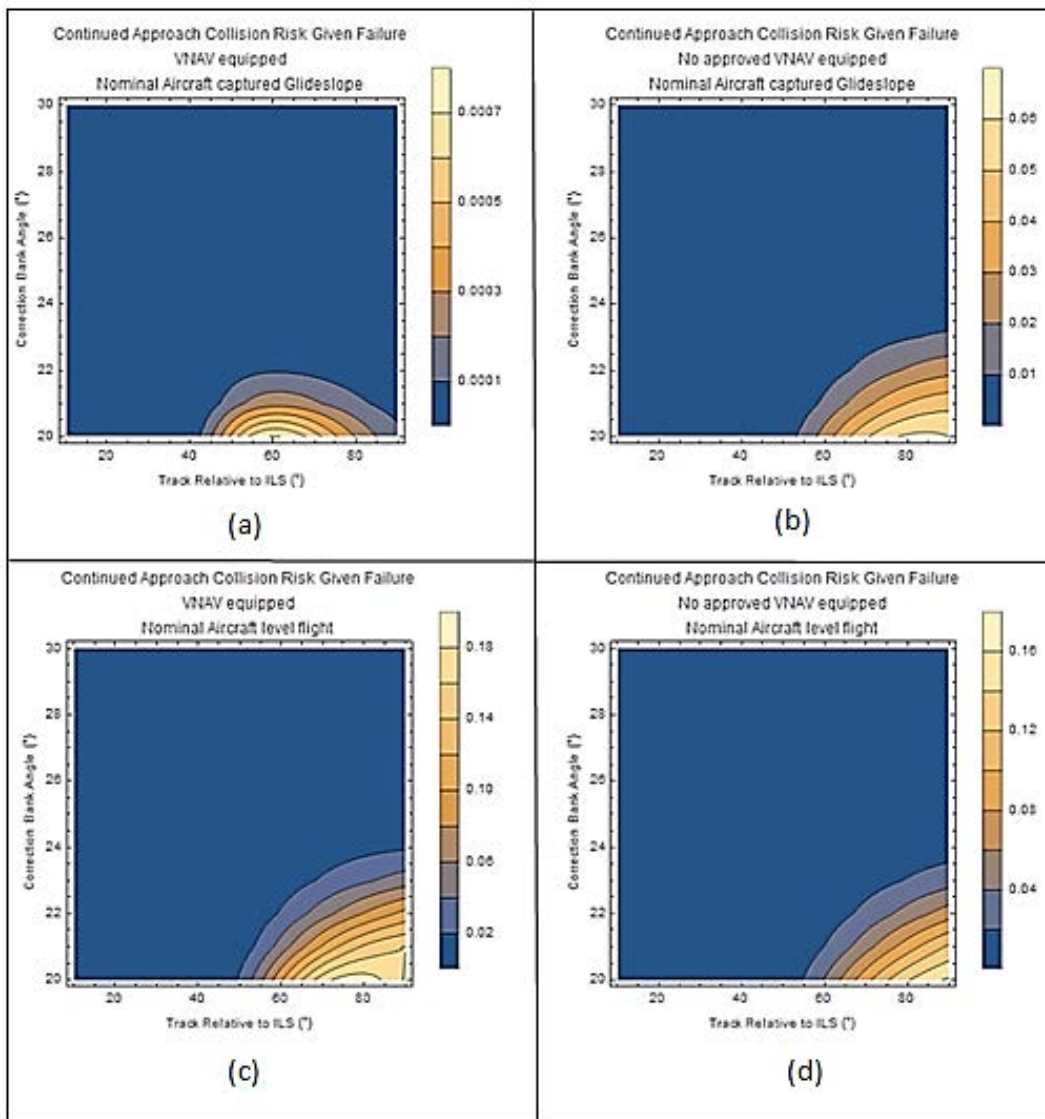


Figure M-25: Collision Risk Sensitivity to Correction Bank Angle for Nominal Aircraft Continuing Approach with Captured Glideslope and in Level Flight

Figure M-26 depicts nominal aircraft that executed a go-around with a captured glideslope and in level flight. Graphs (a) and (b) show the aircraft that have captured the glideslope, and graphs (c) and (d) show aircraft in level flight. Graphs (a) and (b) show an increased collision risk at the 20° to 30° angle of bank at the 70° track. Graphs (c) and (d) indicate increased collision risk at the 20° to 30° angle of bank at the 30° and 45° tracks.

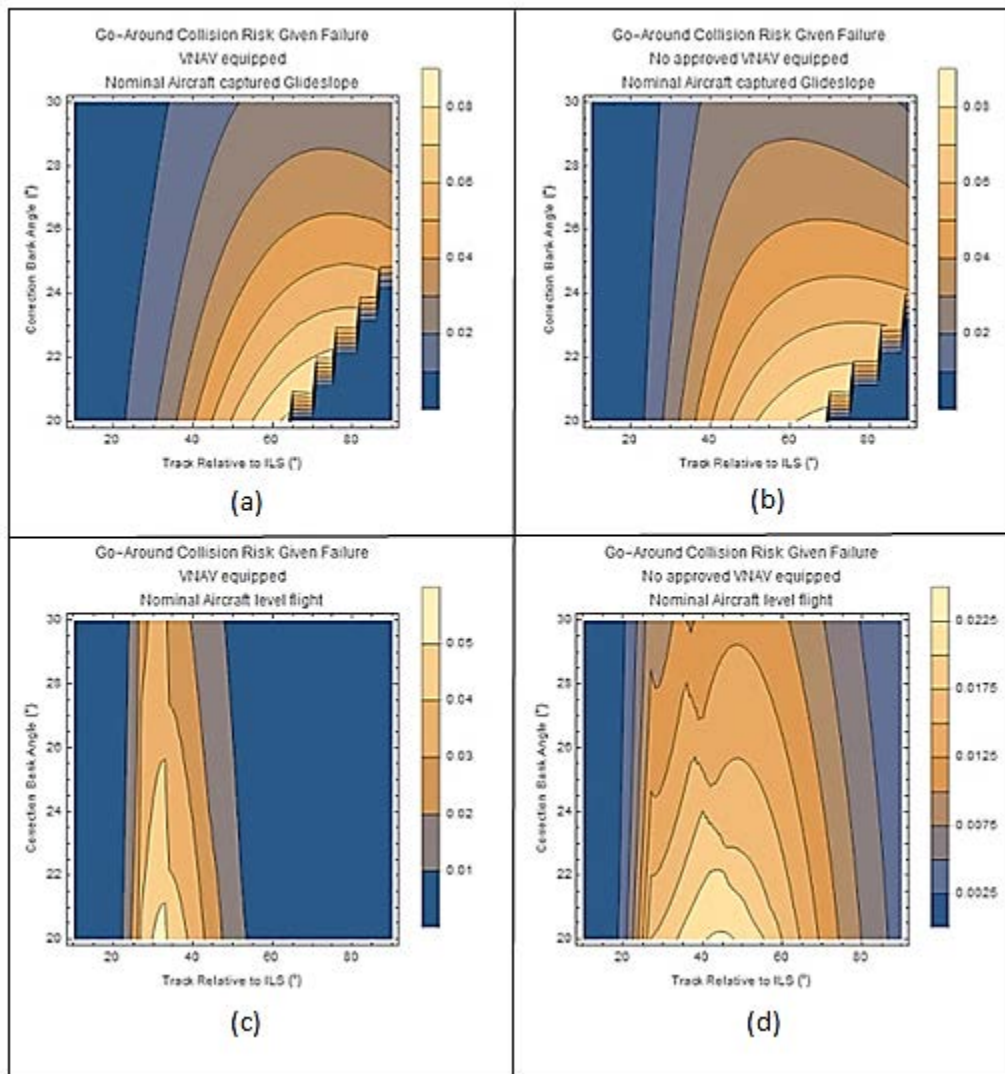


Figure M-26: Collision Risk Sensitivity to Correction Bank Angle for Nominal Aircraft Executing a Go-around with Captured Glideslope and in Level Flight